AD_____

Award Number: W81XWH-09-1-0279

TITLE: Regulation of mTOR by Nutrients

PRINCIPAL INVESTIGATOR: Kun-Liang Guan

CONTRACTING ORGANIZATION: University of California, San Diego
La Jolla, CA 92093

REPORT DATE: July 2012

TYPE OF REPORT: Final

PREPARED FOR: U.S. Army Medical Research and Materiel Command
Fort Detrick, Maryland 21702-5012

DISTRIBUTION STATEMENT: Approved for Public Release;
Distribution Unlimited

REPORT DOCUMENTATION PAGE

Form Approved
OMB No. 0704-0188

1. REPORT DATE	2. REPORT TYPE	3. DATES COVERED
July 2012	Final	1 July 2009 - 30 June 2012

4. TITLE AND SUBTITLE
Regulation of mTOR by Nutrients

5a. CONTRACT NUMBER

5b. GRANT NUMBER
W81XWH-09-1-0279

5c. PROGRAM ELEMENT NUMBER

6. AUTHOR(S)
Kun-Liang Guan

E-Mail: kuguan@ucsd.edu

5d. PROJECT NUMBER

5e. TASK NUMBER

5f. WORK UNIT NUMBER

7. PERFORMING ORGANIZATION NAME(S) AND ADDRESS(ES)

University of California, San Diego
La Jolla, CA 92093

8. PERFORMING ORGANIZATION REPORT NUMBER

9. SPONSORING / MONITORING AGENCY NAME(S) AND ADDRESS(ES)
U.S. Army Medical Research and Materiel Command
Fort Detrick, Maryland 21702-5012

10. SPONSOR/MONITOR'S ACRONYM(S)

11. SPONSOR/MONITOR'S REPORT NUMBER(S)

12. DISTRIBUTION / AVAILABILITY STATEMENT
Approved for Public Release; Distribution Unlimited

13. SUPPLEMENTARY NOTES

14. ABSTRACT
The mammalian target of rapamycin complex 1, mTORC1, is constitutively activated in TSC 1 or TSC2 mutant cells and contributes to the pathogenesis of TSC. Rapamycin, which is a potent inhibitor of TORC1, is in clinical trials for TSC and related diseases. Amino acids are key signals for mTORC1 activation. We have shown that the Rag family GTPases play a critical role in mTORC1 activation in response to amino acid stimulation. Gtr1 and Gtr2 are Rag homologs in yeast and they are also involved amino acid-induced TORC1 activation in yeast. We have solved the three dimensional structure of Gtr1-Gtr2 complex. This is the first GTPase dimmer structure ever to be solved. Our structure provides key molecular insights into the mechanism of Rag GTPase interaction with raptor and the "regulators", which consists of MP1/P14/P18 complex. Remarkably, the C-terminal diner structure of Gtr1-Gtr2 is highly similar to the structure of P14/MP1 dimmer although there is not primarily sequence homology between Gtr and P14/MP1. Our study also reveals the molecular basis how Rag is recruited to the lysosomes by "regulators" and the mechanism of mTORC1 activation by amino acids.

15. SUBJECT TERMS
TSC, mTORC1, Rag GTPase, Gtr1/Gtr2, VAM6, PRAK, cell growth

16. SECURITY CLASSIFICATION OF:			17. LIMITATION OF ABSTRACT	18. NUMBER OF PAGES	19a. NAME OF RESPONSIBLE PERSON
					USAMRMC
a. REPORT	b. ABSTRACT	c. THIS PAGE			19b. TELEPHONE NUMBER *(include area code)*
U	U	U	UU	114	

Table of Contents

Page

Introduction

The mammalian target of rapamycin (mTOR) is a central controller of cell growth (Wullschleger et al., 2006). TOR is highly conserved from yeast to mammals and forms two distinct complexes, TORC1 and TORC2. The two TOR complexes differ in subunit composition, sensitivity to rapamycin, and biological functions. Only TORC1 is inhibited by rapamycin. TORC1 promotes cell growth by stimulating translation and directly phosphorylating S6K and 4EBP1. High TORC1 activity also plays an important role to inhibit autophagy under nutrient sufficiency. In fact, inhibition of TORC1 by nutrient starvation is sufficient to induce autophagy. The functional importance of TORC1 in tuberous sclerosis complex (TSC) is demonstrated by the fact that mutation in TSC1 or TSC2 results in constitutive activation of TORC1(Cheadle et al., 2000; Inoki et al., 2002). Moreover, uncontrolled TORC1 activity contribute to cell over growth and tumor formation in TSC. Therefore, TORC1 regulation is key to TSC disease development and therapeutic treatment (Lee et al., 2007).

As a key growth controller, TORC1 is regulated by a wide range of extracellular and intracellular signals, including growth factors, cellular energy levels, and stress conditions(Kim and Guan, 2011). Moreover, nutrients, particularly amino acids, play a major role in TORC1 activation. In the absence of amino acids, neither growth factor or glucose can efficiently activate TORC1. Therefore, amino acid signaling is one of the most important signals for TORC1 regulation.

TSC1/TSC2 inhibit TORC1 by acting through the Rheb GTPase(Inoki et al., 2003), which is a member of the Ras super family. TSC1/TSC2 inhibits Rheb by stimulating GTP hydrolysis of Rheb, which is a direct activator of TORC1. This mechanism plays a key role in mediate growth factor signals to TORC1 activation. In contrast, the Rag GTPases were identified to mediate signals from amino acids to TORC1 activation(Kim and Guan, 2009; Sancak et al., 2008). Rag GTPases differ from other Ras family members in that they have a long C-terminal extension and form a GTPase hetero dimer. They also lack the C-terminal lipid modification site that is a characteristic feature for many Ras GTPases. Rag GTPase is localized to lysosome via interaction with lysosomal membrane protein p18(Sancak et al., 2010). Rag GTP loading (activation) is stimulated by amino acids. The active RagA/B can directly binds to raptor, which is a key subunit of TORC1. Therefore, in response to amino acid stimulation, Rag recruits TORC1 to lysosome where it presumably is activated by Rheb, which is also resides on lysosome. A major issue in TORC1 regulation, hence TSC research, is how RAG GTPase is regulated. In addition, the in vivo physiological functions of Rag have not been fully understood although in vitro studies suggest that Rag GTPases have critical role in TORC1 activation in response to amino acids.

Body

Amino acids are the most important activator of TORC1 (Wullschleger et al., 2006) (Kim and Guan, 2011). In the absence of amino acids, neither growth factors nor glucose can effectively activate TORC1 (Hara et al., 1998). Studies from our laboratory identified Rag GTPases as key regulators of TORC1 in response to amino acids (Kim et al., 2008). Expression of constitutively active RagA caused TORC1 activation even in the absence of amino acids (Fig. 1A). In contrast, expression of dominant negative RagA blocked mTORC1 activation by amino acids (Fig.1B). These studies have established Rag GTPases as key signaling molecules acting between amino acids and TORC1.

Rag GTPases are unique that they form a hetero dimer (Kim et al., 2008). RagA or RagB forms a hetero dimer with either RagC or RagD. It is the heterodimer that is functional in TORC1 activation. However, overexpression of the RagA or RagB can activate TORC1 though less efficiently. In contrast, overexpression of either RagC or RagD cannot activate TORC1. These results suggest that the two Rag subunits in the heterodimer do not functional equally. The N-terminal region of Rag contains the GTP binding and GTPase domain. To further support the importance of Rag dimer in TORC1 activation, we have mapped that the C-terminal regions of both RagA/B and RagC/D are important for dimmer formation (Fig.2). Without the C-terminal region, the truncated Rag GTPases are not functional in TORC1 activation. These data demonstrate that both the N-terminal GTPase domain and the C-terminal dimerization domain are important for Rag function in vivo.

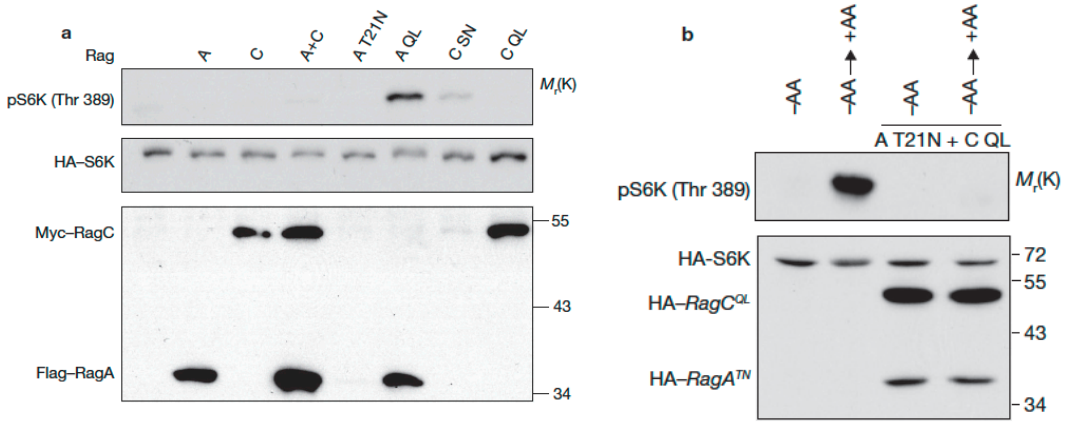

Fig.1. Rag GTPases are involved in TORC1 activation in response to amino acids. **(B)** Constitutively active RagA and RagB stimulate S6K phosphorylation. Mammalian RagA, RagB, RagC, or RagD construct was co-transfected with HA-S6K into HEK293 cells. Their corresponding dominant negative mutants (RagA T21N, RagB T54N, RagC S75N, RagD S76N), and constitutively active mutants (RagA Q66L, RagB Q99L, RagC Q120L, RagD Q121L), were also tested. Phosphorylation and protein levels were determined by immunoblotting with appropriate antibodies, as indicated. Expression of RagA Q66L and RagC S75N (to a less degree) activated TORC1 in the absence of amino acids as indicated by the increased S6K phosphorylation. **(B)** RagA has a dominant role over RagC in regulating S6K phosphorylation. Each indicated Rag constructs were co-transfected with HA-S6K. The different Rag mutants used in the transfection are indicated on the top of each lane. The presence or absence of amino acids (AA) is also indicated. Phosphorylation of S6K was determined.

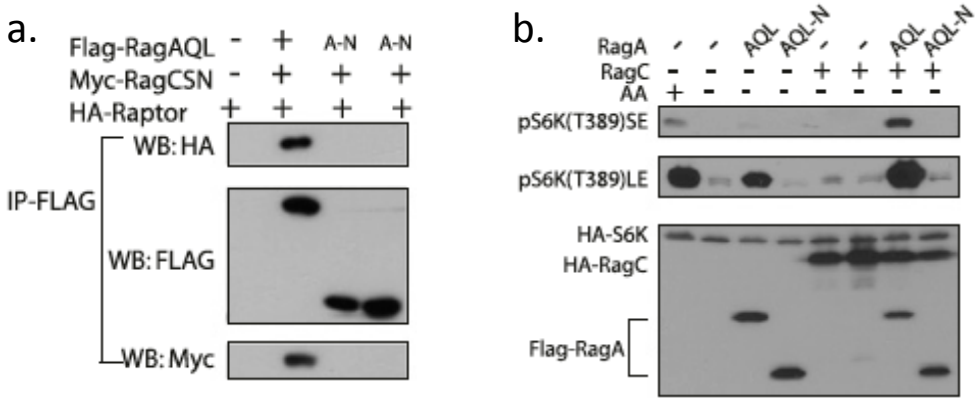

Fig.2. Dimerization is required for RagA/C to activate TORC1. **(A)** The C-terminal domain is required for RagA to interact with raptor. Flag-RagA full length or N-terminal domain (A-N) was

co-transfected with Myc-RagC and HA-Raptor. Cell lysates were precipitated with Flag antibody and the co-immunoprecipitated HA-Raptor was detected by Western blot (top panel). **(B)** The C-terminal domain is required for RagA to stimulate S6K phosphorylation. HA-S6K was co-transfected with full length or N-terminal domain of RagA-QL in the presence or absence of RagC as indicated. The transfected cells were treated with medium with or without amino acids (AA) as indicated. Phosphorylation of S6K was determined to indirectly measure TORC1 activity. SE and LE denote for short exposure and long exposure, respectively.

We investigated the relationship between Rag and Rheb, which is also a Ras family GTPase. Rheb is inactivated by the TSC1/TSC2 GAP activity (Li et al., 2004). Rheb can directly activate TORC1. Dominant negative RagA mutant can block amino acid-induced but not Rheb-induced TORC1 activation, indicating that Rag does not function downstream of Rheb (Fig.3). Given the fact that Rheb can directly bind to and activate TORC1 and RagA can potently bind Raptor, a key subunit of TORC1, our data suggest a model that Rag functions parallel to the TSC-Rheb signaling branch.

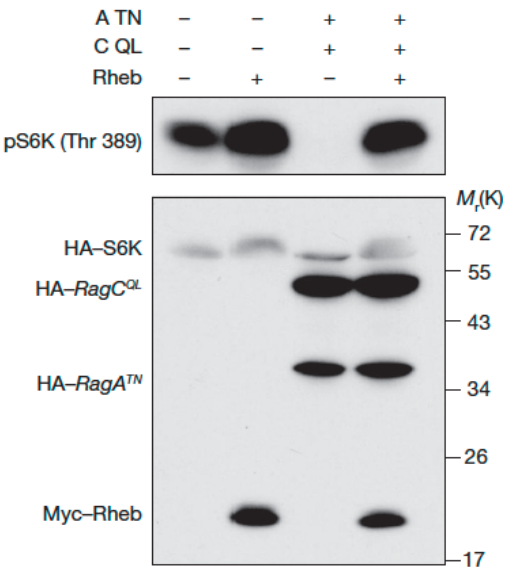

Fig.3. Rag GTPases act parallel to Rheb in TORC1 activation. Dominant negative RagA T21N and RagC Q120L were transfected into HEK293 cells with or without Rheb construct. S6K was included in the co-transfection. Phosphorylation and protein levels of the transfected proteins were determined by immunoblotting with appropriate antibodies, as indicated. Dominant negative RagA does not inhibit TORC1 activation by Rheb.

We performed functional screen to search for novel TORC1 regulators, especially in response to amino acid stimulation. Our RNA interference screen using Drosophila S2 cells has also isolated Rab and Arf as potential regulators of TORC1 (Fig.4) (Li et al.). Both Rab and Arf are Ras family GTPases and have been implicated in intracellular trafficking (Gillingham and Munro, 2007; Zerial and McBride, 2001). Uncontrolled Rab5 and Arf1 potently inhibit TORC1. This inhibitory effect is specific to amino acid stimulation but does not interfere TORC1 activation by glucose. We tested several members of the Rab family and found that expression of constitutively active Rab suppressed TORC1 activity even in the presence of amino acids (Fig. 5A). It is the active Rab5 but not the dominant negative Rab5 that could potently inhibit mTORC1 (Fig. 5B). These observations demonstrate a critical role of intracellular trafficking in amino acid induced TRC1 activation. Our data are consistent with a recent report that amino acid stimulation promotes TORC1 recruitment to lysosomal membrane where TORC1 is activated by Rheb (Sancak et al., 2010).

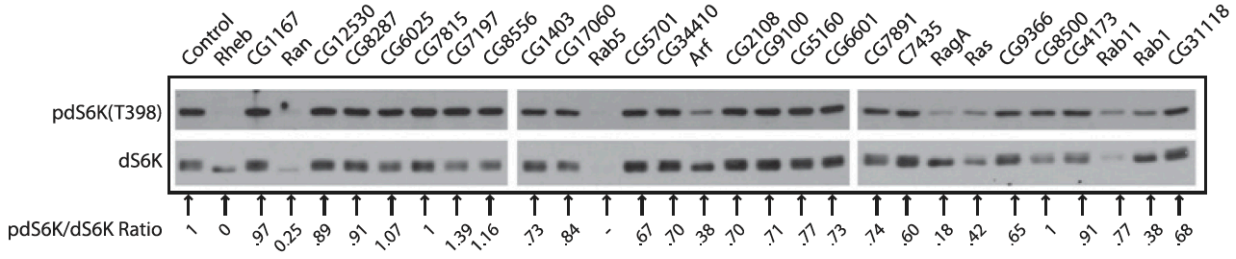

Fig.4. Rab and Arf proteins are involved in regulating TORC1 activity in *Drosophila* S2 cells. *Drosophila* S2 cells untreated (lane 1) or treated with the double stranded RNA against individual genes (as indicated by the Drosophila genome CG numbers) were starved of amino

acids for 1 h followed by amino acid stimulation for 30 min. Phosphorylation and protein levels of dS6K were determined by immunoblotting with the indicated antibodies. Signals detected by anti-pdS6K and anti-dS6K were quantified and the ratio was calculated. An example of the screen results is shown. The control ratio is set to be 1 and all other ratio is the comparison with the control.

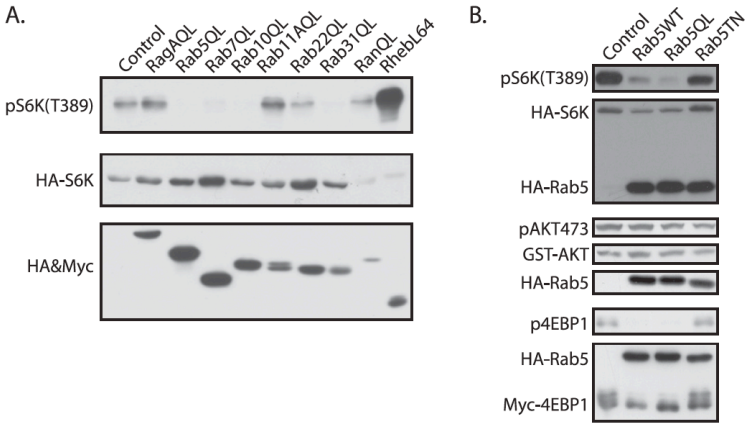

Fig.5. **(A).** Inhibition of TORC1 by various Rab. Constitutively active Rab mutants were co-transfected with HA-S6K into HEK293 cells. Cells were cultured in the presence of amino acids. Phosphorylation of HA-S6K was determined. **(B).** Constitutively active Rab5 but not the dominant negative Rab5 inhibits TORC1. Phosphorylation of S6K and 4EBP1 were used as indicators for TORC1 activity. Rab5 has no effect on ATK phosphorylation, indicating that TORC2 is not inhibited by Rab5.

Amino acids are the most important activator of TORC1 (Kim and Guan, 2011; Wullschleger et al., 2006). In the absence of amino acids, neither growth factors nor glucose can effectively activate TORC1 (Hara et al., 1998). Studies from our laboratory identified Rag GTPases as key regulators of TORC1 in response to amino acids (Kim et al., 2008). Similar observations were also reported by David Sabatini's group (Sancak et al., 2008). Moreover, it has been proposed that Rag functions to recruit mTOR to lysosomes where mTORC1 is activated by the Rheb GTPase (Sancak et al., 2010). The interaction between Rag and mTOR is controlled by amino acids. In contrast, the interaction between Rag and lysosome is not regulated but is medicated by the "regulator" complex (Sancak et al., 2010).

To understand the mechanism of Rag in mTORC1 regulation, we attempted to solve the three dimensional structure of the Rag GTPases, which form a heterodimer in vivo. We succeeded in expression and purification of RagA/C complex. However, they failed to crystalize. We then shifted our attention to the yeast Rag homologs. Activation of mTORC1 by amino acids is highly conserved from yeast to mammalian cells. Gtr1 and Gtr2 are yeast homologs of the mammalian RagA/B and RagC/D, respectively, and they also stimulate TORC1 activation in yeast. We purified Gtr1/Gtr2 protein complex and obtained high quality crystals of Gtr1/Gtr2. The three dimensional structure of the Gtr1p-Gtr2p complex was solved at 2.8 Å resolution (Fig.6A). This is the first GTPase dimer structure ever reported and it reveals a pseudo 2-fold symmetric organization. Structure-guided functional analyses of RagA-RagC, the human homologs of Gtr1p-Gtr2p, show that both G domains and dimerization are important for raptor binding (Fig.7). In particular, the switch regions of the G domain in RagA are indispensible for interaction with raptor and hence TORC1 activation. Based on mutagenesis and structure-function studies, we have mapped the Rag surface that is important for Raptor interaction and mTORC1 activation (Fig.7). The dimerized C-terminal domains of RagA-RagC display a remarkable structural similarity to MP1/p14 (Fig.6B), which is in a complex with lysosome membrane protein p18, and directly interact with p18, therefore recruiting mTORC1 to the lysosome for activation by Rheb. Our results reveal a structural model for the mechanism of the Rag GTPases in TORC1 activation and amino acid signaling (Gong et al., 2011).

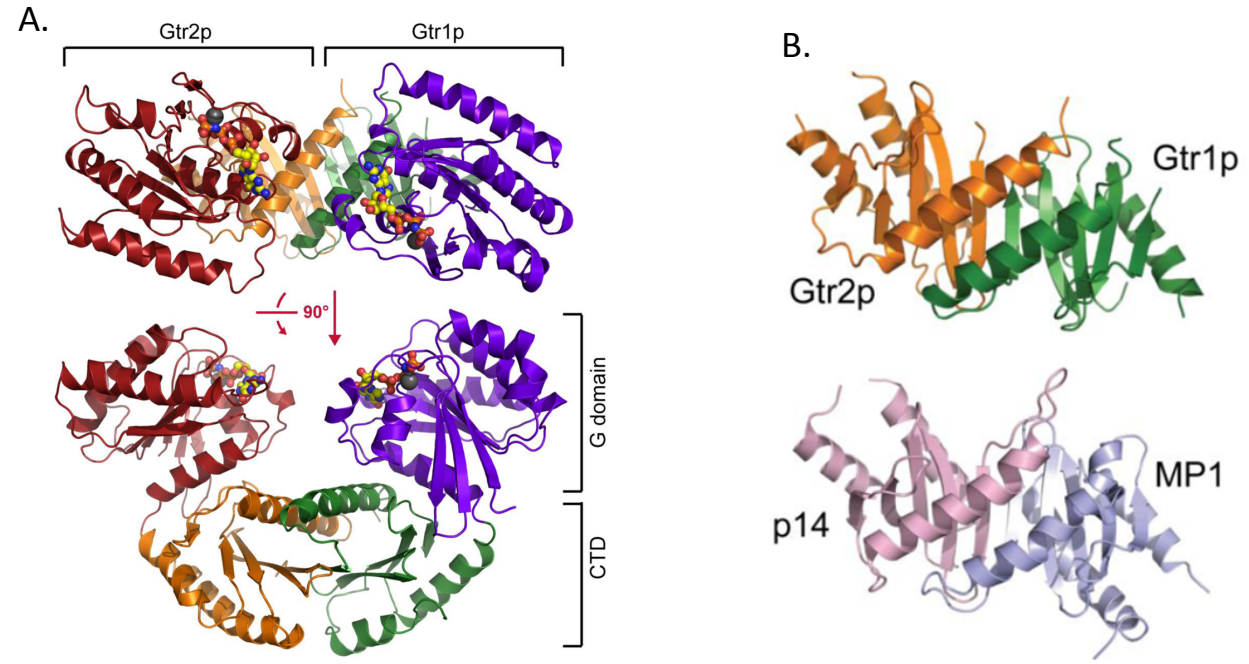

Fig.6. Three dimensional structure of Gtr1/Gtr2 dimer. **(A)** Overall structure of Gtr1p-Gtr2p complex as ribbon representation in two different views. N terminal GTPase domains (G domain) of Gtr1p and Gtr2p bound to GMPPNP are colored in blue and red, and C terminal domains (CTD) are colored in green and orange, respectively. GMPPNP is shown as stick representation and magnesium atoms are shown as black ball. **(B)** Structure comparison of Gtr1p-Gtr2p CTDs and p14/MP1 complex. The structures are shown in ribbon representation and Gtr1p, Gtr2p CTDs are colored green and orange, respectively while p14 and MP1 are colored pink and light blue, respectively. P14/MP1 are critical in recruiting Rag GTPases to lysosome. P14/MP1 show high three-dimensional structure similarity with the CTD of Gtr1/Gtr2 although there is no primary amino acid sequence similarity between P14/MP1 and the CTD of Gtr1/2.

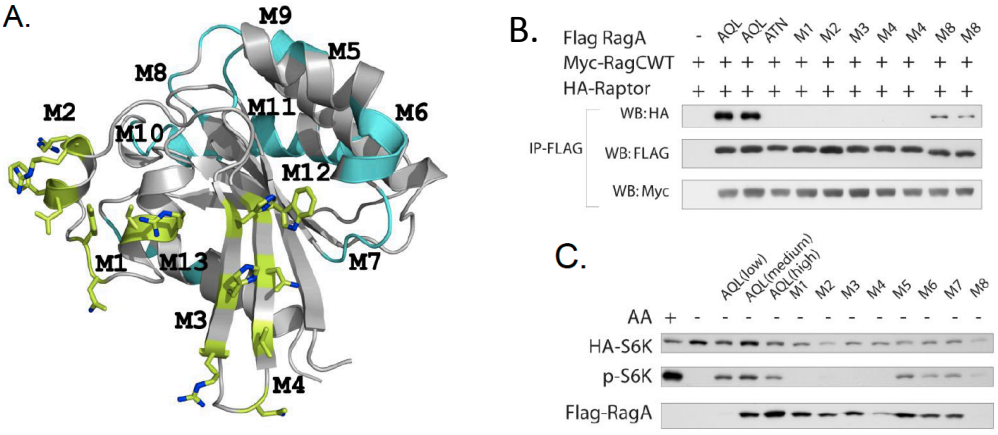

Fig.7 Mapping the raptor interaction surface on RagA that is important for mTORC1 activation. **(A)** G domain of Gtr1p is shown in ribbon representation. Corresponding residues involved in composite RagA mutations (M1-M4) are indicated with stick representation and colored in green and residues mutated in M5-M13 are colored in cyan. All mutants were generated based on RagAQL(RagA^{GTP}). **(B)** The regions close to switch I and II in RagA G domain are important for raptor interaction. Interaction between raptor and co-transfected RagA mutants was examined by co-immunoprecipitation. IP and WB denote immunoprecipitation and Western blotting, respectively. **(C)** The raptor interaction defective RagA mutants cannot activate TORC1. RagA

mutants were co-transfected with HA–S6K into HEK293 cells and phosphorylation of HA-S6K in the absence of amino acids (indicating the activity of RagA) was determined.

Works from our lab and others have demonstrated that Rag GTPases play a major role in mTORC1 activation in response to amino acid signals (Kim et al., 2008; Sancak et al., 2008). Rag A/B are capable of binding raptor, which is a key subunit in mTORC1, only when they are in the active GTP-bound form. Amino acids stimulate GTP loading of RagA/B. Therefore, GTP loading, hence activation, of Rag A/B is the key event in mTORC1 activation by amino acids. Recent genetic studies in yeast have suggested that VAM6 may play a role in Grt1 activation (Binda et al., 2009). VAM6 is conserved in mammalian cells. We made efforts to investigate whether Rag may be regulated by VAM6. We observed that VAM6 could be co-immunoprecipitated with Rag GTPases (Fig.8A). We found that the C-terminal region of VAM6 is responsible for a direct interaction with RagA by an in vitro pull-down assay (Fig.8B). Notably, VAM6 appears to preferentially interact with the inactive GDP-bound form of RagA (Fig.8C). These observations are consistent with a possible role of VAM6 as a guanine nucleotide exchange factor (GEF) for Rag GTPases. Future experiments will focus on the establishment of an in vitro nucleotide binding and exchange assay for Rag GTPases and then investigation of the function VAM6 in Rag regulation in response to amino acid stimulation.

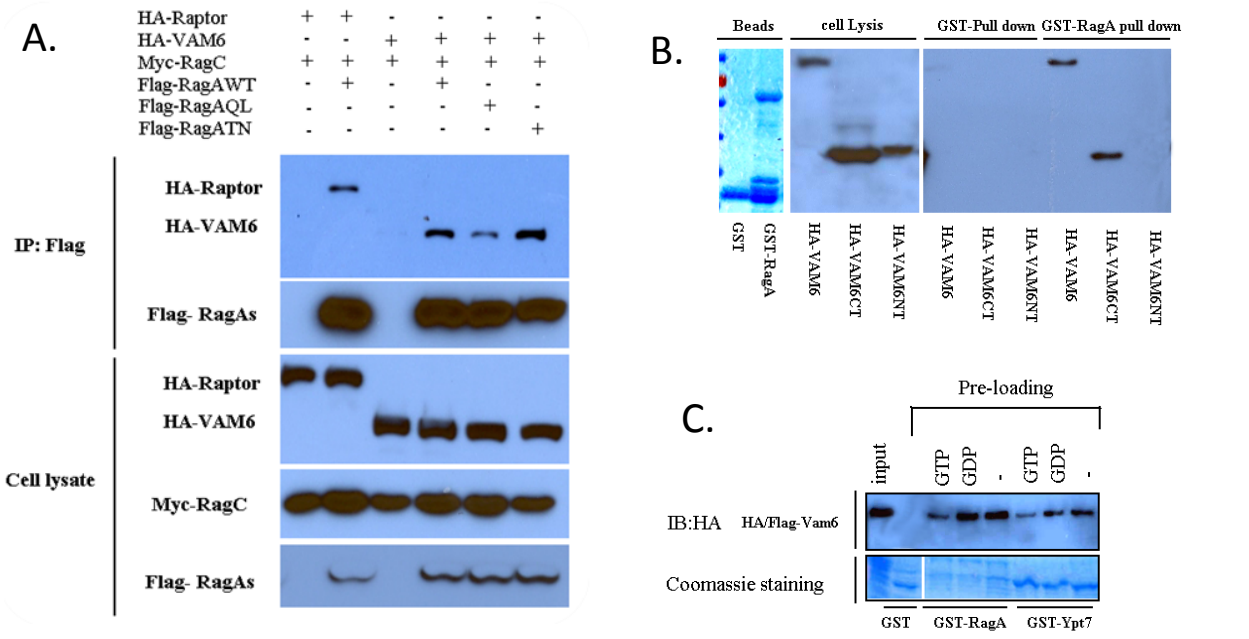

Fig. 8. Vam6 interacts with Rag GTPases. **(A)** Co-immunoprecipitation between VAM6 and Rag A/C. VAM6 was co-transfected with RagC and different mutants of RagA as indicated. Raptor was included as a positive control for RagA/C interaction. Flag-RagA was immunoprecipitated and the co-precipitated HA-Raptor or HA-VAM6 was detected by HA Western blot. Expression levels of transfected proteins in total cell lysates were detected by Western blot. IP denotes immunoprecipitation. **(B)** In vitro pull-down of VAM6 by GST-RagA. Wild type or different deletion constructs of HA-VAM6 were expressed by transfection in HEK293 cells (middle panel). Recombinant GST or GST-RagA was purified from E. coli (left panel). In vitro binding was performed by incubating HA-VAM6 with GST-RagA (right panel). The binding of VAM6 to GST-RagA was detected by Western blot for HA (right panel). GST was included as a negative control. GST-RagA interacted with the full length and the C-terminal domain but not the N-terminal domain of VAM6. **(C)** VAM6 preferentially interacts with GTP-bound RagA. Recombinant GST-RagA was un-treated (indicated by -, which was probably largely in GDP-bound form) or preloaded with GDP or GTP as indicated before it was used for in vitro pull-down assays. Binding of HA-VAM6 to GST-RagA was detected by Western blot

with HA antibody. GST and GST-YPT7 were used as negative and positive control, respectively.

Mutations in the TSC1 or TSC2 tumor suppressors are responsible for TSC disease. A unique feature of the TSC cells is the constitutive activation of mTORC1. We have found that the TSC mutant cells display high basal endoplasmic reticulum (ER) stress (Fig.9A). Moreover, the TSC cells are supersensitive to cellular stress, such as ER stress (Kang et al., 2011). We observed that ER stress inducers could selectively kill TSC cells (Fig.9B). These findings have important therapeutic implication. One may selectively kill TSC cells by ER stress, thus could provide a potential treatment for TSC.

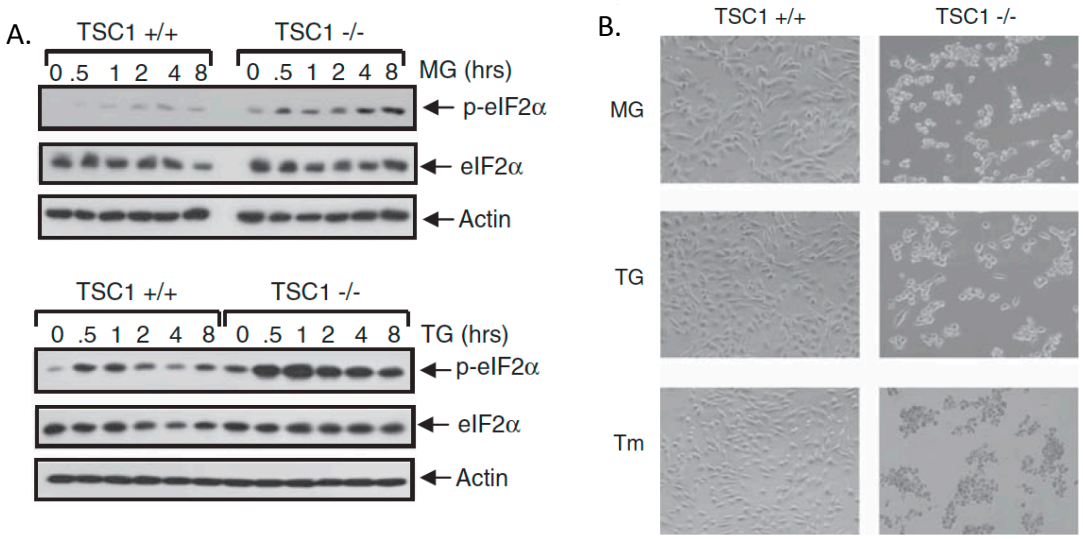

Fig.9. TSC1-/- cells have elevated ER stress response and hypersensitive to ER stress-induced cell death. **(A)** TSC2-/- cells display elevated ER stress response. Wild type and TSC1-/- cells were treated with endoplasmic reticulum (ER) stress agent MG132 (MG) or thapsigargin (TG) for indicated times. ER stress response was detected by the increased phosphorylation of eIF2α. Note that TSC1-/- had a higher basal and increased eIF2α phosphorylation. **(B)** TSC1-/- cells are hypersensitive to ER stress. TSC1+/+ and -/- cells were treated with MG132 (MG), thapsigargin (TG), or tunicamycin (TM) for 18 hours. Cell death was monitored by microscopy.

mTORC1 is activated by growth factors and nutrient sufficiency and is also inhibited by stress conditions. The p38 mitogen-activated protein kinase plays a major role in cellular stress response. We have observed that the p38 regulated/activated kinase (PRAK) contributes to energy starvation-induced mTORC1 inactivation. PRAK phosphorylates Rheb, which is a Ras-related GTPase and a potent direct mTORC1 activator. Phosphorylation of Rheb by PRAK decreases its GTP binding, therefore results in Rheb inactivation. These results reveal a novel mechanism of mTORC1 regulation in response to energy starvation(Zheng et al., 2011).

To understand the physiological functions of Rag in mTORC1 regulation, especially in response to amino acid stimulation, we have generated RagA and RagB double knockout mouse fibroblast cells (Fig.10A). Our initial characterizations showed normal mTORC1 activation by insulin (Fig.10A). However, the RagA/B double knockout cells displayed a slower and weaker response to amino acids (Fig.10B). Surprisingly, the RagA/B double KO cells still retained significant mTORC1 activation by amino acids. These data support a physiological role of RagA/B in amino acid signaling. More importantly, our data indicate that amino acids can activate mTORC1, though compromised, in the absence of Rag GTPases. These observations suggest that a RagA/B independent mechanism in mTORC1 activation by amino acids. We will further investigate the amino acid-induced mTORC1 activating using the knockout cells.

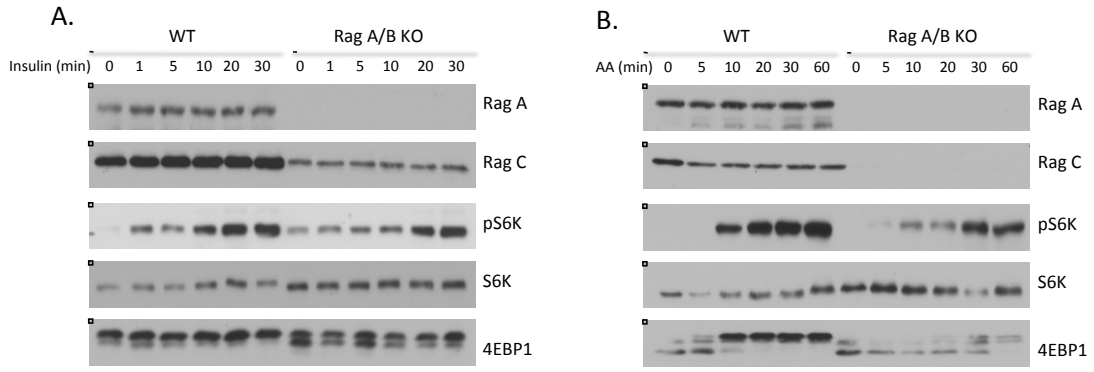

Fig.10. RagA/B double knockout MEFs are partially defective in mTORC1 activation by amino acids. **(A)** Activation of mTORC1 by insulin. Wild type and RagA/B double knockout (KO) MEFs were cultured in serum free medium overnight. Cells were stimulated with insulin for indicated time. Phosphorylation of S6K (pS6K) was determined by immunoblot. RagA protein was detected in the WT but not the KO cells (RagB deletion was verified by genomic PCR, data not shown). In addition, protein level of RagC was also significantly decreased because RagC is stabilized by dimer formation with RagA/B. Phosphorylation of S6K (pS6K) was determined to measure mTORC1 activation. **(B)** Amino acids induce a delayed and weaker mTORC1 activation in RagA/B double knockout MEFs. Cells were cultured in amino acid free medium for two hours before stimulation with amino acids for indicated times. Phosphorylation of S6K was determined by immunoblotting with phosphospecific antibody. Phosphorylation of 4EBP1 could be observed by the alteration of mobility shift. The slower migrating and faster migrating forms represent the phosphorylated and unphosphorylated 4EBP1, respectively. Note, the RagA/B double knockout MEFs display a weaker and slower phosphorylation of both S6K and 4EBP1 in response to amino acid stimulation.

Cells have to respond to a large numbers of signals to regulate cell growth. Signals from different pathways have to be integrated in order for the cell to have a concert response, either to grow or not to grow. cAMP is one of the major intracellular second message in cellular regulation. We have observed that increasing cellular cAMP levels by forskolin, which increases cAMP by stimulating adenyl cyclase, inhibits TORC1, as indicated by the decreased phosphorylation of S6K and 4EBP1 (Fig.11). Consistent with the increase of cellular cAMP, forskolin also increased the phosphorylation of Creb, which is a physiological substrate of protein kinase A. Forskolin treatment caused a dose and time dependent inhibition of TORC1. In most cell types, cAMP has growth inhibitory effects. Our data indicate that inhibition of TORC1 by cAMP may contribute to its cell growth inhibitory effect.

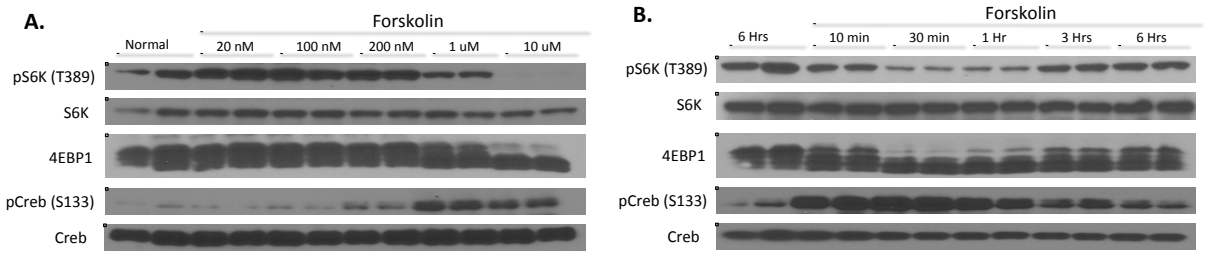

Fig.11. Forskolin inhibits TORC1. **A.** Forskolin decreases the phosphorylation of S6K and 4EBP1 in a dose dependent manner. HEK293 cells were treated with different concentrations of forskolin (from 20nM to 10uM) for one hour. Total cell lysates were probed with various antibodies as indicated. As expected, forskolin increased Creb phosphorylation (pCreb(S133)). **B.** A time course of TORC1 inhibition by forskolin.

We also examined the effect of forskolin on amino acid stimulation. Forskolin was particularly potent in blocking TORC1 activation by amino acids (Fig. 12A). In fact, forskolin completely blocked S6K phosphorylation upon amino acid re-addition. We have further tested the functional role of protein kinase A (PKA), which is directly activated by cAMP, in TORC1 regulation. H89 is a potent PKA inhibitor. We found that H89 strongly suppressed the inhibitory effect of forskolin on S6K phosphorylation (Fig. 12B). Consistent with PKA inhibition, H89 inhibited Creb phosphorylation by forskolin. These observations indicate that cAMP acts through PKA to inhibit TORC1, possibly by blocking amino acid signaling. Future studies are needed to demonstrate the molecular mechanism of TORC1 inhibition by cAMP and PKA.

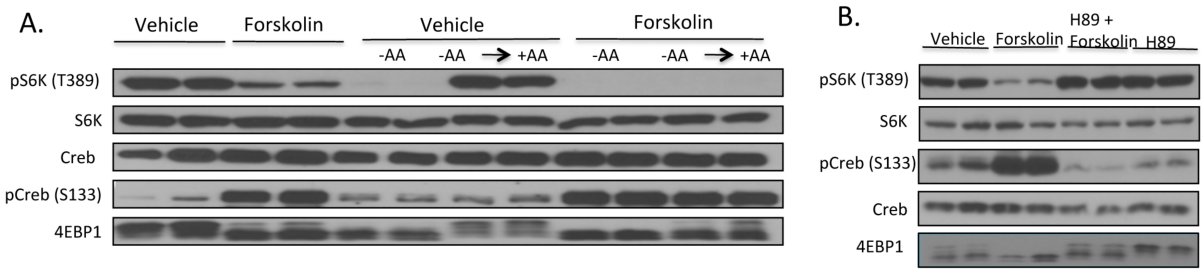

Fig. 12. A. Forskolin blocked amino acid-induced TORC1 activation. Experiments are similar to figure 11. **B.** Inhibition of PKA by H89 blocks the effect of forskolin on S6K phosphorylation.

Key Research Accomplishments

The research accomplishments in the last three years are

1. We have identified the switch I as the effector domain important for Raptor binding and TORC1 activation.
2. We have mapped the C-terminal region of RagA and RagC as important for GTPase dimerization and TORC1 activation.
3. We showed that amino acid-stimulated TORC1 activation is completely blocked by dominant negative RagA mutant, suggesting an essential role of Rag in amino acid signaling.
4. We observed that Rag acts parallel to TSC-Rheb in TORC regulation. In the absence of Rheb, Rag GTPases cannot activate TORC1.
5. We discovered that the Rab family GTPases are also involved in TORC1 regulation in response to amino acid stimulation, indicating a role of intracellular trafficking in amino acid-induced TORC1 activation.
6. We have solved the three dimensional structure3 of Gtr1-Gtr2 complex, which are the yeast homologs of the mammalian RagA/B-RagC/D.
7. We have mapped the domain in RagA-RagC complex responsible for interaction with Raptor.
8. We showed a novel mechanism of Rheb, which is a key activator of mTOR, regulation by phosphorylation.

9. We demonstrated that TSC1 or TSC2 mutant cells are supersensitive to stress, especially ER stress.
10. We have expressed VAM6 and shown a physical interaction between VAM6 and RagA. We have generated reagents to test if RagA can be activated by VAM6.
11. We have shown that RagA and RagB are important for TORC1 activation by amino acids using the RagA/B double knockout cells.
12. We demonstrated that elevation of cAMP by forskolin inhibits TORC1.
13. Our data show that PKA mediates the cAMP effect to inhibit TORC1, particularly in amino acid response.

Reportable Outcomes

Papers published on this project.

Kim, E., Goraksha, P., Li, L., Neufeld, T.P., and Guan, K-L. (2008) Regulation of TORC1 by Rag GTPases in nutrient response. Nature Cell Biol. 10, 935-945.

Kim, E. and Guan, K-L. (2009) RAG GTPases in Nutrient-mediated TOR Signaling Pathway. Cell Cycle 8, 1014-1018.

Li, L. and Guan, K-L. (2009) Amino acid signaling to TOR activation: Vam6 functioning as a Gtr1 GEF. Mol. Cell 35, 543-545.

Li, L., Kim, E., Yuan, H., Inoki, K., Goraksha-Hicks, Schiesher, R. L., Neufeld, T.P., Guan, K-L., (2010) Regulation of mTORC1 by the Rab and ARF GTPases. J. Biol. Chem. 285, 19705-9.

Gong, R., Li., L., Liu, Y., Wang, P., Yang, H., Wang, L., Cheng, J., Guan, K-L., and Xu, Y. (2011) Crystal Structure of Gtr1p-Gtr2p complex reveals new insights into the amino acid-induced TORC1 activation. Genes & Dev. 25, 1668-73.

Kang, Y.J., Lu, M-K., and Guan, K-L. (2011) The TSC1 and TSC2 tumor suppressors are required for proper ER stress response and protect cells from ER stress-induced apoptosis. Cell Death & Differentiation. 18, 133-44.

Kim, J. and Guan, K-L. (2011) Amino acid signaling in mTOR activation. Ann. Rev. Biochem. 80, 1001-32.

Zheng, M, Wang, Y.H, Wu, X.N, Wu, S.Q, Lu, B.J, Dong, M.Q, Zhang, H, Sun, P, Lin, S.C, Guan, K-L, and Han. J. (2011). Inactivation of Rheb by PRAK-mediated phosphorylation is essential for energy-depletion-induced suppression of mTORC1. Nature Cell Biol. 13, 263-272.

Inoki, K. Kim, J., and Guan, K-L. (2011) AMPK and mTOR in cellular energy homeostasis and drug targets. Ann. Rev. Pharmacol. Toxicol. 52, 381-400.

Conclusion

During the past three years, we have made great progresses on this project and have satisfactorily addressed the major questions. We have established that Rag GTPases as key signaling mediators between amino acids and TORC1. This conclusion is supported by both the cell biology study of overexpression, knockdown, and most importantly using RagA/B double knockout cells. The Rag GTPases form a herterodimer to stimulate TORC1 activation by directly binding to raptor. Rag acts in a pathway parallel to TSC-Rheb upstream of TORC1. In addition, we have identified the Rab and Arf GTPases as important regulators of TORC1, especially in response to amino acid stimulation. These observations suggest an important role of intracellular trafficking in TORC1 activation by amino acids. We have also resolved the three

dimensional structure of Gtr1-Gtr2 complex, which are the yeast homologs of the mammalian Rag GTPases. This is the first GTPase dimmer structure ever to be solved. Our structure provides key molecular insights into the mechanism of Rag GTPase interaction with raptor and the "regulators", which consists of MP1/P14/P18 complex. Remarkably, the C-terminal diner structure of Gtr1-Gtr2 is highly similar to the structure of P14/MP1 dimmer although there is not primarily sequence homology between Gtr and P14/MP1. Our study also reveals the molecular basis how Rag is recruited to the lysosomes by "regulators". Our data have shown an important crosstalk between the mTOR pathway and the cAMP-PKA singling. Cellular cAMP and its effector PKA can inhibit TORC1. This PKA-mediated TORC1 inhibition may explain the growth inhibitory role of PKA under most physiological conditions.

References

Appendices

PDF files of the four papers are attached.

Binda, M., Peli-Gulli, M.P., Bonfils, G., Panchaud, N., Urban, J., Sturgill, T.W., Loewith, R., and De Virgilio, C. (2009). The Vam6 GEF controls TORC1 by activating the EGO complex. Mol Cell *35*, 563-573.

Cheadle, J.P., Reeve, M.P., Sampson, J.R., and Kwiatkowski, D.J. (2000). Molecular genetic advances in tuberous sclerosis. Hum Genet *107*, 97-114.

Gillingham, A.K., and Munro, S. (2007). The small G proteins of the Arf family and their regulators. Annu Rev Cell Dev Biol *23*, 579-611.

Gong, R., Li, L., Liu, Y., Wang, P., Yang, H., Wang, L., Cheng, J., Guan, K.L., and Xu, Y. (2011). Crystal structure of the Gtr1p-Gtr2p complex reveals new insights into the amino acid-induced TORC1 activation. Genes Dev *25*, 1668-1673.

Hara, K., Yonezawa, K., Weng, Q.P., Kozlowski, M.T., Belham, C., and Avruch, J. (1998). Amino acid sufficiency and mTOR regulate p70 S6 kinase and eIF-4E BP1 through a common effector mechanism. J Biol Chem *273*, 14484-14494.

Inoki, K., Li, Y., Xu, T., and Guan, K.L. (2003). Rheb GTPase is a direct target of TSC2 GAP activity and regulates mTOR signaling. Genes Dev *17*, 1829-1834.

Inoki, K., Li, Y., Zhu, T., Wu, J., and Guan, K.L. (2002). TSC2 is phosphorylated and inhibited by Akt and suppresses mTOR signalling. Nat Cell Biol *4*, 648-657.

Kang, Y.J., Lu, M.K., and Guan, K.L. (2011). The TSC1 and TSC2 tumor suppressors are required for proper ER stress response and protect cells from ER stress-induced apoptosis. Cell Death Differ *18*, 133-144.

Kim, E., Goraksha-Hicks, P., Li, L., Neufeld, T.P., and Guan, K.L. (2008). Regulation of TORC1 by Rag GTPases in nutrient response. Nat Cell Biol *10*, 935-945.

Kim, E., and Guan, K.L. (2009). RAG GTPases in nutrient-mediated TOR signaling pathway. Cell Cycle *8*, 1014-1018.

Kim, J., and Guan, K.L. (2011). Amino acid signaling in TOR activation. Annu Rev Biochem *80*, 1001-1032.

Lee, C.H., Inoki, K., and Guan, K.L. (2007). mTOR pathway as a target in tissue hypertrophy. Annu Rev Pharmacol Toxicol *47*, 443-467.

Li, L., Kim, E., Yuan, H., Inoki, K., Goraksha-Hicks, P., Schiesher, R.L., Neufeld, T.P., and Guan, K.L. Regulation of mTORC1 by the Rab and Arf GTPases. J Biol Chem *285*, 19705-19709.

Li, Y., Corradetti, M.N., Inoki, K., and Guan, K.L. (2004). TSC2: filling the GAP in the mTOR signaling pathway. Trends Biochem Sci *29*, 32-38.
Sancak, Y., Bar-Peled, L., Zoncu, R., Markhard, A.L., Nada, S., and Sabatini, D.M. Ragulator-Rag complex targets mTORC1 to the lysosomal surface and is necessary for its activation by amino acids. Cell *141*, 290-303.
Sancak, Y., Bar-Peled, L., Zoncu, R., Markhard, A.L., Nada, S., and Sabatini, D.M. (2010). Ragulator-Rag complex targets mTORC1 to the lysosomal surface and is necessary for its activation by amino acids. Cell *141*, 290-303.
Sancak, Y., Peterson, T.R., Shaul, Y.D., Lindquist, R.A., Thoreen, C.C., Bar-Peled, L., and Sabatini, D.M. (2008). The Rag GTPases bind raptor and mediate amino acid signaling to mTORC1. Science *320*, 1496-1501.
Wullschleger, S., Loewith, R., and Hall, M.N. (2006). TOR signaling in growth and metabolism. Cell *124*, 471-484.
Zerial, M., and McBride, H. (2001). Rab proteins as membrane organizers. Nat Rev Mol Cell Biol *2*, 107-117.
Zheng, M., Wang, Y.H., Wu, X.N., Wu, S.Q., Lu, B.J., Dong, M.Q., Zhang, H., Sun, P., Lin, S.C., Guan, K.L.*, et al.* (2011). Inactivation of Rheb by PRAK-mediated phosphorylation is essential for energy-depletion-induced suppression of mTORC1. Nat Cell Biol *13*, 263-272.

nature cell biology

Regulation of TORC1 by Rag GTPases in nutrient response

Eunjung Kim[1,3,4], Pankuri Goraksha-Hicks[2,4], Li Li[1], Thomas P. Neufeld[2,5] and Kun-Liang Guan[1,5]

TORC1 (target of rapamycin complex 1) has a crucial role in the regulation of cell growth and size. A wide range of signals, including amino acids, is known to activate TORC1. Here, we report the identification of Rag GTPases as activators of TORC1 in response to amino acid signals. Knockdown of *Rag* gene expression suppressed the stimulatory effect of amino acids on TORC1 in *Drosophila melanogaster* S2 cells. Expression of constitutively active (GTP-bound) Rag in mammalian cells activated TORC1 in the absence of amino acids, whereas expression of dominant-negative Rag blocked the stimulatory effects of amino acids on TORC1. Genetic studies in *Drosophila* also show that Rag GTPases regulate cell growth, autophagy and animal viability during starvation. Our studies establish a function of Rag GTPases in TORC1 activation in response to amino acid signals.

A wide range of signals regulates the activity of TOR (target of rapamycin) in the control of cell growth. TOR exists in two distinct complexes[1,2], TORC1 and TORC2, which share mTOR and mLST8, and each have their unique subunits. Rapamycin directly inhibits TORC1 (ref. 3) but not TORC2 (refs 4–6). TORC1 positively regulates cell growth and size by promoting anabolic processes, such as protein synthesis[1,7], and inhibiting catabolic processes, such as autophagy[8–10]. TORC1 activation causes phosphorylation of the S6-kinase and the translation factor 4EBP1. These proteins mediate TOR-induced translational regulation[11,12] and their phosphorylation has been used to assess TOR activation *in vivo*.

TORC1 is regulated by mitogenic growth factors, cellular energy levels and amino acids[1,2]. The mechanisms involved in TORC1 regulation by growth factors and energy levels have been characterized. For example, growth factors activate TORC1 partly through phosphatidylinositol-3-kinase (PI(3)K), Akt, TSC1/TSC2 and Rheb[13–15], a small GTPase of the Ras family that directly binds to and stimulates TORC1[16–18]. Amino acids are potent activators of TORC1 (ref. 19); however, the mechanism by which they activate TORC1 is largely unknown. Although studies have implicated the VPS34 PI(3)K in the nutrient response[20,21], its precise function in TORC1 activation remains to be established.

Gtr1 and Gtr2 are unique members of the Ras GTPase family in *Saccharomyces cerevisiae*[22], which has a long carboxy-terminal extension that is required for Gtr1/Gtr2 heterodimer formation[23,24]. In *S. cerevisiae*, Gtr1/Gtr2 function in a multifunctional protein complex involved in nuclear transport regulation, intracellular protein trafficking, microautophagy and exit from rapamycin-induced growth arrest[22,24–26]. RagA and RagB are mammalian homologues of Gtr1, and RagC and RagD are corresponding homologues of Gtr2 (refs 27, 28). Although the physiological functions of Rag family GTPases are largely unknown, RagA and RagB can form heterodimers with RagC and RagD[28], and Rag complexes may interact functionally with Ran to modulate nuclear transport[22,29]. Here, we identify Rag GTPases as regulators of TORC1 in cultured mammalian cells and *Drosophila*. Our data indicate that Rag promotes cell growth and inhibits autophagy by activating TORC1 in response to amino acid signals.

RESULTS

dRagA and dRagC are positive regulators of S6K phosphorylation in *Drosophila* S2 cells

As the GTPase family of proteins are involved in almost every aspect of cell signalling, we hypothesized that amino acid signalling to TORC1 may involve a GTPase(s). We performed an RNA interference (RNAi) screen of 132 annotated *Drosophila* GTPases using *Drosophila* S2 cells, looking for GTPases whose silencing prevents amino-acid-induced phosphorylation and mobility shift of dS6K in S2 cells (Fig. 1a). CG11968 and CG8707 were identified as important for dS6K phosphorylation in response to amino acids (Fig. 1a). Sequence comparison analyses showed that CG11968 is most closely homologous to yeast Gtr1 and mammalian RagA and RagB, whereas CG8707 is homologous to yeast Gtr2 and mammalian RagC and RagD. We therefore named them dRagA and dRagC, respectively (Fig. 1a). Consistent with results in yeast and mammalian cells, these proteins were previously found to interact in large-scale two-hybrid screens[30]. Knockdown of many other GTPases, such as Rho family members, had no effect on dS6K phosphorylation (Fig. 1a).

[1]Department of Pharmacology and Moores Cancer Center, University of California San Diego, La Jolla, CA 92093-081, USA. [2]Department of Genetics, Cell Biology and Development, University of Minnesota, Minneapolis, Minnesota 55455, USA. [3]Current address: Department of Food Sciences and Nutrition, Catholic University of Daegu, Gyeongsan, Korea.
[4]These authors contributed equally to this study.
[5]Correspondence should be addressed to K.-L. G. or T.N. (e-mail: kuguan@ucsd.edu; neufe003@umn.edu)

Received 17 April 2008; accepted 19 June 2008; published online 6 July 2008; DOI: 10.1038/ncb1753

[Cell Cycle 8:7, 1014-1018; 1 April 2009]; ©2009 Landes Bioscience

Perspective

RAG GTPases in nutrient-mediated TOR signaling pathway

Eunjung Kim[1] and Kun-Liang Guan[2,*]

[1]Department of Food Sciences and Nutrition; Catholic University of Daegu; Gyeongsan-si, Gyeongbuk, Repulic of Korea; [2]Department of Pharmacology and Moores Cancer Center; University of California San Diego; La Jolla, California USA

Key words: Rag GTPases, amino acid, mTORC1, Rheb, cell growth

Amino acids are key nutrients for protein synthesis and many metabolic processes. There is compelling evidence that amino acids themselves regulate protein synthesis, degradation and cell growth. Mammalian target of rapamycin complex 1 (mTORC1) plays a central role in cellular growth regulation. Amino acids potently activate mTORC1, however, the mechanism of amino acid signaling is largely unknown. Recent studies have identified Rag small GTPases as key components mediating amino acid signals to mTORC1 activation.

A typical notion of the amino acids is that they serve as building blocks for protein synthesis and as precursors of many vital metabolic pathways. Despite this fundamental function as nutrient that make life possible, it has long been thought that amino acids participate in these processes in a passive way. However, accumulating data indicate that amino acids take a rather active role by initiating signal transduction.

The mammalian target of rapamycin (mTOR) is a central player in cell growth regulation. mTOR is a serine/threonine protein kinase and a member of phosphatidylinositol kinase-related kinase (PIKK) family.[1] As suggested by its name, TOR was originally identified as a cellular target of antifungal macrolide rapamycin, which is currently used as a FDA-approved immunosuppressant and anticancer drug.[2] mTOR exists in two distinct complexes, mTORC1 and mTORC2. The two TOR complexes differ in subunit compositions, downstream targets and regulation (reviewed in ref. 3). mTORC1 is a rapamycin-sensitive complex consisting of mTOR, mLST8 (GβL), Raptor and PRAS40 (proline-rich Akt/PKB substrate 40 kDa). Two well known substrates for mTORC1 are S6K1 (p70 ribosomal S6 kinase 1) and 4EBP1 (eukaryotic initiation factor 4E binding protein 1), which are involved in protein synthesis and cell growth.[4,5] In contrast, association of Rictor, Protor (protein observed with Rictor),[6] and Sin1 with mTOR-mLST8 constitute the rapamycin-insensitive mTORC2, which has been implicated in the phosphorylation and regulation of Akt,[7,8] SGK (serum and glucocorticoid-inducible kinase),[9] and PKC.[10,11] This phosphorylation is proposed to play a role in kinase activation, protein maturation and stability. Although both mTORC1 and mTORC2 are activated downstream of the PI3K in response to growth factor stimulation, amino acids potently stimulate mTORC1 but not mTORC2.[12] Collectively, these observations demonstrate the complexity of mTOR biology.

*Correspondence to: Kun-Liang Guan; UCSD; Pharmacology; UCSD Moores Cancer Center; 3855 Health Sciences Dr.; La Jolla, California 92093 USA; Tel.: 858.822.7945; Fax: 858.822.5433; Email: kuguan@ucsd.edu

Submitted: 02/04/09; Accepted: 02/09/09

Previously published online as a *Cell Cycle* E-publication: http://www.landesbioscience.com/journals/cc/article/8124

Amino Acids in mTORC1 Regulation

The activity of mTORC1 is precisely regulated by upstream positive and negative regulators.[5] Rheb (Ras-homolog enriched in brain) directly binds[13] and activates mTOR in vitro and in vivo.[14] Rheb knockdown abolishes S6K1 and 4EBP1 phosphorylation,[15] whereas, overexpression of Rheb stimulates S6K1 and 4EBP1 phosphorylation.[16,17] The TSC (tuberous sclerosis complex) 1 and TSC2 heterodimer has been established as a major negative regulator of mTORC1 in response to a variety of signals including insulin, growth factors and energy status.[18] It has been shown that TSC1/2 act as a GAP (GTPase activating protein) towards Rheb and convert Rheb from GTP-bound active form to GDP-bound inactive form, therefore, suppressing mTORC1 activity.[16,17,19]

TSC1/2, however, is not required for amino acid-mediated mTORC1 regulation[20,21] because amino acid starvation still induces dephosphorylation of S6K1, S6 and 4EBP1 in $TSC2^{-/-}$ MEFs.[20] On the other hand, when Rheb is ectopically expressed, cells are resistant to amino acid withdrawal in terms of S6K1 or 4EBP1 phosphorylation.[13,22,23] Then do amino acids regulate mTOR activity by modulating Rheb-mTOR interaction or Rheb-GTP level? In fact, it has been shown that amino acid withdrawal substantially reduced the interaction between endogenous mTOR with GST-Rheb, whereas, amino acid addition alone to D-PBS was sufficient to fully restore the interaction between GST-Rheb and mTOR.[23] Rheb also interacts with Raptor and mLST8, however, the interaction was not affected by amino acids.[23] Curiously, however, nucleotide binding status of Rheb does not appear to affect Rheb-mTOR interaction in vivo and in vitro. Nucleotide-free Rheb mutants bind to mTOR even stronger than does wild-type Rheb even though mTOR kinase activity was lacking with this mutant.[13] It is also still under debate whether amino acids modulate Rheb-GTP/GDP loading status.[20,21,24]

Therefore it is unclear whether the degree of mTOR-Rheb interaction represents the critical event in mTORC1 activation by amino acids. Further studies are needed to clarify whether amino acids regulate physiological Rheb GTP binding.

Modulation of mTOR-Raptor interaction has also been proposed as a mechanism of amino acid-mediated mTOR signaling.[25] The amount of Raptor co-immunoprecipitated with mTOR was significantly increased in the amino acid starved HEK293T cells whereas Raptor and mTOR co-precipitation was significantly decreased with amino acid stimulation. Interestingly, mTOR kinase activity was inversely correlated with the strength of Raptor binding to mTOR in vitro. On the other hand, insulin stimulation did not affect mTOR-Raptor interaction although it increased S6K1 phosphorylation. Unlike the mTOR-Raptor interaction, the mTOR-mLST8 interaction does not appear to be regulated by amino acids. This suggests that mTOR-Raptor interaction is modulated specifically by amino acids to regulate mTOR kinase activity.

Rag: A New Player in Amino Acid Signaling

How amino acids regulate mTORC1 activity has been a key question in the mTOR field. Recently, both functional screen and biochemical purification studies have discovered that Rag (Ras-related GTPases) GTPases play an important role in amino acid signaling.[26,27] RagA and B genes (97.8% amino acids sequence identity to each other) were originally identified in an effort to isolate novel Ras family members[28] and RagC and D (81.1% sequence identity) were subsequently identified from yeast two-hybrid screening using RagA as a bait.[29] The closest structural RagA/B and RagC/D orthologs are the yeast (*Saccharomyces cerevisiae)* Gtr1 and Gtr2, respectively. Like interaction of yeast Gtr1 and Gtr2, RagA/B bind with RagC/D through C-terminal region and form a heteromeric complex. The interaction appears to be important for the stability of Rag protein as well as for the Rag function since deletion of this mutual interaction domain abolished RagA or RagC function (Kim E and Guan K-L, unpublished data). Interestingly, a combination of GTP-bound form of RagA/Gtr1 and GDP-bound form of RagC/Gtr2 show the highest functionality. However, nucleotide-bound state of RagA/Gtr1 has a dominant role over that of RagC/Gtr2.[26,30] Besides the heteromeric complex formation, considerably bigger size (36 kDa RagA, 50 kDa RagC) than other Ras homologues and lack of lipid modification motifs in C-terminal regions are also distinct features of Rag GTPases from other GTP binding proteins.

The involvement of Rag in amino acid-mediated mTOR signaling was identified in an extensive RNAi screening in which suppression of dRag expression impaired activation of dS6K upon amino acid stimulation in Drosophila S2 cells.[26] In mammalian cells, expression of GDP-bound inactive RagA/B ($RagA^{TN}$/$RagB^{TN}$) inhibited mTORC1 even in the presence of amino acid stimulation whereas GTP-bound active RagA/B ($RagA^{QL}$/$RagB^{QL}$) induced S6K and 4EBP1 phosphorylation in the absence of amino acids. In Drosophila, $dRagA^{QL}$ overexpressing cells showed bigger cell size than neighboring wild type cells and this difference was more prominent in the nutrient starved condition. The function of Rag in amino acid signaling is specific as shown by $RagA^{QL}$/$RagB^{QL}$ could not overcome other mTORC1 inhibitory signals such as osmotic stress. Moreover, expression of $RagA^{TN}$-$RagC^{QL}$ in HeLa cells suppressed insulin-stimulated S6K phosphorylation as amino acid starvation did.

How then Rag mediates amino acid signaling to mTORC1? Rag specifically interacts with Raptor and this interaction is increased upon ectopic expression of $RagB^{QL}$ as observed in amino acid starved cells.[27] In fact, amino acid stimulation increases GTP loading of Rag. However, Rag heterodimer does not appear to directly modulate the kinase activity of mTORC1 in vitro.[27] It rather plays a critical role in mTOR translocation. mTOR translocates from cytoplasm to the peri-nuclear region and forms a large vesicular structure upon amino acid stimulation.[27] Interestingly, in $RagB^{QL}$ expressing cells mTOR was co-stained with Rab7 positive peri-nuclear and vesicular structures containing Rheb in the amino acid deprivation condition. Moreover, when Rag or Raptor expression was genetically knocked-down by RNA interference, amino acid-mediated mTOR translocation was no longer observed. Although there is no direct evidence showing Rag and Raptor translocation upon amino acid level, it is very tempting to speculate that increased interaction of Rag with Raptor upon amino acid stimulation results in mTORC1 localization to proximity with Rheb, which activates mTORC1. However, Rag does not appear to modulate Rheb GTP binding.[26] Increased Drosophila cell size by Rheb overexpression was not diminished by dRagC knockdown. Moreover, decreased cell size of $Rheb^{-/-}$ cells was not compensated by $dRagA^{QL}$ overexpression. Nevertheless, RagC mutation dominantly suppressed the lethality of TSC1 null homozygous mutant animals and $RagA^{QL}$ overexpression compensated TSC1/2 inhibitory signals in HEK293 cells. This suggests that Rag functions independent and in parallel to TSC1/2 and Rheb.

In yeast, Gtr1 and Gtr2 have been shown to play an important role in specific recycling of general amino acid permease, Gap1p, from the late endosome to the plasma membrane.[30] Rag, however, does not appear to regulate mTORC1 by modulating intracellular amino acid concentration in mammalian cells. Amino acid incorporation rate was not affected by stable expression of Rag.[26] Moreover, treatment of protein synthesis inhibitor, cycloheximide, reverses the inhibition of mTORC1 caused by leucine deprivation, but not by $RagB^{TN}$-$RagC^{QL}$ expression.[27] Since $RagA^{QL}$ expression could complement Gtr1 and Gtr2 mutant, it will be of interest to pursuit the question whether mammalian Rag is also involved in amino acid transporter trafficking to the cell membrane as yeast Gtr protein does.

Upon amino acid starvation, cells degrade cellular organelles by autophagy to provide necessary nutrients for cell survival. In yeast, Gtr2 has been shown to function in microautophagy (small vesicle formation and release into the vacuole lumen) and plays an essential role in the resumption of growth after rapamycin removal. $RagA^{QL}$ expression also inhibited starvation-induced autophagy in vitro and in vivo.[26] On the other hand, Drosophila fat body specific expression of $dRagA^{QL}$ significantly decreased survival rate of the animals under starvation condition. This is probably because

constitutive activation of mTORC1 and lack of autophagy by dRagA^{QL} makes the animals more sensitive to nutrient deficiency.

Vps34 and MAP4K3 in Amino Acid Signaling

There have been many indications that wortmannin sensitive, but not Class I PI3K, protein(s) is involved in mTORC1 activation by amino acids. Vps34 was discovered as a responsible protein in amino acid signaling by two independent research groups in 2005.[24,31]

Vps34 (vacuolar protein sorting 34) is a Class III PI3K, which forms an active complex with another protein kinase Vps15[32] and generates PtdIns(3)P (reviewed in refs. 33–35). Vps34 was initially identified as an essential protein in vesicular trafficking,[36,37] and recent studies showed a function of Vps34 in amino acid sensing. In the study of Nobukuni T, et al. hVps34 activity as well as PtdIns(3)P was increased and decreased by amino acid stimulation and deprivation, respectively, in accordance with S6K phosphorylation.[24] Genetic knockdown of hVps34 or overexpression of GFP-FYVE expression vector, which acts as a dominant negative to Vps34 signaling by sequestering PtdIns(3)P, also impaired S6K phosphorylation. These data suggest that class III PI3K, hVps34 mediates amino acid signaling to mTOR whereas class I PI3K mediates insulin signaling to Akt, which in turn phosphorylates TSC2 and modulates mTOR signaling pathway. Interestingly, hVps34 and hVps15 are also co-localized to Rab7-positive late endosome. Taken together, this suggests that the function of Rag, mTOR and hVps34 in amino acid signaling can be interconnected on Rab7 positive endosome membrane.

A mechanism of hVps34 to activate mTORC1 was not known, however, Gulati P, et al. presented intriguing results connecting Ca^{2+}, hVps34 and amino acid signaling.[38] Addition of amino acid evoked a rapid increase in intracellular Ca^{2+} concentration and S6K phosphorylation. In addition, hVps34 activity and PtdIns(3)P production were inhibited by pre-incubation with Ca^{2+} chelator, BAPTA-AM. These results suggest that Vps34 and mTOR is downstream of Ca^{2+}. Although biological meaning has not been described, it has been reported that hVps34 interacts with mTOR. hVps34-mTOR interaction was not changed by either Ca^{2+} or amino acid but calmodulin (CaM)-mTOR interaction was changed in Ca^{2+} and hVps34-dependent manner. This led to a proposed model that amino acid increases Ca^{2+} influx, which increases the interaction of Ca^{2+}/CaM with the hVps34-mTOR signalosome and confers conformational change of the signalosome and consequently activates mTORC1.

A perplexing issue regarding hVps34 in mTORC1 activation is that hVps34 and its product PtdIns(3)P are essential for autophagy in amino acid deprivation condition but mTOR is known to be activated by amino acids and to suppress autophagy. This appears contradictory to hVps34 activation upon amino acid stimulation. However, two elegant studies gave a clue about this question.[39,40] They showed that some, but not all, of mammalian hVps34 is bound to beclin1, the mammalian homologue of Atg6/Vps30p, and that the beclin1-associated hVps34 and the beclin1-free hVps34 appear to be localized to trans-Golgi network and endosome, respectively. This suggests that there are distinct pools of hVps34 in which beclin1-free hVps34 recruits mTOR to endosome and form signalosome upon amino acids stimulation and the other beclin1-hVps34 pool regulates autophagy.

The model of Vps34 in amino acid signaling has recently been challenged by the results showing that the activity of hVps34 is not affected by Ca^{2+} chelators or CaM inhibitors and hVps34 activity is CaM binding independent.[41] More importantly, genetic studies in Drosophila argue against a role of Vps34 in amino acid signaling.[42] Mutation in Drosophila Vps34 showed disrupted autophagosome/autolysosome formation in larval fat body cells and also disrupted endocytosis. However, cell size of the Vps34 mutant or Vps34^{KD} expressing animals were similar to that of wild-type cells. Vps34 mutant had no effect in TSC1 mutant animal viability as well. On the other hand, amino acid starvation or co-expression of TSC1/2 induced autophagy in control animals but not in Vps34 mutant animals. Collectively, these data suggest that Vps34 does not act upstream of TOR. This raises a question on the proposed function of hVps34 in amino acid sensing.

Recent genetic RNAi screening targeting Drosophila protein kinases has also identified that MAP4K3 protein kinase is involved in amino acid signaling.[43] It was shown that amino acids regulate the kinase activity of MAP4K3 from which S6 and 4EBP1 phosphorylation is regulated in a rapamycin sensitive but TSC1/2 independent manner. MAP4K3 overexpression, however, only partially delayed dephosphorylation of S6K upon amino acid withdrawal. It will be interesting to determine the relationship between MAP4K3, Rag GTPases and Vps34.

Future Perspective

Our body responds to amino acid limitation by repressing protein synthesis and activating protein degradation. This phenomenon implicates that our body senses the level of extracellular and intracellular amino acids and regulates protein synthesis/degradation, where mTORC1 has been long believed to play a central role. In fact, dysregulation of mTORC1 signaling pathway is found in many detrimental human diseases including cancer and tissue hypertrophy.[44-46] However, how mTORC1 senses the level of amino acids or conversely how amino acids regulate mTORC1 activity is largely unknown. This seemingly simple question in fact is rather complex. The amino acid sensor(s) has yet to be identified. Does the cell have one sensor detecting all amino acids or does the cell have multiple sensors detecting different amino acids? Regardless of the answer, activation of mTORC1 is apparently a common consequence in response to amino acid sufficiency (Fig. 1).

In this aspect, identification of Rag proteins makes a significant step forward in our understanding of amino acid signaling. The Rag GTPases may indirectly sense intracellular amino acids by changing bound nucleotide and relays signal to mTORC1. Moreover, Rag regulates mTORC1 in parallel to TSC1/2-Rheb axis, which is consistent with previous reports that TSC1/2 is dispensable for amino acid regulation of mTORC1. These findings suggest that Rag can be most appropriately fit into a place for amino acid sensor relaying signal to mTORC1. There are, however, still many remaining questions. How amino acids relay

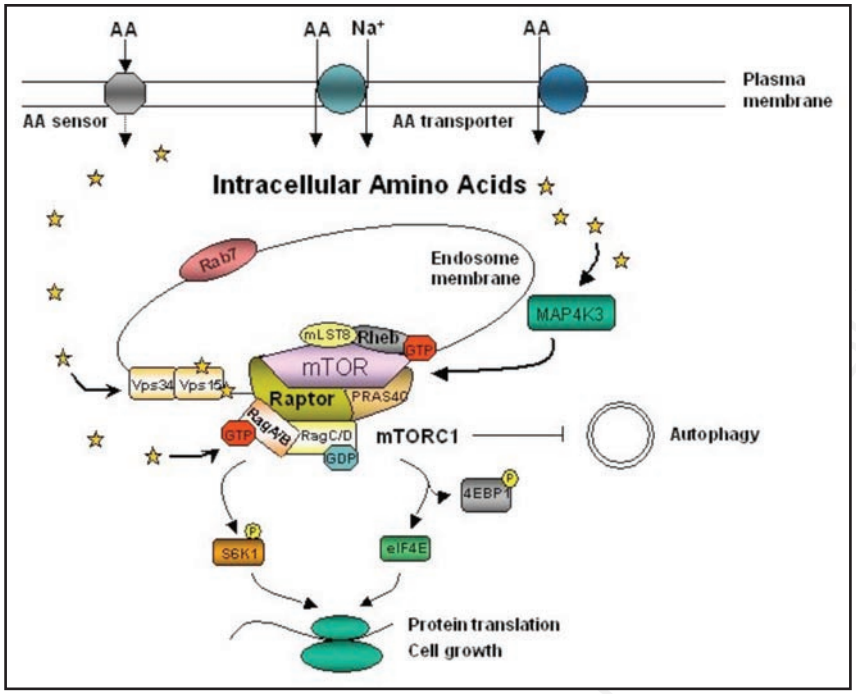

Figure 1. Regulation of mTORC1 by amino acids. Amino acid stimulation increases mTORC1 activity by activating Rag, which binds to Raptor and facilitate the translocation of mTORC1 to Rab7 positive perinuclear endosome membrane. A hVps34/hVps15 complex also localize on the Rab7 positive endosome membrane. Amino acid regulation of mTORC1 activity through MAP4K3 is also shown.

signals to Rag? What is the exact mechanism for Rag to activate mTORC1? Is the biological function of Rag interconnected with that of hVps34 or MAP4K3 in amino acid signaling? Also, identification of Rag regulators, such as GEF and GAP, and elucidation of the mechanism of mTORC1 translocation to Rab7 positive vesicular structures may fill key gaps between amino acids and mTORC1 activation.

Acknowledgements

We appreciate Joungmok Kim and Bin Zhao for their critical reading of the manuscript. This work was supported by the Science Research Center (SRC) program of Korea Science and Engineering Foundation granted to E. Kim (R11-2008-0106) and grants from National Institutes of Health and Department of Defense to K.L.G.

References

1. Schmelzle T, Hall MN. TOR, a central controller of cell growth. Cell 2000; 103:253-62.
2. Abraham RT, Wiederrecht GJ. Immunopharmacology of rapamycin. Annu Rev Immunol 1996; 14:483-510.
3. Yang Q, Guan KL. Expanding mTOR signaling. Cell Res 2007; 17:666-81.
4. Fingar DC, Salama S, Tsou C, Harlow E, Blenis J. Mammalian cell size is controlled by mTOR and its downstream targets S6K1 and 4EBP1/eIF4E. Genes Dev 2002; 16:1472-87.
5. Hay N, Sonenberg N. Upstream and downstream of mTOR. Genes Dev 2004; 18:1926-45.
6. Pearce LR, Huang X, Boudeau J, Pawlowski R, Wullschleger S, Deak M, et al. Identification of Protor as a novel Rictor-binding component of mTOR complex-2. Biochem J 2007; 405:513-22.
7. Jacinto E, Loewith R, Schmidt A, Lin S, Ruegg MA, Hall A, et al. Mammalian TOR complex 2 controls the actin cytoskeleton and is rapamycin insensitive. Nat Cell Biol 2004; 6:1122-8.
8. Loewith R, Jacinto E, Wullschleger S, Lorberg A, Crespo JL, Bonenfant D, et al. Two TOR complexes, only one of which is rapamycin sensitive, have distinct roles in cell growth control. Mol Cell 2002; 10:457-68.
9. Garcia-Martinez JM, Alessi DR. mTOR complex 2 (mTORC2) controls hydrophobic motif phosphorylation and activation of serum- and glucocorticoid-induced protein kinase 1 (SGK1). Biochem J 2008; 416:375-85.
10. Ikenoue T, Inoki K, Yang Q, Zhou X, Guan KL. Essential function of TORC2 in PKC and Akt turn motif phosphorylation, maturation and signalling. EMBO J 2008; 27:1919-31.
11. Facchinetti V, Ouyang W, Wei H, Soto N, Lazorchak A, Gould C, et al. The mammalian target of rapamycin complex 2 controls folding and stability of Akt and protein kinase C. EMBO J 2008; 27:1932-43.
12. Hara K, Yonezawa K, Weng QP, Kozlowski MT, Belham C, Avruch J. Amino acid sufficiency and mTOR regulate p70 S6 kinase and eIF-4E BP1 through a common effector mechanism. J Biol Chem 1998; 273:14484-94.
13. Long X, Lin Y, Ortiz-Vega S, Yonezawa K, Avruch J. Rheb binds and regulates the mTOR kinase. Curr Biol 2005; 15:702-13.
14. Sancak Y, Thoreen CC, Peterson TR, Lindquist RA, Kang SA, Spooner E, et al. PRAS40 is an insulin-regulated inhibitor of the mTORC1 protein kinase. Mol Cell 2007; 25:903-15.
15. Zhang Y, Gao X, Saucedo LJ, Ru B, Edgar BA, Pan D. Rheb is a direct target of the tuberous sclerosis tumour suppressor proteins. Nat Cell Biol 2003; 5:578-81.
16. Inoki K, Li Y, Xu T, Guan KL. Rheb GTPase is a direct target of TSC2 GAP activity and regulates mTOR signaling. Genes Dev 2003; 17:1829-34.
17. Tee AR, Manning BD, Roux PP, Cantley LC, Blenis J. Tuberous sclerosis complex gene products, Tuberin and Hamartin, control mTOR signaling by acting as a GTPase-activating protein complex toward Rheb. Curr Biol 2003; 13:1259-68.
18. Inoki K, Ouyang H, Li Y, Guan KL. Signaling by target of rapamycin proteins in cell growth control. Microbiol Mol Biol Rev 2005; 69:79-100.
19. Garami A, Zwartkruis FJ, Nobukuni T, Joaquin M, Roccio M, Stocker H, et al. Insulin activation of Rheb, a mediator of mTOR/S6K/4E-BP signaling, is inhibited by TSC1 and 2. Mol Cell 2003; 11:1457-66.
20. Smith EM, Finn SG, Tee AR, Browne GJ, Proud CG. The tuberous sclerosis protein TSC2 is not required for the regulation of the mammalian target of rapamycin by amino acids and certain cellular stresses. J Biol Chem 2005; 280:18717-27.
21. Roccio M, Bos JL, Zwartkruis FJ. Regulation of the small GTPase Rheb by amino acids. Oncogene 2006; 25:657-64.
22. Saucedo LJ, Gao X, Chiarelli DA, Li L, Pan D, Edgar BA. Rheb promotes cell growth as a component of the insulin/TOR signalling network. Nat Cell Biol 2003; 5:566-71.
23. Long X, Ortiz-Vega S, Lin Y, Avruch J. Rheb binding to mammalian target of rapamycin (mTOR) is regulated by amino acid sufficiency. J Biol Chem 2005; 280:23433-6.
24. Nobukuni T, Joaquin M, Roccio M, Dann SG, Kim SY, Gulati P, et al. Amino acids mediate mTOR/raptor signaling through activation of class 3 phosphatidylinositol 3OH-kinase. Proc Natl Acad Sci USA 2005; 102:14238-43.

25. Kim DH, Sarbassov DD, Ali SM, King JE, Latek RR, Erdjument-Bromage H, et al. mTOR interacts with raptor to form a nutrient-sensitive complex that signals to the cell growth machinery. Cell 2002; 110:163-75.
26. Kim E, Goraksha-Hicks P, Li L, Neufeld TP, Guan KL. Regulation of TORC1 by Rag GTPases in nutrient response. Nat Cell Biol 2008; 10:935-45.
27. Sancak Y, Peterson TR, Shaul YD, Lindquist RA, Thoreen CC, Bar-Peled L, et al. The Rag GTPases bind raptor and mediate amino acid signaling to mTORC1. Science 2008; 320:1496-501.
28. Schurmann A, Brauers A, Massmann S, Becker W, Joost HG. Cloning of a novel family of mammalian GTP-binding proteins (RagA, RagBs, RagB1) with remote similarity to the Ras-related GTPases. J Biol Chem 1995; 270:28982-8.
29. Sekiguchi T, Hirose E, Nakashima N, Ii M, Nishimoto T. Novel G proteins, Rag C and Rag D, interact with GTP-binding proteins, Rag A and Rag B. J Biol Chem 2001; 276:7246-57.
30. Gao M, Kaiser CA. A conserved GTPase-containing complex is required for intracellular sorting of the general amino-acid permease in yeast. Nat Cell Biol 2006; 8:657-67.
31. Byfield MP, Murray JT, Backer JM. hVps34 is a nutrient-regulated lipid kinase required for activation of p70 S6 kinase. J Biol Chem 2005; 280:33076-82.
32. Volinia S, Dhand R, Vanhaesebroeck B, MacDougall LK, Stein R, Zvelebil MJ, et al. A human phosphatidylinositol 3-kinase complex related to the yeast Vps34p-Vps15p protein sorting system. EMBO J 1995; 14:3339-48.
33. Nobukuni T, Kozma SC, Thomas G. hvps34, an ancient player, enters a growing game: mTOR Complex1/S6K1 signaling. Curr Opin Cell Biol 2007; 19:135-41.
34. Yan Y, Backer JM. Regulation of class III (Vps34) PI3Ks. Biochem Soc Trans 2007; 35:239-41.
35. Backer JM. The regulation and function of Class III PI3Ks: novel roles for Vps34. Biochem J 2008; 410:1-17.
36. Odorizzi G, Babst M, Emr SD. Phosphoinositide signaling and the regulation of membrane trafficking in yeast. Trends Biochem Sci 2000; 25:229-35.
37. Lindmo K, Stenmark H. Regulation of membrane traffic by phosphoinositide 3-kinases. J Cell Sci 2006; 119:605-14.
38. Gulati P, Gaspers LD, Dann SG, Joaquin M, Nobukuni T, Natt F, et al. Amino acids activate mTOR complex 1 via Ca^{2+}/CaM signaling to hVps34. Cell Metab 2008; 7:456-65.
39. Kihara A, Kabeya Y, Ohsumi Y, Yoshimori T. Beclin-phosphatidylinositol 3-kinase complex functions at the trans-Golgi network. EMBO Rep 2001; 2:330-5.
40. Kihara A, Noda T, Ishihara N, Ohsumi Y. Two distinct Vps34 phosphatidylinositol 3-kinase complexes function in autophagy and carboxypeptidase Y sorting in *Saccharomyces cerevisiae*. J Cell Biol 2001; 152:519-30.
41. Yan Y, Flinn RJ, Wu H, Schnur RS, Backer JM. hVps15, but not Ca(2+)/CaM, is required for the activity and regulation of hVps34 in mammalian cells. Biochem J 2009; 417:747-55.
42. Juhasz G, Hill JH, Yan Y, Sass M, Baehrecke EH, Backer JM, et al. The class III PI(3)K Vps34 promotes autophagy and endocytosis but not TOR signaling in Drosophila. J Cell Biol 2008; 181:655-66.
43. Findlay GM, Yan L, Procter J, Mieulet V, Lamb RF. A MAP4 kinase related to Ste20 is a nutrient-sensitive regulator of mTOR signalling. Biochem J 2007; 403:13-20.
44. Lee CH, Inoki K, Guan KL. mTOR pathway as a target in tissue hypertrophy. Annu Rev Pharmacol Toxicol 2007; 47:443-67.
45. Inoki K, Corradetti MN, Guan KL. Dysregulation of the TSC-mTOR pathway in human disease. Nat Genet 2005; 37:19-24.
46. Guertin DA, Sabatini DM. Defining the role of mTOR in cancer. Cancer Cell 2007; 12:9-22.

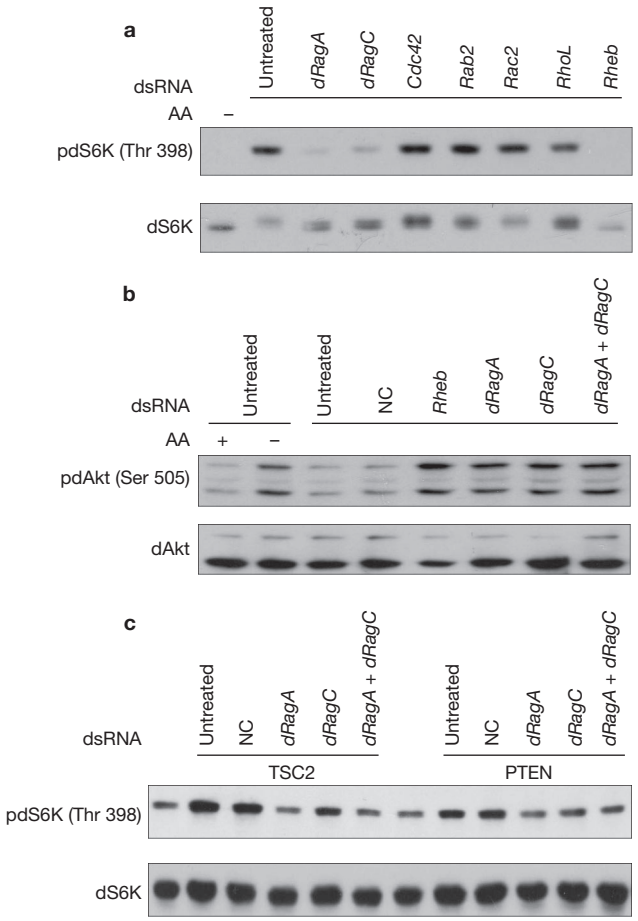

Figure 1 dRagA and dRagC are activators of TORC1 in *Drosophila* S2 cells. (**a**) Knockdown of *dRagA* and *dRagC* decreased dS6K phosphorylation (Thr 398). *Drosophila* S2 cells untreated (lane 2) or treated with the indicated RNAi were starved of amino acids for 1 h followed by amino acid stimulation for 30 min Phosphorylation and protein levels of dS6K were determined by immunoblotting with the indicated antibodies. (**b**) dRagA and dRagC are not required for dAkt phosphorylation. *Drosophila* S2 cells untreated (lanes 1–3) or treated with the indicated RNAi were starved of amino acids for 1 h and stimulated with amino acids for 30 min. Phosphorylation and protein levels of dAkt were determined by immunoblotting with appropriate antibodies as indicated. NC, negative control RNAi. (**c**) dRagA and dRagC function in parallel with TSC2 and PTEN. *dRagA* and/or *dRagC* RNAi was added to S2 cells in combination with *dTSC2* or *dPTEN* RNAi, as indicated. *dTSC2* or *dPTEN* RNAi treatment increased pdS6K (Thr 398) and this increase was compromised by *dRagA* or/and *dRagC* RNAi. Full scans of blots are provided in Supplementary Information, Fig. S6.

Rheb was also isolated in our screen. It is worth noting that *Rheb* knockdown reproducibly caused a stronger inhibition of S6K phosphorylation, compared with *dRagA* and *dRagC* knockdown (Fig. 1a), consistent with the notion that Rheb is a direct activator of TORC1 (refs 17, 18). Knockdown of several other GTPases, such as *Rab5* and *Ran*, also decreased dS6K phosphorylation. However, knockdown of *Rab5* and *Ran* also caused a significant decrease in cell numbers (data not shown), indicating a general effect of these GTPases on cell proliferation/apoptosis. Therefore, we focused on the Rag GTPases.

Amino acids are known to stimulate TORC1 but not TORC2 (ref. 2). Indeed, amino acid starvation indirectly elevates TORC2 activity as inactivation of S6K by amino acid starvation removes the feedback inhibition on TORC2 (refs 31, 32; Fig. 1b). We tested the effect of dRag on dAkt phosphorylation, a TORC2 substrate. Knockdown of *dRagA* or *dRagC* caused a significant increase in dAkt phosphorylation (Fig. 1b), which is consistent with the notion that dRagA and dRagC have a positive role in TORC1, but not TORC2, activation.

To determine the functional relationship between dRag and the components of the TOR signalling pathway, we performed knockdown of *dTSC2* and *dPTEN*, two negative regulators of dTOR, in combination with *dRag*. As expected, *dTSC2* knockdown increased dS6K phosphorylation (Fig. 1c); however, knockdown of either *dRagA* or *dRagC* compromised this effect of *dTSC2* knockdown (Fig. 1c). Notably, knockdown of *dRagA* or *dRagC* did not decrease dS6K phosphorylation below the basal level when *dTSC2* was also knocked down. In contrast, *dRheb* knockdown eliminated dS6K phosphorylation even when *dTSC2* was knocked down (data not shown). Similar results were observed for dRag and dPTEN (Fig. 1c). These data suggest that RagA and RagC may function in parallel with PTEN and TSC2 to activate TORC1.

Rag GTPases regulate mammalian TORC1

We next examined the function of Rag GTPases in the regulation of mammalian TORC1 in cultured cells. Human *RagA* shares over 90% sequence identity with RagB but only 25% sequence identity with *RagC* and *RagD*, whereas *RagC* shares 87% sequence identity with *RagD*[28]. Wild-type as well as constitutively active and dominant-negative mutants of human *RagA*, *B*, *C* and *D* were constructed. *In vivo* labelling of *RagA* showed that both wild-type and $RagA^{Q66L}$ contained high levels of GTP, whereas $RagA^{T21N}$ bound little nucleotide (Supplementary Information, Fig. S1). We found that expression of Rag, especially the constitutively active $RagA^{Q66L}$ and $RagB^{Q99L}$, increased phosphorylation of co-transfected HA–S6K (Fig. 2a). In contrast, expression of dominant-negative $RagA^{T21N}$ and $RagB^{T54N}$ decreased S6K phosphorylation. The effect of dominant-negative *RagA* and *RagB* expression on S6K was also shown by an increase in S6K mobility (Fig. 2a). On the other hand, expression of constitutively active and dominant-negative *RagC* or *RagD* had only a minor effect on S6K phosphorylation (Fig. 2a). Surprisingly, the dominant-negative mutants $RagC^{S75N}$ and $RagD^{S76N}$ decreased S6K mobility (Fig. 2a), indicating a possible increase in phosphorylation (see results later).

We confirmed that there is a physical interaction between *RagA* and *RagC* (data not shown) and further investigated the relationship between *RagA* and *RagC* in S6K phosphorylation. $RagA^{T21N}$ dominantly inhibited S6K phosphorylation regardless of the nucleotide-binding status of the co-expressed *RagC* (Fig. 2b). Moreover, $RagA^{Q66L}$ dominantly activated S6K phosphorylation regardless of the nucleotide-binding status of the co-transfected *RagC*. Notably, $RagA^{T21N}$ and $RagC^{S75N}$ were poorly expressed when they were transfected alone. However, when they were co-transfected with either wild-type or mutant versions of *RagC* or *RagA*, the expression levels were markedly increased (Fig. 2b), suggesting that dimer formation stabilizes the dominant-negative mutants of *RagA* and *RagC*, which are unstable.

To further examine the role of Rag GTPases in mTORC1 regulation, we determined the phosphorylation status of the S6K site Thr 421/Ser 424, which is not directly phosphorylated by mTORC1, and 4EBP1, another direct substrate of mTORC1. $RagA^{T21N}$ did not decrease S6K Thr 421/Ser 424 phosphorylation as much as Thr 389. In contrast, $RagA^{T21N}$ completely blocked 4EBP1 phosphorylation (S65) and also caused a dramatic mobility shift of the co-transfected 4EBP1 (Fig. 2c). On the other hand, Rag had little effect on Akt (Ser 473) phosphorylation, a TORC2 substrate[33].

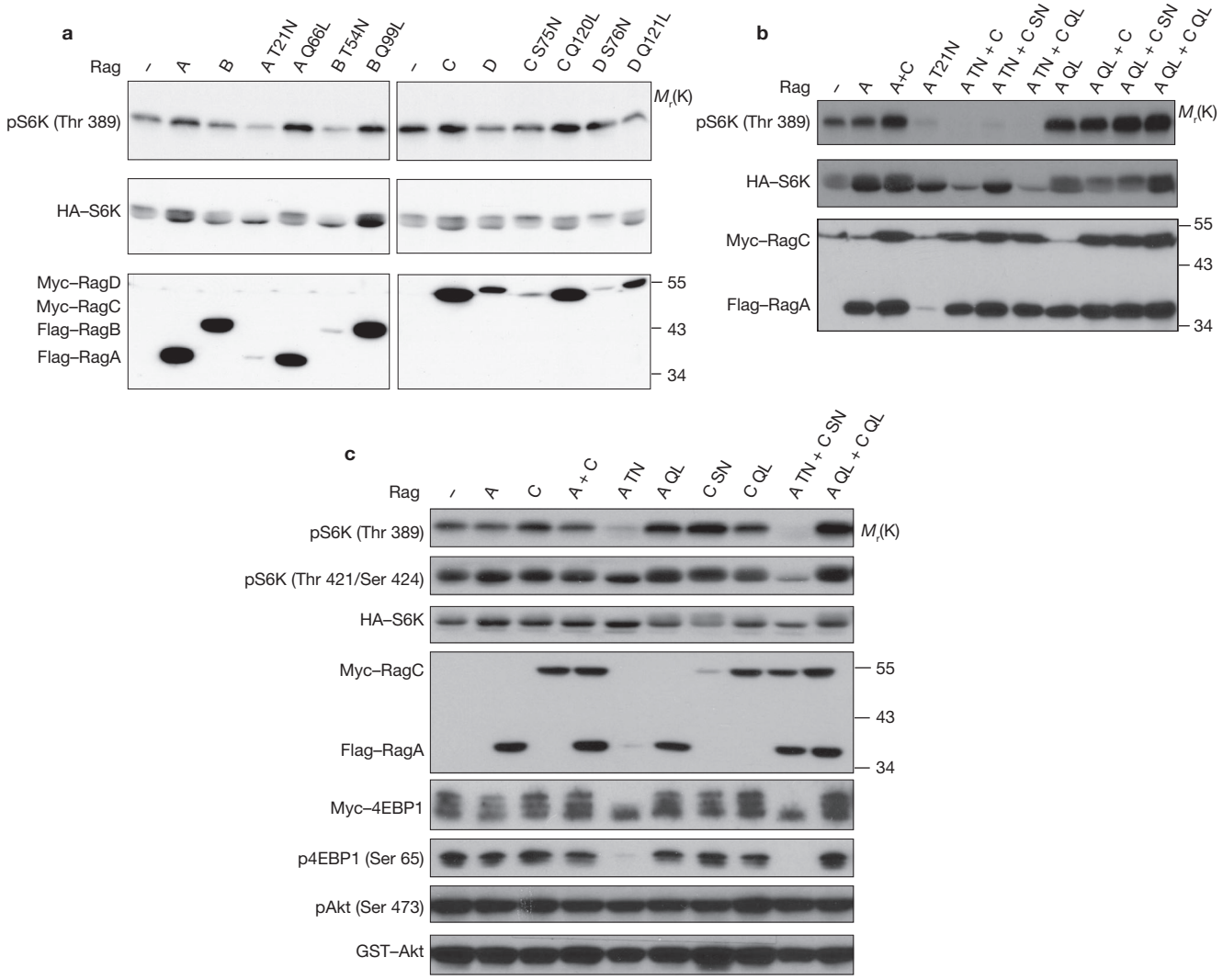

Figure 2 Mammalian Rag GTPases regulate TORC1 activity. (**a**) Constitutively active RagA and RagB stimulate S6K phosphorylation. 200 ng of each mammalian *RagA*, *RagB*, *RagC* or *RagD* construct was co-transfected with *HA–S6K* (20 ng) into HEK293 cells. Their corresponding dominant-negative mutants (*RagA*^{T21N}, *RagB*^{T54N}, *RagC*^{S75N}, *RagD*^{S76N}) and constitutively active mutants (*RagA*^{Q66L}, *RagB*^{Q99L}, *RagC*^{Q120L}, *RagD*^{Q121L}) were also tested. Phosphorylation and protein levels were determined by immunoblotting with the appropriate antibodies, as indicated. (**b**) RagA has a dominant role over RagC in regulating S6K phosphorylation. Each *Rag* construct (200 ng) indicated was co-transfected with *HA–S6K* (20 ng). The different *Rag* mutants used in the transfection are indicated at the top of each lane. (**c**) Rag regulates TORC1 but not TORC2 activity. Each indicated *Rag* construct (200 ng) was co-transfected with either *HA–S6K* (20 ng), *Myc–4EBP1* (20 ng) or of *GST–Akt* (100 ng). Phosphorylation and protein levels were determined by immunoblotting with the appropriate antibodies, as indicated. Full scans of blots are provided in Supplementary Information, Fig. S6.

These results support the notion that Rag GTPases specifically activate mTORC1 but not mTORC2.

Rag GTPases regulate amino acid response

The stimulatory effect of constitutively active RagA on S6K phosphorylation was not significant in normal culture medium (Fig. 2). Previously, we had also observed that stimulation of S6K phosphorylation by Rheb was weak in rich medium but was greatly enhanced under nutrient-poor conditions[34]. We therefore tested the effects of amino acid deprivation on S6K phosphorylation. Expression of constitutively active *RagA*^{Q66L}, but neither wild-type *RagA* nor dominant-negative *RagA*^{T21N}, increased S6K phosphorylation (Fig. 3a). Moreover, expression of *RagA*^{T21N} and *RagC*^{Q120L} completely blocked S6K phosphorylation in response to amino acid stimulation (Fig. 3b). Surprisingly, expression of dominant-negative *RagC*^{S75N}, but not constitutively active *RagC*^{Q120L}, reproducibly increased S6K phosphorylation (Fig. 3a). Although less marked, this effect on S6K is significant, given the low expression of *RagC*^{S75N}. Transfection with as little as 20 ng of *RagA*^{Q66L} DNA markedly increased S6K phosphorylation in the absence of amino acids and this effect persisted for more than 12 h (Supplementary Information, Fig. S2a, data not shown). Expression of *RagA*^{T21N} blocked amino acid stimulation, despite its low level of expression (Supplementary Information, Fig. S2a).

TORC1 is known to be inhibited by various conditions, such as osmotic stress. We tested whether *RagA*^{Q66L} can overcome inhibition by osmotic stress. As shown in Supplementary Information, Fig. S2b, osmotic stress still inhibited *RagA*^{Q66L}-induced S6K phosphorylation. We found that neither *RagA*^{Q66L} nor *RagA*^{T21N} affected AMPK phosphorylation (data not shown), excluding an involvement of AMPK.

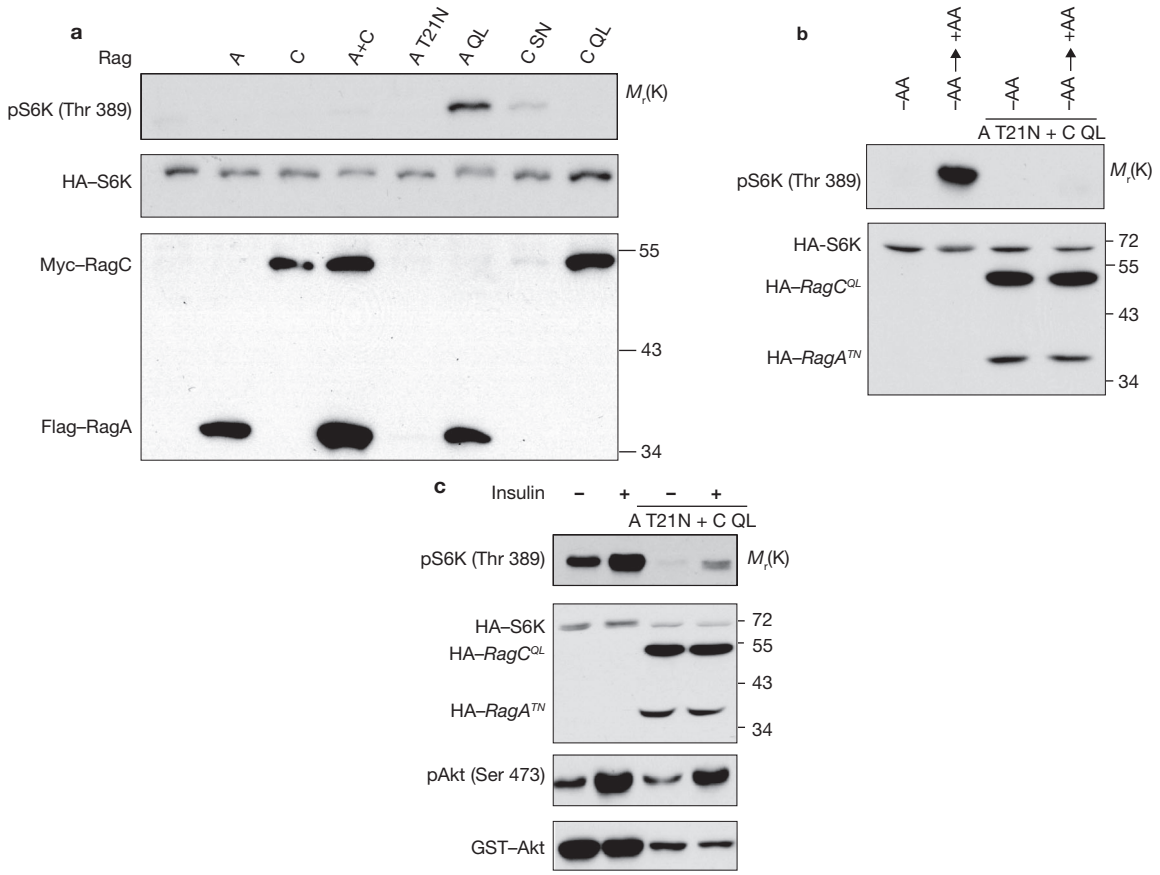

Figure 3 Rag GTPases are involved in the response to amino acids. (**a**) *RagA*^{Q66L} and *RagC*^{S75N} activate TORC1 in the absence of amino acids. Each *Rag* construct (200 ng) indicated was co-transfected with *HA–S6K* (20 ng) into HEK293 cells. Cells were starved of amino acids for 1 h before collection. Phosphorylation and protein levels were determined by immunoblotting with the appropriate antibodies, as indicated. (**b**) *RagA*^{T21N} and *RagC*^{Q120L} block S6K phosphorylation in response to amino acid (AA) stimulation. *pcDNA3* (200 ng, lanes 1 and 2) or each indicated *Rag* construct was co-transfected with *HA–S6K* into HEK293 cells. Cells were starved of amino acids for 1 h (–AA) and either remained in the starvation medium or were stimulated with amino-acid-containing-medium (+AA) for 30 min before collection. Phosphorylation and protein levels were determined by immunoblotting with the appropriate antibodies, as indicated. (**c**) *RagA*^{T21N} and *RagC*^{Q120L} suppress insulin-induced stimulation of S6K phosphorylation. *pcDNA3* (200 ng, lanes 1 and 2) or each indicated *Rag* construct was co-transfected with *HA–S6K* (20 ng) or *GST–Akt* (100 ng) into HeLa cells. Cells were serum-starved overnight and stimulated with insulin (400 nM) for 30 min. Phosphorylation and protein levels were determined by immunoblotting with the appropriate antibodies, as indicated. Full scans of blots are provided in Supplementary Information, Fig. S6.

In the absence of amino acids, the ability of insulin to stimulate S6K is significantly compromised (Supplementary Information, Fig. S3; refs 8, 19). We therefore examined the effect of Rag on insulin signalling. Co-expression of *RagA*^{T21N} and *RagC*^{Q120L} potently reduced the ability of insulin to stimulate S6K phosphorylation (Fig. 3c), consistent with the results obtained under conditions of amino acid starvation (Supplementary Information, Fig. S3). In contrast, insulin-induced Akt phosphorylation was not affected by Rag (Fig. 3c). These data further support the notion that Rag GTPases may be specifically involved in amino acid signalling.

Rag GTPases regulate cell size in *Drosophila*

As TOR signalling in the regulation of cell and organ size in *Drosophila* is well established [35,36], we examined the effect of dRagA and dRagC on cell growth *in vivo*. Wild-type *dRagA*, constitutively active *dRagA*^{Q61L} and dominant-negative *dRagA*^{T16N} were each expressed in posterior wing compartments using the posterior driver *en–GAL4*. We found that expression of the constitutively active *dRagA*^{Q61L}, but not the wild-type *dRagA*, significantly increased posterior compartment size, compared with that of the control anterior compartment (Fig. 4a). In contrast, expression of the dominant-negative *dRagA*^{T16N} decreased posterior wing compartment size. Consistent with these results, expression of *dRagA*^{Q61L} increased individual cell size of the wing, whereas expression of *dRagA*^{T16N} reduced cell size (Fig. 4b). We also expressed dRagA in the dorsal wing surface using the dorsal-specific *ap–GAL4*. As predicted, expression of *dRagA*^{Q61L} or *dRagA*^{T16N} caused wing curvature downwards or upwards, respectively (Supplementary Information, Fig. S4a, b). These results support the suggestion that high activity of dRagA promotes cell growth and low activity of dRagA inhibits cell growth.

The *Drosophila* larval fat body is involved in TOR-dependent nutrient sensing, as well as in relaying a nutritional response during development[37]. We thus examined the role of dRagA in cell size regulation in this tissue under conditions of normal feeding or after amino acid starvation for 48 h. Under starvation conditions, clonal overexpression of wild-type *dRagA* resulted in a modest increase in individual cell size, whereas expression of constitutively active *dRagA*^{Q61L} resulted in a 3-fold increase in cell size, compared with neighbouring control cells (Fig. 4c, d). Expression of wild-type *dRagA* and *dRagA*^{Q61L} had little effect on cell size under normal-fed conditions (Fig. 4c), consistent with a specific effect of

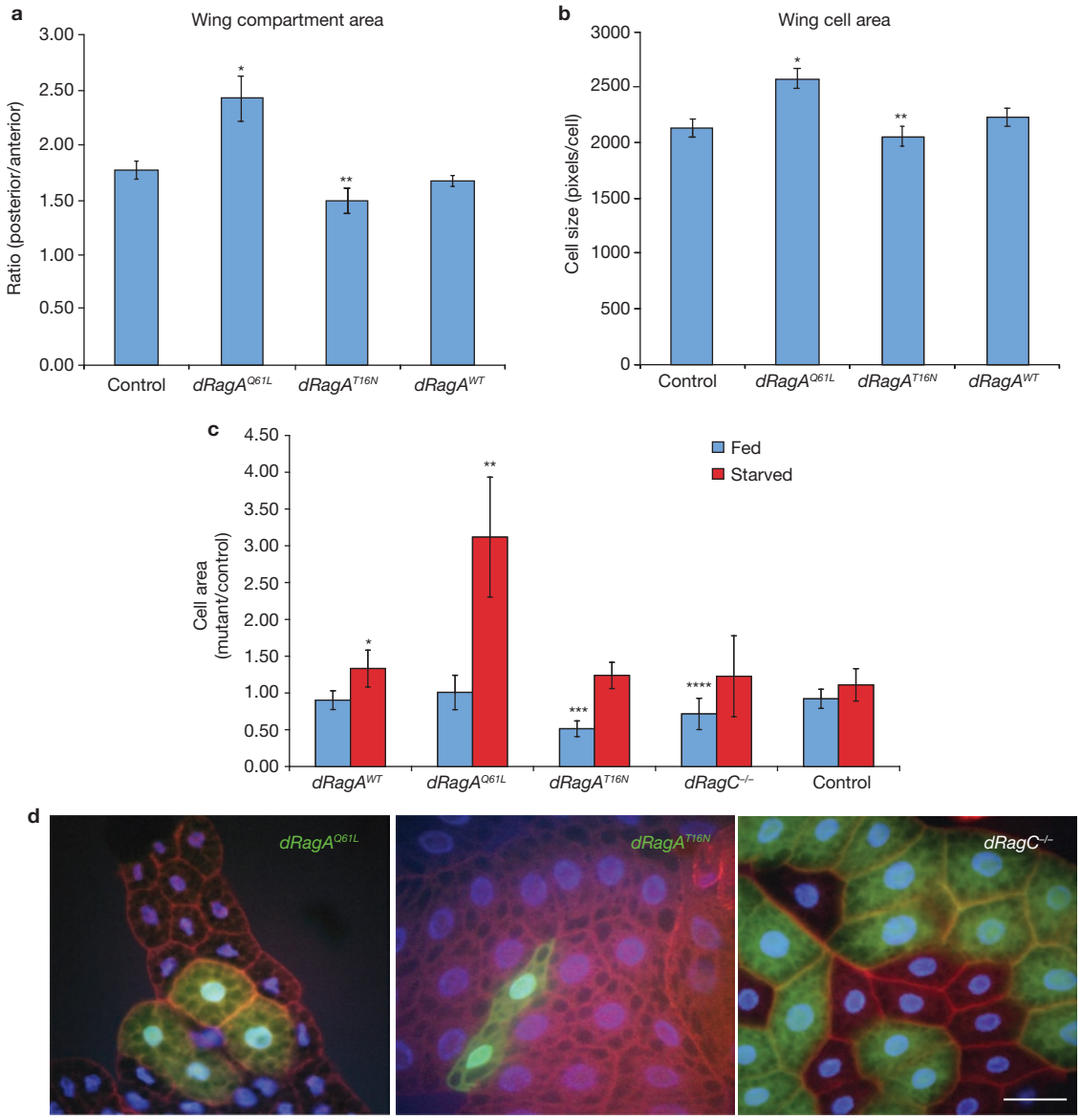

Figure 4 dRagA and dRagC promote cell and organ growth in *Drosophila*. (**a**) dRagA positively regulates wing compartment size. Wild-type or mutant *dRagA* transgenes were expressed in posterior compartments with the *en–GAL4* driver. The ratios of representative posterior to anterior compartment areas are shown. Posterior compartment area was significantly increased in response to $dRagA^{Q61L}$ expression and decreased in response to $dRagA^{T16N}$ expression. Data are mean ± s.d., $*P = 7.32 \times 10^{-4}$ ($n = 7$), $**P = 6.18 \times 10^{-4}$ ($n = 12$), Student's two-tailed *t*-test, (*n* is the number of adult wings analysed). (**b**) dRagA positively regulates wing cell size. The average area of posterior compartment cells from *en–GAL4* UAS–*dRagA* adult wings is shown. Cells expressing $dRagA^{Q61L}$ are significantly larger and $dRagA^{T16N}$-expressing cells are smaller than controls. Data are mean ± s.d., $*P = 1.15 \times 10^{-3}$ (n=7), $**$ $P = 0.025$ ($n = 12$), Student's 2-tailed *t*-test (*n* represents number of adult wings analysed). (**c**, **d**) dRag GTPases positively regulate larval fat body cell size. (**c**) Cell area of clonally-induced *dRagA*-expressing cells or *dRagC* homozygous mutant cells relative to neighbouring wild-type control cells is shown. Cell area was determined from phalloidin-stained fixed fat body samples from fed or 48 h starved larvae. Expression of $dRagA^{WT}$ or $dRagA^{Q61L}$ significantly increased relative cell area under starvation but not fed conditions. Cells expressing $dRagA^{T16N}$ and *dRagC* loss-of-function cells were significantly smaller than control cells only under nutrient replete conditions. Data are means ± s.d., $*P = 2.04 \times 10^{-3}$ ($n = 5$), $**P = 2.94 \times 10^{-6}$ ($n = 14$), $***P = 3.79 \times 10^{-7}$ ($n = 14$), $****P = 1.36 \times 10^{-5}$ ($n = 30$), Student's two-tailed *t*-test. (**d**) Representative examples of fat body cells with altered dRagA activity. Cells expressing *dRagA* transgenes are marked by the expression of GFP in the left and middle panels, and *dRagC* homozygous mutant cells are marked by absence of GFP in the right panel. Scale bar represents 50 μm.

dRagA in the nutrient response. Furthermore, expression of $dRagA^{T16N}$ potently decreased cell size, and this effect was observed only during nutrient sufficiency but not nutrient starvation (Fig. 4c, d). These data are consistent with the effect of RagA on S6K phosphorylation observed in mammalian cells (see Fig. 3a, b) and strongly support a role of dRagA specifically involved in the nutrient response.

To investigate the function of endogenous dRag, we identified a P element insertion in the 5′ untranslated region of the *dRagC* gene. In animals homozygous for this insertion, growth was arrested at the early third instar larval stage, which is similar to the growth arrest observed in *Tor* loss-of-function mutants[36], and could be restored to viability by mobilization of the P element (data not shown). In the larval fat body,

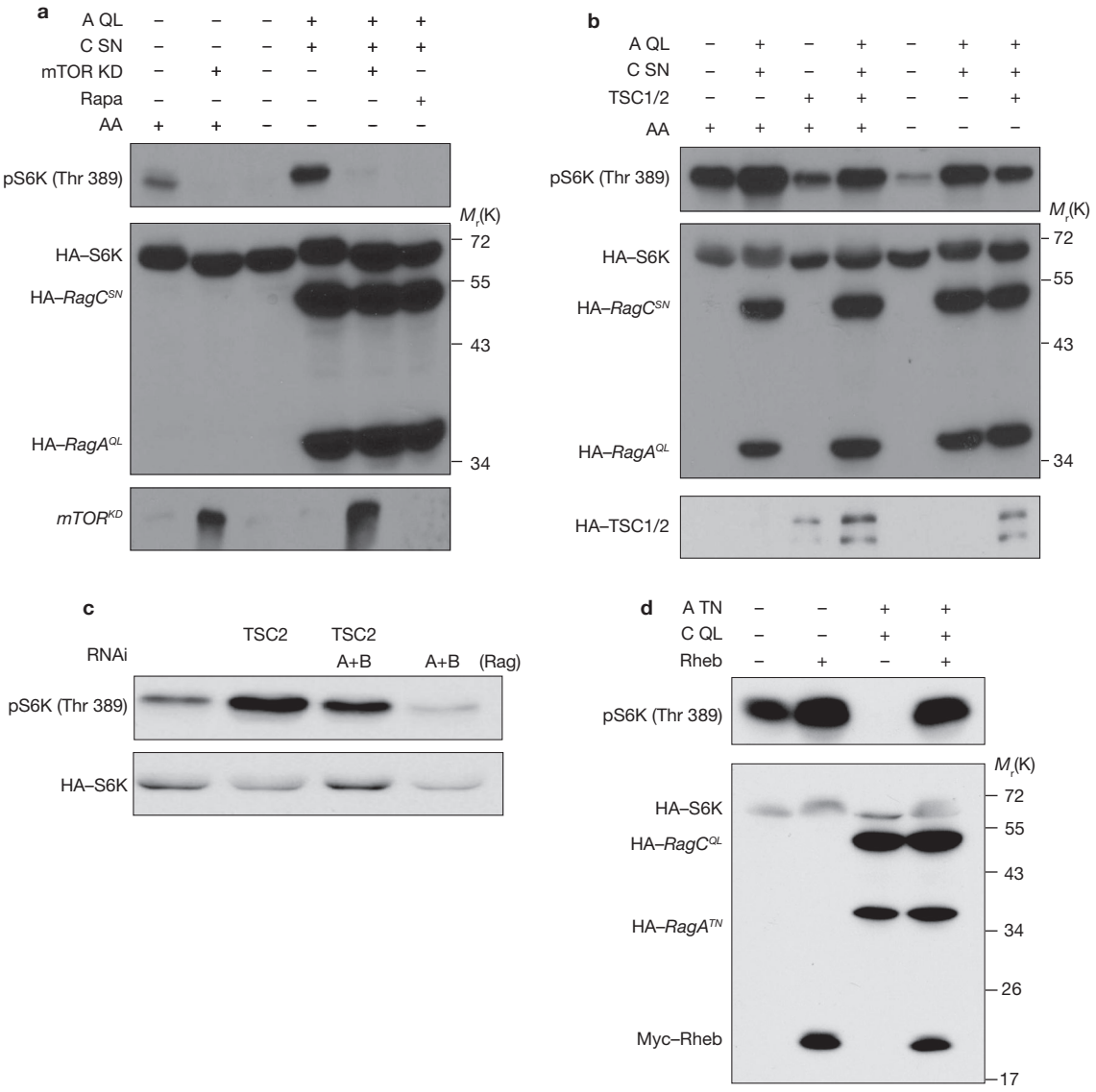

Figure 5 Relationship between Rag and components of the TOR pathway. (**a**) Rag acts through TORC1 to regulate S6K phosphorylation. HEK293 cells were transfected with constructs as indicated. Co-expression of of *mTOR*^{KD} construct (600 ng) or rapamycin treatment (rapa, 20 nM, 30 min) abolished the effect of *RagA*^{Q66L} and *RagC*^{S75N} on S6K phosphorylation. The protein level of mTOR^{KD} was determined by immunoblotting with anti-mTOR antibody. (**b**) RagA/RagC and TSC1/TSC2 independently regulate S6K phosphorylation. HEK293 cells were transfected with 200 ng of each *Rag* and/or ′ constructs as indicated. Amino acid starvation for 1 h (–AA) is indicated. Phosphorylation and protein levels of the transfected proteins were determined by immunoblotting with appropriate antibodies, as indicated. (**c**) TSC2 and RagA/B independently affect S6K phosphorylation. *HA–S6K* (20 ng) was transfected into HeLa cells with or without RNAi against human *TSC2*, *RagA* and *RagB* as indicated. (**d**) *RagA*^{T21N} and *RagC*^{Q120L} do not block Rheb-induced S6K phosphorylation. *RagA*^{T21N} and *RagC*^{Q120L} (200 ng each) were transfected into HEK293 cells with or without *Rheb* construct (20 ng). *S6K* was included in the co-transfection. Phosphorylation and protein levels of the transfected proteins were determined by immunoblotting with appropriate antibodies, as indicated. Full scans of blots are provided in Supplementary Information, Fig. S6.

clones of cells homozygous for this *dRagC* mutation showed a statistically significant reduction in cell size during fed but not starved conditions (Fig. 4c, d), highlighting a requirement for endogenous *dRagC* in cell growth regulation and nutrient response.

Rag and TSC1/2 function independently and in parallel to promote TORC1 signalling

We next examined the relationship between Rag and TORC1 pathway components in further detail. In mammalian cells, rapamycin treatment completely blocked *RagA*^{Q66L}/*RagC*^{S75N}-induced S6K phosphorylation (Fig. 5a). Consistent with this, co-expression of an mTOR kinase dead mutant (*mTOR*^{KD}) also effectively inhibited *RagA*^{Q66L}/*RagC*^{S75N}-induced S6K phosphorylation. These results show that Rag functions upstream of mTOR. On the other hand, expression of TSC1/TSC2 partially inhibited the stimulatory effect of *RagA*^{Q66L}/*RagC*^{S75N} (Fig. 5b). Conversely, expression of *RagA*^{Q66L}/*RagC*^{S75N} partially reversed the inhibitory effect of TSC1/TSC2. To further investigate the relationship between Rag and TSC, we examined the endogenous proteins. Both *RagA* and *RagB* genes are expressed in HeLa cells (data not shown). Knockdown of both *RagA* and *RagB* decreased S6K phosphorylation and also compromised the

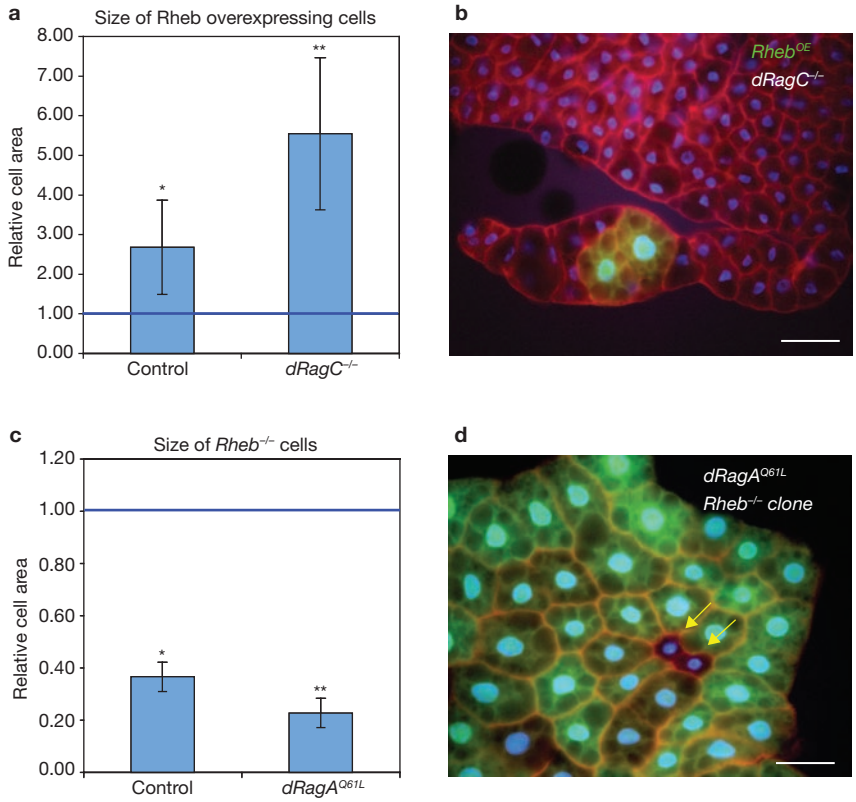

Figure 6 Rag GTPases act in parallel with Rheb to promote fat body cell growth. (**a**, **b**) dRagC is not required for Rheb-induced cell growth. (**a**) The area of *Rheb*-overexpressing cells in control or *dRagC* mutant (*dRagC*$^{-/-}$) backgrounds under fed conditions, relative to that of neighbouring control cells which were assigned a value of 1. Overexpression of *Rheb* led to a significant increase in cell area in both control and *dRagC* mutant backgrounds. Data are mean ± s.d., $*P = 0.034$ ($n = 5$), $**P = 6.1 \times 10^{-3}$ ($n = 5$), Student's two-tailed *t*-test (*n* represents number of experimental samples). (**b**) A representative example of a clone of *Rheb*-overexpressing cells in a *dRagC*$^{-/-}$ animal. *Rheb* transgene-expressing cells are marked by co-expression of GFP. Cell boundaries are labelled by phalloidin staining in red; nuclei are labelled by DAPI in blue. Scale bar represents 50 μm. (**c**, **d**) Expression of *dRagA*^{Q61L} fails to rescue the growth impairment of *Rheb* mutant cells. (**c**) Relative area of clonally-induced *Rheb*$^{26.2}$ homozygous mutant cells in a control background and in animals expressing *dRagA*^{Q61L} throughout the fat body. Clonally induced *Rheb*$^{26.2}$ homozygous mutant cells were significantly smaller than neighbouring control cells both in wild-type and in *dRagA*^{Q61L} expressing backgrounds. Data are mean ±s.d., $*P = 2.91 \times 10^{-4}$ ($n = 7$), $**P = 2.59 \times 10^{-8}$ ($n = 5$), Student's two-tailed *t*-test (fed conditions where *n* represents number of experimental samples). (**d**) A representative example of *Rheb* homozygous mutant cells (marked by lack of GFP, arrows) in fat body ubiquitously expressing UAS–*dRagA*^{Q61L}. GFP-positive control cells in this experiment are a mixture of *Rheb*$^{+/-}$ and *Rheb*$^{+/+}$. Scale bar represents 50 μm.

increased S6K phosphorylation caused by *TSC2* knockdown (Fig. 5c). These results indicate that Rag and TSC1/2 may function in parallel pathways and independently regulate mTORC1 activity.

We then tested the effect of *RagA*^{T21N} on Rheb-induced S6K phosphorylation. Expression of *RagA*^{T21N} and *RagC*^{Q120L} potently blocked basal S6K phosphorylation but did not inhibit Rheb-induced S6K phosphorylation (Fig. 5d). Amino acid starvation also failed to block the stimulatory effect of Rheb on S6K phosphorylation (data not shown). These data exclude a model that Rag functions downstream of Rheb, but are consistent with Rag acting either in parallel with or upstream of Rheb.

We also investigated the functional relationship between Rag and Rheb *in vivo* through genetic studies in *Drosophila*. To test whether *dRagC* is required for Rheb to stimulate cell growth, the effect of Rheb overexpression on fat body cell size was examined in *dRagC*$^{-/-}$ cells. Mutation of *dRagC* did not block the stimulatory effect of Rheb overexpression on growth (Fig.6a, b). Indeed, Rheb overexpression induced a greater relative increase in cell size in a *dRagC*$^{-/-}$ genetic background. Similarly, Rheb overexpression has been shown to have a more marked effect on cell size during starvation[38], further suggesting that nutrient signalling is impaired in *dRagC* mutants. We also examined the effect of *Rheb* loss-of-function under conditions of *dRagA*^{Q61L} activation, and found that *Rheb* mutant cells were smaller than neighbouring wild-type cells both in control animals and in animals that express *dRagA*^{Q61L} ubiquitously throughout the fat body (Fig 6c, d). These data indicate that dRagA and dRagC are not required for Rheb to stimulate cell growth. We also found that the increase in cell size in response to *dRagA*^{Q61L} expression was partially or completely suppressed in two different *Rheb* hypomorphic mutant backgrounds (data not shown), indicating that Rheb activity may be required for the growth effects of dRagA. Together, these data suggest that Rag acts in parallel with, or upstream of, Rheb to stimulate cell growth.

Tsc1 mutant animals die at an early larval stage because of hyperactive TOR signalling, and this lethality can be rescued by heterozygous mutation of TOR or dS6K[39,40]. Similarly, we observed that heterozygous disruption of *dRagC* partially suppressed the early larval lethality caused by *Tsc1* mutation (Supplementary Information, Fig. S4c, d). This incomplete rescue suggests that dRagC may be responsive to Tsc1/Tsc2 signalling.

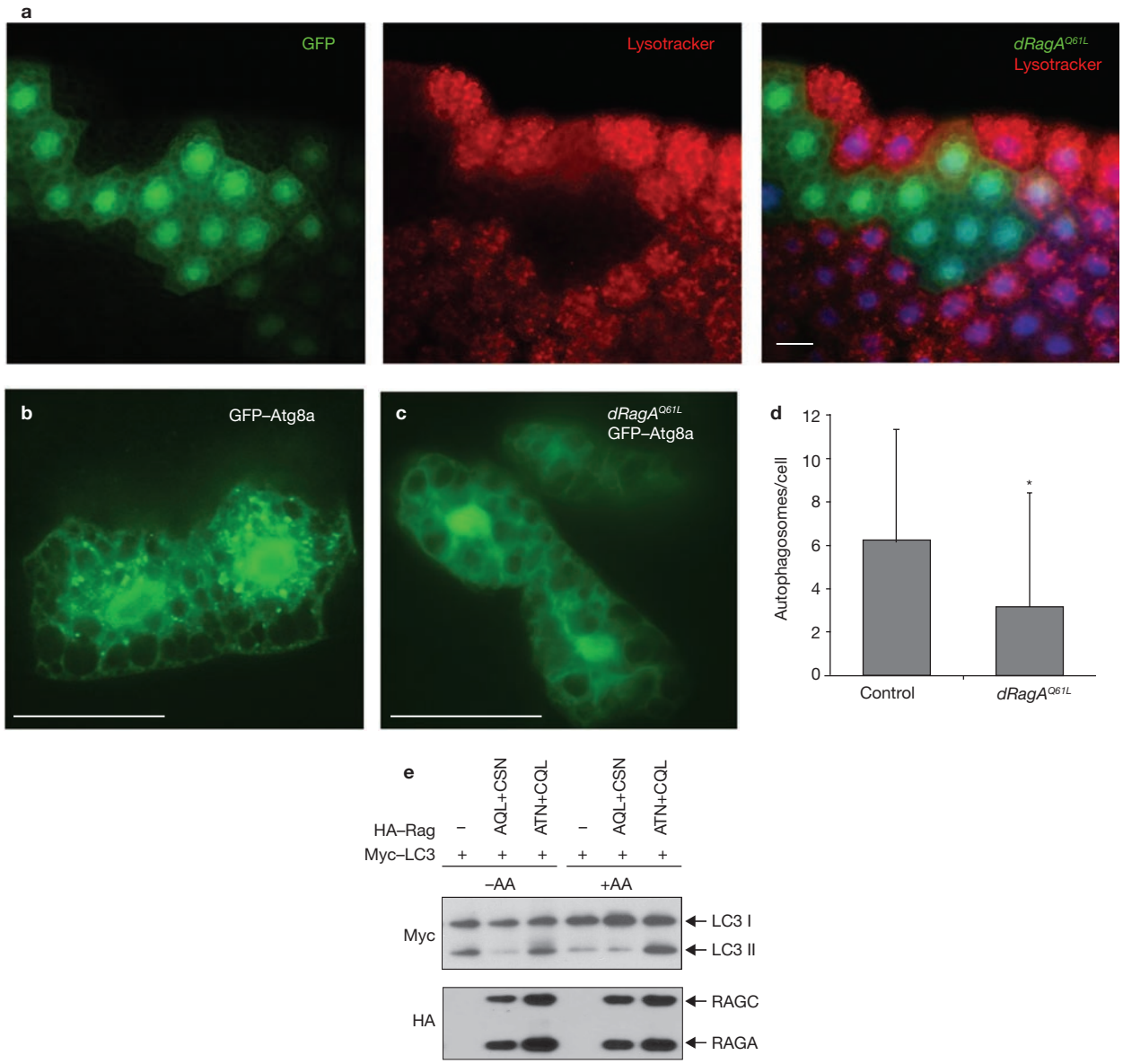

Figure 7 Regulation of autophagy by Rag. (**a**–**d**) *dRagA*^{Q61L} suppresses autophagy. (**a**) *Drosophila* fat body cells clonally expressing *dRagA*^{Q61L} (marked in green by GFP expression) failed to accumulate autolysosomes (shown in surrounding control cells by punctate Lysotracker Red staining) in response to starvation for 4 h. Nuclei are marked in blue by DAPI. (**b**–**d**) Induction of autophagosomes in response to 4-h starvation is shown by the punctate pattern of GFP–Atg8a expression in control fat body cells (**b**), but not in cells expressing *dRagAQ61L* (**c**). The average number of GFP–Atg8a-marked autophagosomes per cell in control and *dRagA*^{Q61L}-expressing clones is shown (**d**). Data are mean ± s.d., $*P = 2.91 \times 10^{-6}$, Students two-tailed *t*-test ($n = 33$ fat body samples imaged per genotype). Scale bars represent 25 μm in each panel. (**e**) RagA regulates LC3 conversion in mammalian cells. *Myc–LC3* was co-transfected with *RagA*^{QL} and *RagC*^{SN} or *RagA*^{TN} and RagC^{QL} into HEK293 cells as indicated. One day after transfection, cells were cultured in amino-acid-sufficienct medium (+AA) or amino-acid-depleted medium (–AA) for 4 h before collection. Western blotting for Myc–LC3 and HA–Rag were performed. Autophagic conversion of LC3I into the lipidated LC3II form was blocked by active RagA and stimulated by dominant-negative RagA. Full scans of blots are provided in Supplementary Information, Fig. S6.

Rag proteins regulate starvation responses in *Drosophila*

Autophagy is strongly induced in the *Drosophila* fat body in response to starvation, and this is dependent on downregulation of TOR signalling. Autophagy can be readily imaged *in vivo* using markers such as GFP–Atg8 and Lysotracker[41]. We found that overexpression of *dRagA*^{Q61L} markedly inhibited starvation-induced punctate Lysotracker and GFP–Atg8a staining (Fig. 7a–d) in response to starvation in *Drosophila*. This observation indicates that active dRagA suppresses the nutrient starvation response, suggesting that high dRagA activity may generate false signals mimicking nutrient sufficiency, thereby suppressing autophagy.

LC3, the mammalian Atg8 homologue, undergoes a set of modifications resulting in conversion from LC3I to LC3II during autophagy[42]. To further test the function of Rag in autophagy, we examined the LC3 modification in HEK293 cells. Expression of *RagA*^{QL} and *RagC*^{SN} inhibited LC3 conversion in response to amino acid starvation (Fig.7e). Furthermore, expression of *RagA*^{TN} and *RagC*^{QL} enhanced LC3 conversion even in the presence of amino acids. These results are consistent with the

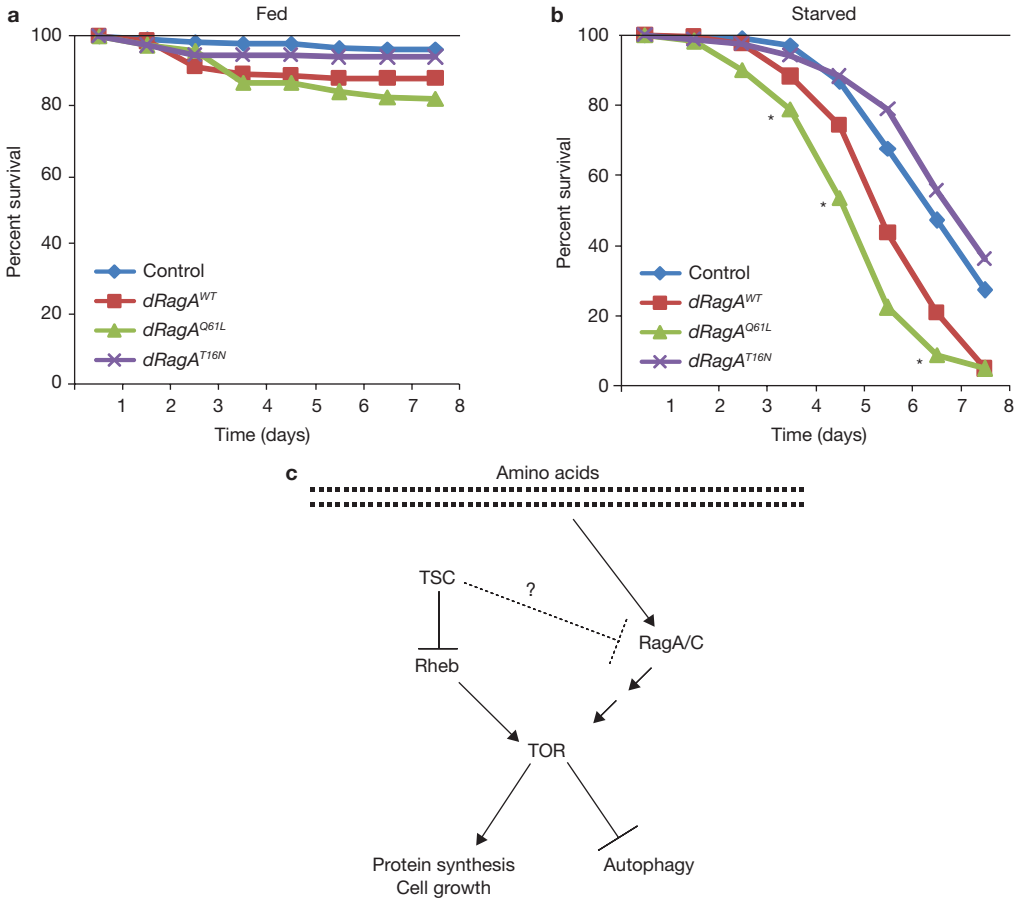

Figure 8 High dRagA activity sensitizes *Drosophila* to starvation. (**a**, **b**) dRagA activation increases sensitivity to starvation. Expression of $dRagA^{Q61L}$ using the fat-body-specific *Cg–GAL4* driver significantly decreased survival of adult female flies under starvation (**b**) but not fed (**a**) conditions, relative to controls (Cg–GAL4 alone). Asterisks indicate significant difference, compared with controls. Data are mean ± s.d., $*P < 0.05$, Students two-tailed *t*-test ($n = 150$ flies/genotype/treatment). (**c**) A proposed model of Rag GTPase in regulation of TORC1 activity. Rag GTPases act independently of and in parallel to TSC–Rheb to activate TOR signalling, possibly by transducing a nutrient-dependent signal. The mechanism of TOR regulation by Rag GTPases is indirect, and probably involves additional unidentified factors.

data observed in *Drosophila* and further demonstrate a role of the Rag GTPases in autophagy regulation in response to nutrient signals.

As a proper response to nutrient limitation is also important for organisms to survive under unfavourable conditions[43,44], we investigated the effect of dRagA activity on adult animal viability in response to starvation. Targeted expression of constitutively active $dRagA^{Q61L}$ to the fat body had no significant effect on survival in animals given a normal diet, but resulted in a significantly accelerated rate of death under conditions of starvation (Fig. 8a, b). In contrast, animals expressing the dominant-negative $dRagA^{T16N}$ were more resistant to death induced by starvation. Similar effects on starvation survival were observed with ubiquitous expression of *dRagA* transgenes (data not shown). Taken together these data suggest that the activity of dRagA is important for signalling in response to nutrient starvation and also is crucial for animal survival.

DISCUSSION

Amino acids are important activators of TORC1; however, the mechanism involved in amino acid signalling remains uncertain. Although VPS34 was proposed to mediate nutrient signals to TOR[20,21], we recently found that *Drosophila* with *Vps34*-null mutations have normal TOR activity[45]; *Vps34* knockdown had no effect on dS6K phosphorylation (data not shown). In this report, we have identified Rag GTPases as important activators of the TORC1 pathway in response to amino acids both in *Drosophila* and in mammals. Knockdown of *dRagA* or *dRagC* markedly decreased dS6K phosphorylation in response to amino acid stimulation. Overexpression of constitutively active $dRagA^{Q61L}$ increased cell size in fat body and wings, especially in starved *Drosophila*. Expression of dominant-negative $dRagA^{T16N}$ decreased cell size and this effect was stronger when nutrient levels were sufficient. Furthermore, $dRagA^{Q61L}$ expression and *dRagC* mutation suppressed starvation-induced autophagy and the lethality of *Tsc1* mutant animals, respectively. In mammalian cells, overexpression of constitutively active RagA activated TORC1 even in the absence of amino acids, and expression of dominant-negative RagA blocked TORC1 activation in response to amino acid stimulation. The relationship between Rag and amino acids is specific, as shown by the failure of constitutively active RagA to overcome the effects of osmotic stress.

The physiological role of Rag in the nutrient response is further supported by the finding that during starvation flies expressing $dRagA^{Q61L}$ die earlier than controls, presumably because of a failure to attenuate their metabolic activity and growth, owing to a false sense of nutrient sufficiency. Additionally, animals expressing $dRagA^{T16N}$ are more resistant to starvation and survive longer in the absence of nutrients.

Our data indicate that dimer formation between RagA/B and RagC/D is important for TORC1 activation. Within the dimer, the function of RagA/B is dominant. In other words, *RagA*^{Q66L} dominantly activates and *RagA*^{T21N} dominantly inhibits TORC1 regardless of the nucleotide binding status of the RagC/D in the complex. Nevertheless, RagC/D is likely to be critical for dimer function, given the effects of *dRagC* knockdown in S2 cells and the phenotypes of *dRagC* mutant animals. Interestingly, yeast Gtr1 and Gtr2 must be in GTP-bound and GDP-bound states, respectively, to function[26]. Our results suggest that the relationship between RagA and RagC is similar to that of Gtr1 and Gtr2. In addition, RagC may have a GTPase-independent role in stabilizing RagA and may regulate RagA localization or activity, or aid in TORC1 activation.

Studies in *S. cerevisiae* have shown that Gtr1/Gtr2 could control intracellular protein trafficking, thereby regulating the localization of the general amino acid permease Gap1 (ref. 26). This observation suggests a possible mechanism whereby Gtr1/2 activates TORC1 by promoting amino acid import and thus regulating nutrient availability. However, our data from mammalian cells are not consistent with this model for two reasons. First, complete and extended amino acid depletion fails to inhibit TORC1 activity in cells overexpressing *RagA*^{Q66L}. Second, we found that amino acid import was not significantly affected by RagA expression (Supplementary Information, Fig.S5). Therefore, it is unlikely that Rag regulates TORC1 by promoting the availability of nutrients. Instead, we favour a model in which Rag acts between amino acids and TORC1 in a pathway parallel to the TSC–Rheb axis (Fig. 8c). An interesting possibility is that Rag regulates localization of TORC1 pathway components.

This study identifies Rag GTPases as positive regulators of TORC1 in amino acid signalling, a conclusion supported by biochemical studies in mammalian cells and genetic studies in *Drosophila*. Future studies to elucidate the molecular mechanism of Rag in amino acid sensing and TORC1 activation will provide new insight into this important pathway.

METHODS

Antibodies, plasmids and reagents. Anti-*Drosophila* S6 kinase antibody was provided by Mary Stewart (University of North Dakota State University, Fargo, ND). Anti-phospho *Drosophila* S6K, anti-S6K, anti-phospho S6K, anti-Akt, anti-phospho Akt and anti-phospho 4EBP1 antibodies were from Cell Signaling. Anti-mTOR and anti-Myc antibodies were from Santa Cruz Biotechnology. Anti-HA and anti-Flag antibodies were from Covance and Sigma, respectively, and diluted 1:1000 for western blotting. The cDNAs encoding human RagA and RagC were obtained from the American Tissue Culture Collection and amplified by PCR. *RagA* was subcloned into the *Bam*HI/*Xho*I restriction enzyme site of pcDNA3–HA and pcDNA3–FLAG, and *RagC* was subcloned into the *Bam*HI/*Eco*RI restriction enzyme site of pcDNA3–HA and Myc–pRK5 vectors. The cDNAs encoding RagB and RagD were amplified by PCR from the human brain cDNA library and cDNA library generated from HEK293 cells, respectively. *RagB* and *RagD* were subcloned into *Eco*RV/*Xho*I and *Bam*HI/*Eco*RI site of pcDNA3–FLAG and pRK5–Myc vectors, respectively. All mutant constructs of *RagA*, *B*, *C* and *D* were created by PCR mutagenesis and were verified by DNA sequencing. Primers used for Rag construct cloning are listed in Supplementary Information, Table S1. All other DNA constructs, including HA–*S6K*, Myc–*4EBP1*, GST–*Akt*, Flag–*mTOR*^{KD}, HA–*TSC1*, HA–*TSC2* and Myc–*Rheb*, were from laboratory stock. Insulin and rapamycin were obtained from Sigma and Cell Signaling, respectively. siRNAs targeting human TSC2, RagA and RagB were obtained from Dharmacon.

Cell culture. *Drosophila* S2 cells (Invitrogen) were cultured in *Drosophila* serum-free medium (Invitrogen) supplemented with L-glutamine (45 ml of 200 mM L-glutamine in 500 ml medium) and maintained at 27 °C. HEK293 cells and HeLa cells were cultured in Dulbecco's modified Eagle's medium (DMEM, Invitrogen, Cat. No. 12430) supplemented with 10% fetal bovine serum (FBS) in a 37 °C humidified incubator with 5% CO_2.

Amino-acid-containing (SDMK) or -free (SDMK-AA) media used for *Drosophila* S2 cells were made using Schneider's *Drosophila* medium (Invitrogen) formulation. Stocks for amino acids (2×), inorganic salts (2.5×) and other components (5×) were made individually and mixed together to a final concentration of 1× SDMK or 1× SDMK-AA. For SDMK-AA, double-distilled water was added instead of AA. The final pH and osmolality were adjusted to 6.6–6.8 and 345–365 mOsm kg^{-1}, respectively. SDMK and SDMK-AA were used for amino acid stimulation and starvation, respectively, for *Drosophila* S2 cells.

Amino-acid-containing (DMEMK) -free (DMEMK-AA) media used for HEK293 and HeLa cells were made using DMEM medium (Invitrogen, Cat. No.12430) formulation. Stocks for amino acids (10×), inorganic salts and other components (2×) were made individually. For vitamins, minimum essential medium (MEM) vitamin solution (100×, Invitrogen) was used at a 1:25 dilution (final concentration, 4×). Stocks were mixed together to final concentration of 1× DMEMK or 1× DMEMK-AA. For DMEMK-AA, double-distilled water was added instead of amino acids. The final pH and osmolality were adjusted to 7.0–7.4 and 295–340 mOsm kg^{-1}, respectively. DMEMK and DMEMK-AA were used for amino acid stimulation and starvation, respectively for HEK293 and HeLa cells.

RNA interference. *Drosophila* RNA interference (RNAi) experiments were performed as described previously[46] with minor modifications. Briefly, primers flanked with a T7 RNA polymerase binding site (GAATTAATACGACTCACTATAGGGAGA) at the 5′ end followed by gene-specific sequences (Supplementary Information, Table S2) were designed to amplify approximately 600 bp of the coding region of the gene of interest. Each individual DNA fragment was amplified with this primer by PCR from *Drosophila* genomic DNA and the PCR products were purified using the High Pure PCR purification kit (Roche). Using the purified PCR products as templates, *in vitro* transcription was performed to produce dsRNA using a MEGAscript T7 transcription kit (Ambion). The transcribed RNAs were annealed *in vitro* by incubation at 65 °C for 30 min followed by slow cooling down to room temperature. dsRNAs were analysed by 1% agarose gel electrophoresis for integrity as well as length, and quantified. *Drosophila* S2 cells were cultured in 12-well plates for 4 days with a starting density of 2×10^5 cells per well. On days 1 and 3, dsRNA (4 μg) targeting the gene of interest was added directly to the culture wells. Cells were lysed at the end of day 4, with 150 μl per well of mild lysis buffer (10 mM Tris-HCl (pH 7.5), 100 mM NaCl, 1% NP-40, 50 mM NaF, 2 mM EDTA (pH 8.0), 1 mM dithiothreitol, 1 mM PMSF, 10 μg/ml leupeptin, and 10 μg/ml aprotinin). Cell lysates were subjected to SDS–PAGE.

For RNAi experiments, HeLa cells were diluted and plated into 6-well plates at about 30% confluency. Twenty-four hours later, of siRNAs (20 μM, final concentration) were transfected using Lipofectamine (Invitrogen) following the manufacturer's protocol.

Transfection and western blot analysis. Transfection was performed in serum-free conditions using Lipofectamine reagent (Invitrogen) as described by the manufacturer. Cells were lysed in mild lysis buffer (10 mM Tris-HCl (pH 7.5), 100 mM NaCl, 1% NP-40, 50 mM NaF, 2 mM EDTA (pH 8.0), 1 mM DTT, 1 mM PMSF, 10 μg ml^{-1} leupeptin and 10 μg ml^{-1} aprotinin). Samples were resolved by SDS–PAGE, transferred to polyvinylidene difluoride membrane and blotted with the desired antibodies.

***Drosophila* stocks and genetic manipulations.** ESTs GH04846 and GH16429 encoding dRagA/CG11968 and dRagC/CG8707, respectively, were purchased from the *Drosophila* Genomics Resource Center. Wild-type and PCR-generated mutant versions of these cDNAs were subcloned into pUAST and injected into *w*^{1118} embryos using standard procedures (Model System Genomics, Duke University). P[EPgy2]EY11726 is a lethal insertion in the 5′-UTR of *dRagC/CG8707*. Transposase-mediated excision of this line completely restored viability. To generate homozygous *dRagC* clones, the EY11726 element was recombined with FRT42D. Clones of cells for *dRagC*^{EY11726} or *Rheb*^{2D1} mutant or expressing *dRag* transgenes were generated as described previously[47]. Flies were cultured on standard cornmeal/molasses/agar medium at 25 °C.

Histology and size quantification. Culture and starvation of larvae, fat body dissection, Texas Red-phalloidin treatment and Lysotracker staining were performed as described previously[48]. GFP–Atg8a was expressed in spontaneous larval fat body clones as described[45]. Images were captured using ACT1 software to run a DXM 1200 Nikon digital camera attached to a Zeiss Axioscope 2 epifluorescence microscope with Plan-Neoflar ×5 and ×40 objective lenses. The average area of mutant

and surrounding control fat body cells was determined using the histogram function of Adobe Photoshop 7.0. To quantify transgene effects on adult wing cell and compartment size, the average area and number of cells within a representative anterior region (the area between wing margin and L1) and a representative posterior region (the area between L3 and L4) was determined using Photoshop 7.0. Statistical analyses were performed on a minimum of six samples per genotype and significance was determined using Student's two-tailed unpaired *t*-test.

Viability assays. Fifty female adult flies expressing the indicated UAS–*dRag* transgenes using the fat-body-specific *cg–GAL4* driver were fed on regular food for 24–48 h post eclosion and then transferred to vials containing either plain agar (starved) or standard fly media (fed). Viable flies were counted and transferred to fresh vials every 24 h. These experiments were carried out in triplicate.

Note: Supplementary Information is available on the Nature Cell Biology website.

ACKNOWLEDGEMENTS

The authors wish to thank Ken Inoki for discussions and Mary Stewart for the dS6K antibody. This work is supported by NIH grants to K.L.G. (GM62694 and CA108941) and T.P.N. (GM62509).

AUTHOR CONTRIBUTIONS

K.L.G. conceived the idea of GTPase screen; K.L.G. and E.K. designed, and E.K. performed, the screen and mammalian experiments; P.G.H. and T.P.N. designed and performed the *Drosophila* experiments with the assistance of E.K.; L.L. performed the LC3 experiments; K.L.G. and T.P.N. coordinated the study; K.L.G., E.K., P.G.H. and T.P.N. wrote the paper; all authors commented on the manuscript.

COMPETING FINANCIAL INTERESTS

The authors declare no competing financial interests.

Published online at http://www.nature.com/naturecellbiology/
Reprints and permissions information is available online at http://npg.nature.com/reprintsandpermissions/

1. Hay, N. & Sonenberg, N. Upstream and downstream of mTOR. *Genes Dev.* **18,** 1926–1945 (2004).
2. Wullschleger, S., Loewith, R. & Hall, M. N. TOR signaling in growth and metabolism. *Cell* **124,** 471–484 (2006).
3. Sabatini, D. M., Erdjument-Bromage, H., Lui, M., Tempst, P. & Snyder, S. H. RAFT1: a mammalian protein that binds to FKBP12 in a rapamycin-dependent fashion and is homologous to yeast TORs. *Cell* **78,** 35–43 (1994).
4. Jacinto, E. *et al.* Mammalian TOR complex 2 controls the actin cytoskeleton and is rapamycin insensitive. *Nature Cell Biol.* **6,** 1122–1128 (2004).
5. Loewith, R. *et al.* Two TOR complexes, only one of which is rapamycin sensitive, have distinct roles in cell growth control. *Mol. Cell* **10,** 457–468 (2002).
6. Sarbassov, D. D. *et al.* Rictor, a novel binding partner of mTOR, defines a rapamycin-insensitive and raptor-independent pathway that regulates the cytoskeleton. *Curr. Biol.* **14,** 1296–1302 (2004).
7. Fingar, D. C., Salama, S., Tsou, C., Harlow, E. & Blenis, J. Mammalian cell size is controlled by mTOR and its downstream targets S6K1 and 4EBP1/eIF4E. *Genes Dev.* **16,** 1472–1487 (2002).
8. Blommaart, E. F., Luiken, J. J., Blommaart, P. J., van Woerkom, G. M. & Meijer, A. J. Phosphorylation of ribosomal protein S6 is inhibitory for autophagy in isolated rat hepatocytes. *J. Biol. Chem.* **270,** 2320–2326 (1995).
9. Noda, T. & Ohsumi, Y. Tor, a phosphatidylinositol kinase homologue, controls autophagy in yeast. *J. Biol. Chem.* **273,** 3963–3966 (1998).
10. Shigemitsu, K. *et al.* Regulation of translational effectors by amino acid and mammalian target of rapamycin signaling pathways. Possible involvement of autophagy in cultured hepatoma cells. *J. Biol. Chem.* **274,** 1058–1065 (1999).
11. Gingras, A. C., Kennedy, S. G., O'Leary, M. A., Sonenberg, N. & Hay, N. 4E-BP1, a repressor of mRNA translation, is phosphorylated and inactivated by the Akt(PKB) signaling pathway. *Genes Dev.* **12,** 502–513 (1998).
12. Thomas, G. The S6 kinase signaling pathway in the control of development and growth. *Biol. Res.* **35,** 305–313 (2002).
13. Inoki, K., Li, Y., Zhu, T., Wu, J. & Guan, K. L. TSC2 is phosphorylated and inhibited by Akt and suppresses mTOR signalling. *Nature Cell Biol.* **4,** 648–657 (2002).
14. Manning, B. D., Tee, A. R., Logsdon, M. N., Blenis, J. & Cantley, L. C. Identification of the tuberous sclerosis complex-2 tumor suppressor gene product tuberin as a target of the phosphoinositide 3-kinase/akt pathway. *Mol. Cell* **10,** 151–162 (2002).
15. Potter, C. J., Pedraza, L. G. & Xu, T. Akt regulates growth by directly phosphorylating Tsc2. *Nature Cell Biol.* **4,** 658–665 (2002).
16. Kwiatkowski, D. J. Rhebbing up mTOR: new insights on TSC1 and TSC2, and the pathogenesis of tuberous sclerosis. *Cancer Biol. Ther.* **2,** 471–476 (2003).
17. Long, X., Ortiz-Vega, S., Lin, Y. & Avruch, J. Rheb binding to mammalian target of rapamycin (mTOR) is regulated by amino acid sufficiency. *J. Biol. Chem.* **280,** 23433–23436 (2005).
18. Sancak, Y. *et al.* PRAS40 is an insulin-regulated inhibitor of the mTORC1 protein kinase. *Mol. Cell* **25,** 903–915 (2007).
19. Hara, K. *et al.* Amino acid sufficiency and mTOR regulate p70 S6 kinase and eIF-4E BP1 through a common effector mechanism. *J. Biol. Chem.* **273,** 14484–14494 (1998).
20. Byfield, M. P., Murray, J. T. & Backer, J. M. hVps34 is a nutrient-regulated lipid kinase required for activation of p70 S6 kinase. *J. Biol. Chem.* **280,** 33076–33082 (2005).
21. Nobukuni, T. *et al.* Amino acids mediate mTOR/raptor signaling through activation of class 3 phosphatidylinositol 3OH-kinase. *Proc. Natl Acad. Sci. USA* **102,** 14238–14243 (2005).
22. Nakashima, N., Noguchi, E. & Nishimoto, T. *Saccharomyces cerevisiae* putative G protein, Gtr1p, which forms complexes with itself and a novel protein designated as Gtr2p, negatively regulates the Ran/Gsp1p G protein cycle through Gtr2p. *Genetics* **152,** 853–867 (1999).
23. Bun-Ya, M., Harashima, S. & Oshima, Y. Putative GTP-binding protein, Gtr1, associated with the function of the Pho84 inorganic phosphate transporter in *Saccharomyces cerevisiae*. *Mol. Cell Biol.* **12,** 2958–2966 (1992).
24. Nakashima, N., Hayashi, N., Noguchi, E. & Nishimoto, T. Putative GTPase Gtr1p genetically interacts with the RanGTPase cycle in *Saccharomyces cerevisiae*. *J. Cell Sci.* 109 (Pt 9), 2311–2318 (1996).
25. Dubouloz, F., Deloche, O., Wanke, V., Cameroni, E. & De Virgilio, C. The TOR and EGO protein complexes orchestrate microautophagy in yeast. *Mol. Cell* **19,** 15–26 (2005).
26. Gao, M. & Kaiser, C. A. A conserved GTPase-containing complex is required for intracellular sorting of the general amino-acid permease in yeast. *Nature Cell Biol.* **8,** 657–667 (2006).
27. Schurmann, A., Brauers, A., Massmann, S., Becker, W. & Joost, H. G. Cloning of a novel family of mammalian GTP-binding proteins (RagA, RagBs, RagB1) with remote similarity to the Ras-related GTPases. *J. Biol. Chem.* **270,** 28982–28988 (1995).
28. Sekiguchi, T., Hirose, E., Nakashima, N., Ii, M. & Nishimoto, T. Novel G proteins, Rag C and Rag D, interact with GTP-binding proteins, Rag A and Rag B. *J. Biol. Chem.* **276,** 7246–7257 (2001).
29. Hirose, E., Nakashima, N., Sekiguchi, T. & Nishimoto, T. RagA is a functional homologue of *S. cerevisiae* Gtr1p involved in the Ran/Gsp1–GTPase pathway. *J. Cell Sci.* **111,** 11–21 (1998).
30. Giot, L. *et al.* A protein interaction map of *Drosophila melanogaster*. *Science* **302,** 1727–1736 (2003).
31. Harrington, L. S. *et al.* The TSC1-2 tumor suppressor controls insulin–PI3K signaling via regulation of IRS proteins. *J. Cell Biol.* **166,** 213–223 (2004).
32. Shah, O. J., Wang, Z. & Hunter, T. Inappropriate activation of the TSC/Rheb/mTOR/S6K cassette induces IRS1/2 depletion, insulin resistance, and cell survival deficiencies. *Curr. Biol.* **14,** 1650–1656 (2004).
33. Sarbassov, D. D., Guertin, D. A., Ali, S. M. & Sabatini, D. M. Phosphorylation and regulation of Akt/PKB by the rictor–mTOR complex. *Science* **307,** 1098–1101 (2005).
34. Inoki, K., Li, Y., Xu, T. & Guan, K. L. Rheb GTPase is a direct target of TSC2 GAP activity and regulates mTOR signaling. *Genes Dev.* **17,** 1829–1834 (2003).
35. Oldham, S., Montagne, J., Radimerski, T., Thomas, G. & Hafen, E. Genetic and biochemical characterization of dTOR, the *Drosophila* homolog of the target of rapamycin. *Genes Dev.* **14,** 2689–2694 (2000).
36. Zhang, H., Stallock, J. P., Ng, J. C., Reinhard, C. & Neufeld, T. P. Regulation of cellular growth by the *Drosophila* target of rapamycin dTOR. *Genes Dev.* **14,** 2712–2724 (2000).
37. Colombani, J. *et al.* A nutrient sensor mechanism controls *Drosophila* growth. *Cell* **114,** 739–749 (2003).
38. Saucedo, L. J. *et al.* Rheb promotes cell growth as a component of the insulin/TOR signalling network. *Nature Cell Biol.* **5,** 566–571 (2003).
39. Radimerski, T., Montagne, J., Hemmings-Mieszczak, M. & Thomas, G. Lethality of *Drosophila* lacking TSC tumor suppressor function rescued by reducing dS6K signaling. *Genes Dev.* **16,** 2627–2632 (2002).
40. Zhang, Y., Billington, Jr., C. J., Pan, D. & Neufeld, T. P. *Drosophila* target of rapamycin kinase functions as a multimer. *Genetics* **172,** 355–362 (2006).
41. Scott, R. C., Schuldiner, O. & Neufeld, T. P. Role and regulation of starvation-induced autophagy in the *Drosophila* fat body. *Dev. Cell* **7,** 167–178 (2004).
42. Klionsky, D. J., Cuervo, A. M. & Seglen, P. O. Methods for monitoring autophagy from yeast to human. *Autophagy* **3,** 181–206 (2007).
43. Britton, J. S., Lockwood, W. K., Li, L., Cohen, S. M. & Edgar, B. A. *Drosophila's* insulin/PI3-kinase pathway coordinates cellular metabolism with nutritional conditions. *Dev. Cell* **2,** 239–249 (2002).
44. Juhasz, G., Erdi, B., Sass, M. & Neufeld, T. P. Atg7-dependent autophagy promotes neuronal health, stress tolerance, and longevity but is dispensable for metamorphosis in *Drosophila*. *Genes Dev.* **21,** 3061–3066 (2007).
45. Juhasz, G. *et al.* The class III PI(3)K Vps34 promotes autophagy and endocytosis but not TOR signaling in *Drosophila*. *J. Cell Biol.* **181,** 655–666 (2008).
46. Clemens, J. C. *et al.* Use of double-stranded RNA interference in *Drosophila* cell lines to dissect signal transduction pathways. *Proc. Natl Acad. Sci. USA* **97,** 6499–6503 (2000).
47. Scott, R. C., Juhasz, G. & Neufeld, T. P. Direct induction of autophagy by Atg1 inhibits cell growth and induces apoptotic cell death. *Curr. Biol.* **17,** 1–11 (2007).
48. Hennig, K. M., Colombani, J. & Neufeld, T. P. TOR coordinates bulk and targeted endocytosis in the *Drosophila melanogaster* fat body to regulate cell growth. *J. Cell Biol.* **173,** 963–974 (2006).

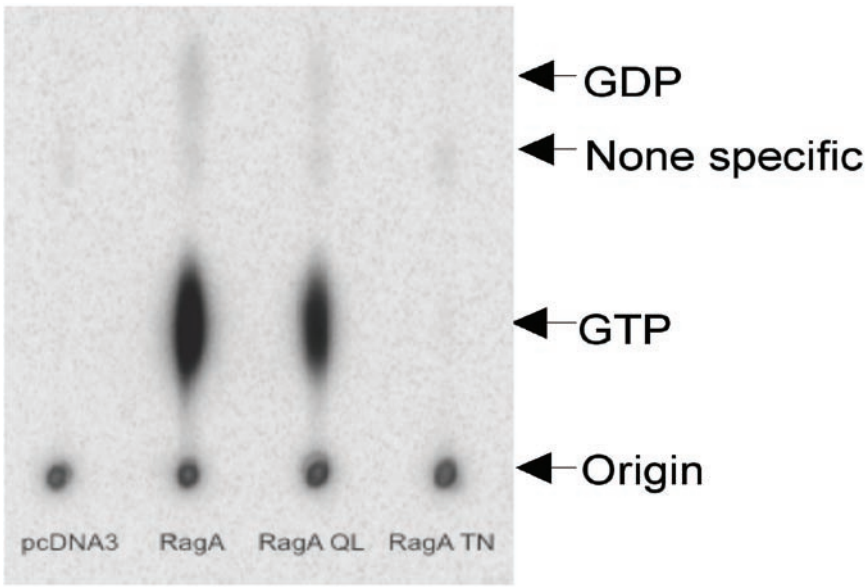

Figure S1 Nucleotide binding status of RagA mutants. Wild type and mutant forms of Myc-RagA was transfected into HEK293 cells and the transfected cells were labeled with ^{32}P-phosphate. Myc-RagA was immunoprecipitated and the bound nucleotides were eluted and analyzed by thin layer chromatography. Transfection of pCDNA3 vector was included as a negative control.

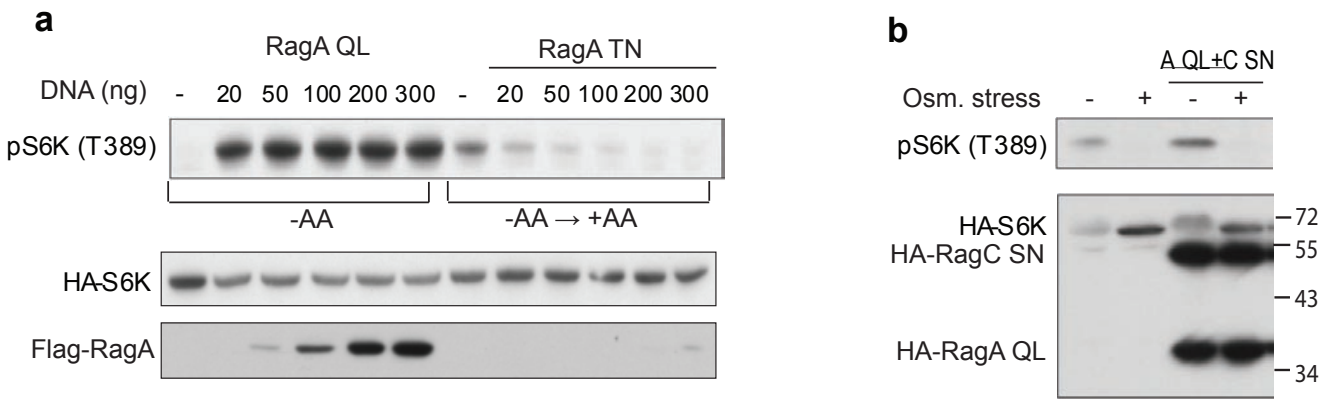

Figure S2 Rag is specifically involved in nutrient signaling. (**a**) RagA T21N inhibits S6K phosphorylation in a dose dependent manner. Each indicated amount (ng) of RagA Q66L or RagA T21N was co-transfected with HA-S6K. RagA Q66L transfected cells were AA starved for 1 h and RagA T21N transfected cells were AA starved for 1 h and stimulated with AA for 30 min. Phosphorylation and protein levels were determined by immunoblotting with appropriate antibodies, as indicated. A low protein level of RagA T21N could be detected with 300 ng of transfection. (**b**) Rag cannot reverse the inhibitory effect by osmotic stress. 200 ng of pcDNA3 or each indicated Rag construct was co-transfected with HA-S6K into HEK293 cells. For osmotic stress, cells were treated with 600 mM of sorbitol for 30 min before harvest. Phosphorylation and protein levels were determined by immunoblotting with appropriate antibodies, as indicated.

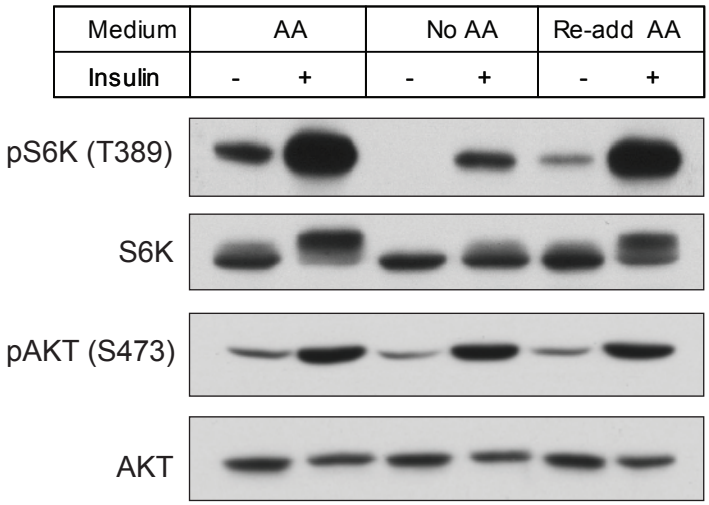

Figure S3 Amino acid starvation diminishes the stimulatory effect of insulin on TORC1 but not TORC2. HeLa cells were serum starved for 16 h. Cells were then remained in serum starvation media or switched to AA starvation media (No AA). After 1 h of AA starvation, cells were either remained in AA starvation media or stimulated with AA containing media (re-add AA) for 30 min. Insulin (400 nM) was added for 30 min before harvest. Phosphorylation and expression levels of endogenous proteins were detected by immunoblotting with the indicated antibodies.

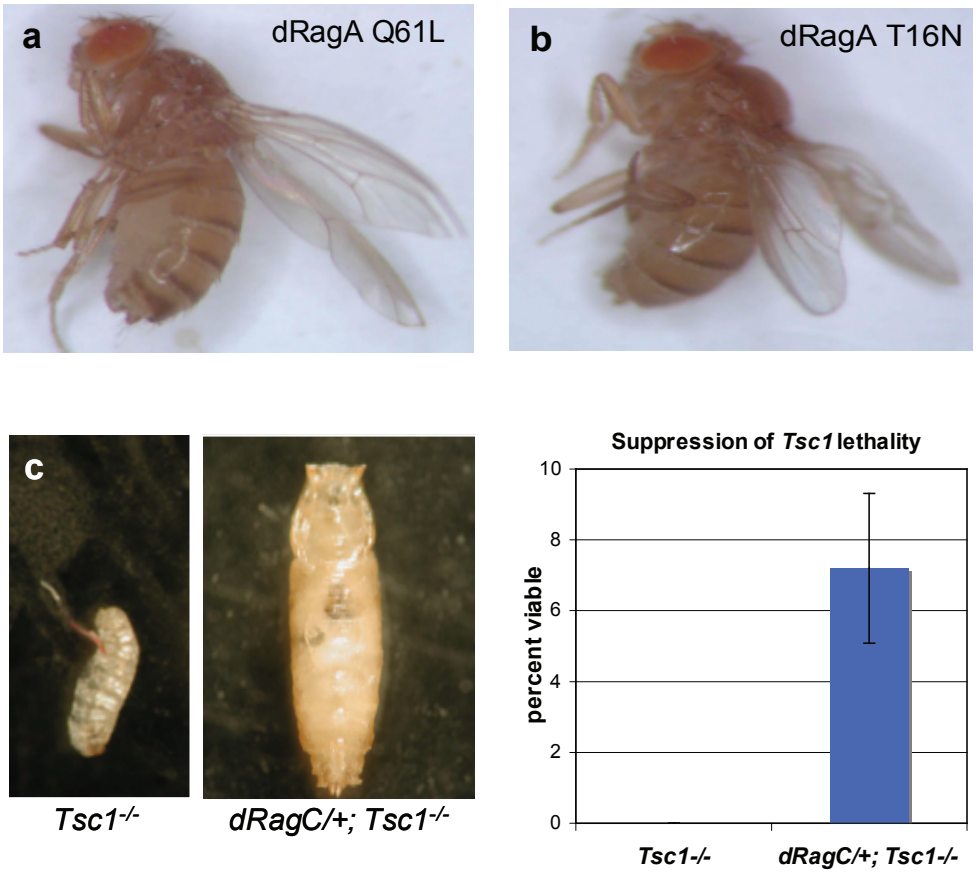

Figure S4 Genetic interactions and growth effects of dRag GTPases in *Drosophila*. (**a, b**) dRagA expression affects wing growth. Expression of dRagA Q61L (**a**) or dRagA T16N (**b**) in the dorsal epithelial cells of the wing using the ap-GAL4 driver results in downward (increased rate of growth) or upward (decreased rate of growth) curvature of the wing blade, respectively, reflecting an altered rate of growth in these cells. (**c, d**) *dRagC* mutation dominantly suppresses the lethality of *Tsc1* null homozygous mutant animals. $Tsc1^{29}$ mutants die at the early second instar larval stage. Mutation of a single copy of *dRagC* in the $Tsc1^{29}$ null background partially rescues the lethality, allowing survival to the pupal stage in 7.4% of animals (n = 474).

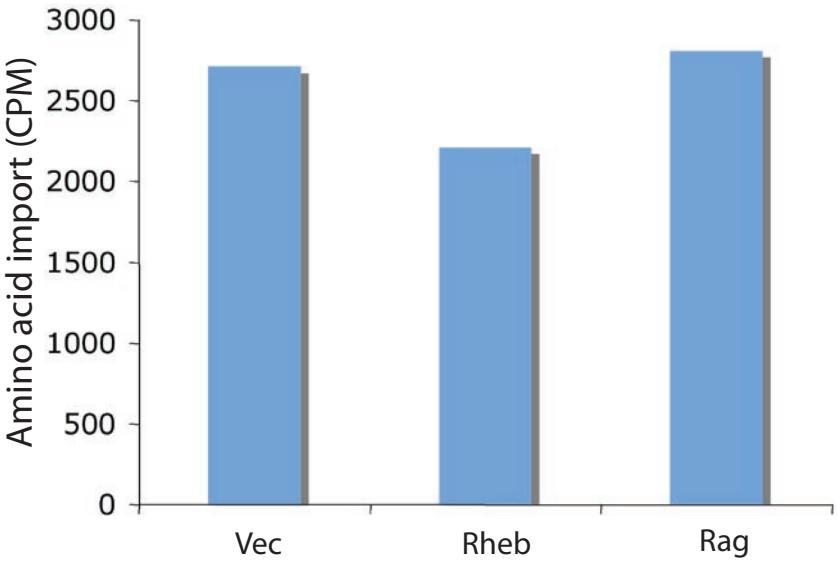

Figure S5 Rag does not affect amino acid import. Rheb S16H (labeled as Rheb) or RagA Q66L and RagC S75N (labeled as Rag) expressing stable clones of HeLa cells were incubated with [^{3}H]-labeled amino acid mixture in the presence of 2 mM cold amino acids. Cells were washed with PBS before lysis and radioactivity in the lysates were counted. The amino acid import is specific because the increase of radioactivity inside cells could be completely competed by a high concentration of amino acid in the culture medium in a dose dependent manner (data not shown).

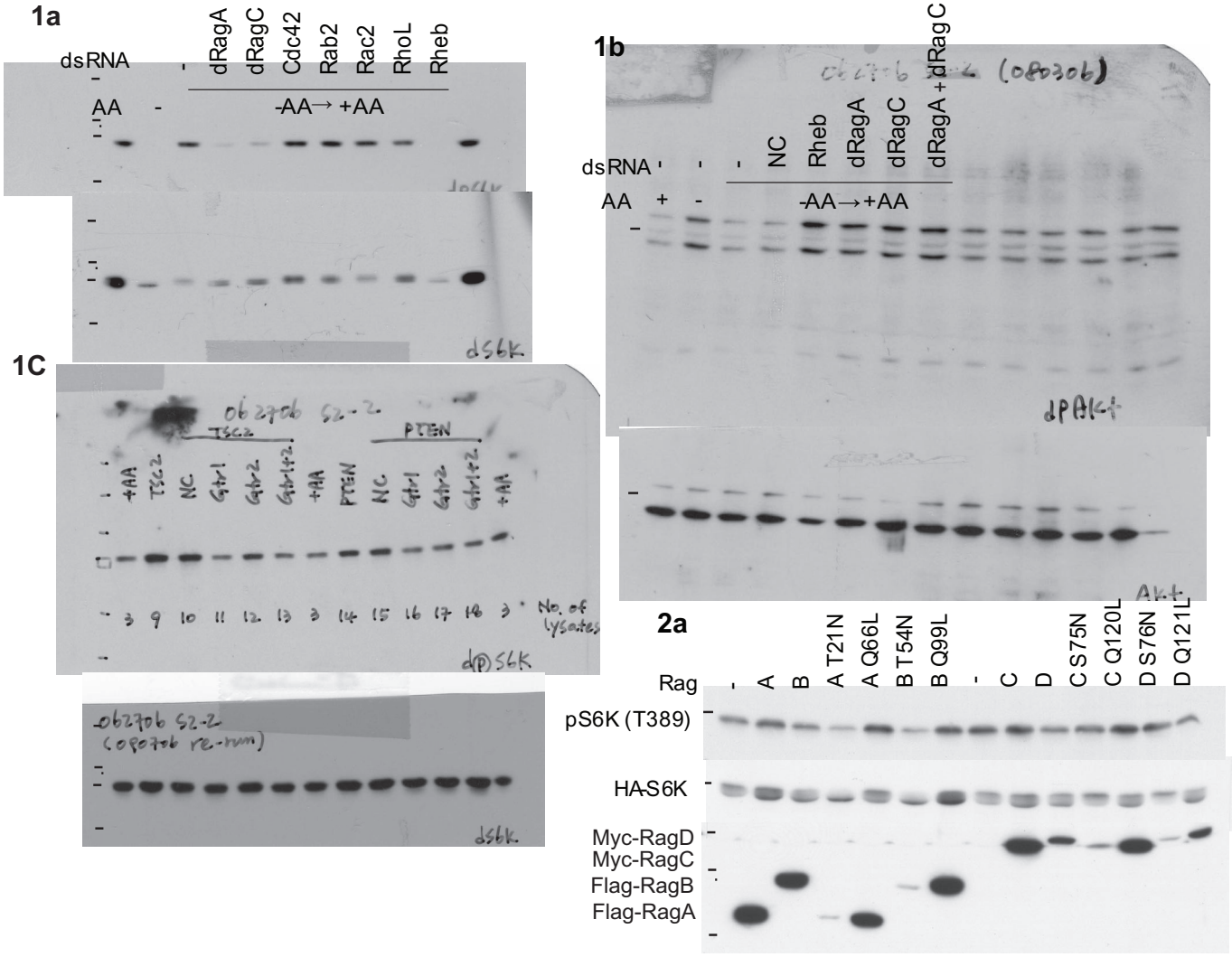

Figure S6 Full scans of original blots for data in figure 1, 2, 3, 5, and 7e. Panels corresponding to the figures in the paper are indicated.

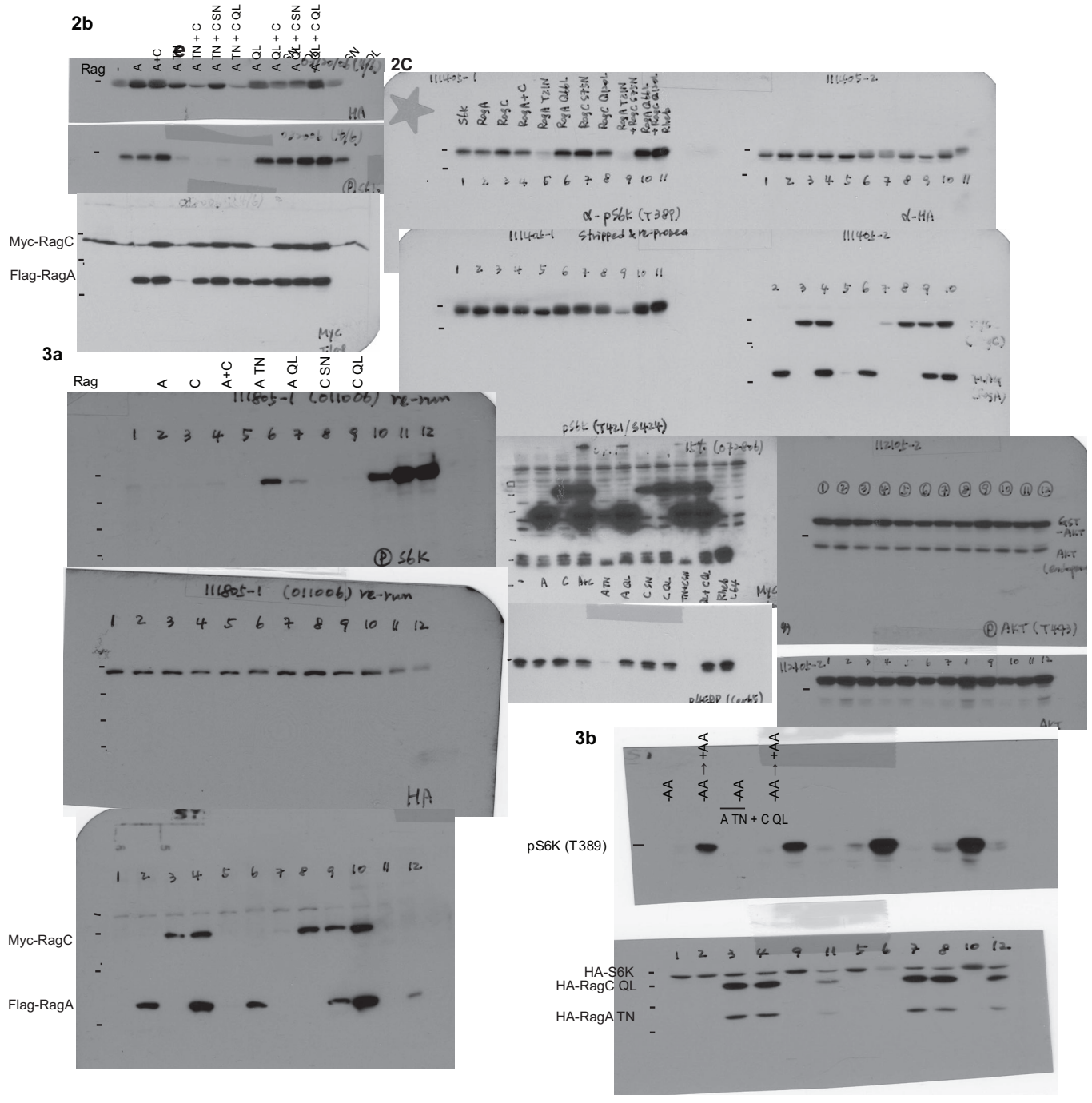

Figure S6 continued

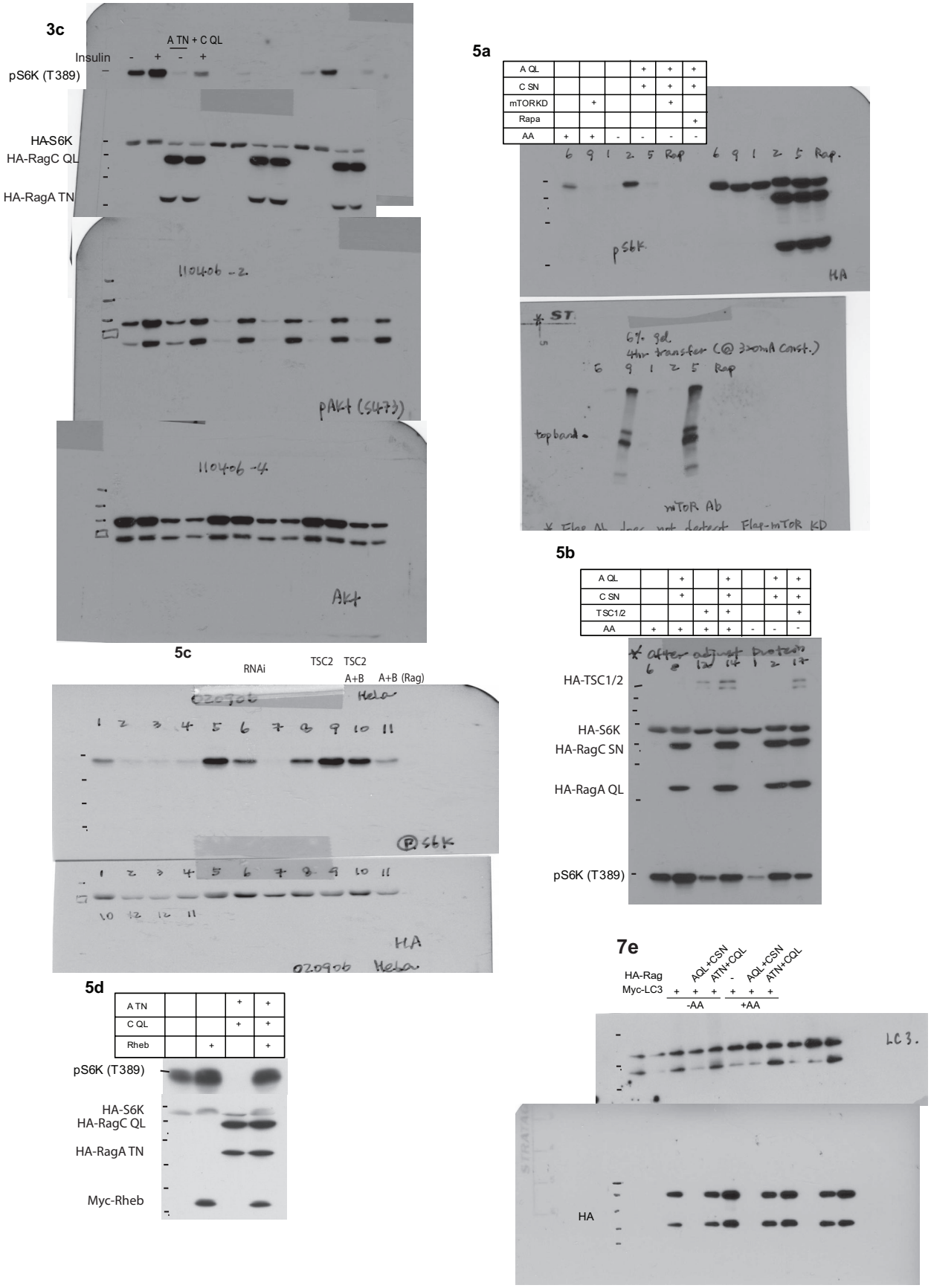

Figure S6 continued

Supplementary Methods

GTP Labeling Assay

GTP labeling assay was performed as described[1]. Briefly, HEK293 cells were cultured in six-well plates and transfected with either pcDNA3 or Myc-RagA constructs using Lipofectamine reagent (Invitrogen). Thirty six hours later, cells were washed with phosphate-free DMEM (GIBCO Cat. No. 11971) and incubated with 1 ml of phosphate-free DMEM for 90 min. Cells were then incubated with 25 μCi of [^{32}P]phosphate/ml for 4 hr. After labeling, cells were lysed with prechilled lysis buffer (0.5% NP-40, 50 mM Tris [pH 7.5], 100 mM NaCl, 10 mM $MgCl_2$, 1 mM dithiothreitol(DTT), 1 mM phenylmethylsulfonyl fluoride, 10 μg of leupeptin/ml, 10 μg of aprotinin/ml) for just 30 sec on ice. The lysates were then centrifuged at 12,000 X g for 15 min at 4°C. The supernatant (160 μl) was transferred to a fresh tube and 16 μl of NaCl (500 mM) was added to inhibit GAP activity. Myc-RagA was then immunoprecipitated with anti-Myc antibody and protein-G sepharose bead slurry (50%, Amersham Biosciences) for 1 hr at 4°C. The beads were washed with wash buffer 1 (50 mM Tris [pH 8.0], 500 mM NaCl, 5 mM $MgCl_2$, 1 mM DTT, 0.5% Triton X-100) three times at 4°C and then washed with wash buffer 2 (50 mM Tris [pH 8.0], 100 mM NaCl, 5 mM $MgCl_2$, 1 mM DTT, 0.1% Triton X-100) three times at 4°C. The RagA-bound nucleotides were eluted with 20 μl of elution buffer (2 mM EDTA, 0.2% sodium dodecyl sulfate, 1 mM GDP, 1 mM GTP) at 68°C for 10 min. The eluted nucleotides were applied onto polyethyleneimine cellulose plates (Baker-flex) and developed in 0.75 M KH_2PO_4[pH 3.4] solution. GTP and GDP was visualized and quantified by a phosphoimager.

Amino Acids Incorporation Assay

Tritiated-amino acids uptake was determined as described with modifications[2]. Rheb S16H or RagA Q66L and RagC S75N expressing stable clones of HeLa cells were cultured in 12-well plates. When cells reached approximately 70-80% confluency, the culture medium was replaced by amino acid deprived media (DMEMK-AA) for 2 h at 37°C. The medium was then replaced by 1 ml of amino acids sufficient media (DMEMK, total amino acids concentration: 2 mM) containing [^{3}H]-labeled amino acids mixture (GE Health Care, TRK440) at a concentration of 2 μCi/ml (~ 0.02 μM amino acid mixture) for 15 min at 37°C. Cells were washed three times with ice-cold PBS on ice and 250 μl of 1 M NaOH were added to lyse cells. After incubation for 10 min at 4°C, 250 μl of 1 M HCl was added to neutralize pH. Cell lysates were centrifuged at 13,200 rpm for 10 min at 4°C and the supernatant was used for protein quantification as well as for radioactivity counting.

Supplementary references

1. Li, Y., Inoki, K. & Guan, K.L. Biochemical and functional characterizations of small GTPase Rheb and TSC2 GAP activity. *Mol Cell Biol* **24**, 7965-7975 (2004).
2. Fang, J., Mao, D., Smith, C.H. & Fant, M.E. IGF regulation of neutral amino acid transport in the BeWo choriocarcinoma cell line (b30 clone): evidence for MAP kinase-dependent and MAP kinase-independent mechanisms. *Growth Horm IGF Res* **16**, 318-325 (2006).

Amino Acid Signaling to TOR Activation: Vam6 Functioning as a Gtr1 GEF

Li Li[1,2] and Kun-Liang Guan[1,*]
[1]Department of Pharmacology and Moores Cancer Center, University of California, San Diego, La Jolla, CA 92093, USA
[2]Department of Biological Chemistry, University of Michigan, Ann Arbor, MI 48109, USA
*Correspondence: kuguan@ucsd.edu
DOI 10.1016/j.molcel.2009.08.010

In this issue of *Molecular Cell*, Binda et al. identify Vam6/Vps39 as a guanine nucleotide exchange factor for Gtr1, a Rag family GTPase, to promote TORC1 activation in response to amino acids.

In unicellular organisms, such as the budding yeast *Sachromyces cerevisiae*, cell growth is largely governed by the availability of nutrients. However, growth of higher eukaryotic cells requires growth factors in addition to nutrients. The target of rapamycin (TOR) is a central cell growth controller in both yeast and mammalian cells. TOR is a member of the phosphoinositide 3-kinase-related protein kinase family that is important for normal physiology and development in various species (Wullschleger et al., 2006). Uncontrolled mammalian TOR (mTOR) activation also contributes to tumor development (Sarbassov et al., 2005). TOR exists in two distinct complexes, TORC1 and TORC2, which differ in subunit compositions and biological functions (Loewith et al., 2002). TORC1 is potently and specifically inhibited by the drug rapamycin, whereas TORC2 is not directly sensitive to rapamycin. In mammalian cells, TORC1 phosphorylates S6K1 and 4EBP1, two proteins in translation control, whereas TORC2 is required for phosphorylation and activation of Akt, SGK, and conventional PKC (Yang and Guan, 2007).

As a key growth regulator, TORC1 is activated by nutrients, such as amino acids, and cellular energy status (Wullschleger et al., 2006). The molecular mechanisms of mTORC1 regulation by growth factors and cellular energy status have been extensively studied (Figure 1). However, the mechanism of TORC1 activation by amino acids is largely unknown, although amino acids are the most potent activators of TORC1 (Hara et al., 1998). Significant progress has been made with recent biochemical and genetic studies demonstrating that Rag family GTPases, which belong to the Ras superfamily, are key mediators between amino acids and TORC1 activation (Kim et al., 2008; Sancak et al., 2008). The Rag GTPases are highly conserved from yeast to mammals. In humans, there are four Rag genes, RagA, B, C, and D. RagA and RagB are closely related to each other, and RagC and RagD are closely related to each other, whereas the homology between RagA/B and RagC/D is limited (Sekiguchi et al., 2001). A unique feature of these GTPases is that they form heterodimers. RagA or RagB forms stable heterodimers with RagC or RagD via their respective C-terminal regions, and it is the heterodimer that fully activates mTORC1 (Kim et al., 2008; Sancak et al., 2008). It is worth noting that no other Ras family GTPase is known to form a dimer. Another unique property of the Rag GTPases is that, within the heterodimer, the two GTPases bind different forms of guanine nucleotides; one binds GTP, and the other binds GDP. Only when RagA/B is in GTP form and RagC/D is in GDP form is the heterodimer fully active and able to stimulate TORC1. In addition, RagA/B has a dominant role over RagC/D in TORC1 activation. The active Rag heterodimer can directly bind to raptor, which is a key subunit in TORC1. This interaction between Rag and raptor depends on the GTP-binding status of RagA/B. However, unlike Rheb, which can activate TORC1 kinase activity by binding (Figure 1), Rag is unable to activate TORC1 by binding alone. It has been proposed that Rag may activate TORC1 by transporting TORC1 to the vicinity of Rheb (Sancak et al., 2008), but this model needs further verification. Furthermore, how Rags are activated in response to amino acids remains unknown. Now, Binda et al. provide some insights into this process.

The budding yeasts Gtr1 and Gtr2 are highly homologous to RagA/B and RagC/D, respectively, and also form a heterodimer (Figure 1). Interestingly, Gtr1 and Gtr2 are important for recovery from rapamycin treatment, indicating their possible roles in TOR regulation (Dubouloz et al., 2005). In the report by Binda et al., the authors showed that Gtr1 and Gtr2 indeed play an important role in TORC1 activation in response to amino acids, indicating that the function of Rag family GTPase is conserved in eukaryotes (Binda et al., 2009). Similar to the mammalian Rag GTPases, the Gtr1-GTP and Gtr2-GDP complex is the active form in TORC1 activation. The yeast genetic study also identified two additional proteins required for TORC1 activation: EGO1 and EGO3. These two factors are components of a complex involved in microautophagy regulation known as the EGO complex, and the identification of these proteins in TORC1 activation indicates that it is the EGO complex, not just Gtr1/Gtr2, that stimulates TORC1 activation in response to amino acids. However, unlike RagA/B-GTP, which can completely restore mammalian TORC1 activation in amino-acid-free conditions, Gtr1-GTP only partially activates yeast TORC1. Another noticeable difference between yeast and mammalian cells is that amino acids apparently do not alter the subcellular localization of Tor1 and Tco89 (a TORC1 component). In addition, the subcellular localization of Gtr1 and Gtr2 is not affected by amino acids. Therefore, the proposed mechanism of TORC1 activation via the amino-acid-induced subcellular localization of TORC1 may not be conserved.

In an attempt to isolate Gtr1 regulators, the authors performed a synthetic

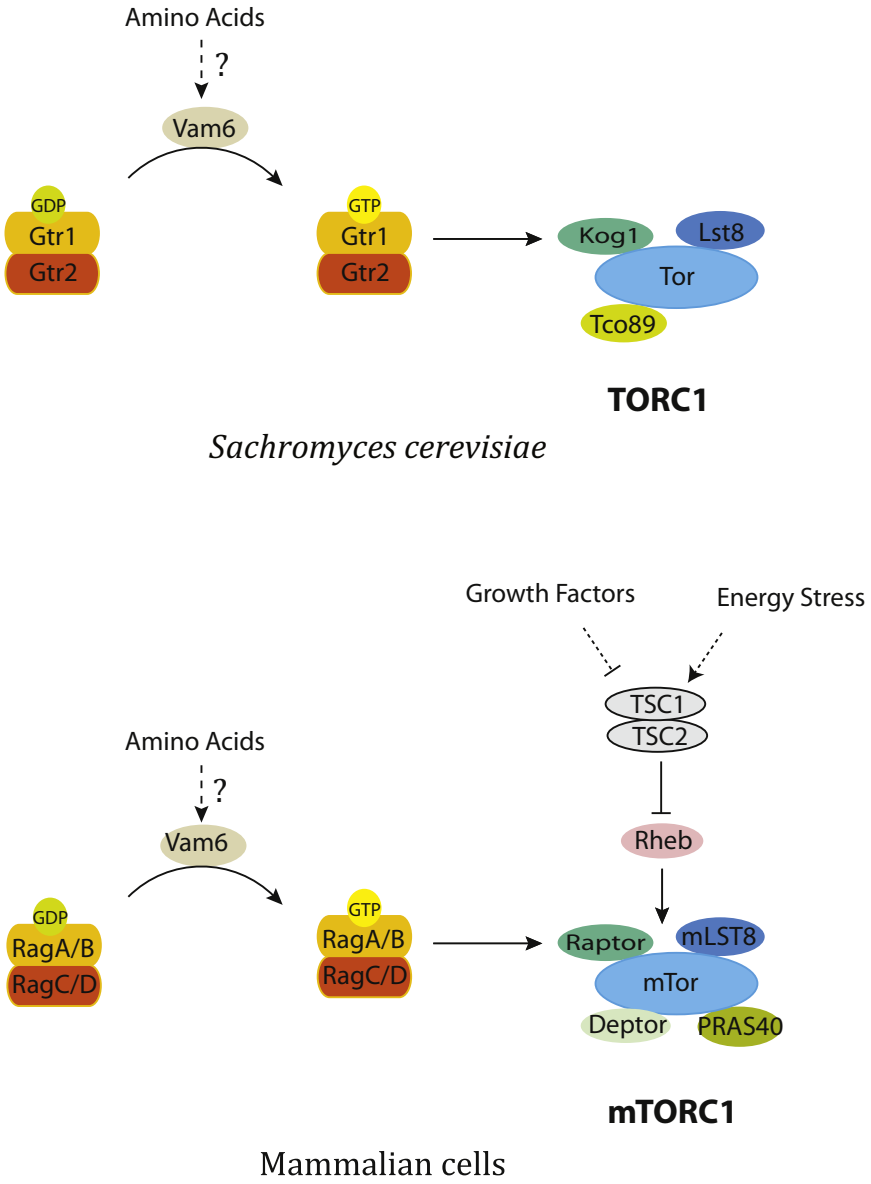

Figure 1. Functions of Vam6 and Rag GTPases in TORC1 Activation by Amino Acids
Corresponding genes in *S. cerevisiae* and human are shown in the same color. Dashed lines denote an indirect connection, whereas solid arrows indicate a direct effect. Because whether Vam6 stimulates Gtr2 nucleotide exchange is unknown, the guanine nucleotides in Gtr2 and RagC/D are not shown in order to avoid potential confusion.

genetic screen. Overexpression of a GDP-binding mutant of Gtr1-GDP partially inhibits yeast growth. The authors hypothesized that mutation of a Gtr1 activator, such as a guanine nucleotide exchange factor (GEF), would further enhance the Gtr1-GDP-expressing phenotype. Based on this synthetic genetic screen, the two strongest hits isolated are *gtr1Δ* and *vam6Δ*. Indeed, further genetic studies demonstrate that overexpression of Vam6 (also known as Vps39) suppresses the defects caused by Gtr1-GDP overexpression, consistent with the prediction that Vam6 might be a Gtr1 GEF. Notably, Vam6 is a known GEF for Ypt7, a Rab7 homolog that is involved in intracellular trafficking. This prompted the authors to test whether Vam6 has direct GEF activity toward Gtr1.

In vitro nucleotide exchange experiments using purified recombinant proteins unequivocally showed that Vam6 strongly promotes nucleotide exchange of Gtr1. Recombinant Vam6 stimulated GDP release from Gtr1 as efficiently as it did for Ypt7. In contrast, Vam6 did not affect the nucleotide release of a control protein Ras. Moreover, TORC1 activation is blunted in *vam6Δ* mutant yeast in response to amino acid stimulation, as determined by a decreased phosphorylation of Sch9. To determine the in vivo role of *VAM6* in *GTR1* regulation, the authors used an assay based on the interaction between Gtr1 and Ego1, which is a key component of the EGO complex that includes Gtr1 and Gtr2. Gtr1 interacts with Ego1 in a manner depending on Gtr1 GTP binding. The authors found that the interaction between Gtr1 and Ego1 was dramatically decreased in *vam6Δ* strain, indicating an in vivo role of *VAM6* in *GTR1* activation. Collectively, these results strongly demonstrate that Vam6 is a Gtr1 GEF and may mediate amino acid signals to Gtr1 activation, therefore leading to TORC1 activation (Figure 1).

The current study not only confirmed the Rag family GTPases as key upstream activators of TORC1 in response to amino acids in yeast, but more importantly, identified Vam6 as a GEF for Gtr1. These observations significantly advanced our current understanding of amino acid signaling and TORC1 activation. Given the fact that Gtr1 GTP binding is stimulated by amino acids, Vam6 may mediate the amino acid signals to TORC1 activation. However, several key issues remain to be addressed. Because amino acids do not affect Tor1 and Tco89 localization, how does Gtr1/Gtr2 affect the TORC1 activity in yeast? TORC1 regulation in *S. cerevisiae* is rather different from that in higher eukaryotes, as the budding yeast has no TSC1 and TSC2, which are important upstream negative regulators of TORC1. Is the function of *VAM6/VPS39* conserved in the high eukaryotes? Furthermore, does Vam6 directly sense intracellular amino acids? And how is Vam6 activity regulated in response to amino acid signals? Given the fact that *VAM6* is involved in intracellular vesicle trafficking, does this machinery play a role in TORC1 regulation? What is the function of the EGO complex in TORC1 activation? Does the

amino acid sensing and Gtr1 activation occur on intracellular vesicles where Vam6 is localized? The identification of Vam6 as the Rag family GTPase GEF certainly raises many exciting new questions for understanding the mechanism of TORC1 activation by amino acids and the coordination between cell growth and nutrient sensing.

REFERENCES

Binda, M., Peli-Gulli, M.-P., Bonfils, G., Panchaud, N., Urban, J., Sturgill, T.W., Loewith, R., and De Virgilio, C. (2009). Mol. Cell *35*, this issue, 563–573.

Dubouloz, F., Deloche, O., Wanke, V., Cameroni, E., and De Virgilio, C. (2005). Mol. Cell *19*, 15–26.

Hara, K., Yonezawa, K., Weng, Q.P., Kozlowski, M.T., Belham, C., and Avruch, J. (1998). J. Biol. Chem. *273*, 14484–14494.

Kim, E., Goraksha-Hicks, P., Li, L., Neufeld, T.P., and Guan, K.L. (2008). Nat. Cell Biol. *10*, 935–945.

Loewith, R., Jacinto, E., Wullschleger, S., Lorberg, A., Crespo, J.L., Bonenfant, D., Oppliger, W., Jenoe, P., and Hall, M.N. (2002). Mol. Cell *10*, 457–468.

Sancak, Y., Peterson, T.R., Shaul, Y.D., Lindquist, R.A., Thoreen, C.C., Bar-Peled, L., and Sabatini, D.M. (2008). Science *320*, 1496–1501.

Sarbassov, D.D., Ali, S.M., and Sabatini, D.M. (2005). Curr. Opin. Cell Biol. *17*, 596–603.

Sekiguchi, T., Hirose, E., Nakashima, N., Ii, M., and Nishimoto, T. (2001). J. Biol. Chem. *276*, 7246–7257.

Wullschleger, S., Loewith, R., and Hall, M.N. (2006). Cell *124*, 471–484.

Yang, Q., and Guan, K.L. (2007). Cell Res. *17*, 666–681.

The Alternating Power Stroke of a 6-Cylinder AAA Protease Chaperone Engine

Wolfgang Kress[1] and Eilika Weber-Ban[1,*]
[1]ETH Zurich, Institute of Molecular Biology and Biophysics, 8093 Zurich, Switzerland
*Correspondence: eilika@mol.biol.ethz.ch
DOI 10.1016/j.molcel.2009.08.013

In this issue of *Molecular Cell*, Augustin et al. (2009) describe the regulatory coupling of adjacent ATP subunits in the mitochondrial AAA protease ring along with the responsible molecular determinants and uncover its importance for membrane dislocation of substrates.

The functional integrity of prokaryotic and eukaryotic cells critically depends on ATP-dependent proteolysis for homeostasis in the cytoplasm and in cellular organelles (Leidhold and Voos, 2007). This activity is carried out by complexes consisting of ATPase rings associated or fused to a protease chamber enclosing the active sites (Striebel et al., 2009). Protein substrates are recruited to the ATPase rings, threaded through their central pores by expending energy and then transferred into the proteolytic chamber for degradation.

At the heart of the activities mediated by these degradation machines lies their engine, the molecular AAA motor that converts the chemical energy of ATP hydrolysis into a mechanical force exerted on protein substrates (Hanson and Whiteheart, 2005). How the energy conversion is achieved and which molecular elements participate are key questions in the field. AAA ATPases form hexameric rings around a central pore with ATP-binding sites located at subunit interfaces. The ATP-binding sites feature the canonical Walker A and B motifs for binding and hydrolysis, respectively, and an arginine from the adjacent subunit (R finger) that contacts the γ-phosphate of bound ATP (Ogura et al., 2004). ATP hydrolysis is coupled to up and down movements of conserved loops contacting the substrate in the central pore of the ATPase ring (Hinnerwisch et al., 2005; Martin et al., 2008; Wang et al., 2001). Described mechanisms for hydrolysis within a ring range from a stochastic model for ClpXP (Martin et al., 2005) to sequential hydrolysis around the ring for an AAA helicase (Enemark and Joshua-Tor, 2006).

In the present study Augustin and colleagues (Augustin et al., 2009) investigate ATP hydrolysis in the hetero-oligomeric mitochondrial m-AAA protease from yeast, which is located in the inner membrane, exposing its catalytic sites to the matrix (Leidhold and Voos, 2007). This system has some unique features. (1) A hetero-oligomeric complex with alternating subunits around the ring allows manipulation of only every other subunit. (2) Due to the essential role m-AAA protease plays in mitochondria, respiratory impairment provides an in vivo read-out of m-AAA protease activity and allows for genetic screening.

By designing Walker A and Walker B variants of the two subunits building the m-AAA ring in yeast (Yta10 and Yta12), the authors show that an allosteric inhibitory effect is exerted by ATP-binding of one subunit on the ability of the following neighboring subunit to hydrolyse ATP. "Empty" Yta12 subunits (Walker A variants defective in ATP-binding) are uncoupled from the allosteric effect and cannot inhibit their Yta10 neighbor,

REPORT

This paper is available online at www.jbc.org

THE JOURNAL OF BIOLOGICAL CHEMISTRY VOL. 285, NO. 26, pp. 19705–19709, June 25, 2010

Regulation of mTORC1 by the Rab and Arf GTPases*[S]

Received for publication, January 12, 2010, and in revised form, May 3, 2010
Published, JBC Papers in Press, May 10, 2010, DOI 10.1074/jbc.C110.102483

Li Li[‡§], Eunjung Kim[¶], Haixin Yuan[‡], Ken Inoki[‖], Pankuri Goraksha-Hicks[**], Rachel L. Schiesher[**], Thomas P. Neufeld[**], and Kun-Liang Guan[‡1]

*From the [‡]Department of Pharmacology and Moores Cancer Center, University of California San Diego, La Jolla, California 92093, the [§]Department of Biological Chemistry and [‖]Life Sciences Institute, University of Michigan, Ann Arbor, Michigan 48109, the [¶]Department of Food Sciences and Nutrition, Catholic University of Daegu, Gyeongsan 712-702, Korea, and the **Department of Genetics, Cell Biology and Development, University of Minnesota, Minneapolis, Minnesota 55455*

The mammalian target of rapamycin (mTOR) is a key cell growth regulator, which forms two distinct functional complexes (mTORC1 and mTORC2). mTORC1, which is directly inhibited by rapamycin, promotes cell growth by stimulating protein synthesis and inhibiting autophagy. mTORC1 is regulated by a wide range of extra- and intracellular signals, including growth factors, nutrients, and energy levels. Precise regulation of mTORC1 is important for normal cellular physiology and development, and dysregulation of mTORC1 contributes to hypertrophy and tumorigenesis. In this study, we screened *Drosophila* small GTPases for their function in TORC1 regulation and found that TORC1 activity is regulated by members of the Rab and Arf family GTPases, which are key regulators of intracellular vesicle trafficking. In mammalian cells, uncontrolled activation of Rab5 and Arf1 strongly inhibit mTORC1 activity. Interestingly, the effect of Rab5 and Arf1 on mTORC1 is specific to amino acid stimulation, whereas glucose-induced mTORC1 activation is not blocked by Rab5 or Arf1. Similarly, active Rab5 selectively inhibits mTORC1 activation by Rag GTPases, which are involved in amino acid signaling, but does not inhibit the effect of Rheb, which directly binds and activates mTORC1. Our data demonstrate a key role of Rab and Arf family small GTPases and intracellular trafficking in mTORC1 activation, particularly in response to amino acids.

The target of rapamycin (TOR)[2] is a large (~280 kDa) protein kinase that regulates cell growth and cell size (1). The function of TOR in promoting cell growth is conserved from yeast to mammals. TOR forms two structurally and functionally distinct complexes, TORC1 and TORC2 (2). Only TORC1, but not TORC2, is directly inhibited by rapamycin. The mammalian TORC1, mTORC1, directly phosphorylates and activates the ribosomal S6 kinase, S6K (3). Because direct kinase assay of mTORC1 is rather challenging, phosphorylation of S6K is the most frequently used readout for mTORC1 activation.

As a key cell growth regulator, TORC1 activity is tightly regulated by mitogenic growth factors, the availability of amino acids, and cellular ATP levels (1). Extensive studies have elucidated the signaling mechanisms of growth factors and cellular energy levels in mTORC1 activation. The TSC1 and TSC2 tumor suppressors are key upstream negative regulators of mTORC1 (4). TSC1 and TSC2 form a complex and function as a GTPase-activating protein (GAP) to inhibit the Rheb GTPase, which can directly bind to and activate mTORC1 (5–9). AKT, which is a protein kinase activated by numerous growth-stimulating signals, such as growth factors, can phosphorylate and inhibit TSC2 and therefore relieve the inhibitory effect of TSC2 on mTORC1 (10, 11). Furthermore, AKT can directly phosphorylate PRAS40, which is a subunit of mTORC1, and thus contribute to mTORC1 activation (9). The mechanism of mTORC1 regulation by cellular energy status has been elucidated. The AMP-activated protein kinase is a key cellular energy sensor and regulates a large number of cellular responses upon energy starvation. The AMP-activated protein kinase inhibits the mTORC1 pathway by phosphorylating TSC2 and raptor, a key subunit of mTORC1, and thereby coordinates cell growth with the availability of cellular energy (12, 13).

Amino acids are the most potent stimulator of mTORC1. In the absence of amino acids, mTORC1 activation by insulin is severely compromised (14). We have recently shown that the Rag family GTPases play an essential role in mTORC1 activation in response to amino acid stimulation (15, 16). In mammalian cells, the RagA or RagB forms heterodimers with either RagC or RagD, and the resulting heterodimers strongly bind to raptor in a manner depending on GTP binding of RagA or RagB (16). It has been suggested that amino acids modulate the subcellular translocation of mTORC1 through Rag GTPases (16). These results indicate that intracellular trafficking may be important in mTORC1 regulation. In this report, we demonstrate that members of the Rab and Arf family GTPases play important roles in mTORC1 activation.

EXPERIMENTAL PROCEDURES

Antibodies, Plasmids, and Chemicals—Anti-*Drosophila* S6 kinase antibody was provided by Mary Stewart (North Dakota State University, Fargo, ND). Anti-phospho *Drosophila* S6K, anti-S6K, anti-phospho S6K, anti-Akt, anti-phospho Akt, and anti-phospho 4EBP1 antibodies were from Cell Signaling. Anti-Myc, anti-HA, and anti-FLAG antibodies were from Santa Cruz Biotechnology, Covance, and Sigma, respectively. RagA/C constructs were made as described previously. Rab5A, Rab7A, Rab10, Rab11A, Rab22, Rab31, and Ran constructs were ob-

* This work was supported, in whole or in part, by National Institutes of Health Grants GM62694 and GM51586 (to K.-L. G.). This work was also supported by Grant DOD W81XWH-09-1-0279 from the United States Department of Defense (to K.-L. G.).

[S] The on-line version of this article (available at http://www.jbc.org) contains supplemental Methods and Figs. S1–S5.

[1] To whom correspondence should be addressed: Moores Cancer Center, University of California San Diego, 3855 Health Sciences Dr., La Jolla, CA 92093-0815. Fax: 858-822-5433; E-mail: kuguan@ucsd.edu.

[2] The abbreviations used are: TOR, target of rapamycin; mTOR, mammalian TOR; S6K, S6 kinase; dS6K, *Drosophila* S6K; GAP, GTPase-activating protein; GFP, green fluorescent protein; HA, hemagglutinin; DMEM, Dulbecco's modified Eagle's medium; RNAi, RNA interference; UAS, upstream activation sequence.

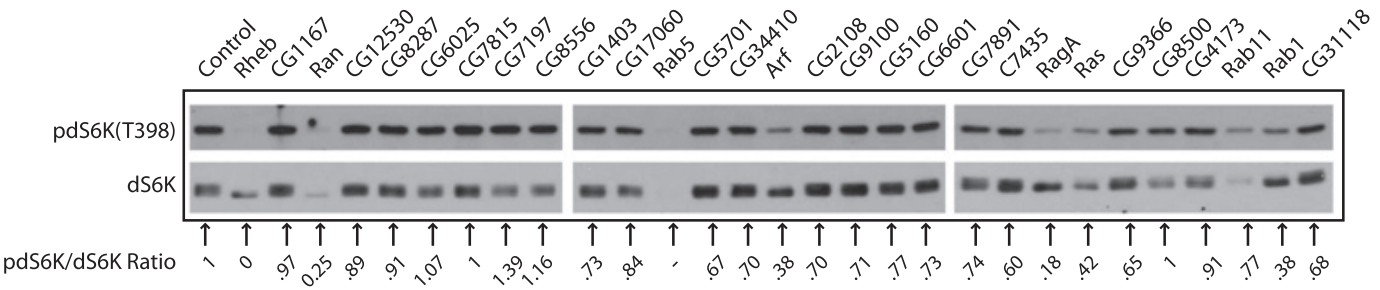

FIGURE 1. **Rab and Arf proteins are indispensable in regulating TORC1 activity in *Drosophila* S2 cells.** *Drosophila* S2 cells untreated (*lane 1*) or treated with the double-stranded RNA against individual genes (as indicated by the *Drosophila* genome CG numbers) were starved of amino acids for 1 h followed by amino acid stimulation for 30 min. Phosphorylation and protein levels of dS6K were determined by immunoblotting with the indicated antibodies. Signals detected by anti-phospho-dS6K (*pdS6K*) and anti-dS6K were quantified, and the ratio was calculated. The control ratio is set to be 1, and all other ratios are the comparison with the control. − means protein signal not detectable.

tained from Drs. X. Chen and A. Saltiel (University of Michigan). Rab5A was subcloned into pBABE-puro retroviral vector. All other DNA constructs, including HA-S6K, Myc-4EBP1, GST-Akt, and Myc-Rheb, were from laboratory stock. Insulin and brefeldin A were obtained from Sigma.

Cell Culture—Drosophila S2 cells (Invitrogen) were cultured in *Drosophila* serum-free medium (Invitrogen) supplemented with 18 mM L-glutamine and maintained at 28 °C. HEK293 cells and HeLa cells were cultured in DMEM supplemented with 10% fetal bovine serum. PC3 cells were cultured in F-12K medium supplemented with 10% fetal bovine serum. Amino acid-containing or -free medium used for *Drosophila* S2 cells were made using Schneider's *Drosophila* medium (Invitrogen) formulation as described previously (15). Amino acid-containing (DMEMK) or amino acid-free (DMEMK-AA) media used for HEK293 and HeLa cells were made using DMEM medium (Invitrogen, catalog number 12430) formulation.

RNA Interference—Drosophila RNA interference (RNAi) experiments were performed as described previously (17).

Transfection and Cell Lysis—Transfection was performed in serum-free conditions using Lipofectamine reagent (Invitrogen) as described by the manufacturer. Cells were lysed in SDS lysis buffer (1% SDS, 0.1 M Tris, pH 7.5).

Drosophila Genetics and Histology—Clonal knockdown of Arf1 in larval fat body cells was performed using the double-stranded RNA UAS line GD12522 from the Vienna *Drosophila* RNAi Center. This line was co-expressed with UAS-dicer to increase RNAi efficiency. Spontaneous flippase-mediated induction of GFP-marked cells and staining with Texas Red-phalloidin and LysoTracker Red (Invitrogen) were performed as described previously (15). Cell area measurements were determined from confocal images of fixed fat body tissues using Adobe Photoshop, as described previously (15). mCherry-Atg8a was expressed and analyzed as described previously (18).

RESULTS AND DISCUSSION

Knockdown of Rab and Arf Decreases TORC1 Activity in Drosophila S2 Cells—To search for GTPases that may regulate TORC1, we used RNAi to knock down all putative small GTPases predicted in the *Drosophila* genome. Examples of GTPase knockdown on dS6K phosphorylation are shown in Fig. 1. Besides Ras, Rheb, and Rag, which are known to regulate TORC1, knockdown of several other small GTPases also significantly decreased dS6K phosphorylation (Fig. 1). Ran GTPase is essential for nuclear import and export (19). In cells treated with double-stranded RNA against Ran, both dS6K protein and phosphorylation were decreased dramatically, possibly due to a reduction of total cell numbers. However, the remaining dS6K displayed a fast migration, indicating that dS6K was dephosphorylated in Ran knockdown S2 cells.

We found that knockdown of Rab5 and Rab11 similarly decreased both dS6K protein and phosphorylation (Fig. 1). Due to a dramatic reduction in dS6K protein, it is unclear whether the relative dS6K phosphorylation was decreased by knockdown of these two GTPases. However, knockdown of Rab1 caused a significant decrease of dS6K phosphorylation as indicated by both the phosphorylation-specific antibody and an increased electrophoretic mobility. Similar results were observed with Arf1 knockdown, and the effects of Rab1 and Arf1 knockdown on dS6K phosphorylation were similar to that caused by RagA knockdown. These results strongly indicate that Rab1 and Arf1 are important for TORC1 activity in *Drosophila* S2 cells.

Constitutive Activation of Rab Inhibits mTORC1—In mammalian cells, there are large numbers of Rab and Arf family GTPases that often have overlapping functions in intracellular trafficking (20, 21). The data from *Drosophila* S2 cells indicate that intracellular vesicle trafficking may play a key role in TORC1 activation. To test this possibility, we overexpressed several constitutively active Rab GTPases in 293 cells to determine their effect on mTORC1 in mammalian cells. As positive controls, expression of either constitutive RagAQL or RhebL64 increased S6K phosphorylation (Fig. 2*A*). We observed that expression of active mutants of Rab5, Rab7, Rab10, and Rab31 potently inhibited S6K phosphorylation. In contrast, expression of active Rab11 had little effect, whereas Rab22 had a minor inhibitory effect on S6K phosphorylation. The inhibitory effect of the Rab GTPases on S6K phosphorylation was surprising because knockdown of these GTPases in *Drosophila* S2 cells also decreased dS6K phosphorylation. However, it is well documented that disruption of GTP cycling of Rab proteins can disrupt normal cellular trafficking (20, 22). Our data suggest that normal intracellular trafficking is critical for proper mTORC1 activation.

To further elucidate the effect of Rab proteins on mTORC1, we picked Rab5 as a representative for further characterization. We tested the effects of wild type, constitutively active, and dominant negative Rab5 on the phosphorylation of S6K

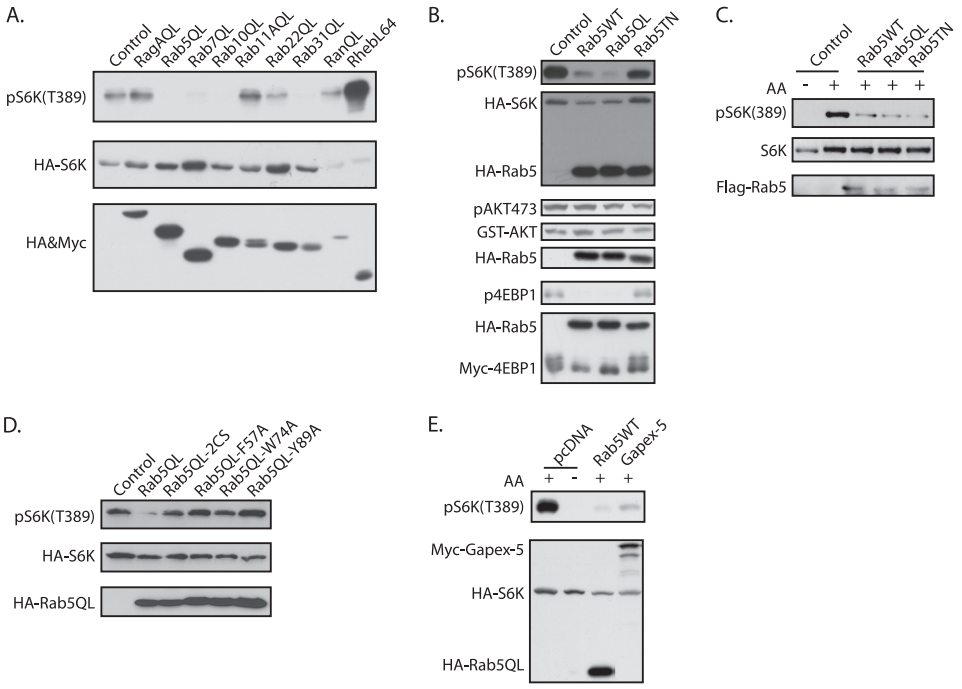

FIGURE 2. **Several mammalian Rab proteins inhibit mTORC1 activity.** *A*, constitutively active Rab proteins inhibit S6K phosphorylation. Each mammalian Rab construct was co-transfected with HA-S6K into HEK293 cells. Phosphorylation and protein levels were determined by immunoblotting with the indicated antibodies. *B*, Rab5 regulates TORC1 but not TORC2 activity. Each indicated Rab protein construct was co-transfected with HA-S6K, Myc-4EBP1, or GST-Akt. Phosphorylation and protein levels were determined by immunoblotting with the indicated antibodies. *Rab5WT*, wild type Rab5. *C*, Rab5 regulates TORC1 activity in PC3 cells. PC3 cells stably express pBABE-puro vector; corresponding Rab5 constructs were generated, and the protein and phosphorylation levels were determined by immunoblotting with the indicated antibodies. *AA+*, amino acid stimulation; *AA−*, amino acid starvation. *D*, the effect of Rab5 on mTORC1 is dependent on its membrane localization and effector binding. Each Rab5 mutant construct was co-transfected with HA-S6K into HEK293 cells. Phosphorylation and protein levels were determined by immunoblotting with the indicated antibodies. *E*, GAPex overexpression inhibits S6K phosphorylation. Either Rab5 or GAPex construct was transfected into HEK293 cells together with HA-S6K. Phosphorylation and protein levels were determined by immunoblotting with the indicated antibodies.

and 4EBP1, two direct substrates of mTORC1 (23). We found that both the wild type and the constitutively active Rab5 strongly inhibited the phosphorylation of co-transfected S6K and 4EBP1, although the Rab5QL was more potent (Fig. 2*B*). The dominant negative Rab5TN also inhibited S6K phosphorylation but was significantly less effective than the active Rab5QL. In addition, the endogenous S6K phosphorylation was also inhibited by either Rab5QL or Rab5TN overexpression (supplemental Fig. S1). These data support a notion that too much or too little Rab5 activity inhibits mTORC1, suggesting that continuous intracellular trafficking is important for mTORC1 activation. We also determined the effect of Rab5 on AKT phosphorylation, which is phosphorylated by mTORC2 but not mTORC1 (24), and found that neither the constitutively active nor the dominant negative Rab5 affected AKT phosphorylation (Fig. 2*B*, supplemental Fig. S1), indicating that the effect of Rab5 is specific on mTORC1. In PC3 cells, which have elevated phosphatidylinositol 3-kinase pathway activity, Rab5 overexpression still inhibited S6K phosphorylation (Fig. 2*C*).

We tested whether Rab5 interacts with mTORC1 by co-immunoprecipitation. Our data showed that Rab5 could not co-immunoprecipitate with either Raptor or mTOR, whereas the positive control RagA-RagC interacted with both (supplemental Fig. S2). Immunofluorescence of transfected Rab5 showed that a significant fraction of endogenous mTOR co-localized with Rab5 (supplemental Fig. S3), indicating that Rab5 and mTOR can exist in the same subcellular compartment.

We then examined the importance of Rab5 membrane localization, which is required for its function in vesicle trafficking (25), in mTORC1 inhibition. Expression of the Rab5QL-2CS, which has the two C-terminal membrane-targeting essential cysteines substituted by serines and not associated with membrane (supplemental Fig. S4), failed to inhibit S6K phosphorylation (Fig. 2*D*), supporting that membrane localization is essential for Rab5 to influence mTORC1 activity. Next, we tested the importance of Rab5 signaling in mTORC1 inhibition. Mutations of Phe-57, Trp-74, or Tyr-89 of Rab5 are known to compromise Rab5 signaling *in vivo* (26). Our data showed that mutations of these residues abolished the ability of Rab5 to inhibit mTORC1 (Fig. 2*D*). Together, these observations further support the notion that a proper Rab5 signaling is important for physiological mTORC1 regulation.

To further investigate a role of Rab5 in mTORC1 regulation, GAPex, a guanine nucleotide exchange factor for Rab5 and Rab31 (27), was co-expressed with S6K1. We reasoned that hyperactivation of endogenous Rab5 might also inhibit mTORC1. Indeed, we observed that GAPex overexpression decreased S6K1 phosphorylation (Fig. 2*E*). The above data are consistent with a critical role of endogenous Rab5 and Rab31 in mTORC1 regulation.

Rab5 Specifically Affects Amino Acid- or Rag-induced but Not Glucose- or Rheb-induced mTORC1 Activation—It has been proposed that amino acids activate TORC1 possibly by affecting intracellular mTORC1 localization through Rag GTPases (16). We tested the effect of Rab5 on mTORC1 activation by amino acids. Co-expression of Rab5QL inhibited S6K phosphorylation in response to amino acid stimulation (Fig. 3*A*). In contrast to the amino acid stimulation, Rab5QL had no inhibitory effect on S6K phosphorylation when cells were stimulated by glucose (Fig. 3*B*). These results show that the effect of Rab5 is pathway-specific and consistent with the model that amino acids stimulate mTORC1 activation by regulating its intracellular localization.

Previous studies have shown that transient overexpression of Rheb-induced mTORC1 activation is insensitive to amino acid deprivation, whereas Rag mediates amino acid signals to regulate mTORC1 localization (16). We tested the relationship between Rab5 and RagA or Rheb. Co-expression of Rab5QL strongly inhib-

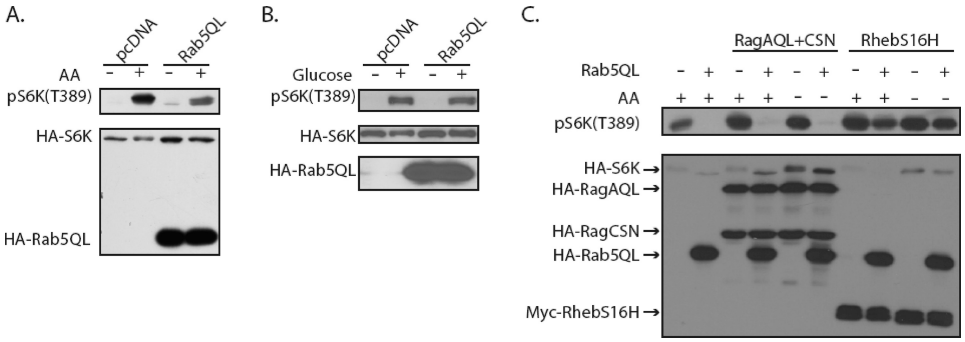

FIGURE 3. **The active Rab5QL blocks amino acid-stimulated but not glucose- or Rheb-induced mTORC1 activation.** *A*, Rab5 inhibits mTORC1 activity induced by amino acids. Rab5 construct was co-transfected with HA-S6K into HEK293 cells. Cells were starved for amino acids (*AA*−) for 1 h followed by amino acid stimulation (*AA*+) for 30 min before harvesting. Phosphorylation and protein levels were determined by immunoblotting with the indicated antibody. *B*, Rab5 does not affect glucose-induced mTORC1 activity. Rab5 construct was co-transfected with HA-S6K into HEK293 cells. Cells were deprived of glucose for 1 h followed by glucose stimulation for 30 min before collection. Phosphorylation and protein levels were determined by immunoblotting with the indicated antibodies. *C*, Rab5 blocks Rag- but not Rheb-induced S6K phosphorylation. Rab5 was transfected into HEK293 cells with or without RagA/C or Rheb construct as indicated. S6K was included in the co-transfection. Phosphorylation and protein levels of the transfected proteins were determined by immunoblotting with the indicated antibodies.

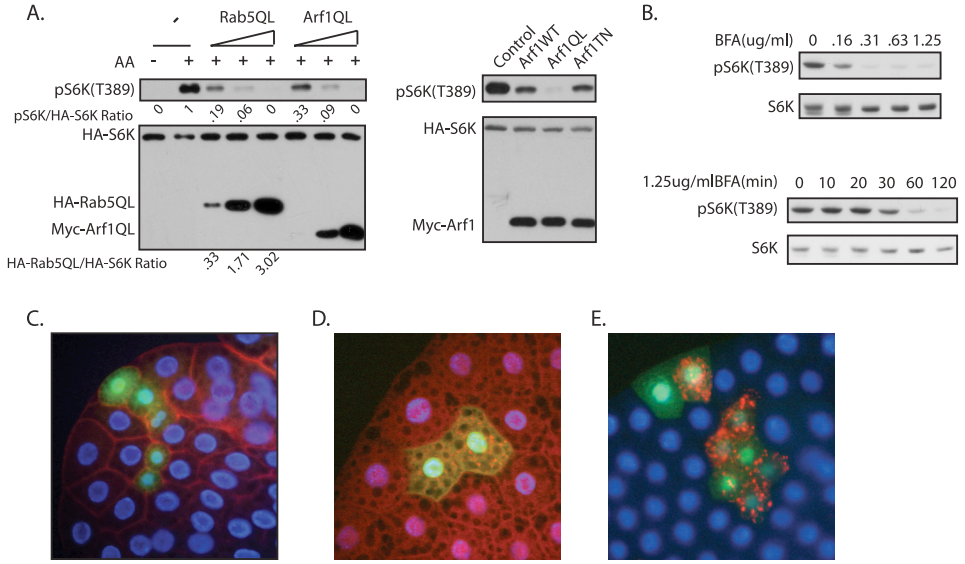

FIGURE 4. **Regulation of TORC1 by Arf1.** *A*, Arf1 inhibits S6K phosphorylation. HA-S6K was co-transfected with increasing amounts of Rab5QL (50, 100, 200 ng) or Arf1QL (50, 100, 200 ng) into HEK293 cells. Phosphorylation and protein levels were determined by immunoblotting with the indicated antibodies. Signals detected by anti-pS6K, anti-HA-S6K, and anti-HA-Rab5QL were quantified, and the ratio was calculated. *AA*−, amino acid starvation; *AA*+, amino acid stimulation. *B*, brefeldin A (*BFA*) inhibits S6K phosphorylation. Mouse embryonic fibroblast cells were treated with the indicated concentrations or times of brefeldin A. Phosphorylation and protein levels were determined by immunoblotting with the indicated antibodies. *C*, down-regulation of Arf1 expression reduces cell size. Fat body cells expressing UAS-Arf1-RNAi (GFP-positive clone) have a decreased area when compared with surrounding wild type control cells (GFP-negative). 4′,6-Diamidino-2-phenylindole (*blue*) labels the nuclei; phalloidin staining of F-actin (*red*) helps to visualize the cell boundary. *D* and *E*, Arf1 down-regulation induces autophagy. Clonal expression of UAS-Arf1-RNAi results in punctate staining of mCherry-Atg8a (*D*) and LysoTracker Red (*E*) under fed conditions.

ited mTORC1 activation by active RagAQL (Fig. 3*C*). On the other hand, Rab5QL only had a minor effect on S6K phosphorylation in the presence of active RhebS16H mutant. These data demonstrate that Rab5 is particularly important for mTORC1 activation by amino acids and Rag GTPase but not required for mTORC1 activation by glucose and Rheb. Similar observations were made with active Rab7, Rab10, and Rab31 (data not shown). Given the fact that both amino acids and Rag affect mTORC1 localization (16), our data support that intracellular trafficking, at least the steps regulated by Rab5, Rab7, Rab10 and Rab31, is important for mTORC1 activation in response to amino acid stimulation.

Arf1 Regulates mTORC1 in Both Drosophila and Mammalian Cells—The RNA interference screen revealed that knockdown of Arf1 homolog in S2 cells significantly decreased dS6K phosphorylation (Fig. 1). Arf family GTPases are also involved in intracellular vesicle trafficking (23). We tested the effect of Arf1 in mammalian cells. Co-expression of the constitutively active Arf1QL inhibited S6K phosphorylation as strongly as Rab5QL (Fig. 4*A*). Similar to the results observed with Rab5 mutants, the constitutively active Arf1QL was more potent than the wild type or dominant negative Arf1TN in inhibiting S6K1 phosphorylation (Fig. 4*A*). We also found that a significant fraction of mTOR was co-localized with the transfected Arf1 (supplemental Fig. S3). On the other hand, Arf1 did not show a direct interaction with either Raptor or mTOR (supplemental Fig. S2) by our co-immunoprecipitation experiments.

Brefeldin A is a drug that inhibits Arf1 guanine nucleotide exchange factor, thereby inhibiting Arf1 activity (28, 29). We tested the effect of brefeldin A on S6K1 phosphorylation and found that it potently inhibited endogenous S6K phosphorylation in a dose-dependent manner (Fig. 4*B*). The inhibitory effect was rather rapid as an almost complete inhibition of S6K1 phosphorylation was observed with a 60-min brefeldin A treatment. These data support a role of endogenous Arf in mTORC1 regulation.

Two well characterized cellular functions of TORC1 are to promote cell growth and to inhibit autophagy (1, 30). We investigated the role of Arf1 in cell size regulation in *Drosophila*. Knockdown of Arf1 in clones of GFP-marked cells in the larval fat body resulted in a 40% reduction in cell area (Fig. 4*C*), consistent with a decreased TORC1 activity in these cells. In parallel, we examined the effect of Arf1 on autophagy, which is inhibited by high TORC1 activity. Arf1 knockdown caused a strong induction of autophagy, as indicated by punctate localization of mCherry-Atg8a and LysoTracker Red, which mark early (autophagosome) and late (autolysosome) stages of autophagy, respectively (Fig. 4, *D* and *E*). These data further support that Arf1 plays an important role in TORC1 regulation *in vivo*.

The TORC1 complex has an essential role in cell growth in response to various growth-promoting and inhibitory signals (1). Two GTPase families, Rheb and Rag, have previously been shown to stimulate mTORC1 activation (8, 9, 15, 16). However, the mechanisms of these GTPases in mTORC1 regulation are different. Rheb, acting downstream of TSC1-TSC2, binds to and activates mTORC1 (5–9). Therefore, the effect of Rheb on mTORC1 is direct. On the other hand, the Rag GTPases act downstream of amino acids to promote mTORC1 activation (15, 16). Although RagA and RagB bind directly to raptor with high affinity, they cannot directly activate mTORC1 without the help of Rheb (16). A model has been proposed that Rag GTPases may regulate the intracellular localization of mTORC1 in response to amino acids. When amino acids are sufficient, the active RagA and RagB recruit mTORC1 to subcellular compartments where Rheb is localized (16). Therefore, active Rag presents mTORC1 to a location where it can be activated by Rheb. This model suggests that intracellular trafficking would be important for mTORC1 activation.

In this study, we have discovered Rab and Arf GTPases as having an important function in mTORC1 activation. However, the roles of these GTPases in mTORC1 regulation are different from Rag or Rheb. Neither Rab5 nor Arf1 is sufficient to activate mTORC1, and they do not interact with mTORC1 (supplemental Fig. S2). Their effects on mTORC1 are likely to indirectly influence the subcellular localization of mTORC1 or its regulators. Consistently, both Rab and Arf are key regulators of intracellular trafficking. Unlike Rheb or Rag, which promote mTORC1 activation when in GTP-bound form and inhibit mTORC1 in GDP-found form, overexpression of both the GTP-bound and the GDP-bound forms of Rab5 or Arf1 inhibits mTORC1. These results are consistent with an important role of GTPase cycling of Rab or Arf for proper intracellular vesicle trafficking. Overexpression of either GTP-bound or GDP-bound forms of these proteins might result in trapping of target proteins in a certain step and disruption of normal cycling. It is worth noting that Rab5 selectively blocks the stimulating effect of RagA but not Rheb on mTORC1 activation. Furthermore, Rab5 inhibits the effect of amino acids but not glucose on mTORC1 activation. These data support a model that intracellular trafficking is critical for amino acid signaling to mTORC1 activation that is mediated by the Rag GTPases. Future studies are needed to clarify the subcellular compartment where mTORC1 localizes.

Acknowledgments—We appreciate the gifts of Rab and GAPex plasmids from Drs. Alan Saltiel and Xiaowei Chen (University of Michigan) and thank Dr. Mary Stewart (North Dakota State University) for Drosophila S6K antibody.

REFERENCES

1. Wullschleger, S., Loewith, R., and Hall, M. N. (2006) *Cell* **124,** 471–484
2. Loewith, R., Jacinto, E., Wullschleger, S., Lorberg, A., Crespo, J. L., Bonenfant, D., Oppliger, W., Jenoe, P., and Hall, M. N. (2002) *Mol. Cell* **10,** 457–468
3. Thomas, G. (2002) *Biol. Res.* **35,** 305–313
4. Inoki, K., Li, Y., Zhu, T., Wu, J., and Guan, K. L. (2002) *Nat. Cell Biol.* **4,** 648–657
5. Inoki, K., Li, Y., Xu, T., and Guan, K. L. (2003) *Genes Dev.* **17,** 1829–1834
6. Zhang, Y., Gao, X., Saucedo, L. J., Ru, B., Edgar, B. A., and Pan, D. (2003) *Nat. Cell Biol.* **5,** 578–581
7. Tee, A. R., Manning, B. D., Roux, P. P., Cantley, L. C., and Blenis, J. (2003) *Curr. Biol.* **13,** 1259–1268
8. Long, X., Ortiz-Vega, S., Lin, Y., and Avruch, J. (2005) *J. Biol. Chem.* **280,** 23433–23436
9. Sancak, Y., Thoreen, C. C., Peterson, T. R., Lindquist, R. A., Kang, S. A., Spooner, E., Carr, S. A., and Sabatini, D. M. (2007) *Mol. Cell* **25,** 903–915
10. Manning, B. D., Tee, A. R., Logsdon, M. N., Blenis, J., and Cantley, L. C. (2002) *Mol. Cell* **10,** 151–162
11. Potter, C. J., Pedraza, L. G., and Xu, T. (2002) *Nat. Cell Biol.* **4,** 658–665
12. Inoki, K., Zhu, T., and Guan, K. L. (2003) *Cell* **115,** 577–590
13. Gwinn, D. M., Shackelford, D. B., Egan, D. F., Mihaylova, M. M., Mery, A., Vasquez, D. S., Turk, B. E., and Shaw, R. J. (2008) *Mol. Cell* **30,** 214–226
14. Hara, K., Yonezawa, K., Weng, Q. P., Kozlowski, M. T., Belham, C., and Avruch, J. (1998) *J. Biol. Chem.* **273,** 14484–14494
15. Kim, E., Goraksha-Hicks, P., Li, L., Neufeld, T. P., and Guan, K. L. (2008) *Nat. Cell Biol.* **10,** 935–945
16. Sancak, Y., Peterson, T. R., Shaul, Y. D., Lindquist, R. A., Thoreen, C. C., Bar-Peled, L., and Sabatini, D. M. (2008) *Science* **320,** 1496–1501
17. Clemens, J. C., Worby, C. A., Simonson-Leff, N., Muda, M., Maehama, T., Hemmings, B. A., and Dixon, J. E. (2000) *Proc. Natl. Acad. Sci. U.S.A.* **97,** 6499–6503
18. Arsham, A. M., and Neufeld, T. P. (2009) *PloS One* **4,** e6068
19. Yudin, D., and Fainzilber, M. (2009) *J. Cell Sci.* **122,** 587–593
20. Zerial, M., and McBride, H. (2001) *Nat. Rev. Mol. Cell Biol.* **2,** 107–117
21. Gillingham, A. K., and Munro, S. (2007) *Annu. Rev. Cell Dev. Biol.* **23,** 579–611
22. Rink, J., Ghigo, E., Kalaidzidis, Y., and Zerial, M. (2005) *Cell* **122,** 735–749
23. Gingras, A. C., Kennedy, S. G., O'Leary, M. A., Sonenberg, N., and Hay, N. (1998) *Genes Dev.* **12,** 502–513
24. Sarbassov, D. D., Guertin, D. A., Ali, S. M., and Sabatini, D. M. (2005) *Science* **307,** 1098–1101
25. Gomes, A. Q., Ali, B. R., Ramalho, J. S., Godfrey, R. F., Barral, D. C., Hume, A. N., and Seabra, M. C. (2003) *Mol. Biol. Cell* **14,** 1882–1899
26. Merithew, E., Hatherly, S., Dumas, J. J., Lawe, D. C., Heller-Harrison, R., and Lambright, D. G. (2001) *J. Biol. Chem.* **276,** 13982–13988
27. Lodhi, I. J., Bridges, D., Chiang, S. H., Zhang, Y., Cheng, A., Geletka, L. M., Weisman, L. S., and Saltiel, A. R. (2008) *Mol. Biol. Cell* **19,** 2718–2728
28. Helms, J. B., and Rothman, J. E. (1992) *Nature* **360,** 352–354
29. Donaldson, J. G., Finazzi, D., and Klausner, R. D. (1992) *Nature* **360,** 350–352
30. Chang, Y. Y., Juhász, G., Goraksha-Hicks, P., Arsham, A. M., Mallin, D. R., Muller, L. K., and Neufeld, T. P. (2009) *Biochem. Soc. Trans.* **37,** 232–236

nature cell biology

Inactivation of Rheb by PRAK-mediated phosphorylation is essential for energy-depletion-induced suppression of mTORC1

Min Zheng[1], Yan-Hai Wang[1], Xiao-Nan Wu[1], Su-Qin Wu[1], Bao-Ju Lu[2], Meng-Qiu Dong[2], Hongbing Zhang[3], Peiqing Sun[4], Sheng-Cai Lin[1], Kun-Liang Guan[5] and Jiahuai Han[1,6]

Cell growth can be suppressed by stressful environments, but the role of stress pathways in this process is largely unknown. Here we show that a cascade of p38β mitogen-activated protein kinase (MAPK) and p38-regulated/activated kinase (PRAK) plays a role in energy-starvation-induced suppression of mammalian target of rapamycin (mTOR), and that energy starvation activates the p38β–PRAK cascade. Depletion of p38β or PRAK diminishes the suppression of mTOR complex 1 (mTORC1) and reduction of cell size induced by energy starvation. We show that p38β–PRAK operates independently of the known mTORC1 inactivation pathways—phosphorylation of tuberous sclerosis protein 2 (TSC2) and Raptor by AMP-activated protein kinase (AMPK)—and surprisingly, that PRAK directly regulates Ras homologue enriched in brain (Rheb), a key component of the mTORC1 pathway, by phosphorylation. Phosphorylation of Rheb at Ser 130 by PRAK impairs the nucleotide-binding ability of Rheb and inhibits Rheb-mediated mTORC1 activation. The direct regulation of Rheb by PRAK integrates a stress pathway with the mTORC1 pathway in response to energy depletion.

The p38 MAPK signalling pathway is evolutionarily conserved from yeast to humans and participates in a variety of cellular responses[1–4]. There are four mammalian members in the p38 group of MAPK: p38α, p38β, p38γ and p38δ (refs 5–8). Similarities in activation and function have been observed, but each p38 isoform also has specific functions[9]. Although activation of p38 MAPKs by different stimuli is dependent on cell type, various stress stimuli, including energy stress, activate the p38 pathway in all cells, and thus the p38 pathway is considered to be a major stress-activated signalling pathway[10]. A number of substrates of p38 group MAPKs have been identified, including transcription factors and protein kinases, and the p38 pathway not only regulates gene expression, but also some other cellular responses to stress.

mTOR is a highly conserved protein kinase that plays a critical role in controlling cell growth and metabolism[11–13]. mTOR exists in two distinct complexes called mTORC1 and mTORC2 (ref. 14). The immunosuppression drug rapamycin inhibits mTORC1 (ref. 15), but not mTORC2 (ref. 16). The two complexes catalyse phosphorylation of different substrates, and thus execute different functions[17]. mTORC1 integrates signals from growth factors, nutrients, stress and energy levels in regulating cell growth. mTORC2 phosphorylates the hydrophobic motif of AKT (also known as protein kinase B) and modulates cytoskeletal organization[18]. mTORC1 contains regulatory-associated protein of mTOR (Raptor)[19], mammalian lethal with Sec13 protein 8 (mLST8, also known as GβL; ref. 20), proline-rich AKT substrate 40 kDa (PRAS40; ref. 21) and DEP-domain-containing mTOR interacting protein (Deptor)[22]. AMPK is upstream of mTORC1 in the energy-starvation-induced cellular response[23,24]. Energy depletion activates AMPK, which phosphorylates TSC2, thereby increasing its GTPase-activation protein (GAP) activity[25]. TSC2 is a GAP for the small G-protein Rheb (ref. 26), and Rheb is a key regulator of mTORC1 (refs 27,28). As the GTP-bound form of Rheb activates mTORC1, TSC2 negatively regulates mTORC1 (refs 26,29,30). Direct phosphorylation of Raptor by AMPK has been reported, and Raptor phosphorylation also negatively regulates the activity of mTORC1 (ref. 31). The p70 S6 kinase (S6K1) and eIF4E binding protein 1 (4EBP1) are key regulators of translation, and are the most well-characterized targets of mTORC1 (ref. 32). Phosphorylation of S6K and 4EBP1 by mTORC1 leads to increased translation of specific messenger RNAs, which is part of the mechanism used by mTORC1 to regulate cell growth.

[1]The Key Laboratory of the Ministry of Education for Cell Biology and Tumor Cell Engineering, School of Life Sciences, Xiamen University, Xiamen, Fujian 361005, China. [2]The National Institute of Biological Sciences, Beijing 102206, China. [3]Department of Physiology, National Laboratory of Medical Molecular Biology, Institute of Basic Medical Sciences, Chinese Academy of Medical Sciences and Peking Union Medical College, Beijing 100005, China. [4]The Scripps Research Institute, La Jolla, California 92037, USA. [5]Department of Pharmacology and Moores Cancer Center, University of California, San Diego, La Jolla, California 92093-0815, USA. [6]Correspondence should be addressed to J.H. (e-mail: jhan@scripps.edu or jhan@xmu.edu.cn)

Received 30 April 2010; accepted 12 December 2010; published online 20 February 2011; DOI: 10.1038/ncb2168

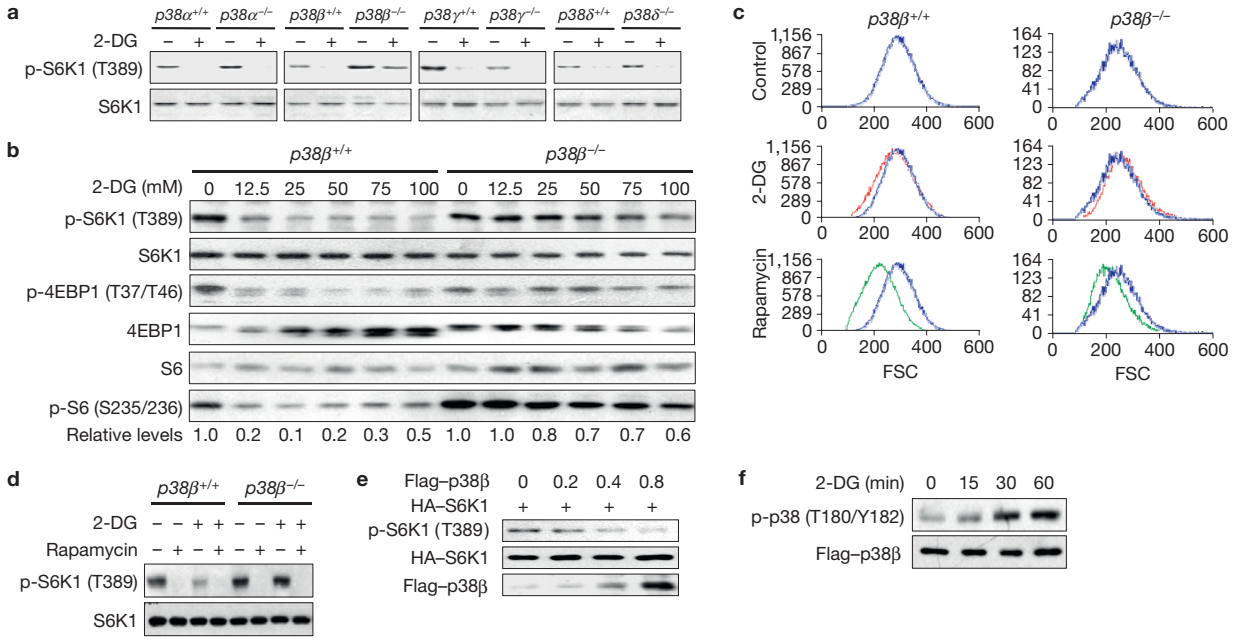

Figure 1 p38β is essential for the 2-DG-induced cellular response. (**a**) 2-DG-induced dephosphorylation of S6K1 is compromised in $p38\beta^{-/-}$ MEF cells. $p38\alpha^{-/-}$, $p38\beta^{-/-}$, $p38\gamma^{-/-}$ and $p38\delta^{-/-}$ cells, and their corresponding wild-type (+/+) MEF cells, were treated with or without 25 mM 2-DG for 60 min. Cell lysates were analysed by immunoblotting for the levels of the indicated proteins and phosphorylation states. (**b**) $p38\beta^{+/+}$ and $p38\beta^{-/-}$ MEF cells were treated with different doses of 2-DG for 30 min and analysed as in **a**. The relative levels of phosphorylated S6 were determined by ImageJ software (as indicated at the bottom). (**c**) The 2-DG-induced, but not rapamycin-induced, cell-size decrease is compromised in $p38\beta^{-/-}$ MEF cells. $p38\beta^{+/+}$ and $p38\beta^{-/-}$ MEF cells were treated with nothing (control), 6.25 mM 2-DG or 20 nM rapamycin for 60 h. FACS analysis was carried out to determine cell size. FCS (forward scatter) is a relative measure of cell size. Cell-size distribution of the control, as indicated by the blue line, is included in each image for comparison. (**d**) 2-DG-induced, but not rapamycin-induced, S6K1 dephosphorylation is compromised in $p38\beta^{-/-}$ MEF cells. The cells treated as in **c** were analysed as in **a** to determine the phosphorylation levels of S6K1. (**e**) p38β overexpression suppresses S6K1 phosphorylation. The HA–S6K1 expression plasmid (0.1 μg) was co-transfected with 0, 0.2, 0.4 and 0.8 μg of the Flag–p38β expression plasmid into HEK293 cells. Cell lysates were analysed as in **a**. (**f**) 2-DG induces phosphorylation of p38β. MEF cells were transfected with Flag–p38β and treated with 25 mM 2-DG for 0, 15, 30 and 60 min. Flag–p38β phosphorylation levels and Flag–p38β levels in Flag–immunoprecipitates were determined by western blotting using anti-phospho-p38 and anti-Flag antibodies, respectively. (Note, owing to the similar size of p38 family members, there is no method available at present to specifically detect p38β phosphorylation. Therefore, we used transiently expressed Flag–p38β to determine whether 2-DG can activate p38β. Uncropped images of blots are shown in Supplementary Fig. S9.

Crosstalk between the p38 and mTOR pathways has been reported. Phosphorylation of Ser 1210 of TSC2 by MK2, a downstream kinase of p38α, creates a 14-3-3 binding site, which prevents TSC2 from inhibiting mTORC1 (ref. 33). Involvement of the p38 pathway in H_2O_2- and other stimuli-induced mTORC1 activation was also reported recently[34]. As both mTOR and p38 pathways are evolutionarily conserved signal pathways, we are interested in their relationship during the cellular response to energy stress, and found that the p38β–PRAK cascade is essential for energy-starvation-induced inactivation of mTORC1.

RESULTS

p38β is essential for energy-depletion-induced inhibition of mTORC1

To determine the involvement of the p38 pathway in energy-depletion-induced inactivation of mTORC1, we analysed whether knockout of p38α, p38β, p38γ or p38δ could affect 2-deoxy-glucose (2-DG)-induced dephosphorylation of p70 S6K1, an *in vitro* model for measuring energy-depletion-induced inactivation of mTORC1 (ref. 25). 2-DG-induced dephosphorylation of S6K1 in p38α, p38γ and p38δ knockout MEF cells is similar to that in their corresponding $p38\alpha^{+/+}$, $p38\gamma^{+/+}$ and $p38\delta^{+/+}$ MEF cells, but the dephosphorylation of S6K1 was blocked in $p38\beta^{-/-}$ MEF cells in comparison with $p38\beta^{+/+}$ MEF cells (Fig. 1a), indicating that p38β is important for S6K1 dephosphorylation. A concentration of 25 mM 2-DG can effectively inhibit the phosphorylation of S6K1, 4EBP1 and S6 in wild-type MEF cells, but not in $p38\beta^{-/-}$ cells, even at higher 2-DG doses (Fig. 1b). Dynamic analysis also shows the impaired 2-DG response in $p38\beta^{-/-}$ cells (Supplementary Fig. S1a). The p38β-specific effect on 2-DG-induced dephosphorylation of S6K1 was also observed in HEK293 cells (Supplementary Fig. S1b). As mTORC1 controls cell size[35,36], we analysed the size of wild-type and $p38\beta^{-/-}$ MEFs before and after 2-DG and rapamycin treatment. Interestingly, 2-DG did not reduce the size of $p38\beta^{-/-}$ cells as it did in wild-type MEF cells, whereas inhibition of mTORC1 by rapamycin reduced cell size in both cell types (Fig. 1c). Consistent with the cell size data, rapamycin eliminated phospho-S6K1 in both cells, whereas the effect of 2-DG on phospho-S6K1 was impaired in $p38\beta^{-/-}$ cells (Fig. 1d). In support of the role of p38β in 2-DG-induced inactivation of mTORC1, overexpression of p38β, but not other p38 group members, suppressed S6K1 phosphorylation (Fig. 1e and Supplementary Fig. S1c), although 2-DG activated not only p38β, but also some other p38 group members (Fig. 1f and Supplementary Fig. S1d).

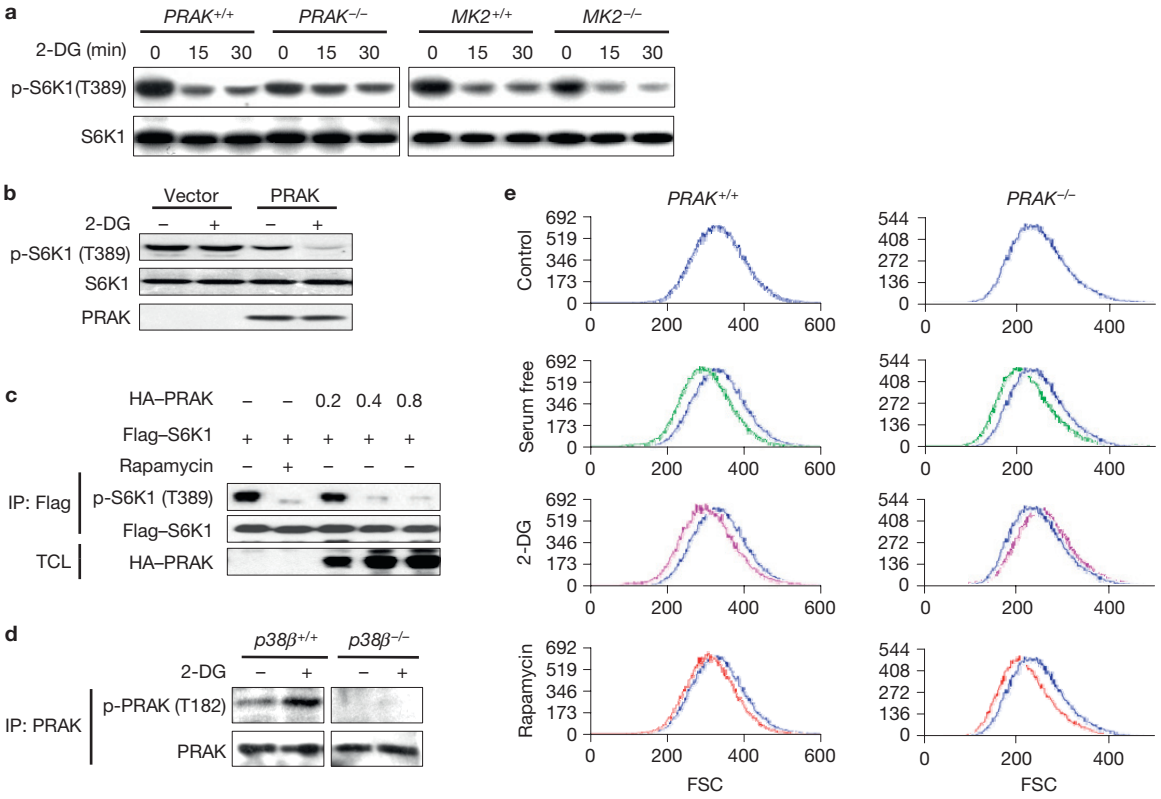

Figure 2 PRAK is essential for the 2-DG-induced cellular response. (**a**) 2-DG-induced dephosphorylation of S6K1 is compromised in *PRAK*$^{-/-}$ MEF cells. *PRAK*$^{+/+}$, *PRAK*$^{-/-}$, *MK2*$^{+/+}$ and *MK2*$^{-/-}$ MEF cells were treated with 25 mM 2-DG for 0, 15 or 30 min, then analysed by immunoblotting for the levels of the indicated proteins and phosphorylation states. (**b**) Reconstitution of PRAK restores 2-DG-induced dephosphorylation of S6K1 in *PRAK*$^{-/-}$ MEF cells. *PRAK*$^{-/-}$ MEF cells were infected with an empty viral vector or a PRAK-expressing lentivirus 36 h before treatment with nothing or 25 mM 2-DG for 30 min. Phosphorylation of S6K1, S6K1 protein levels and PRAK protein levels were determined by immunoblotting with corresponding antibodies. (**c**) PRAK overexpression suppresses S6K1 phosphorylation in a dose-dependent manner. The Flag–S6K1 expression plasmid (0.1 μg) was co-transfected with 0, 0.2, 0.4 and 0.8 μg of the HA–PRAK expression plasmid. Cells treated with 20 nM rapamycin were included as a control. Flag–S6K1 was immunoprecipitated by anti-Flag antibody-conjugated protein A/G-Sepharose beads and phosphorylation of Flag–S6K1 was determined by immunoblotting with corresponding antibodies. IP, immunoprecipitates; TCL, total cell lysates. (**d**) Activation of PRAK by 2-DG is defective in *p38β*$^{-/-}$ MEF cells. *p38β*$^{+/+}$ and *p38β*$^{-/-}$ MEF cells were treated with nothing or 25 mM 2-DG for 30 min. PRAK was immunoprecipitated with mouse anti-PRAK antibodies; then the phosphorylation of PRAK and PRAK protein levels were determined by immunoblotting with corresponding antibodies. (**e**) The 2-DG-induced, but not serum-starvation- and rapamycin-induced, cell-size decrease is compromised in *PRAK*$^{-/-}$ MEF cells. *PRAK*$^{+/+}$ and *PRAK*$^{-/-}$ MEF cells were treated with nothing (control), were serum-starved for 36 h, or were treated with 6.25 mM 2-DG or 20 nM rapamycin for 60 h. Cells were collected for FACS analysis to determine cell size. FCS (forward scatter) is a relative measure of cell size. The cell size distribution curve of the control, as indicated by the blue line, is included in each image for comparison purposes. Uncropped images of blots are shown in Supplementary Fig. S9.

PRAK is essential for energy-depletion-induced inhibition of mTORC1

One means by which the p38 group kinases execute their function is through their downstream kinases. To evaluate the possibility that p38β regulates mTORC1 through activation of its downstream kinases, we analysed whether deletion of PRAK (ref. 37) or MK2 (refs 38, 39), the kinases that can be activated by p38β (refs 40,41), affects 2-DG-induced dephosphorylation of S6K1 in MEF cells. Deletion of PRAK, but not MK2, impaired 2-DG-induced dephosphorylation of S6K1 (Fig. 2a). In support of the role of PRAK in mTORC1 inactivation, reconstitution of PRAK expression in *PRAK*$^{-/-}$ MEFs restored 2-DG-induced dephosphorylation of S6K1 in *PRAK*$^{-/-}$ cells (Fig. 2b), and overexpression of PRAK inhibited S6K1 phosphorylation (Fig. 2c). Knockdown of PRAK, but not MK2, in HEK293 cells also impaired 2-DG-induced dephosphorylation of S6K1 (Supplementary Fig. S2a,b). 2-DG can activate PRAK, as demonstrated by Thr 182 phosphorylation, and this activation is eliminated by p38β knockout (Fig. 2d), indicating that the p38β-mediated regulation of mTORC1 activity occurs at least partly through PRAK. As with p38β, PRAK is also required for the 2-DG-induced decrease in cell size and has no role in the serum-deprivation- or rapamycin-induced change in cell size (Fig. 2e).

p38β–PRAK cascade is selectively involved in certain forms of energy-depletion-induced mTORC1 inactivation

As 2-DG functions through inhibition of glycolysis to cause energy depletion in cells, glucose deprivation in culture medium should induce a similar phenotype. As anticipated, glucose deprivation induced activation of p38β and PRAK, as indicated by the increase in phosphorylation levels of these proteins (Fig. 3a), and low-glucose-induced dephosphorylation of S6K1 was impaired in *p38β*$^{-/-}$ and *PRAK*$^{-/-}$ cells (Fig. 3b,c). PRAK deletion sensitized MEF cells to

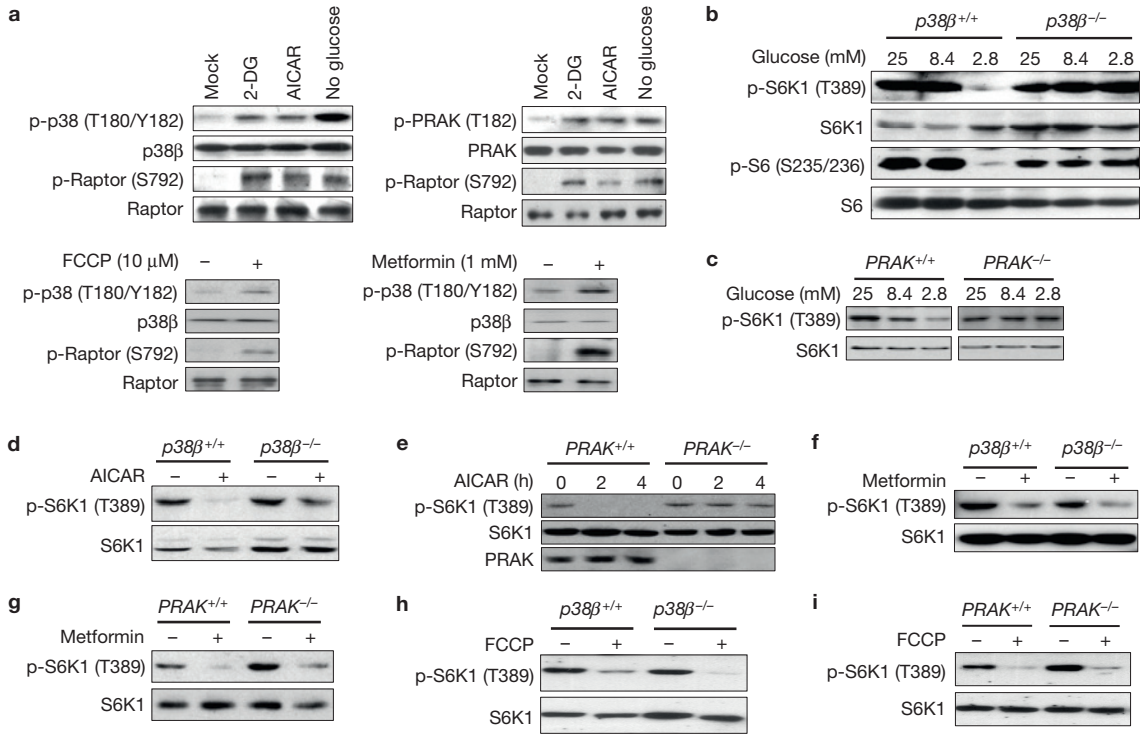

Figure 3 p38β and PRAK selectively participate in certain forms of energy-depletion-induced mTORC1 inactivation. (**a**) MEF cells were infected with a lentivirus expressing p38β (top left and bottom panels) or PRAK (top right panel), and treated with 50 mM 2-DG for 30 min, 2 mM AICAR for 4 h, glucose-free medium as indicated for 24 h (top), or 10 μM FCCP for 15 min or 1 mM metformin for 24 h (bottom). Phosphorylation and protein levels of p38β, PRAK and Raptor were determined by immunoblotting with corresponding antibodies. (**b**) Glucose-starvation-induced dephosphorylation of S6K1 is compromised in p38β-deficient MEF cells. $p38\beta^{+/+}$ and $p38\beta^{-/-}$ MEF cells were cultured in DMEM containing 25, 8.4 or 2.8 mM glucose for 24 h. Phosphorylation and protein levels of S6K1 or S6 were determined by immunoblotting with corresponding antibodies. (**c**) Glucose-starvation-induced dephosphorylation of S6K1 is compromised in PRAK-deficient MEF cells. Experiments performed as in **b** except $PRAK^{+/+}$ and $PRAK^{-/-}$ MEF cells were used. (**d**) $p38\beta^{+/+}$ and $p38\beta^{-/-}$ MEF cells were stimulated with 0.5 mM AICAR as indicated for 4 h. Cell lysates were analysed by immunoblotting for protein and phosphorylation levels of S6K1. (**e**) $PRAK^{+/+}$ and $PRAK^{-/-}$ MEF cells were stimulated with 0.5mM AICAR for the indicated times. Cell lysates were analysed as in **d**. (**f**) Metformin-induced dephosphorylation of S6K1 is not affected by p38β deficiency in MEF cells. $p38\beta^{+/+}$ and $p38\beta^{-/-}$ MEF cells were stimulated with 1 mM metformin as indicated for 24 h. Cell lysates were analysed by immunoblotting for protein and phosphorylation levels of S6K1. (**g**) Metformin-induced dephosphorylation of S6K1 is not affected by PRAK deficiency in MEF cells. Experiments performed as in **f**, except $PRAK^{+/+}$ and $PRAK^{-/-}$ MEF cells were used. (**h**) FCCP-induced dephosphorylation of S6K1 is not affected by p38β deficiency in MEF cells. $p38\beta^{+/+}$ and $p38\beta^{-/-}$ MEF cells were stimulated with 10 μM FCCP as indicated for 15 min. Phosphorylation and protein levels of S6K1 were determined by immunoblotting with corresponding antibodies. (**i**) FCCP-induced dephosphorylation of S6K1 is not affected by PRAK deficiency in MEF cells. Experiments performed as in **h**, except $PRAK^{+/+}$ and $PRAK^{-/-}$ MEF cells were used. Uncropped images of blots are shown in Supplementary Fig. S9.

death induced by glucose deprivation, and rapamycin treatment was able to rescue this phenotype (Supplementary Fig. S2c). AMPK plays a key role in cellular energy homeostasis by sensing changes in the AMP/ATP ratio[42]. Its activity can be determined by phosphorylation of its substrate Raptor. We treated cells with 5-aminoimidazole-4-carboxamide 1-β-D-ribofuranoside (AICAR) and metformin[24], compounds that can activate AMPK, and found that both can activate p38β and AMPK (Fig. 3a), but only AICAR-induced dephosphorylation of S6K1 was impaired in $p38\beta^{-/-}$ and $PRAK^{-/-}$ cells (Fig. 3d–g). We also examined carbonyl cyanide 4-(trifluoromethoxy) phenylhydrazone (FCCP), an uncoupler of oxidative phosphorylation, and found that it activated p38β and AMPK (Fig. 3a), but its mediated dephosphorylation of S6K1 was not p38β–PRAK dependent (Fig. 3h,i). It is unclear why p38β–PRAK has no role in metformin- and FCCP-induced inactivation of mTORC1. A recent report showed that the metformin-induced inactivation of mTORC1 is independent of AMPK (ref. 43), which is consistent with our observation that the mechanism used by metformin to induce mTORC1 inactivation is different from that used by AICAR.

We also tested other stimuli that can affect mTORC1 activity and found that PRAK deletion has little or no effect on the insulin-induced phosphorylation of S6K1 (Supplementary Fig. S3a), or on the dephosphorylation of S6K1 mediated by the depletion of serum or amino acids (Supplementary Fig. S3b,c). Rapamycin- and high-osmolarity (sorbitol)-mediated dephosphorylation of S6K1 were also not affected by PRAK knockout (Supplementary Fig. S3c). Collectively, the p38β–PRAK pathway selectively participates in 2-DG-, AICAR- and glucose-deprivation-induced inactivation of mTORC1.

p38β–PRAK cascade is independent of AMPK and TSC2

The p38β–PRAK cascade should function upstream of mTORC1, because deletion of p38β or PRAK does not affect rapamycin-mediated dephosphorylation of S6K1 and cell-size reduction (Fig. 1c–e). To determine whether p38β is downstream of AMPK in suppressing

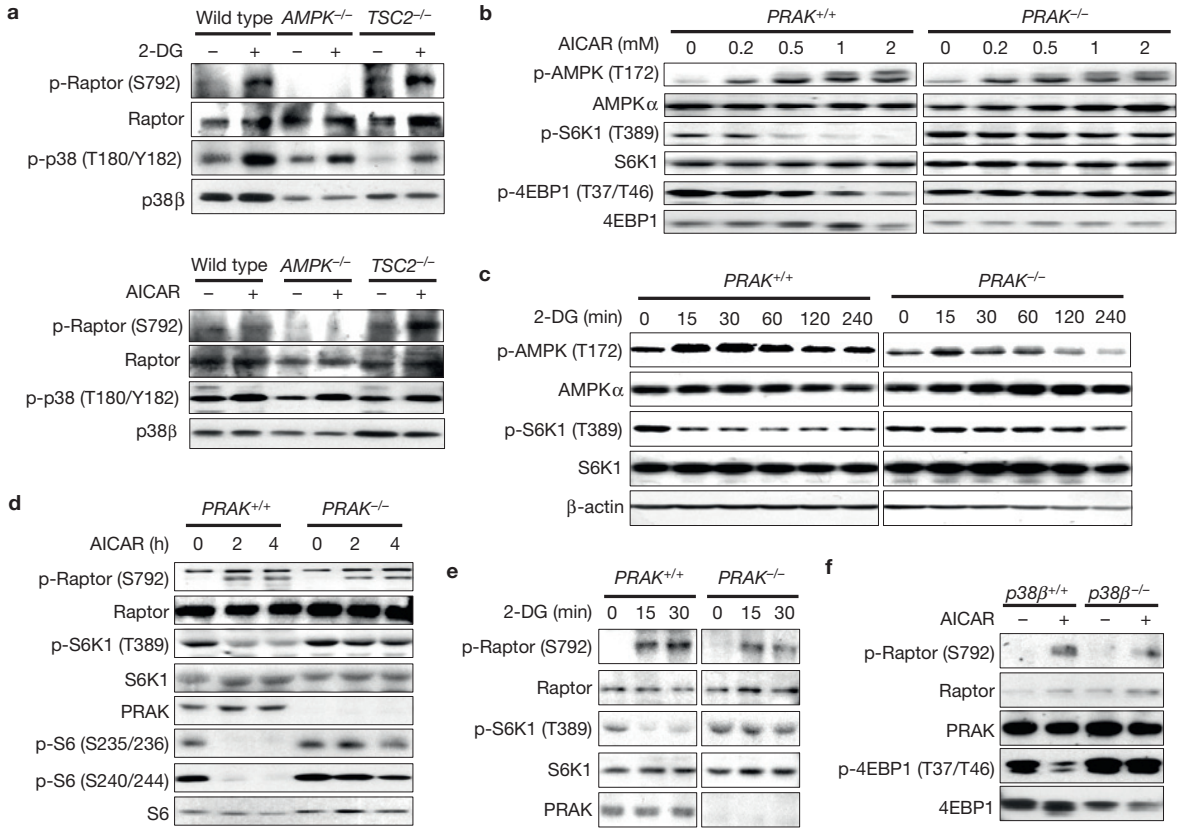

Figure 4 Suppression of mTORC1 by PRAK is independent of AMPK. (**a**) MEF cells with the indicated gene deletions were infected with a lentivirus expressing p38β and stimulated with or without 25 mM 2-DG for 30 min (top) or 2 mM AICAR for 4 h (bottom). Cell lysates were analysed by immunoblotting for the protein and phosphorylation levels of Raptor and p38β. (**b**) AICAR-induced AMPK phosphorylation is comparable in *PRAK*$^{+/+}$ and *PRAK*$^{-/-}$ cells. *PRAK*$^{+/+}$ and *PRAK*$^{-/-}$ MEF cells were stimulated with different doses of AICAR for 2 h. Phosphorylation and protein levels of AMPK, S6K1 and 4EBP1 were determined by immunoblotting with corresponding antibodies. (**c**) 2-DG-induced AMPK activation in MEF cells is not affected by PRAK knockout. *PRAK*$^{+/+}$ and *PRAK*$^{-/-}$ MEF cells were treated with 25 mM 2-DG for 0, 15, 30, 60, 120 or 240 min. Cell lysates were analysed by immunoblotting for the levels of the indicated proteins and their phosphorylation states. (**d**) *PRAK*$^{+/+}$ and *PRAK*$^{-/-}$ MEF cells were treated with 0.5 mM AICAR for 0, 2 and 4 h. Cell lysates were analysed by immunoblotting for the levels of the indicated proteins and their phosphorylation states. (**e**) 2-DG-induced Raptor phosphorylation is not compromised in PRAK-deficient MEF cells. *PRAK*$^{+/+}$ and *PRAK*$^{-/-}$ MEF cells were treated with 25 mM 2-DG for 0, 15 or 30 min. Cell lysates were analysed by immunoblotting for the levels of the indicated proteins and their phosphorylation states. (**f**) AICAR-induced Raptor phosphorylation is not compromised in p38β-deficient MEF cells. *p38β*$^{+/+}$ and *p38β*$^{-/-}$ MEF cells were stimulated with 0.5 mM AICAR as indicated for 4 h. Cell lysates were analysed by immunoblotting for the levels of the indicated proteins and their phosphorylation states. Uncropped images of blots are shown in Supplementary Fig. S9.

mTORC1, we used AMPKα1/α2 double-knockout MEFs. Consistent with published data[31], 2-DG and AICAR were not able to induce Raptor phosphorylation in AMPK-deficient cells (Fig. 4a). As 2-DG- and AICAR-induced p38β phosphorylation was not affected by AMPK deletion (Fig. 4a), AMPK is not upstream of p38β activation. Consistently, p38β phosphorylation was also not affected by deletion of TSC2, a downstream target of AMPK (Fig. 4a). As treatment with AICAR or 2-DG induced similar Thr 172 phosphorylation of AMPK in wild-type and *PRAK*$^{-/-}$ MEF cells (Fig. 4b,c), p38β–PRAK should have no role in AMPK activation. The activation of AMPK by AICAR and 2-DG in wild-type and *PRAK*$^{-/-}$ cells was confirmed by the phosphorylation of the AMPK substrate Raptor (Fig. 4d,e). Similar data were obtained using *p38β*$^{-/-}$ cells (Fig. 4f). Thus, AMPK and p38β–PRAK are parallel pathways.

TSC2 is a suppressor of mTORC1 and acts downstream of AMPK (ref. 25). It is known that 2-DG- or AICAR-induced dephosphorylation of S6K1 is impaired in *TSC2*$^{-/-}$ cells[25]. Both 2-DG and AICAR can downregulate S6K1 phosphorylation in PRAK-overexpressing TSC2 cells, but not in vector-transfected *TSC2*$^{-/-}$ cells (Fig. 5a,b), indicating that overexpressed PRAK can compensate for the loss of TSC2 function in *TSC2*$^{-/-}$ cells. As a high dose (2 mM) of AICAR can suppress S6K1 phosphorylation in *TSC2*$^{-/-}$ cells[31], we tested whether PRAK knockdown can make *TSC2*$^{-/-}$ cells more resistant to AICAR. *TSC2*$^{-/-}$ cells were resistant to low-dose (0.5 mM) AICAR-induced inactivation of mTORC1 and, as anticipated, we were not able to see any effect of PRAK knockdown (Fig. 5c). We observed that knockdown of PRAK in *TSC2*$^{-/-}$ cells enhances the resistance to 2 mM AICAR in these cells (Fig. 5d), consistent with the conclusion that PRAK is in parallel with TSC2 in regulating mTORC1. In addition, we observed that expression of PRAK further suppresses S6K1 phosphorylation in the presence of overexpressed TSC2 in wild-type cells (Fig. 5e), and that TSC2-overexpression-mediated inhibition of S6K1 phosphorylation does not require PRAK (Fig. 5f). Collectively, our data show that TSC2 and PRAK are independent of each other, and can compensate for each other in the inactivation of mTORC1.

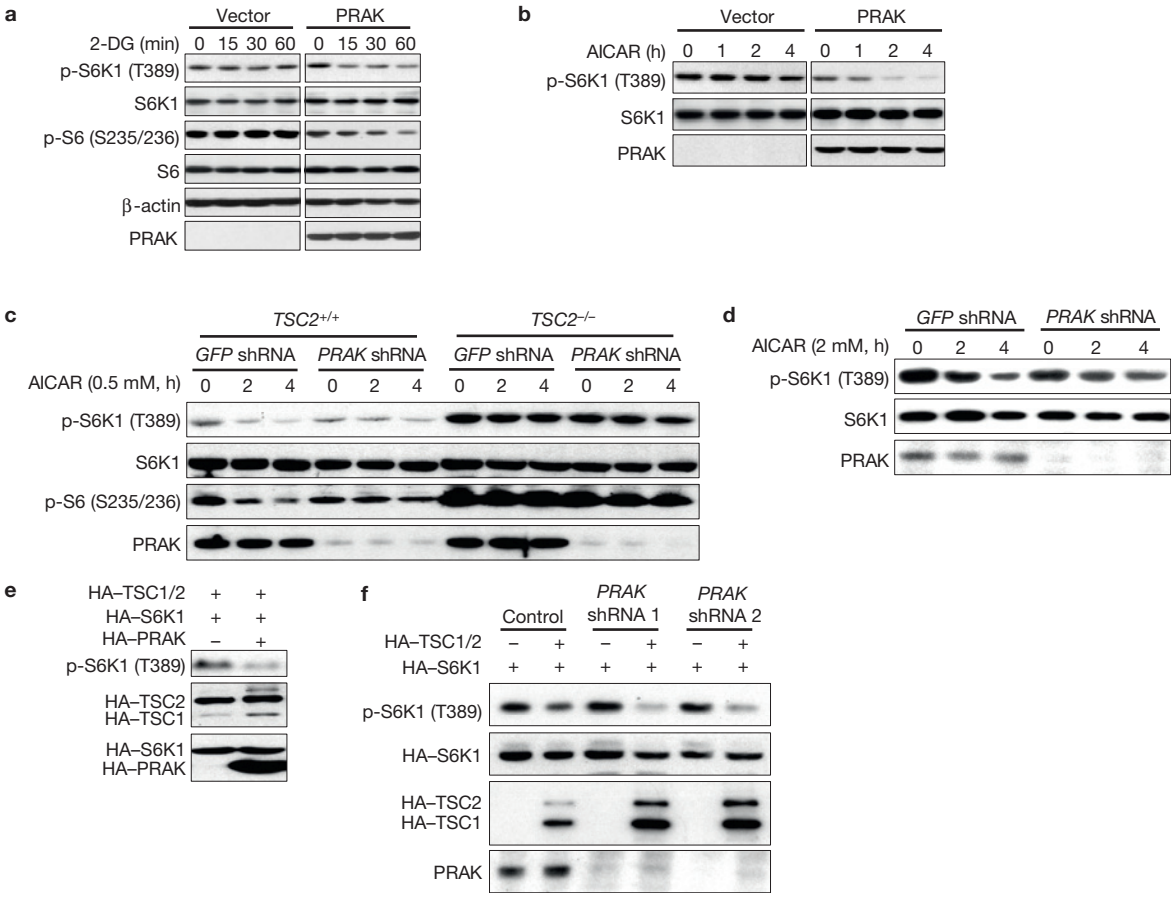

Figure 5 Suppression of mTORC1 by PRAK is independent of TSC2. (**a**) *TSC2*$^{-/-}$ MEF cells were infected with vector or PRAK-expressing lentivirus. At 48 h post-infection, cells were treated with 2-DG for 0, 15, 30 or 60 min and analysed by immunoblotting for the levels of the indicated proteins and their phosphorylation states. (**b**) *TSC2*$^{-/-}$ MEF cells were infected with an empty vector or PRAK-expressing lentivirus. Cells were treated with 0.5 mM AICAR for 0, 1, 2 or 4 h. Cell lysates were analysed as in **a**. (**c**) TSC2$^{+/+}$ and *TSC2*$^{-/-}$ MEF cells were infected with lentiviruses expressing *GFP* shRNA or *PRAK* shRNA. Cells were then stimulated with 0.5 mM AICAR for 0, 2 or 4 h. Cell lysates were analysed as in **a**. (**d**) *TSC2*$^{-/-}$ MEF cells were infected with lentiviruses expressing *GFP* shRNA or *PRAK* shRNA. Cells were then stimulated with 2 mM AICAR for 0, 2 or 4 h. Cell lysates were analysed as in **a**. (**e**) PRAK further enhances S6K1 dephosphorylation in TSC1/2-overexpressing cells. HEK293 cells were transfected with plasmids as indicated. The levels of phospho-S6K1 and HA–TSC1/2, HA–S6K1 and HA–PRAK were determined by western blotting using anti-phospho-S6K1 and anti-HA antibodies, respectively. (**f**) TSC2 suppresses S6K1 phosphorylation in both PRAK wild-type and PRAK knockdown cells. HEK293 cells were infected with lentiviruses expressing control shRNA, *PRAK* shRNA 1 or *PRAK*-shRNA 2. At 48 h post-infection, HA–S6K1 was co-transfected with an empty vector or HA–TSC1 plus HA–TSC2 (HA–TSC1/2). The cell lysates were analysed as in **e**. Uncropped images of blots are shown in Supplementary Fig. S9.

PRAK phosphorylates Rheb at Ser 130 and reduces the ability of Rheb to activate mTORC1

Raptor is a component of mTORC1 and is a target of AMPK in suppressing mTORC1 activity[31]. Neither a knockout cell line nor a dominant-negative mutant of Raptor is available; however, a fusion of Raptor with the carboxy-terminal 20 amino-acid portion of Rheb can create a dominant-active Raptor (Raptor^{DA}; ref. 44; K-L. Guan, unpublished data). Raptor^{DA} expression activated mTOR, as determined by increased phosphorylation of S6K1, and overexpression of wild-type PRAK, but not the kinase-dead mutant of PRAK (PRAK^{KM}), inhibited Raptor^{DA}-induced increase of S6K1 phosphorylation (Fig. 6a). Raptor^{DA}-induced S6K1 phosphorylation requires Rheb (ref. 44). Expression of Rheb enhanced S6K1 phosphorylation, and overexpression of PRAK, but not PRAK^{KM}, inhibited Rheb-induced S6K1 phosphorylation (Fig. 6b), indicating that PRAK is in parallel with Raptor–Rheb or directly regulates Rheb. We then found that PRAK can directly interact with Rheb, but not Raptor, as immunoprecipitation of haemagglutinin (HA)-tagged PRAK in HEK293 cells pulls down endogenous Rheb protein (Fig. 6c). As with other kinase–substrate interactions, PRAK^{KM} was able to more efficiently pull down Rheb when these two proteins were co-expressed (Supplementary Fig. S4a). An *in vitro* kinase assay showed that PRAK phosphorylates Rheb (Fig. 6d), indicating that Rheb is a substrate of PRAK. To identify the phosphorylation site on Rheb, PRAK-phosphorylated Rheb was subjected to phosphopeptide mapping by mass spectrometry. Spectrum searches revealed two potential phosphorylation sites on Rheb (Supplementary Fig. S4b). We mutated these sites to alanine and found that only the mutation of Ser 130 abolished the phosphorylation of Rheb by PRAK (Fig. 6d and Supplementary Fig. S4c), demonstrating that PRAK phosphorylates Ser 130 on Rheb. To determine whether Ser 130 phosphorylation occurs in cells, we generated anti-S130-phospho-Rheb antibodies. Co-expression of Rheb with PRAK, but not PRAK^{KM}, MK2 or an active MK2 mutant (MK2^{EE}), increased Rheb Ser 130 phosphorylation

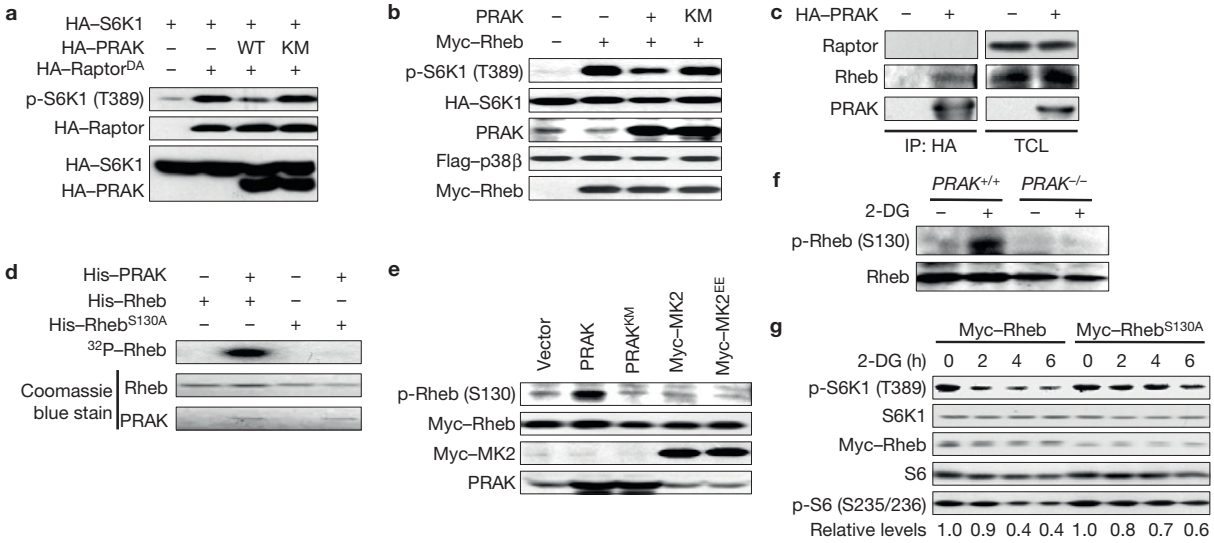

Figure 6 PRAK regulates Rheb by phosphorylation of Rheb on Ser 130. (**a**) PRAK suppresses Raptor^{DA}-mediated S6K1 phosphorylation. HEK293 cells were transfected with plasmids as indicated. The levels of phospho-S6K1, HA–Raptor, HA–S6K1 and HA–PRAK were determined by immunoblotting with corresponding antibodies. (**b**) PRAK inhibits Rheb-induced phosphorylation of S6K1. HEK293 cells were transfected with expression plasmids of Flag–p38β, HA–S6K1, PRAK and Myc–Rheb as indicated. Cell lysates were analysed as in **a**. (**c**) HA–PRAK interacts with endogenous Rheb. The HA–PRAK expression vector was transfected into HEK293 cells. HA–PRAK was immunoprecipitated with anti-HA conjugated protein A/G-Sepharose beads. The immunoprecipitates (IP) and total cell lysate (TCL) were analysed by immunoblotting for HA–PRAK, Rheb and Raptor. (**d**) PRAK phosphorylates Rheb on Ser 130 *in vitro*. His–Rheb or His–Rheb^{S130A} was incubated without or with PRAK in a kinase buffer containing [γ-^{32}P]ATP. Phosphorylation of Rheb was detected by autoradiography. Protein levels of Rheb and PRAK were determined by Coomassie blue staining. (**e**) PRAK, but not MK2, phosphorylates Rheb in mammalian cells. The expression plasmids for PRAK, PRAK^{KM}, Myc–MK2 or Myc–MK2^{EE} were co-transfected with the Myc–Rheb expression plasmid into HEK293 cells, as indicated. Cell lysates were analysed by immunoblotting with corresponding antibodies. (**f**) PRAK is required for 2-DG-induced Rheb phosphorylation. *PRAK*$^{+/+}$ and *PRAK*$^{-/-}$ MEF cells were stimulated with or without 25 mM 2-DG for 30 min. Phosphorylation of Rheb and Rheb protein levels were determined by immunoblotting using anti-phospho-Rheb and anti-Rheb antibodies, respectively. (**g**) Rheb^{S130A} inhibits 2-DG-induced dephosphorylation of S6K1. HEK293 cells were transfected with wild-type Myc–Rheb or Myc–Rheb^{S130A} 24 h before treatment with 25 mM 2-DG for 0, 2, 4 or 6 h. The levels of phospho-S6K1, S6K1, Myc–Rheb, phospho-S6 and S6 were determined by immunoblotting with their corresponding antibodies. The relative levels of phosphorylated S6 (indicated at the bottom) were determined by ImageJ software. Uncropped images of blots are shown in Supplementary Fig. S9.

(Fig. 6e). Ser 130 phosphorylation of endogenous Rheb by PRAK overexpression was also observed (Supplementary Fig. S4d). These data indicate that Ser 130 is an *in vivo* phosphorylation site of PRAK. Ser 130 in Rheb is the only *in vivo* phosphorylation site targeted by PRAK, as co-expression of PRAK, but not PRAK^{KM}, with Rheb led to a single band shift on the Phos-tag gel (Supplementary Fig. S4e). No band shift was observed in Rheb^{S130A} and Rheb$^{S130A/T44A}$ (Supplementary Fig. S4e), confirming the phosphorylation at Ser 130. Therefore, PRAK phosphorylates a single Ser 130 site on Rheb.

We then analysed whether 2-DG or AICAR induces Rheb phosphorylation and found that 2-DG and AICAR induced endogenous Rheb phosphorylation in wild-type, but not *PRAK*$^{-/-}$, MEF cells (Fig. 6f and Supplementary Fig. S4f). Overexpression of wild-type Rheb in HEK293 cells did not affect 2-DG-induced S6K1 dephosphorylation, whereas overexpression of Rheb^{S130A} inhibited 2-DG-induced S6K1 dephosphorylation (Fig. 6g), indicating that the S130A mutant has a dominant-negative effect on 2-DG-induced response. Consistently, overexpression of PRAK can suppress Rheb-mediated S6K1 phosphorylation, but has no effect on Rheb^{S130A}-mediated S6K1 phosphorylation (Supplementary Fig. S4g). The phosphorylated form of Rheb should be less capable of inducing S6K1 phosphorylation, because the phosphomimic mutant Rheb^{S130E} had less effect on S6K1 phosphorylation (Supplementary Fig. S4h). These data indicate that phosphorylation of Ser 130 on Rheb reduces its ability to activate mTORC1.

Phosphorylation of Rheb by PRAK decreases the ability of Rheb to bind guanine nucleotides

To determine why Ser 130 phosphorylation inactivates Rheb, we analysed the amount of non-hydrolysable GTP (GTP-γS) loading on recombinant Rheb or Rheb^{S130A} in the presence of wild-type PRAK or the KM mutant of PRAK *in vitro*. The amount of GTP-γS that is bound to the wild-type PRAK-treated Rheb is about half of that bound to the non-phosphorylatable mutant Rheb^{S130A} or inactive PRAK-treated sample (Fig. 7a). As Rheb cannot hydrolyse GTP in the absence of its GAP TSC2 (ref. 30), a similar result was obtained when [α-^{32}P]GTP was used (Supplementary Fig. S5a). As only about half of Rheb was phosphorylated by PRAK *in vitro* (Supplementary Fig. S5b), Ser 130 phosphorylation should significantly impair GTP binding to Rheb. As we already reached our limit to increase the activity of recombinant PRAK (see Supplementary Information), we were unable to phosphorylate all Rheb *in vitro*, and therefore cannot obtain a precise percentage of inhibition. We also analysed the GTP-γS binding of Rheb mutants. GTP-γS loading in Rheb^{S130A} was about the same as that in wild-type Rheb, GTP-γS loading in Rheb^{S130E} was much less than that in wild-type, and as a negative control, PRAK protein had no GTP-γS binding (Fig. 7b). The GDP loading was also less in Rheb^{S130E} (Supplementary Fig. S5c). Thus, the phosphorylation of Ser 130 decreases guanine nucleotide binding to Rheb.

As Rheb may already bind with GTP before being phosphorylated by PRAK in cells, we loaded GTP onto Rheb first and then analysed

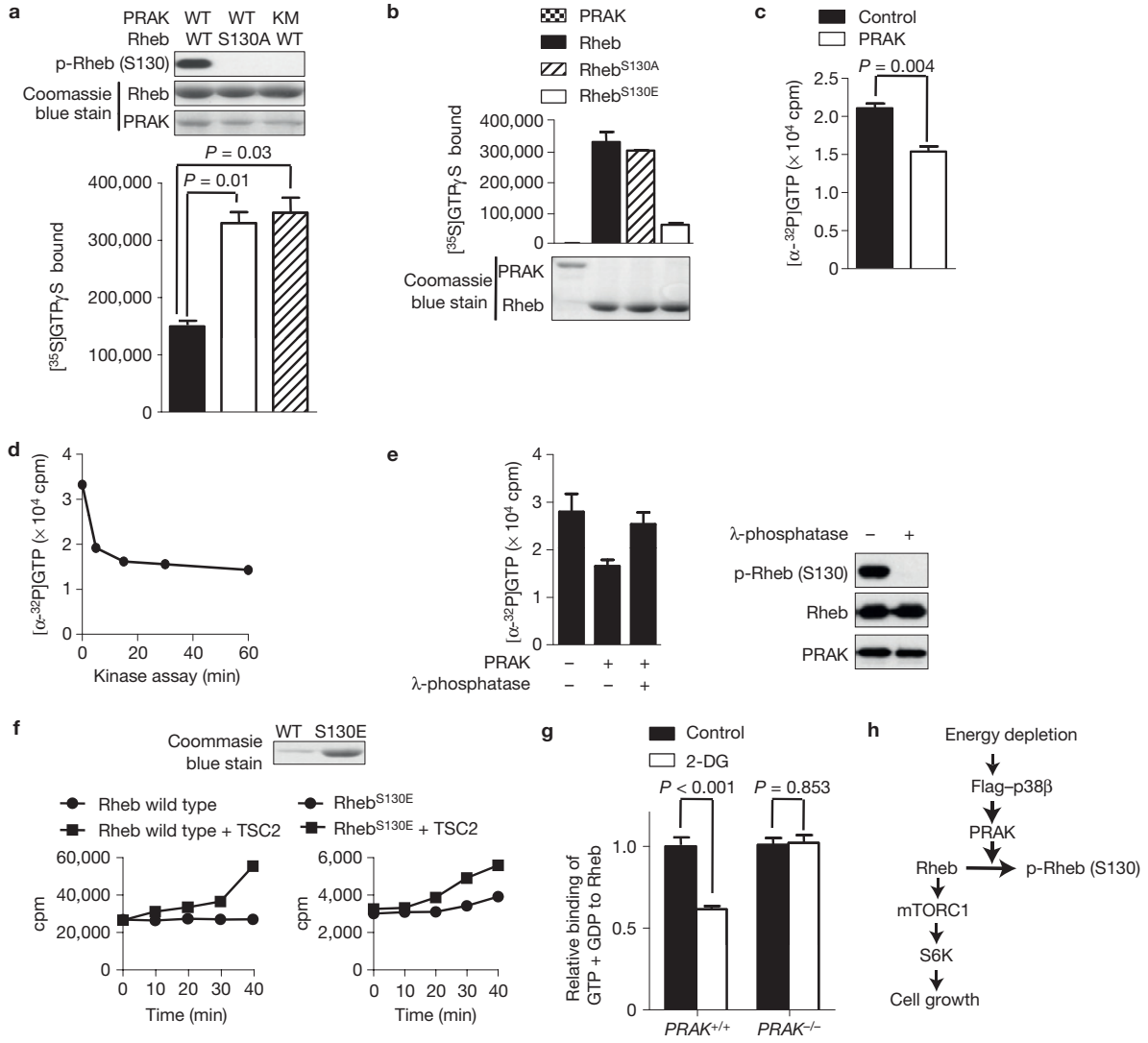

Figure 7 Rheb phosphorylation by PRAK reduces the nucleotide binding ability of Rheb. (**a**) Phosphorylation of Rheb *in vitro* reduces its GTP binding. GST–PRAK and GST–PRAK^{KM} were treated with His–p38β plus constitutively active MKK6 (His–MKK6b^{E}), and were then purified by GST pulldown. GST–Rheb GST–Rheb^{S130A} were incubated with or without activated GST–PRAK or GST–PRAK^{KM} in a kinase buffer containing [^{35}S]GTPγS. The samples were then applied to a GTP loading assay. Top: blots indicate Rheb phosphorylation and levels of proteins in loading assay. Bottom: quantification of loading. Data are means ± s.e.m., $n = 3$ samples, Student's t-test. (**b**) The phospho-Rheb mimic mutant GST–Rheb^{S130E} bound much less GTP. GST–Rheb, GST–Rheb^{S130A} and GST–Rheb^{S130E} were applied to a GTP loading assay (upper panel). The amounts of proteins are shown in the lower panel. (**c**) Phosphorylation of Rheb releases bound GTP. GST–Rheb was loaded with α-^{32}P-GTP first, and was then treated with or without activated PRAK for 60 min at 30 °C. The bound GTP was determined by scintillation counting. (**d**) The reduction of bound α-^{32}P-GTP during Rheb phosphorylation. α-^{32}P-GTP-loaded GST–Rheb was incubated with or without activated GST–PRAK for 0, 5, 15, 30 or 60 min at 30 °C. The bound GTP was determined by scintillation counting. (**e**) Dephosphorylation of phospho-Rheb recovers the ability of Rheb to bind α-^{32}P-GTP. α-^{32}P-GTP-loaded GST–Rheb was treated with or without PRAK and then treated with or without λ-phosphatase, as indicated. The bound GTP was determined by scintillation counting (left panel). The levels of phospho-Rheb, Rheb and PRAK are shown in the right panel. (**f**) Rheb wild type and Rheb^{S130E} were applied to a GTP hydrolysis assay in the absence or presence of HA–TSC2 (bottom two panels). The Coomassie blue staining of Rheb wild-type and Rheb^{S130E} protein is shown in the top panel. (**g**) *PRAK*$^{+/+}$ and *PRAK*$^{-/-}$ MEF cells were metabolically labelled with [^{32}P]phosphate, then treated with or without 25 mM 2-DG for 30 min. Endogenous Rheb was immunoprecipitated. GTP and GDP bound to Rheb was analysed by thin-layer chromatography and quantified by a Phosphorimager. Data are means ± s.e.m., $n = 4$ samples, Student's t-test. The relative binding of GTP + GDP to Rheb was calculated by setting the binding of GTP + GDP to Rheb in control groups to 1.0. (**h**) A proposed model of the p38β–PRAK cascade in regulating the mTORC1 pathway following energy starvation. Uncropped images of blots are shown in Supplementary Fig. S9.

the effect of PRAK phosphorylation of Rheb on the amount of GTP bound to Rheb. Phosphorylation of Rheb by PRAK released GTP that was bound to Rheb (Fig. 7c). Most of the bound GTP was released within 5 min (Fig. 7d). Thus, Ser 130 phosphorylation of Rheb not only made Rheb less capable of accepting GTP loading, but also reduced its ability to retain the already-bound GTP. To further evaluate this hypothesis, we used λ-phosphatase to remove the phosphorylation from *in vitro* phosphorylated Rheb and found that dephosphorylation of phospho-Rheb increased GTP binding (Fig. 7e). To determine whether Ser 130 phosphorylation affects the GTP hydrolysis activity of Rheb, we analysed GTP hydrolysis in wild-type Rheb and Rheb^{S130E} in the presence or absence of TSC2. As a result of the reduced GTP binding

capacity by $Rheb^{S130E}$, we used an excess of $Rheb^{S130E}$ in comparison with wild-type Rheb in the experiment (Fig. 7f, bottom right panel). Both Rheb and $Rheb^{S130E}$ alone had little or no GTP hydrolysing activity, but both can hydrolyse GTP in the presence of TSC2 (Fig. 7f). As a result of the difference in GTP binding activity, we cannot determine whether Ser 130 phosphorylation affects the hydrolysis activity of Rheb. To determine whether PRAK can regulate Rheb in cultured cells, we metabolically labelled wild-type and *PRAK*$^{-/-}$ cells with [^{32}P]phosphate. The cells were treated with or without 2-DG for 30 min, Rheb molecules were immunoprecipitated and bound nucleotides were analysed. Ras was used as a control. The ratio between GTP and GDP is about the same as in wild-type and *PRAK*$^{-/-}$ cells, and is slightly increased after 2-DG treatment in both cells (Supplementary Fig. S5d). 2-DG reduced the ability of Rheb to bind to guanine nucleotides in wild-type cells, but not in *PRAK*$^{-/-}$ cells (Fig. 7g and Supplementary Fig. S5e), whereas 2-DG had no effect on the GTP binding of Ras (Supplementary Fig. S5f), confirming the selective regulation of Rheb by PRAK.

DISCUSSION

Previously published studies and our data described above indicate that activation of the AMPK–TSC2, AMPK–Raptor, and p38β–PRAK pathways are independent events that mediate the suppression of mTORC1. Furthermore, their activation kinetics seem to differ. For example, the activation of p38β–PRAK occurs later than the initial reduction of mTORC1 activity in energy-starved cells (Supplementary Fig. S1a,f), indicating that TSC2 or Raptor suppresses mTORC1 during the early time points. It is important to note that deletion of either TSC2 or PRAK is sufficient to impair energy-depletion-induced inhibition of mTORC1 (no data for Raptor, owing to Raptor$^{-/-}$ cells not being available), indicating that these parallel signalling events are not simply additive. In addition, the overexpression experiments showed that any of these three genes by itself can modulate mTORC1 activity. Overactivation of one pathway can even compensate for the insufficiency of the others, as we observed that overexpression of PRAK is sufficient to suppress mTORC1 in the absence of TSC2 (Fig. 5a,b), overexpression of TSC2 is capable of inhibiting mTORC1 regardless of the presence or absence of PRAK (Fig. 5f) and overexpression of TSC2 in *PRAK*$^{-/-}$ cells can partially rescue the AICAR-induced decrease of S6K1 phosphorylation (Supplementary Fig. S6). It is possible that to inactivate mTORC1, the total activity of these pathways needs to reach a threshold. These three pathways could also operate in a network of offsetting inputs that amplify each other in inactivating mTORC1. It is clear that this is a complicated regulatory system and many other possibilities remain.

mTOR receives input from multiple signalling pathways, including those that regulate growth factors, nutrients and cellular stresses. Recently, it was reported that the p38 pathway participates in the activation of mTORC1 induced by H_2O_2 and other stimuli, and *Drosophila* p38b plays a role in mTORC1 activation[34]. We tested the role of p38β in H_2O_2-mediated changes of mTORC1. We observed suppression of mTORC1 by H_2O_2 (Supplementary Fig. S7a), which is consistent with previous reports[45]. We found that p38β had no role in this response (Supplementary Fig. S7b). On the other hand, we observed that serum starvation reduced basal levels of phospho-S6K1, and under this condition, H_2O_2 can increase the phosphorylation of S6K1 (Supplementary Fig. S7c), which is similar to a previous observation. We determined that H_2O_2-induced mTORC1 activation is not dependent on p38β (Supplementary Fig. S7d). As *Drosophila* p38b is homologous to both mammalian p38α and p38β, we then analysed involvement of p38α. H_2O_2-induced reduction of S6K1 phosphorylation in the cells cultured in serum-containing medium was not affected by p38α deletion (Supplementary Fig. S7e). Under serum-starved conditions, the basal level of phospho-S6K1 in *p38α*$^{-/-}$ MEF cells was higher than that in wild-type cells, and H_2O_2-induced increase of S6K1 phosphorylation was impaired in *p38α*$^{-/-}$ cells (Supplementary Fig. S7f). Thus, it is possible that p38α is responsible for the H_2O_2-induced mTORC1 activation previously observed[34].

Here, we demonstrate that a specific p38 kinase cascade, p38β–PRAK, is essential for energy-depletion-induced inactivation of mTORC1 (Fig. 7h). It was not anticipated that PRAK would be able to directly regulate a component of the mTORC1 pathway. It was also surprising that the GTP binding of Rheb was able to be regulated by phosphorylation on Ser 130, as Ser 130 is located between the second 310 helix and helix IV (ref. 46), a region that is not within or even close to the GTP/GDP binding pocket. It is possible that Ser 130 phosphorylation changes the relative position of the second 310 helix and its flanking loops, profoundly affecting the integrity of the GTP/GDP binding pocket, and leading to a marked decrease in nucleotide binding affinity. It is also possible that Ser 130 phosphorylation affects the interaction between Rheb and its regulators. Ser 130 phosphorylation should be specific for Rheb, as this site was not found in other small GTPases (Supplementary Fig. S8a). RhebL1 has a similar function as Rheb, but does not have a corresponding Ser 130 site[47]. We knocked down Rheb and RhebL1 in MEF cells and found that only Rheb knockdown reduced basal-level phosphorylation of S6K1 (Supplementary Fig. S8b). This could be due to the low expression of RhebL1. As Ser 130 in Rheb is conserved from *Drosophila* to humans (Supplementary Fig. S8c), the regulation of Rheb by phosphorylation could be an evolutionarily conserved mechanism for regulating mTORC1 activity. It seems that cell growth and cellular energy levels need to be precisely coordinated, and cells have evolved multiple checkpoints to regulate Rheb activity. □

METHODS

Methods and any associated references are available in the online version of the paper at http://www.nature.com/naturecellbiology/

Note: Supplementary Information is available on the Nature Cell Biology website

ACKNOWLEDGEMENTS

We would like to thank H. Jiang (Boehringer Ingelheim Pharmaceuticals) for providing p38 conditional knockout mice, B. Viollet (Universite Paris Descartes) and K. R. Laderoute (Stanford University School of Medicine) for *AMPKα1/α2*$^{-/-}$ cells. This work was supported by grants from NSF China 30830092, 30921005, 30828219, 973 program 2009CB22200, National Institutes of Health AI41637 and AI68896.

AUTHOR CONTRIBUTIONS

M.Z., Y-H.W., X-N.W., S-Q.W. and J.H. designed and carried out the experiments. B-J.L. and M-Q.D. carried out mass spectrometry analysis. M.Z., H.Z., P.S., S-C.L., K-L.G. and J.H. participated in the interpretation of the data. M.Z. and J.H. wrote the manuscript.

COMPETING FINANCIAL INTERESTS

The authors declare no competing financial interests.

Published online at http://www.nature.com/naturecellbiology
Reprints and permissions information is available online at http://npg.nature.com/reprintsandpermissions/

1. Cuenda, A. & Rousseau, S. p38 MAP-kinases pathway regulation, function and role in human diseases. *Biochim. Biophys. Acta* **1773,** 1358–1375 (2007).

2. English, J. M. & Cobb, M. H. Pharmacological inhibitors of MAPK pathways. *Trends Pharmacol. Sci.* **23,** 40–45 (2002).
3. Nebreda, A. R. & Porras, A. p38 MAP kinases: beyond the stress response. *Trends Biochem. Sci.* **25,** 257–260 (2000).
4. Ono, K. & Han, J. The p38 signal transduction pathway: activation and function. *Cell Signal.* **12,** 1–13 (2000).
5. Han, J., Lee, J. D., Bibbs, L. & Ulevitch, R. J. A MAP kinase targeted by endotoxin and hyperosmolarity in mammalian cells. *Science* **265,** 808–811 (1994).
6. Jiang, Y. *et al.* Characterization of the structure and function of a new mitogen-activated protein kinase (p38β). *J. Biol. Chem.* **271,** 17920–17926 (1996).
7. Li, Z., Jiang, Y., Ulevitch, R. J. & Han, J. The primary structure of p38γ: a new member of p38 group of MAP kinases. *Biochem. Biophys. Res. Commun.* **228,** 334–340 (1996).
8. Jiang, Y. *et al.* Characterization of the structure and function of the fourth member of p38 group mitogen-activated protein kinases, p38δ. *J. Biol. Chem.* **272,** 30122–30128 (1997).
9. Zarubin, T. & Han, J. Activation and signaling of the p38 MAP kinase pathway. *Cell Res.* **15,** 11–18 (2005).
10. Rincon, M. & Davis, R. J. Regulation of the immune response by stress-activated protein kinases. *Immunol. Rev.* **228,** 212–224 (2009).
11. Reiling, J. H. & Sabatini, D. M. Stress and mTORture signaling. *Oncogene* **25,** 6373–6383 (2006).
12. Wullschleger, S., Loewith, R. & Hall, M. N. TOR signaling in growth and metabolism. *Cell* **124,** 471–484 (2006).
13. Sengupta, S., Peterson, T. R. & Sabatini, D. M. Regulation of the mTOR complex 1 pathway by nutrients, growth factors, and stress. *Mol. Cell* **40,** 310–322 (2010).
14. Sabatini, D. M. mTOR and cancer: insights into a complex relationship. *Nat. Rev. Cancer* **6,** 729–734 (2006).
15. Sabatini, D. M., Erdjument-Bromage, H., Lui, M., Tempst, P. & Snyder, S. H. RAFT1: a mammalian protein that binds to FKBP12 in a rapamycin-dependent fashion and is homologous to yeast TORs. *Cell* **78,** 35–43 (1994).
16. Jacinto, E. *et al.* Mammalian TOR complex 2 controls the actin cytoskeleton and is rapamycin insensitive. *Nat. Cell Biol.* **6,** 1122–1128 (2004).
17. Loewith, R. *et al.* Two TOR complexes, only one of which is rapamycin sensitive, have distinct roles in cell growth control. *Mol. Cell* **10,** 457–468 (2002).
18. Sarbassov, D. D., Guertin, D. A., Ali, S. M. & Sabatini, D. M. Phosphorylation and regulation of Akt/PKB by the rictor-mTOR complex. *Science* **307,** 1098–1101 (2005).
19. Kim, D. H. *et al.* mTOR interacts with raptor to form a nutrient-sensitive complex that signals to the cell growth machinery. *Cell* **110,** 163–175 (2002).
20. Guertin, D. A. *et al.* Ablation in mice of the mTORC components raptor, rictor, or mLST8 reveals that mTORC2 is required for signaling to Akt-FOXO and PKCα, but not S6K1. *Dev. Cell* **11,** 859–871 (2006).
21. Vander, H. E., Lee, S. I., Bandhakavi, S., Griffin, T. J. & Kim, D. H. Insulin signalling to mTOR mediated by the Akt/PKB substrate PRAS40. *Nat. Cell Biol.* **9,** 316–323 (2007).
22. Peterson, T. R. *et al.* DEPTOR is an mTOR inhibitor frequently overexpressed in multiple myeloma cells and required for their survival. *Cell* **137,** 873–886 (2009).
23. Hardie, D. G. Role of AMP-activated protein kinase in the metabolic syndrome and in heart disease. *FEBS Lett.* **582,** 81–89 (2008).
24. Shackelford, D. B. & Shaw, R. J. The LKB1-AMPK pathway: metabolism and growth control in tumour suppression. *Nat. Rev. Cancer* **9,** 563–575 (2009).
25. Inoki, K., Zhu, T. & Guan, K. L. TSC2 mediates cellular energy response to control cell growth and survival. *Cell* **115,** 577–590 (2003).
26. Garami, A. *et al.* Insulin activation of Rheb, a mediator of mTOR/S6K/4E-BP signaling, is inhibited by TSC1 and 2. *Mol. Cell* **11,** 1457–1466 (2003).
27. Aspuria, P. J. & Tamanoi, F. The Rheb family of GTP-binding proteins. *Cell Signal.* **16,** 1105–1112 (2004).
28. Long, X., Lin, Y., Ortiz-Vega, S., Yonezawa, K. & Avruch, J. Rheb binds and regulates the mTOR kinase. *Curr. Biol.* **15,** 702–713 (2005).
29. Zhang, Y. *et al.* Rheb is a direct target of the tuberous sclerosis tumour suppressor proteins. *Nat. Cell Biol.* **5,** 578–581 (2003).
30. Inoki, K., Li, Y., Xu, T. & Guan, K. L. Rheb GTPase is a direct target of TSC2 GAP activity and regulates mTOR signaling. *Genes Dev.* **17,** 1829–1834 (2003).
31. Gwinn, D. M. *et al.* AMPK phosphorylation of raptor mediates a metabolic checkpoint. *Mol. Cell* **30,** 214–226 (2008).
32. Um, S. H., D'Alessio, D. & Thomas, G. Nutrient overload, insulin resistance, and ribosomal protein S6 kinase 1, S6K1. *Cell Metab.* **3,** 393–402 (2006).
33. Li, Y., Inoki, K., Vacratsis, P. & Guan, K. L. The p38 and MK2 kinase cascade phosphorylates tuberin, the tuberous sclerosis 2 gene product, and enhances its interaction with 14-3-3. *J. Biol. Chem.* **278,** 13663–13671 (2003).
34. Cully, M. *et al.* A role for p38 stress-activated protein kinase in regulation of cell growth via TORC1. *Mol. Cell. Biol.* **30,** 481–495 (2010).
35. Fingar, D. C., Salama, S., Tsou, C., Harlow, E. & Blenis, J. Mammalian cell size is controlled by mTOR and its downstream targets S6K1 and 4EBP1/eIF4E. *Genes Dev.* **16,** 1472–1487 (2002).
36. Potter, C. J. & Xu, T. Mechanisms of size control. *Curr. Opin. Genet. Dev.* **11,** 279–286 (2001).
37. New, L. *et al.* PRAK, a novel protein kinase regulated by the p38 MAP kinase. *EMBO J.* **17,** 3372–3384 (1998).
38. Freshney, N. W. *et al.* Interleukin-1 activates a novel protein kinase cascade that results in the phosphorylation of Hsp27. *Cell* **78,** 1039–1049 (1994).
39. Rouse, J. *et al.* A novel kinase cascade triggered by stress and heat shock that stimulates MAPKAP kinase-2 and phosphorylation of the small heat shock proteins. *Cell* **78,** 1027–1037 (1994).
40. Li, Q. *et al.* Determinants that control the distinct subcellular localization of p38α-PRAK and p38β-PRAK complexes. *J. Biol. Chem.* **283,** 11014–11023 (2008).
41. New, L., Jiang, Y. & Han, J. Regulation of PRAK subcellular location by p38 MAP kinases. *Mol. Biol. Cell* **14,** 2603–2616 (2003).
42. Hardie, D. G., Carling, D. & Carlson, M. The AMP-activated/SNF1 protein kinase subfamily: metabolic sensors of the eukaryotic cell? *Annu. Rev. Biochem.* **67,** 821–855 (1998).
43. Kalender, A. *et al.* Metformin, independent of AMPK, inhibits mTORC1 in a rag GTPase-dependent manner. *Cell Metab.* **11,** 390–401 (2010).
44. Sancak, Y. *et al.* Ragulator-Rag complex targets mTORC1 to the lysosomal surface and is necessary for its activation by amino acids. *Cell* **141,** 290–303 (2010).
45. Shaw, R. J. *et al.* The tumor suppressor LKB1 kinase directly activates AMP-activated kinase and regulates apoptosis in response to energy stress. *Proc. Natl Acad. Sci. USA* **101,** 3329–3335 (2004).
46. Yu, Y. *et al.* Structural basis for the unique biological function of small GTPase RHEB. *J. Biol. Chem.* **280,** 17093–17100 (2005).
47. Yuan, J. *et al.* Identification and characterization of RHEBL1, a novel member of Ras family, which activates transcriptional activities of NF-kappa B. *Mol. Biol. Rep.* **32,** 205–214 (2005).

METHODS

Reagents and antibodies. Anti-Rheb (344912; 1:500) was from R&D Systems. Mouse anti-PRAK (A-7; 1:1,000) and anti-Rheb (C-19; 1:500) were from Santa Cruz Biotechnology. Anti-Ras (Y13-259; 1:1,000) was from Transduction Laboratories. Rabbit anti-PRAK antibodies were raised using recombinant PRAK. Anti-phospho-PRAK (T182; 1:1,000) was generated with phospho-peptide[48]. Anti-phospho-Rheb (S130) (1:200) was generated by Abmart. All other antibodies (1:1,000) were from Cell Signaling. 2-DG was obtained from Sigma. AICAR (AICA-Riboside) and rapamycin were obtained from Calbiochem. Phos-tag was obtained from Phos-tag Technology. The expression plasmids of human p38β (Flag–p38β) and PRAK (histidine (His)-tagged PRAK, HA–PRAK and Flag–PRAK) were described previously[49]. The expression plasmids of human S6K (HA–S6K and Flag–S6K) and Rheb (Myc–Rheb) were described previously[50]. To generate His or glutathione *S*-transferase (GST) fusion of Rheb, Rheb was expressed in pET or pGEX vectors. The lentiviral vectors from Invitrogen were used to express protein and shRNA in cultured cells. All mutant constructs of Rheb and PRAK were created by PCR mutagenesis and were verified by DNA sequencing. The real-time PCR primers were as follows: *Rheb*, forward, 5′-TGGCAAATTGTTGGATATGG-3′, reverse, 5′-CCAAAGCTTTCCCTTCTTCA-3′; *RhebL1*, forward, 5′-AAGAAGCTGGCAGAGTCCTG-3′, reverse, 5′-CAATCTCCTGGATGACTTTGG-3′; p38α, forward, 5′-TTGGTCAGTGGGATGCATAA-3′, reverse, 5′-AGTTTCTTGCCTCATGGCTT-3′; p38γ, forward, 5′-GTCATCTTGAATTGGATGCG-3′, reverse, 5′-TGTAGTTCTTGGCCTCATCG-3′; p38δ, forward, 5′-CCAGACAGTGGACATCTGGT-3′, reverse, 5′-CTTTGTCGTTCAGCTTCTGC-3′; *MK2*, forward, 5′-GGTCCCTGGGTGTCATCATGT-3′ reverse, 5′-GCCAGTATGAATTTCCCAACC-3′; p38β, forward, 5′-GCCATATGATGAGAGCGTTG-3′ reverse, 5′-GTGAGCTCCTTCCACTCCTC-3′.

Cell culture, transfection and lentivirus infection. Cells were cultured in Dulbecco's modified Eagle's medium (DMEM; Invitrogen) containing 10% fetal bovine serum (FBS; Invitrogen). Calcium phosphate precipitation or Lipofectamine 2000 was used for cell transfection. HEK293FT was used to prepare the lentivirus, as described in ViraPower Lentiviral Expression System (Invitrogen).

MEFs. Embryonic fibroblasts obtained from $p38\alpha^{lox/lox}$, $p38\beta^{lox/lox}$, $p38\gamma^{lox/lox}$ and $p38\delta^{lox/lox}$ mice were cultured in DMEM supplemented with 10% FBS. MEFs were immortalized with a retrovirus expressing large T antigen. To generate gene-knockout MEF cells, the $p38\alpha^{lox/lox}$, $p38\beta^{lox/lox}$, $p38\gamma^{lox/lox}$ and $p38\delta^{lox/lox}$ MEF cells were infected with a retrovirus expressing Cre to excise the floxed gene. Cells infected with an empty retrovirus vector were also generated and used as control wild-type cells. The gene knockout was confirmed by genomic PCR. The $PRAK^{-/-}$ cell line was generated by immortalizing primary MEF cells with a retrovirus expressing large T antigen. $TSC2^{-/-}$ MEF cells were described previously[51]. $AMPK\alpha1/\alpha2^{-/-}$ cells were obtained from B. Viollet (Universite Paris Descartes) and K. R. Laderoute (Stanford University School of Medicine).

RNA interference. shRNAs were designed using Invitrogen Block-iT RNAi Designer and cloned into a lentiviral vector from Invitrogen. We designed several shRNAs to target human *PRAK*, *MK2*, p38β and *Rheb*, and found the following sequence to be able to effectively knock down the target genes:

GFP shRNA, 5′-GGCACAAGCTGGAGTACAA-3′; *PRAK* shRNA 1, 5′-GCAAGCCAGCCAAGTAACA-3′; *PRAK* shRNA 2, 5′-GCAGGAGGCTTGGAAGTAT-3′; *MK2* shRNA 1, 5′-GGAGAACTCTTTAGCCGAATC-3′; *MK2* shRNA 2, 5′-GGTCCCTGGGTGTCATCATGT-3′; p38β shRNA 1, 5′-CTCAGAACACGCCCGGACA-3′; p38β shRNA 2, 5′- GCTGAAGCGCATCATGGAA-3′.

Lentiviruses were collected 48 h after transfection of HEK293FT cells with lentiviral vectors. The shRNA-expressing lentiviruses were used to infect HEK293 cells. The cells were analysed 3 days after infection. p38α, p38γ and p38δ shRNAs were as previously described[52].

Immunoprecipitation. Cells were lysed in lysis buffer (20 mM Tris at pH 7.5, 150 mM NaCl, 1 mM EDTA, 1 mM EGTA, 1% Triton X-100, 2.5 mM sodium pyrophosphate, 1 mM β-glycerophosphate, 1 mM Na_3VO_4 and 1 μg ml^{-1} leupeptin) and immunoprecipitated with anti-HA or anti-Flag antibody-conjugated protein A/G-Sepharose beads. Immunocomplexes were subjected to SDS–PAGE.

Cell-size assay. Cell-size determination was described previously[3]. Briefly, FACS analysis was carried out on Coulter Epics XL, Beckman. Cells were replated to a 10 cm dish (1:10 split). After 12 h, the cells were treated as indicated. The cultured medium was changed every 24 h. The cells were then collected and fixed on ice in 75% ethanol, then stored at 4 °C until analysis. The fixed cells were treated with 250 μg ml^{-1} RNase A and stained with propidium iodide for FACS analysis, to determine the cell size in the G1-phase population.

***In vitro* kinase assay.** GST–PRAK, His–p38β, His–MKK6b^{E}, GST–Rheb, His–PRAK and His–Rheb were purified from *Escherichia coli* and subjected to a kinase assay in kinase buffer (25 mM Tris at pH 7.5, 10 mM $MgCl_2$, 2 mM dithiothreitol, 5 mM β-glycerophosphate and 0.1 mM Na_3VO_4) at 30 °C for 30 min. To generate activated PRAK, GST–PRAK was subjected to a kinase assay using His–p38β and His–MKK6b^{E} as kinases. GST–PRAK was then repurified using GST beads. To generate phosphorylated Rheb, GST–Rheb was subjected to a kinase assay using activated PRAK as a kinase.

GTP loading assay. GST–Rheb and phosphorylated Rheb, GST–Rheb^{S130A} or GST–Rheb^{S130E} were loaded with [α-^{32}P]GTP in loading buffer (20 mM Tris at pH 8, 5 mM EDTA, 1 mM dithiothreitol and 0.1 mg ml^{-1} BSA) for 15 min at 30 °C (ref. 53). This mixture was applied to a nitrocellulose membrane (Bio-Rad), then rinsed three times with Tris-buffered saline (20 mM Tris at pH 7.6 and 137 mM NaCl). The radioactivity retained on the membrane was determined by scintillation counting.

Mn^{2+}-phos-tag SDS–PAGE. Electrophoresis of the polyacrylamide gel containing Mn^{2+}-phos-tag was conducted as described previously[54], except a 15% polyacrylamide gel was used.

Mass spectra and phosphorylation site mapping. Recombinant Rheb was phosphorylated *in vitro* by active PRAK. The phosphorylated Rheb was resuspended in 8 M urea, 100 mM Tris at pH 8.5, reduced, alkylated, split into three tubes, and digested with trypsin, elastase and thermolysin. The three digests were pooled together for mass spectrometry analysis. The tandem mass spectrograms were searched with SEQUEST (ref. 55), with or without the addition of 80 on serine, threonine or tyrosine (phosphorylation) against a human protein database. The MS3 spectra were searched with SEQUEST with a loss of 18 on serine or threonine (neutral loss of phosphoric acid from phosphorylated serine or threonine). The search results were combined and filtered with DTASelect (ref. 56).

Isoelectric focusing and immunoblotting. Proteins were precipitated with trichloroacetic acid 3-[(3-Cholamidopropyl)-dimethylammonio]-1-propanesulfonate (TCA)/acetone, suspended in IEF sample buffer (7 M urea, 2 M thiourea, 2% CHAPS, 0.8% ampholytes at pH 3–10, 50 mM dithiothreitol and 4% glycerol) and applied to isoelectric focusing using a mini-gel format as described previously[57]. After focusing, IEF gels were incubated in 12% TCA overnight at 4 °C, washed three times with water for 15 min, incubated in 7 M urea, 2 M thiourea and 5 mM dithiothreitol for 10 min to renature the proteins, then soaked in lower gel buffer (0.37 mM Tris at pH 8.8 and 0.1% SDS) three times for 15 min. The focused proteins were then transferred onto a 0.45 μm poly(vinylidene fluoride) membrane and immunoblotted with anti-phospho-Rheb and anti-Rheb antibodies.

Metabolism labelling. $PRAK^{+/+}$ and $PRAK^{-/-}$ MEF cells were washed once with phosphate-free DMEM and incubated with phosphate-free DMEM containing 0.5 mCi/ml ^{32}P-orthophosphate for 4 h. Cells were treated without or with 25 mM 2-DG for 30 min. The cells were lysed with labelling lysis buffer (1% Triton X-100, 50 mM HEPES at pH 7.4, 100 mM NaCl, 5 mM $MgCl_2$, 1 mg ml^{-1} BSA, 1 mM dithiothreitol, 1 mM phenylmethyl sulphonyl fluoride, 10 μg ml^{-1} leupeptin, 10 μg ml^{-1} aprotinin, 1 mM $NaVO_3$ and, 10 mM NaF). Rheb and H-Ras were immunoprecipitated with 20 μl anti-Rheb (C-19) and 10 μl anti-H-Ras (Y13-259) antibodies, respectively[58,59]. Protein A/G beads were added for 1 h at 4 °C. The beads were washed eight times with a washing buffer (0.5% Triton X-100, 50 mM HEPES at pH 7.4, 5 mM $MgCl_2$, 1 mM $NaVO_3$, 0.005% SDS). The bound nucleotides were eluted with 20 μl elution buffer (2 mM EDTA at pH 8.0, 1 mM GDP, 1 mM GTP) at 68 °C for 20 min. SDS-sample buffer was added to beads for analysing the protein in the immuoprecipitates. Methanol (60 μl) and chloroform (30 μl) were added to the eluates, each followed by vortexing and centrifugation at 11,750 *g* for 10 s. Water (45 μl) was added and the samples were centrifuged again at 11,750 *g* for 2 min. The upper phase was collected and dried, then resuspended in 15 μl elution buffer. The eluted nucleotides were subjected to thin-layer chromatography using polyethyleneimine cellulose plates (Baker-flex) in 0.75 M KH_2PO_4 (pH 3.4). Data were collected with a Phosphorimager (Molecular Dynamics) and analysed with the ImageQuant program.

Statistics. Data are expressed as means ± s.e.m. Student's *t*-test was used to compare differences between treated groups and their paired controls. *P* values are indicated in the figures.

48. Sun, P. *et al.* PRAK is essential for ras-induced senescence and tumor suppression. *Cell* **128,** 295–308 (2007).
49. New, L. *et al.* PRAK, a novel protein kinase regulated by the p38 MAP kinase. *EMBO J.* **17,** 3372–3384 (1998).

DOI: 10.1038/ncb2168

50. Inoki, K., Zhu, T. & Guan, K. L. TSC2 mediates cellular energy response to control cell growth and survival. *Cell* **115,** 577–590 (2003).
51. Zhang, H. *et al.* Loss of Tsc1/Tsc2 activates mTOR and disrupts PI3K-Akt signaling through downregulation of PDGFR. *J. Clin. Invest* **112,** 1223–1233 (2003).
52. Kwong, J. *et al.* p38α and p38γ mediate oncogenic ras-induced senescence through differential mechanisms. *J. Biol. Chem.* **284,** 11237–11246 (2009).
53. Inoki, K., Li, Y., Xu, T. & Guan, K. L. Rheb GTPase is a direct target of TSC2 GAP activity and regulates mTOR signaling. *Genes Dev.* **17,** 1829–1834 (2003).
54. Kinoshita, E., Kinoshita-Kikuta, E., Takiyama, K. & Koike, T. Phosphate-binding tag, a new tool to visualize phosphorylated proteins. *Mol. Cell Proteomics* **5,** 749–757 (2006).
55. Yates, J. R. III, Eng, J. K., McCormack, A. L. & Schieltz, D. Method to correlate tandem mass spectra of modified peptides to amino acid sequences in the protein database. *Anal. Chem.* **67,** 1426–1436 (1995).
56. Tabb, D. L., McDonald, W. H. & Yates, J. R. III DTASelect and Contrast: tools for assembling and comparing protein identifications from shotgun proteomics. *J. Proteome Res.* **1,** 21–26 (2002).
57. Anderson, J. C. & Peck, S. C. A simple and rapid technique for detecting protein phosphorylation using one-dimensional isoelectric focusing gels and immunoblot analysis. *Plant J.* **55,** 881–885 (2008).
58. Garami, A. *et al.* Insulin activation of Rheb, a mediator of mTOR/S6K/4E-BP signaling, is inhibited by TSC1 and 2. *Mol. Cell* **11,** 1457–1466 (2003).
59. Roccio, M., Bos, J. L. & Zwartkruis, F. J. Regulation of the small GTPase Rheb by amino acids. *Oncogene* **25,** 657–664 (2006).

nature cell biology

AMPK and mTOR regulate autophagy through direct phosphorylation of Ulk1

Joungmok Kim[1], Mondira Kundu[2], Benoit Viollet[3] and Kun-Liang Guan[1,4]

Autophagy is a process by which components of the cell are degraded to maintain essential activity and viability in response to nutrient limitation. Extensive genetic studies have shown that the yeast ATG1 kinase has an essential role in autophagy induction. Furthermore, autophagy is promoted by AMP activated protein kinase (AMPK), which is a key energy sensor and regulates cellular metabolism to maintain energy homeostasis. Conversely, autophagy is inhibited by the mammalian target of rapamycin (mTOR), a central cell-growth regulator that integrates growth factor and nutrient signals. Here we demonstrate a molecular mechanism for regulation of the mammalian autophagy-initiating kinase Ulk1, a homologue of yeast ATG1. Under glucose starvation, AMPK promotes autophagy by directly activating Ulk1 through phosphorylation of Ser 317 and Ser 777. Under nutrient sufficiency, high mTOR activity prevents Ulk1 activation by phosphorylating Ulk1 Ser 757 and disrupting the interaction between Ulk1 and AMPK. This coordinated phosphorylation is important for Ulk1 in autophagy induction. Our study has revealed a signalling mechanism for Ulk1 regulation and autophagy induction in response to nutrient signalling.

Under nutrient starvation, cells initiate a lysosomal-dependent self-digestive process known as autophagy, whereby cytoplasmic contents, such as damaged proteins and organelles, are hydrolyzed to generate nutrients and energy to maintain essential cellular activities[1–4]. Autophagy is a tightly regulated process and defects in autophagy have been closely associated with many human diseases, including cancer, myopathy and neurodegeneration[5–7]. Autophagy has also been implicated in clearance of pathogens and antigen presentation[8–10]. Genetic studies in *Saccharomyces cerevisiae* have defined the autophagy machinery[11–13]. Among the components of this machinery, the ATG1 kinase, which forms a complex with ATG13 and ATG17, is a key regulator in autophagy initiation[14–18]. Mammals have ATG1 homologues, Ulk1 and Ulk2 (refs 19, 20), and the mammalian counterparts of ATG13 and ATG17 are reported as mATG13 and FIP200, respectively[3,21–22]. However, the mechanism underlying Ulk1 regulation is largely unknown, although a modest Ulk1 activation induced by nutrient starvation has been reported[18,21,23].

The inhibitory function of mTOR complex 1 (mTORC1) in autophagy is well established[24–26]. mTORC1 activity reflects cellular nutritional status[27]. Therefore, understanding how mTORC1 regulates autophagy is of great importance because it may link nutrient signals to regulation of autophagy. The connection between ATG1 kinase and TORC1 has been elucidated in yeast[28]. ATG13 is an essential component of the ATG1 complex[29], and phosphorylation of ATG13 by TORC1 results in the disruption of this complex[16,30]. Accumulating reports have suggested that there is also a relationship between Ulk1 and mTORC1 in mammalian cells[21,23,31]. However, the molecular basis of mTORC1 in autophagy regulation remains to be addressed. Another potential candidate in autophagy regulation is AMPK because it senses cellular energy status to maintain energy homeostasis[32]. There is evidence to support a role for AMPK in autophagy induction in response to various cellular stresses, including glucose starvation[33–37]. However, the molecular mechanism underlying how AMPK regulates autophagy is largely unknown though it is generally assumed that AMPK stimulates autophagy by inhibiting mTORC1 at the level of TSC2 (ref. 38) and Raptor[39]. In this study, we provide molecular insights into how AMPK and mTORC1 regulate autophagy through coordinated phosphorylation of Ulk1.

RESULTS

Glucose starvation activates Ulk1 protein kinase through AMPK-dependent phosphorylation

We examined the effect of glucose starvation on Ulk1 and observed a significant Ulk1 activation on glucose starvation, as indicated by increased Ulk1 autophosphorylation (Fig. 1a). Also, glucose deprivation induced a Ulk1 mobility shift that was reversed by phosphatase treatment, suggesting that glucose starvation induced Ulk1 phosphorylation (Fig. 1b). This shift was more evident on a phos-tag gel[40] and was suppressed by inhibition of AMPK with compound C (6-[4-(2-Piperidin-1-yl-ethoxy)-phenyl)]-3-pyridin-4-yl-pyyrazolo[1,5-a] pyrimidine; ref. 41; Supplementary Information, Fig. S1a). Consistently, the Ulk1 mobility shift induced by glucose starvation was suppressed by co-expression of

[1]Department of Pharmacology and Moores Cancer Center, University of California at San Diego, La Jolla, CA 92130, USA. [2]Department of Pathology, St. Jude Children's Hospital, Memphis, TN 38105, USA. [3]INSERM U1016, Institut Cochin, Université Paris Descartes, CNRS (UMR 8104), Paris, France. [4]Correspondence should be addressed to K.-L.G. (e-mail: kuguan@ucsd.edu)

Received 05 May 2010; accepted 06 December 2010; published online 23 January 2011; DOI: 10.1038/ncb2152

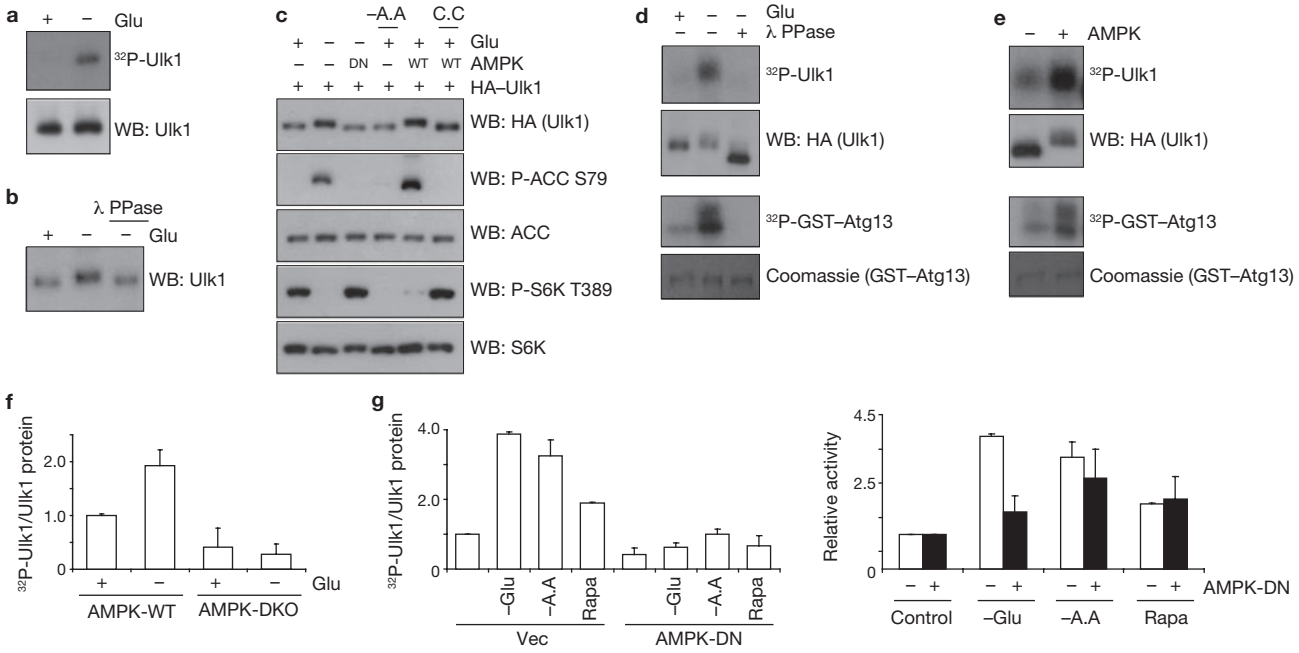

Figure 1 Glucose starvation activates Ulk1 protein kinase through AMPK-dependent phosphorylation. (**a**) HEK293 cells were starved of glucose (4 h) as indicated, endogenous Ulk1 was immunoprecipitated and an autophosphorylation assay was performed. Proteins were resolved by SDS–PAGE and visualized with autoradiography (top) or western blotting (WB; bottom). (**b**) Cells were incubated in glucose-free medium (4 h) as indicated and lysed. Lysates were incubated with lambda phosphatase (λ PPase) as indicated. Endogenous Ulk1 mobility was examined by western blotting. (**c**) HA–Ulk1 was transfected into HEK293 cells together with wild-type (WT) AMPKα1 or a kinase-dead (DN) mutant. Cells were starved of glucose (4 h; Glu) or amino acids (–A.A) and treated with compound C (20 μM, C.C) as indicated. Ulk1 mobility as well as phosphorylation levels of ACC and S6K were determined by western blotting. (**d**) HA–Ulk1 proteins were immunopurified from transfected HEK293 cells, which had undergone glucose starvation (4 h) as indicated. The HA–Ulk1 proteins were treated with λ PPase, and *in vitro* kinase assays were performed in the presence of GST–ATG13. Proteins were resolved by SDS–PAGE; phosphorylated proteins were visualized with autoradiography , HA–Ulk1 by western blotting and GST–Atg13 by Coomassie staining. (**e**) HA–Ulk1 was immunopurified from transfected HEK293 cells under glucose-rich media and treated with AMPK in the presence of cold ATP for 15 min, followed by kinase assays as described in **d**. (**f**) AMPK wild-type (WT) and α1/α2 double knockout (DKO) MEFs were incubated with or without glucose (4 h). Endogenous Ulk1 was immunoprecipitated and autophosphorylation was measured (mean ± s.d., $n = 3$). Autophosphorylation activity was normalized to Ulk1 protein level; relative activity is calculated by normalization to Ulk1 activity from AMPK wild-type MEFs in glucose-rich conditions. (**g**) HA–Ulk1 was transfected into HEK293 cells together with vector (Vec) or an AMPKα1 kinase-dead mutant (DN). The cells were starved of glucose (–Glu) or amino acids (–A.A), or treated with 50 nM rapamycin (Rapa) for 3 h before lysis. Left: autophosphorylation activity was assessed and normalized as in **f** (mean ± s.d., $n = 3$). Right: fold induction in Ulk1 autophosphorylation, compared with Ulk1 autophosphorylation from cells under nutrient-rich conditions. Uncropped images of blots are shown in Supplementary Fig. S5.

the AMPKα kinase-dead (DN) mutant, which dominantly interfered with AMPK signalling as indicated by the decreased phosphorylation of ACC (acetyl-CoA carboxylase), an AMPK substrate, and increased phosphorylation of S6K (p70S6 kinase), an mTORC1 substrate, in response to glucose starvation (Fig. 1c). Moreover, overexpression of wild-type AMPKα was sufficient to induce a Ulk1 mobility shift even under glucose-rich conditions, which was blocked by compound C (Fig. 1c). It is worth noting that amino-acid starvation, which inhibited S6K phosphorylation, did not induce obvious Ulk1 mobility shift or ACC phosphorylation. Together, these data indicate that AMPK might be responsible for Ulk1 phosphorylation induced by glucose starvation.

To determine the effect of the phosphorylation induced by glucose starvation on Ulk1 activity, Ulk1 immune-complex prepared from the glucose-starved cells was treated with lambda phosphatase *in vitro* and then measured for kinase activity. In this experimental setting we confirmed that the phosphatase was efficiently removed because no dephosphorylation of the pre-labelled ^{32}P-GST–TSC2 occurred (Supplementary Information, Fig. S1b). We observed that the phosphatase treatment largely diminished glucose starvation-induced Ulk1 kinase activity as indicated by decreased autophosphorylation and trans-phosphorylation of GST–ATG13 (Fig. 1d). Similarly, lambda phosphatase treatment inactivated the endogenous Ulk1 and increased Ulk1 mobility (Supplementary Information, Fig. S1b). These data suggest that the phosphorylation induced by glucose starvation may contribute to Ulk1 activation.

As glucose starvation activated Ulk1 in a phosphorylation-dependent manner and this phosphorylation was suppressed by dominant-negative AMPK or compound C, we investigated if Ulk1 could be directly activated by AMPK. HA–Ulk1 was immunoprecipitated from the transfected cells cultured on glucose-rich medium and then incubated with AMPK in the presence of cold ATP *in vitro*, followed by a Ulk1 kinase assay. AMPK pre-treatment significantly increased Ulk1 kinase activity and decreased Ulk1 mobility (Fig. 1e). As controls, AMPK could not activate Ulk1 in the absence of ATP or in the presence of AMPK inhibitor (compound C; Supplementary Information, Fig. S1c), indicating that AMPK directly phosphorylated and activated Ulk1. The Ulk1 autophosphorylation visualized by ^{32}P-autoradiogram was not a result of AMPK contamination because an Ulk1 kinase-inactive mutant (K46R) did not show any Ulk1 autophosphorylation in the same experimental setting even though Ulk1^{K46R} was phosphorylated by AMPK as evidenced

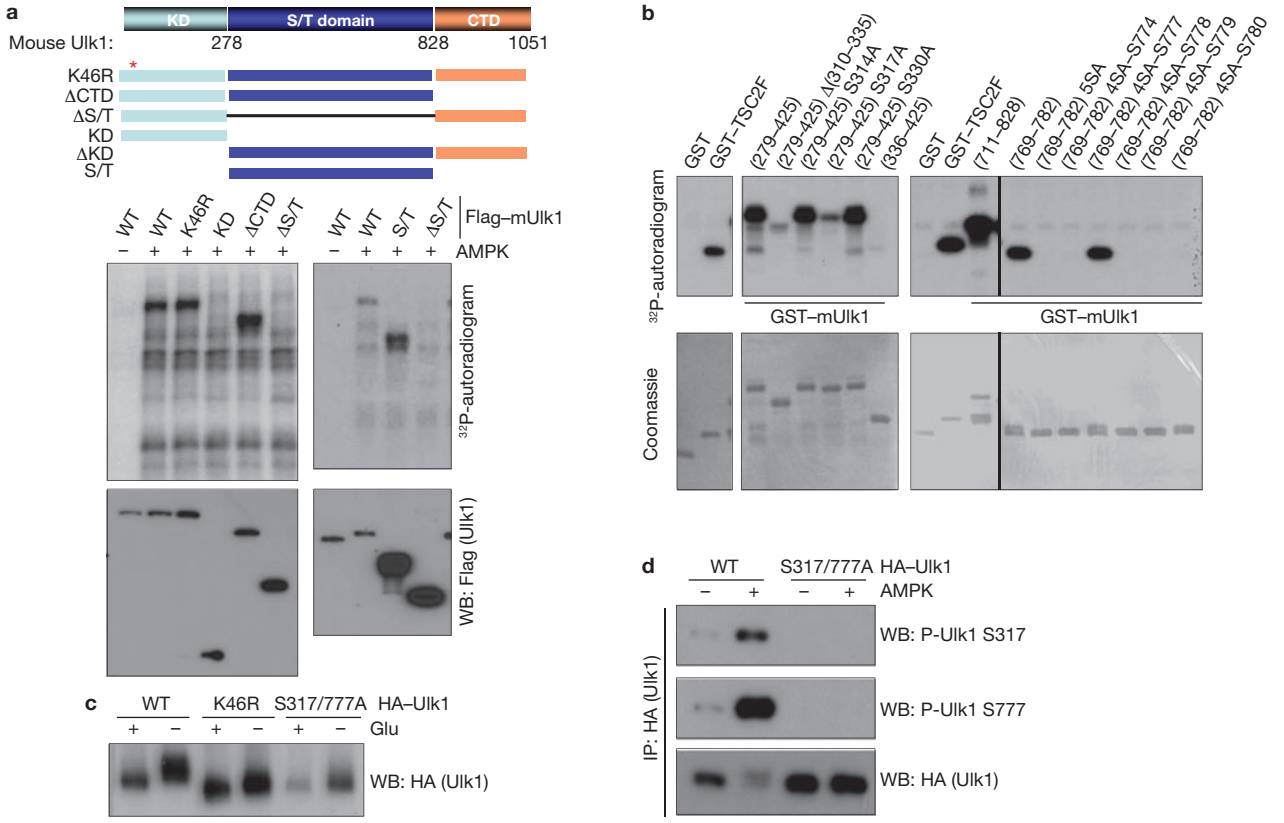

Figure 2 AMPK directly phosphorylates Ulk1 at Ser 317 and Ser 777. (**a**) AMPK phosphorylates the Ulk1 S/T domain *in vitro*. Top: schematic representation of Ulk1 domain structure and deletion constructs used to map phosphorylation sites. The mouse Ulk1 protein consists of an N-terminal kinase domain (KD; 1–278), serine/threonine-rich domain (S/T domain, 279–828), and C-terminal domain (CTD, 829–1051). Bottom: the indicated Flag–Ulk1 deletion mutants were immunopurified from transfected HEK293 cells and were used for *in vitro* AMPK assay as a substrate. Phosphorylation was examined by ^{32}P-autoradiogram and protein level was determined by western blot. (**b**) Determination of AMPK phosphorylation sites in Ulk1. The indicated recombinant GST–Ulk1 mutants were expressed and purified from *Escherichia coli*, and used as substrates for *in vitro* phosphorylation by AMPK. Deletion analyses indicated that two Ulk1 fragments in the S/T domain, 279–425 and 769–782, were highly phosphorylated by AMPK *in vitro*. Mutation of Ser 317 abolished the majority of phosphorylation in the Ulk1 fragment 279–425. Within the fragment 769–782, mutations of five serine residues (Ser 774, Ser 777, Ser 778, Ser 779 and Ser 780) to alanine, denoted as (769–782) 5SA, completely abolished the phosphorylation by AMPK. Reconstitution of Ser 777 in this mutation background, (769–782) 4SA-S777, but not any of the other four residues, restored the phosphorylation by AMPK. GST and GST–TSC2F (TSC2 fragment 1300–1367 containing AMPK phosphorylation site at Ser 1345) were used as negative and positive controls for AMPK reaction, respectively. Phosphorylation was determined by ^{32}P-autoradiograph and the protein levels were detected by Coomassie staining. (**c**) Ser 317/Ser 777 are required for glucose-starvation induced Ulk1 phosphorylation *in vivo*. HA–Ulk1 and mutants were transfected into HEK293 cells. Cells were starved for glucose for 4 h as indicated. HA–Ulk1 was immunoprecipitated and examined by western blot for mobility. (**d**) Phosphorylation of Ulk1 Ser 317 and Ser 777 are induced by AMPK. Wild-type HA–Ulk1 or S317/777A mutant were co-transfected with AMPK into HEK293 cells as indicated. HA–Ulk1 was immunoprecipitated (IP) and phosphorylation of Ser 317 and Ser 777 were determined by western blotting. Uncropped images of blots are shown in Supplementary Fig. S5.

by a decreased mobility (Supplementary Information, Fig. S1d). Also, overexpression of AMPK could activate the co-transfected HA–Ulk1 even in glucose-rich condition, which is comparable to Ulk1 activation by glucose starvation (Supplementary Information, Fig. S1e).

During autophagy, carboxy-terminal lipid modification of LC3 is a well-characterized phenomenon required for autophagosome formation, which can be readily detected by an increased electrophoretic mobility (LC3-II)[42]. Glucose starvation increased LC3-II similarly to rapamycin treatment and this effect was blocked by compound C (Supplementary Information, Fig. S1f), supporting a role for AMPK in induction of autophagy through glucose starvation. To further determine the function of AMPK in Ulk1 activation under physiological conditions, we measured Ulk1 activity in AMPKα1/α2 double knockout (DKO) cells. We observed that endogenous Ulk1 had a lower basal activity, and importantly could not be activated by glucose starvation (Fig. 1f). Together, these data demonstrate that Ulk1 activation induced by glucose starvation is mediated by AMPK, which directly activates Ulk1 by phosphorylation.

The effect of amino-acid starvation, which also induces autophagy, on Ulk1 activity was examined. Consistent with the recent reports[21,23], amino-acid starvation increased Ulk1 autophosphorylation activity (Fig. 1g). Interestingly, amino-acid starvation could still stimulate Ulk1 activation in the cells expressing AMPK-DN mutant although overall Ulk1 activity was lower in these cells. Similarly, rapamycin could activate Ulk1 in these cells. In contrast, Ulk1 activation induced by glucose starvation was largely blocked by AMPK-DN. These observations are consistent with the fact that AMPK is directly involved in cellular energy sensing but not amino-acid signalling. Consistently, amino-acid starvation could induce autophagic markers, LC3 lipidation (LC3-II, Supplementary

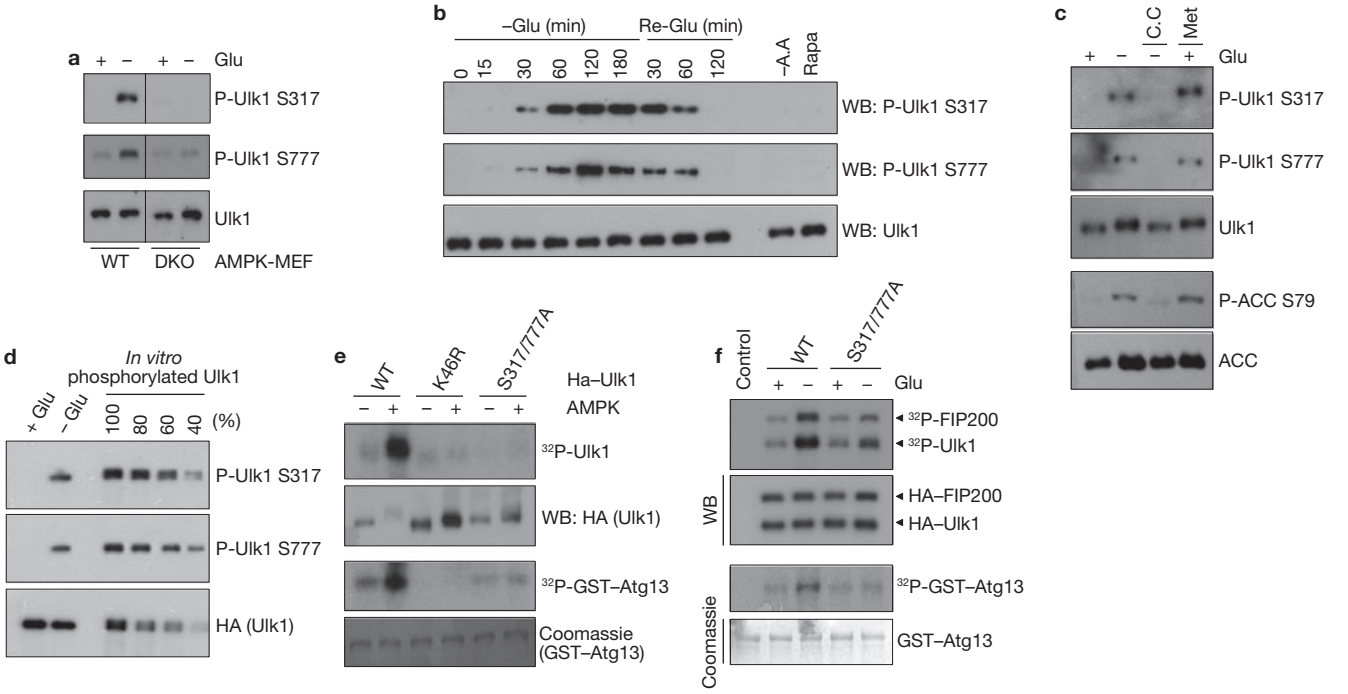

Figure 3 AMPK-dependent Ulk1 Ser 317 and Ser 777 phosphorylation is required for Ulk1 activation in response to glucose starvation. (**a**) AMPK wild-type or DKO MEFs were starved of glucose (4 h) as indicated. Total cell lysates were probed for Ulk1 protein and phosphorylation. (**b**) Time course of Ulk1 Ser 317 and Ser 777 phosphorylation in response to glucose starvation/re-addition. MEFs were starved of glucose (–Glu) for the indicated times. After 3 h starvation, the culture was switched to glucose-containing (25 mM) medium and samples were harvested (Re-Glu). In parallel, cells were treated with amino-acid-free (–A.A) medium or 50 nM rapamycin (Rapa) for 3 h. (**c**) Phosphorylation of Ulk1 Ser 317 and Ser 777 correlates with AMPK activity. MEFs were starved of glucose (4 h) as indicated in the presence or absence of 20 μM compound C (C.C). In parallel, cells were treated with 2 mM Metformin (Met, 2 h) in glucose-rich medium. Phosphorylation of ACC S79 was tested as a positive control for AMPK activation. (**d**) Ulk1 is highly phosphorylated at Ser 317 and Ser 777 by glucose starvation *in vivo*. To determine the Ulk1 phosphorylation level *in vivo*, immunopurified HA–Ulk1 protein was phosphorylated by AMPK *in vitro* (100% represents full phosphorylation of Ulk1 by AMPK). *In vitro* phosphorylated HA–Ulk1 was diluted as indicated, and was immunoblotted along with the immunoprecipitated HA–Ulk1 from cells grown in either glucose-rich (+ Glu) or glucose-free (– Glu, 4 h) medium. The density of the bands was then quantified. By this measurement, approximately 50% of Ulk1 isolated from glucose-starved cells was phosphorylated on Ser 317 and Ser 777. (**e**) The indicated HA–Ulk1 proteins were immunopurified from transfected HEK293 cells grown in high-glucose medium, and then incubated with AMPK in the presence of cold ATP for 15 min *in vitro*. After the reaction, AMPK was removed by extensive washing, the resulting Ulk1 immuno-complexes were assayed for kinase activity in the presence of ^{32}P-ATP. (**f**) HA–Ulk1 proteins (wild type or S317/777A mutant) were immunoprecipitated from the transfected HEK293 cells, which were incubated with or without glucose (4 h) before lysis. An *in vitro* kinase reaction was performed in the presence of GST–ATG13 and FIP200. Uncropped images of blots are shown in Supplementary Fig. S5.

Information, Fig. S1g) and green fluorescent protein (GFP)–LC3 puncta formation (Supplementary Information, Fig. S1h), in AMPK DKO mouse embryonic fibroblasts (MEFs), whereas these cells were defective during autophagy induced by glucose starvation. These data suggest that Ulk1 kinase can be activated by both AMPK-dependent (glucose starvation) and -independent (amino-acid starvation) manners.

AMPK activates Ulk1 by phosphorylating Ser 317 and Ser 777

To understand the mechanism underlying Ulk1 activation by AMPK, we determined the AMPK phosphorylation sites in Ulk1. We initially tested the AMPK consensus sites in Ulk1. Surprisingly, mutation of the AMPK consensus sites (Ser 494, Ser 555, Ser 574, Ser 622, Thr 624, Ser 693 and Ser 811) in Ulk1 had no significant effect on Ulk1 phosphorylation by AMPK *in vitro* (data not shown). Next, we performed systematic Ulk1 deletion experiments and found that AMPK phosphorylated the serine/threonine-rich domain (S/T domain) of Ulk1 (Fig. 2a). Further deletion and mutation analyses identified Ser 317 and Ser 777 as the major AMPK phosphorylation sites (Fig. 2b). Mutation of both Ser 317 and Ser 777 significantly decreased, though not completely, the phosphorylation of full-length Ulk1 by AMPK *in vitro* (Supplementary Information, Fig. S2a), suggesting that there are additional AMPK phosphorylation sites in Ulk1. However, the Ulk1 mobility shift induced by glucose starvation , which was due to both phosphorylation by AMPK and autophosphorylation, was significantly compromised in the S317/777A mutant in the transfected cells (Fig. 2c), indicating that these two residues are major AMPK sites in response to glucose starvation *in vivo*. To confirm Ulk1 phosphorylation *in vivo*, antibodies were prepared and verified for specificity against recombinant Ulk1 fragments phosphorylated by AMPK *in vitro* at Ser 317 and Ser 777 (Supplementary Information, Fig. S2b). Western blot using these antibodies demonstrated that AMPK co-transfection increased Ulk1 Ser 317 and Ser 777 phosphorylation (Fig. 2d).

To determine Ser 317 and Ser 777 phosphorylation of endogenous Ulk1, total lysates of MEF cells were probed with phospho-Ser 317- and phospho-Ser 777-specific antibodies. We found that glucose starvation induced a robust Ulk1 phosphorylation at Ser 317 and Ser 777 (Fig. 3a). Notably, these phosphorylations were completely diminished in AMPK DKO cells. These data demonstrate an essential role for AMPK in phosphorylation of Ulk1 Ser 317 and Ser 777. Phosphorylation of both Ser 317 and Ser 777 appeared at 30 min and peaked at 60–120 min on glucose deprivation and these phosphorylation events gradually decreased

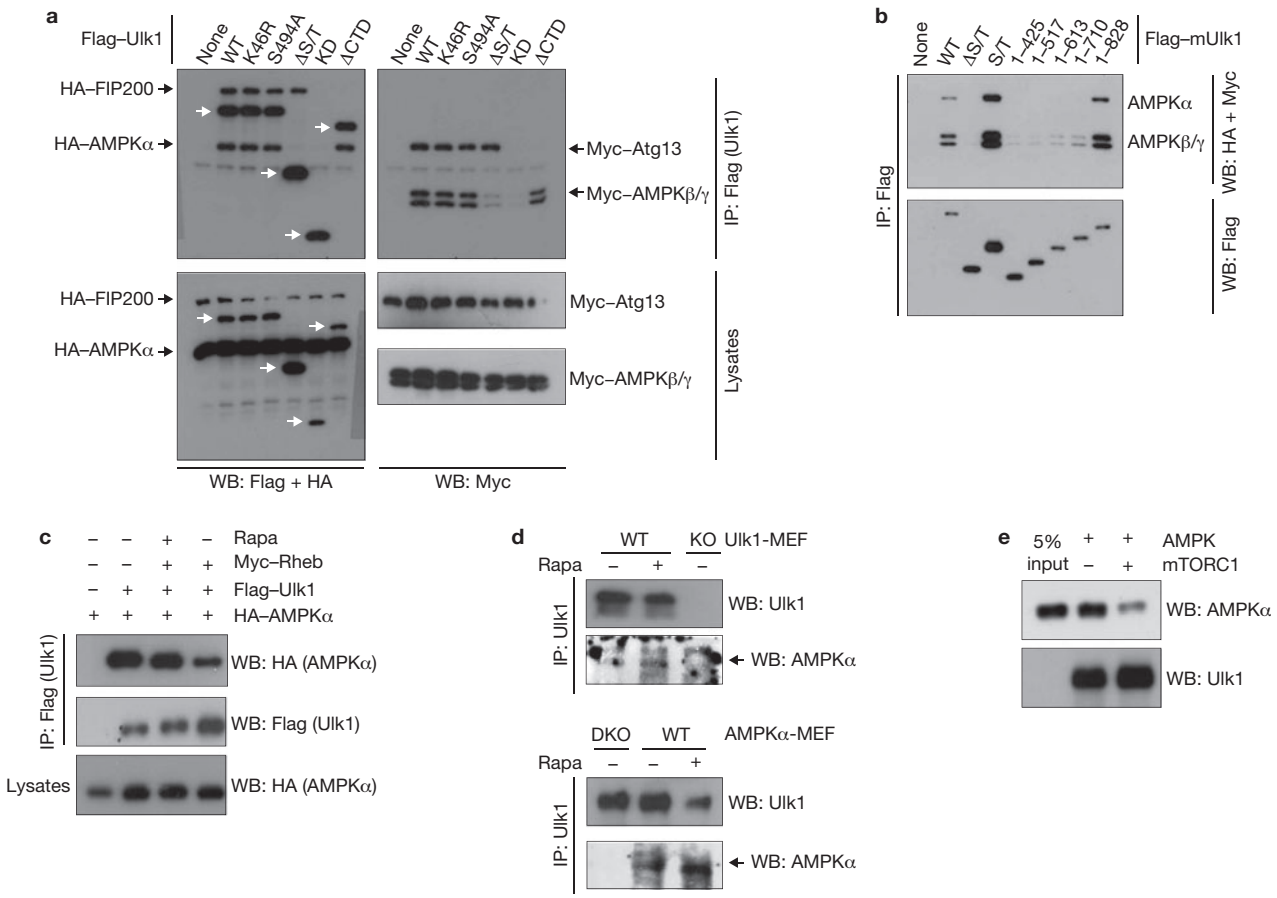

Figure 4 mTORC1 disrupts the Ulk1–AMPK interaction. (**a**) AMPK interacts with Ulk1. HEK293 cells were transfected with the various Flag–Ulk1 deletion mutants together with AMPK α/β/γ, Atg13 and FIP200. Flag–Ulk1 protein (indicated by white arrows) was immunoprecipitated and co-immunoprecipitation of AMPK α/β/γ, Atg13 and FIP200 were examined by western blots. (**b**) Deletion analysis of Ulk1 regions responsible for AMPK interaction. The indicated Flag–Ulk1 truncation mutants were immunoprecipitated from transfected HEK293 cells co-expressing AMPK complex (α/β/γ). Co-immunoprecipitation of AMPK subunits was determined by western blots. (**c**) Rheb inhibits the Ulk1–AMPK interaction. HA–AMPKα, Flag–Ulk1 and Myc–Rheb were co-transfected into HEK293 cells as indicated. Cells were treated with or without rapamycin (50 nM Rapa) for 1 h before lysis. Flag–Ulk1 was immunoprecipitated and co-immunoprecipitates of AMPKα were determined by western blot. (**d**) Rapamycin treatment enhances the interaction of endogenous Ulk1 and AMPK. Endogenous Ulk1 proteins were immunoprecipitated from either Ulk1 or AMPK wild-type and knockout (single-knockout; KO or double-knockout; DKO) MEFs. Treatment with 50 nM rapamycin for 1 h is indicated (Rapa). Co-immunoprecipitation of endogenous AMPKα protein was determined by western blot. The arrow indicates AMPKα protein. (**e**) Phosphorylation by mTORC1 inhibits the ability of Ulk1 to bind AMPK *in vitro*. CBP/SBP–Ulk1 was purified from transfected HEK293 cells by streptavidin beads and the Ulk1–bead complex was incubated with mTORC1, which was prepared by Raptor immunoprecipitation, in the presence of cold ATP, as indicated. The resulting Ulk1 complex was incubated with the cell lysates containing AMPK, then extensively washed. The Ulk1 and associated AMPKα were detected by western blot. Uncropped images of blots are shown in Supplementary Fig. S5.

to basal level at 120 min after glucose re-addition (Fig. 3b). Notably, amino-acid starvation and rapamycin treatment were not sufficient to increase Ulk1 Ser 317 and Ser 777 phosphorylation because AMPK was not activated by these treatments. Moreover, phosphorylation of Ulk1 was inhibited by compound C and stimulated by Metformin (an AMPK activator[43]), similarly to the phosphorylation of AMPK substrate, ACC (Fig. 3c). This result shows that AMPK activation is necessary and sufficient for the phosphorylation of Ulk1 Ser 317 and Ser 777 on glucose starvation. To determine the levels of endogenous Ulk1 Ser 317/Ser 777 phosphorylation in response to glucose starvation, we compared relative phosphorylation of endogenous Ulk1 with the *in vitro* phosphorylated Ulk1, which was almost completely phosphorylated by AMPK based on mobility shift (Fig. 3d). Glucose starvation induced endogenous Ulk1 phosphorylation to a level approximately 50% of the *in vitro* phosphorylated Ulk1, indicating that a significant fraction of endogenous Ulk1 was indeed phosphorylated on glucose starvation. These data demonstrate that Ulk1 Ser 317 and Ser 777 are phosphorylated by AMPK under physiological conditions.

Next, the functional significance of Ser 317 and Ser 777 phosphorylation in Ulk1 activation was examined. AMPK markedly activated wild-type Ulk1, but did not activate the kinase-inactive K46R mutant or the phosphorylation defective S317/777A mutant *in vitro* (Fig. 3e). Additional mutations of individual AMPK consensus sites in the S317/777A background did not markedly further decrease Ulk1 activity, suggesting that Ser 317 and Ser 777 are major sites for AMPK-induced Ulk1 activation (Supplementary Information, Fig. S2c). Consistent with the *in vitro* experimental data, HA–Ulk1$^{S317/777A}$ was minimally activated by glucose starvation in the transfected cells, whereas the wild-type HA–Ulk1 was more efficiently activated (Fig. 3f). Together, our data demonstrate the importance of Ser 317/Ser 777 phosphorylation in

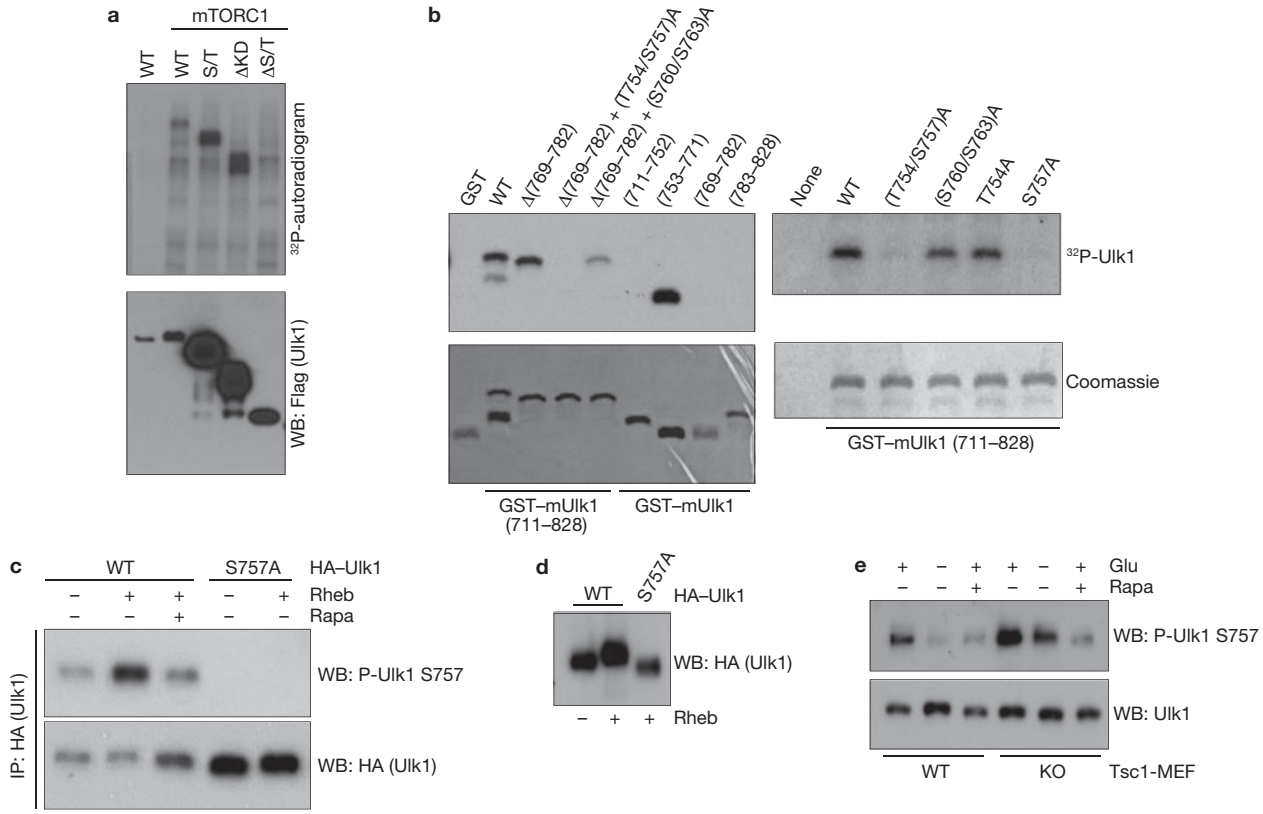

Figure 5 mTORC1 phosphorylates Ulk1 at Ser 757. (**a**) mTORC1 phosphorylates the Ulk1 S/T domain. Ulk1 deletion mutants were prepared from the transfected HEK293 cells and used for *in vitro* mTORC1 assay. Phosphorylation was examined by ^{32}P-autoradiogram (top) and protein level was determined by western blot (bottom). (**b**) Ser 757 is phosphorylated by mTORC1. Left: the indicated recombinant GST–mUlk1 mutants were purified from *E. coli* and used for *in vitro* mTORC1 assay as substrates. Deletion analyses isolated the fragment (753–771) as a target for mTORC1. The Ulk1 (753–771) fragment contains five conserved serine/threonine residues, Thr 754, Ser 757, Ser 760, Thr 763 and Thr 770. Right: mutation of Ser 757 abolished Ulk1 phosphorylation by mTORC1 *in vitro*. GST was used as negative control for mTORC1 phosphorylation reaction. Phosphorylation was determined by ^{32}P-autoradiograph (top), whereas protein levels were detected by Coomassie staining (bottom). (**c**) Rheb increases Ulk1 Ser 757 phosphorylation. HA–Ulk1 wild type and the S757A mutant were immunoprecipitated from transfected HEK293 cells. Co-transfection with Rheb and rapamycin (Rapa) treatment are indicated. Ulk1 Ser 757 phosphorylation was determined by western blot. (**d**) Rheb induces a mobility shift in wild-type Ulk1, but not the Ulk1^{S757A} mutant. HA–Ulk1 was transfected with or without Rheb into HEK293 cells. HA–Ulk1 was immunoprecipitated from the cells under nutrient-rich medium and Ulk1 mobility was examined by western blot. (**e**) Endogenous Ulk1 Ser 757 phosphorylation is elevated in *Tsc1*$^{-/-}$ MEFs. *Tsc1*$^{+/+}$ (WT) and *Tsc1*$^{-/-}$ (KO) MEFs were starved of glucose (4 h), or treated with 50 nM rapamycin (Rapa, 1 h). Ser 757 phosphorylation of endogenous Ulk1 was detected by a phospho-Ulk1 Ser 757 antibody. Uncropped images of blots are shown in Supplementary Fig. S5.

glucose-starvation-induced and AMPK-dependent Ulk1 activation.

mTORC1 disrupts the Ulk1–AMPK interaction by phosphorylating Ulk1 Ser 757

In yeast, nutrient starvation promotes ATG1–ATG13–ATG17 complex formation, and concomitant ATG1-kinase activation[16–17]. However, a similar regulation may not apply to the mammalian Ulk1 because the Ulk1 complex formation is not regulated by nutrients[22–23]. Instead, we observed an interaction between Ulk1 and AMPK (Fig. 4a). Deletion analyses showed that the S/T domain, particularly the fragment (711–828) of Ulk1, was required to bind AMPK (α, β and γ; Fig. 4a, b). Notably, the AMPK-binding domain does not overlap with the ATG13- and FIP200-binding regions (C-terminal domain of Ulk1, CTD). The interactions of Ulk1–AMPK and Ulk1–ATG13–FIP200 were not affected by glucose starvation (data not shown). The yeast TORC1 was reported to disrupt the ATG1 complex[16], but mTORC1 does not have a similar effect on the Ulk1–mAtg13–FIP200 complex[22–23]. Interestingly, we found that the interaction between Ulk1 and AMPK was disrupted by mTORC1. Overexpression of Rheb, an mTORC1 activator[44–45], decreased Ulk1–AMPK co-immunoprecipitation and rapamycin suppressed the effect of Rheb (Fig. 4c). Consistently, rapamycin treatment increased the interaction of endogenous Ulk1 and AMPK (Fig. 4d). Considering the report that mTORC1 could phosphorylate Ulk1 although the phosphorylation sites were not identified[21,23,31], we examined whether mTORC1 could directly regulate the Ulk1–AMPK interaction by phosphorylating Ulk1. Immunoprecipitated Ulk1 was incubated with mTORC1 *in vitro* and then used to pulldown AMPK. Pre-incubation with mTORC1 significantly reduced the ability of Ulk1 to pulldown AMPK (Fig. 4e). These data indicate that mTORC1 inhibits the Ulk1–AMPK interaction by directly phosphorylating Ulk1.

To understand the role of mTORC1 in Ulk1 regulation, we made efforts to identify the mTORC1 phosphorylation site in Ulk1. We tested phosphorylation of various Ulk1 deletions by mTORC1 *in vitro*. As shown in Fig. 5a, the Ulk1 S/T domain (residues 279–828) was phosphorylated by mTORC1. As mTORC1 phosphorylates the residue 651–1051 *in vitro*[23], we assumed that mTORC1 might phosphorylate Ulk1 between residues 651 and 828. Of note, this region includes the fragment (711–828) required for

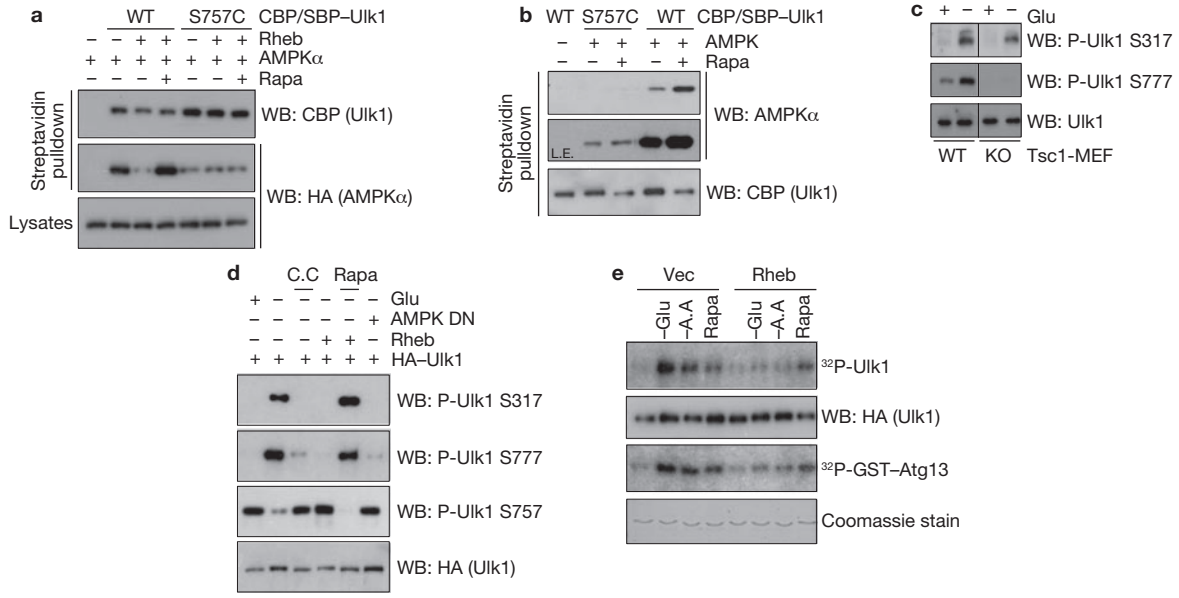

Figure 6 Phosphorylation of Ulk1 Ser 757 by mTORC1 inhibits the Ulk1–AMPK interaction. (**a**) Ulk1 Ser 757 is required for mTORC1 to regulate the interaction of Ulk1 with AMPK *in vivo*. CBP/SBP tagged Ulk1 (wild type or S757C) was co-transfected with HA–AMPKα and Rheb into HEK293 cells as indicated. Ulk1 was purified by streptavidin beads and the co-precipitated HA–AMPKα was examined by western blot (Rapa, 50 nM rapamycin treatment for 1 h before cell lysis). (**b**) Ulk1 Ser 757 is required for rapamycin to enhance the Ulk1–AMPK interaction *in vitro*. CBP/SBP Ulk1 proteins (wild type or S757C) were prepared from transfected HEK293 cells, which were pre-incubated with 50 nM rapamycin (Rapa, 1h) as indicated. The Ulk1 proteins were purified by streptavidin beads and the resulting Ulk1–bead was incubated with the bacterial purified AMPKα/β/γ complex. AMPKα protein levels in the *in vitro* pulldown assays were examined by western blot using AMPKα antibody. L.E.; long exposure. (**c**) Phosphorylation of AMPK sites Ser 317 and Ser 777 in Ulk1 are decreased in *Tsc1*$^{-/-}$ MEFs. *Tsc1*$^{+/+}$ (WT) and *Tsc1*$^{-/-}$ (KO) MEFs were starved of glucose (4 h), or treated with 50 nM rapamycin (Rapa, 1 h). Ser 317 and Ser 777 phosphorylation of endogenous Ulk1 was examined by western blotting with antibodies against Ulk1 phosphorylated at Ser 317 or Ser 777. (**d**) Rheb suppresses Ulk1 Ser 317 and Ser 777 phosphorylation in a manner dependent on mTORC1. HA–Ulk1, AMPKα kinase-dead mutant (DN), and Myc–Rheb were co-transfected into HEK293 cells as indicated. The cells were incubated with glucose-free medium (–Glu, 4 h), in which either 20 μM compound C (C.C.) or 50 nM Rapamycin (Rapa) was added. Total cell lysates were probed with antibodies against Ulk1 phosphorylated at Ser 317, Ser 777, Ser 757, and HA, as indicated. (**e**) Rheb inhibits glucose starvation-induced Ulk1 activation. HA–Ulk1 and Myc–Rheb was transfected into HEK293 cells, which were incubated with glucose-free (–Glu), amino-acid-free (–A.A) medium, or 50 nM rapamycin (Rapa) for 4 h before lysis. HA–Ulk1 was immunoprecipitated and kinase assays were performed. Ulk1 activity was measured by ^{32}P-autoradiogram and the protein level of HA–Ulk1 and GST–Atg13 used in the assay was determined by western blot and by Coomassie staining, respectively. Uncropped images of blots are shown in Supplementary Fig. S5.

AMPK interaction. Therefore, we examined the phosphorylation of Ulk1 fragment (711–828) by mTORC1. Ulk1 (711–828) was phosphorylated by mTORC1, but not by mTORC2 (Supplementary Information, Fig. S3a). Further deletion and mutagenic analyses identified Ser 757 as the mTORC1 phosphorylation site in this fragment (Fig. 5b). Using the antibody specific to phosphorylated Ser 757, we found that Ser 757 phosphorylation was increased when mTORC1 was activated by Rheb co-expression, and that rapamycin treatment inhibited the effect of Rheb (Fig. 5c). As expected, this phosphorylation was not detected in the Ulk1^{S757A} mutant, confirming the specificity of the antibody. Consistently, we observed that Rheb overexpression induced an Ulk1 mobility shift and this shift was abolished in the Ulk1^{S757A} mutant (Fig. 5d), suggesting that Ser 757 is the major mTORC1 phosphorylation site *in vivo*. We also mapped the amino-terminal region of Ulk1 as an important domain for Raptor binding (Supplementary Information, Fig. S3b), which is a substrate-recruiting subunit of mTORC1[46]. To further evaluate a role for mTORC1 in Ulk1 phosphorylation, we examined Ulk1 Ser 757 phosphorylation in the *Tsc1*$^{-/-}$ MEF, which has an elevated mTORC1 activity[47]. Phosphorylation of endogenous Ulk1 Ser 757 was increased in the *Tsc1*$^{-/-}$ MEF, but it was still inhibited by rapamycin (Fig. 5e), confirming the dependence of Ulk1 Ser 757 phosphorylation on mTORC1 activity. Also, glucose starvation, which inhibits mTORC1, decreased endogenous Ser 757 phosphorylation (Fig. 5e). The decrease of Ser 757 phosphorylation by glucose starvation was compromised in the *Tsc1*$^{-/-}$ MEFs, consistent with an inefficient mTORC1 inhibition by glucose starvation in the *Tsc* mutant cells[38]. AMPK is required for mTORC1 inhibition in response to glucose starvation[38–39]. Consistently, glucose starvation was less effective to decrease Ulk1 Ser 757 phosphorylation in the AMPK DKO MEFs (Supplementary Information, Fig. S3c), further supporting a role for mTORC1 in Ulk1 Ser 757 phosphorylation.

Next, we determined the effect of the mTORC1-dependent phosphorylation on the Ulk1–AMPK interaction. Ulk1 Ser 757 was mutated to either aspartate or alanine and we found that both mutations greatly diminished the Ulk1–AMPK interaction (Supplementary Information, Fig. S3d). This was not simply because of a global structural alteration of the mutation because Ulk1^{S757A} could still associate with Atg13 and FIP200 (data not shown). Therefore, we speculated that the chemistry of this position (hydroxyl group) is critical for AMPK interaction. We replaced Ser 757 with a cysteine residue, which is structurally close to serine, and found that it retained some interaction with AMPK although weaker (Supplementary Information, Fig. S3d). Importantly, the interaction between the S757C mutant and AMPK was no longer regulated by Rheb overexpression or rapamycin treatment as determined by co-immunoprecipitation *in vivo* (Fig. 6a). Moreover, in an *in vitro* pulldown assay, wild-type Ulk1 prepared from rapamycin-treated cells had a stronger binding to AMPK than the Ulk1 prepared from

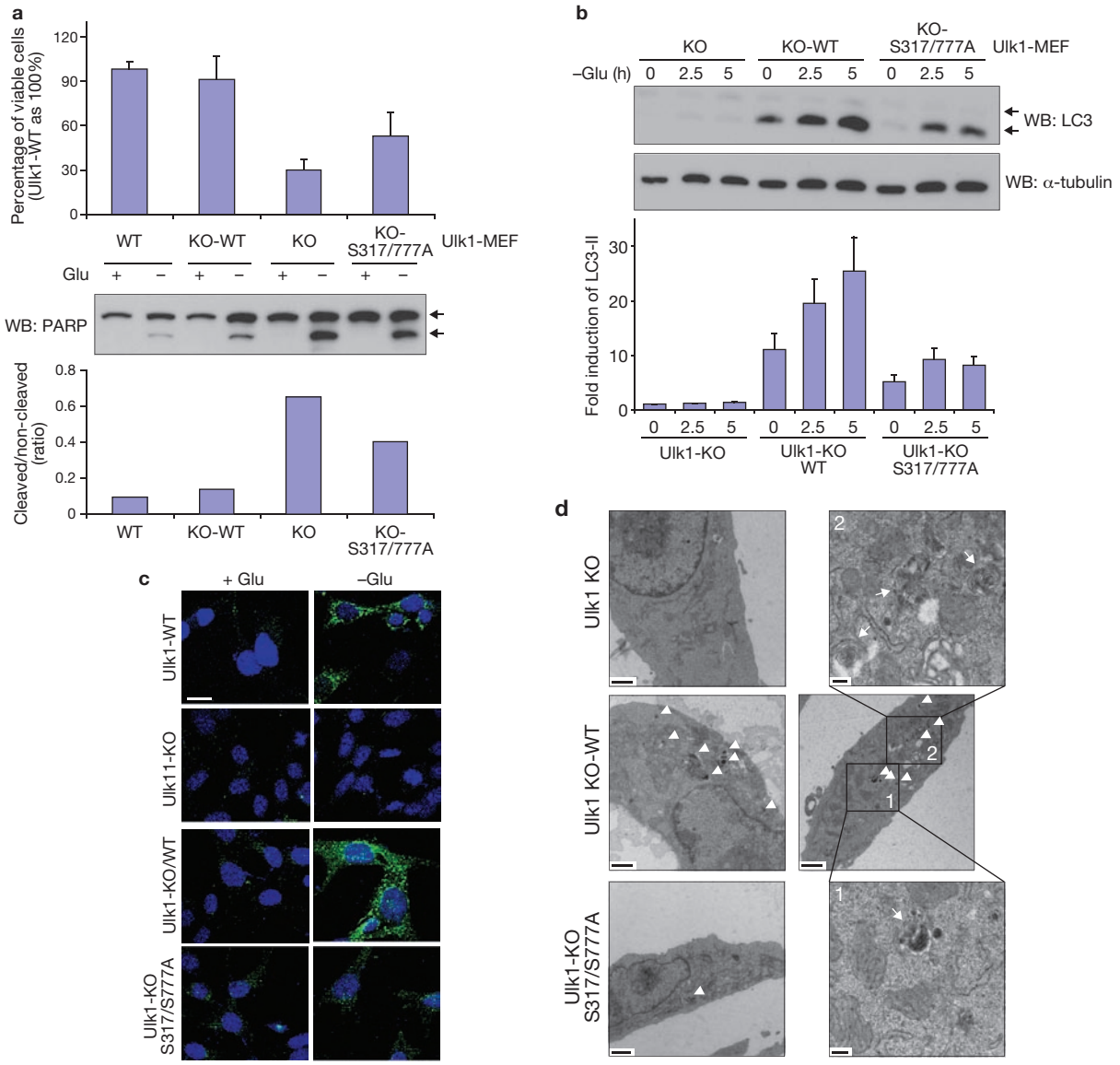

Figure 7 AMPK phosphorylation is required for Ulk1 function in autophagy on glucose starvation. (**a**) Ser 317/Ser 777 is required for Ulk1 to protect cells from glucose starvation. Viability (24 h, mean ± s.d., $n = 4$; top) and PARP cleavage (8 h; western blot, middle; quantification, $n = 2$, bottom) was examined in *Ulk1*$^{+/+}$ (WT), *Ulk1*$^{-/-}$ (KO), *Ulk1*$^{-/-}$ re-expressing wild-type Ulk1 (KO-WT), and *Ulk1*$^{-/-}$ re-expressing Ulk1 S317/777A mutant (KO-S317/777A) MEFs. Arrows in western blot indicate non-cleaved and cleaved PARP. (**b**) The Ulk1 S317/777A mutant is compromised in LC3 lipidation in response to glucose starvation. ULK1 MEFs were cultured in glucose-free medium for the indicated times. LC3-II level was determined by western blotting and the LC3-II accumulation was normalized by α-tubulin and quantified (bottom, $n = 3$, mean ± s.d.). A representative western blot was shown. The LC3 antibody used in this experiment seemed to preferentially recognise the lipid-modified form of LC3-II, which migrated faster on the gel. (**c**) The Ulk1 S317/777A mutant is defective in autophagosome formation. The indicated MEFs were starved of glucose (4 h) and the formation of GFP–LC3-positive autophagosomes was examined by confocal microscopy. GFP–LC3; green and DAPI; blue. Scale bar, 20 μm. (**d**) Autophagy vacuole analysis by electron microscopy. Low-magnification images of *Ulk1*$^{-/-}$ (KO, upper left panel), *Ulk1*$^{-/-}$ reconstituted with wild-type Ulk1 (KO-WT, two middle panels with accompanying higher magnification images), and *Ulk1*$^{-/-}$ reconstituted with Ulk1 S317/777A (KO-S317/777A, lower left panel) are shown. High-magnification images of autophagosomes from KO-WT are shown in upper right and lower right panels. Autophagosome/autolysosome-like structures indicated by arrowheads on the lower-magnification images and arrows in higher-magnification images. Scale bars; lower-magnification, 1 μm; higher-magnification, 200 nm.

the cells cultured in nutrient-rich conditions (Fig. 6b). However, the effect of rapamycin to increase the Ulk1–AMPK interaction was not observed in the S757C mutant. These data indicate that phosphorylation of Ser 757 by mTORC1 is important to regulate the Ulk1–AMPK interaction. Consistent with this hypothesis, phosphorylation of the two AMPK sites, Ser 317 and Ser 777, was suppressed in *Tsc1*$^{-/-}$ MEFs (Fig. 6c) or by Rheb co-transfection (Fig. 6d), both of which are conditions that result in high-mTORC1 activity. As shown in Fig. 6d, the phosphorylations of AMPK site Ser 317 and Ser 777 and of mTORC1 site Ser 757 were reciprocally regulated by the conditions that activate or inhibit AMPK and mTORC1. Glucose starvation decreased Ulk1 Ser 757 phosphorylation but increased Ser 317 and Ser 777 phosphorylation. As expected, the glucose starvation effect was blocked by compound C. In contrast, Rheb stimulated Ser 757 phosphorylation but inhibited Ser 317

and Ser 777 phosphorylation and these effects were reversed by rapamycin. Furthermore, overexpression of Rheb suppressed glucose-starvation induced Ulk1 activation, as demonstrated by autophosphorylation and transphosphorylation of GST–Atg13 (Fig. 6e). These data suggest that mTORC1 disrupts the interaction between Ulk1 and AMPK through phosphorylation of Ulk1 Ser 757, thereby preventing Ulk1 activation by AMPK.

The AMPK phosphorylation is required for Ulk1 function in autophagy

To determine the biological function of Ulk1 phosphorylation by AMPK, Ulk1 wild type and the S317/777A mutant were introduced into the *Ulk1*$^{-/-}$ MEFs (Supplementary Information, Fig. S4a). GFP–LC3 was also introduced into these MEFs to monitor GFP–LC3 positive autophagic vesicles (Supplementary Information, Fig. S4b). The *Ulk1*$^{-/-}$ (KO) cells were sensitive to glucose starvation with marked apoptosis (Fig. 7a). Knockdown of Ulk2 did not further sensitize the *Ulk1*$^{-/-}$ cells to glucose starvation (Supplementary Information, Fig. S4c), indicating that Ulk2 has a minor role in the MEF cells. The *Ulk1*$^{-/-}$ cells were defective in autophagy as indicated by LC3 lipidation, GFP–LC3 puncta formation, and autophagosome/autolysosome formation[42] (Fig. 7b–d). Expression of wild-type Ulk1 (KO-WT) rescued all defective phenotypes in the *Ulk1*$^{-/-}$ cells. In contrast, the Ulk1$^{S317/777A}$ mutant (KO-S317/777A) was less effective in protecting cells from glucose starvation-induced apoptosis (Fig. 7a). The glucose starvation-induced autophagy was also significantly compromised in cells expressing the Ulk1$^{S317/777A}$ mutant as indicated by LC3 lipidation (Fig. 7b and Supplementary Information Fig. S4d). As expected, glucose starvation increased autophagic flux in the wild type but not the *Atg5*$^{-/-}$ or *Ulk1*$^{-/-}$ cells (Supplementary Information, Fig. S4d). Re-expression of Ulk1 but not the S317/777A mutant restored autophagy. Consistently, *Ulk1*$^{-/-}$ cells expressing Ulk1$^{S317/777A}$ were defective in GFP–LC3 aggregation (Fig. 7c, S4e), and autophagosome/autolysosome formation (Fig. 7d, S4f). Based on the above data, we conclude that activation of Ulk1 through phosphorylation of Ser 317/Ser 777 by AMPK has a critical role in autophagy induction in response to glucose starvation.

DISCUSSION

As an autophagy-initiating kinase, the mechanism of Ulk1 regulation is central to understanding autophagy regulation. This study demonstrates a biochemical mechanism of Ulk1 activation by upstream signals and the functional importance of this regulation in autophagy induction. AMPK senses cellular energy status and activates Ulk1 kinase by a coordinated cascade (Fig. 8). Under glucose starvation, the activated AMPK inhibits mTORC1 to relieve Ser 757 phosphorylation, leading to Ulk1–AMPK interaction. AMPK then phosphorylates Ulk1 on Ser 317 and Ser 777, activates Ulk1 kinase, and eventually leads to autophagy induction. Notably, a recent autophagy-interaction proteome[48] and co-immunoprecipitation study[49] have also shown a physical interaction between Ulk1 and AMPK, consistent with our findings. Although AMPK may phosphorylate additional sites that may contribute to Ulk1 activation, phosphorylation of Ser 317/Ser 777 is required for Ulk1 activation and efficient autophagy induction in response to glucose starvation. We noticed that Ser 777 in the mouse Ulk1 is not conserved in human Ulk1, indicating that phosphorylation of other sites in human Ulk1 by AMPK may also contribute to its activation in response to glucose starvation. Moreover, Ser 317 and Ser 777 did not match the AMPK consensus

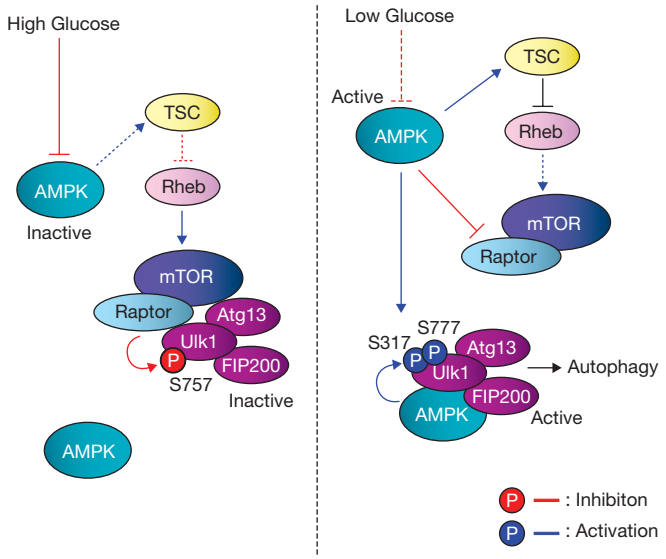

Figure 8 Model of Ulk1 regulation by AMPK and mTORC1 in response to glucose signals. Left: when glucose is sufficient, AMPK is inactive and mTORC1 is active. The active mTORC1 phosphorylates Ulk1 on Ser 757 to prevent Ulk1 interaction with and activation by AMPK. Right: when cellular energy level is limited, AMPK is activated and mTORC1 is inhibited by AMPK through the phosphorylation of TSC2 and Raptor. Phosphorylation of Ser 757 is decreased, and subsequently Ulk1 can interact with and be phosphorylated by AMPK on Ser 317 and Ser 777. The AMPK-phosphorylated Ulk1 is active and then initiates autophagy.

motifs[39,50]. Interestingly, both Ser 317 and Ser 777 are positioned at three residues C-terminal to the putative AMPK consensus sites, Ser 314 and Ser 774. Future studies are needed to test whether this represents a new AMPK recognition motif.

TORC1 is one of the most important autophagy regulators. Recently, DAP1 (death-associated protein 1) has been reported as a novel mTORC1 substrate and has an inhibitory role in autophagy [51]. Here, we show that mTORC1 inhibits Ulk1 activation by phosphorylating Ulk1 Ser 757 and disrupting its interaction with AMPK. Our study expands the mTORC1 regulatory networks, where Ulk1 phosphorylation represents the catabolic arm of mTORC1 biology. However, it is worth noting that inhibition of mTORC1 by amino-acid starvation or rapamycin treatment can activate Ulk1 in an AMPK-independent manner as these conditions are sufficient to activate Ulk1 and induce autophagy, but do not activate AMPK. Therefore, future studies are needed to have a comprehensive understanding of Ulk1 regulation, especially in response to amino-acid starvation.

The coordinated phosphorylation of Ulk1 by mTORC1 and AMPK may provide a mechanism for signal integration and, thus cells can properly respond to the complex extracellular milieu. For example, under conditions of moderate glucose limitation and sufficient amino acids, it is advantageous for cells to modulate metabolism but not to initiate autophagy. Under such conditions, activation of AMPK should alter cellular metabolism by phosphorylating metabolic enzymes to promote amino-acid utilization for energy production. Although AMPK would suppress mTORC1, mTORC1 should not be completely inhibited when amino acids are available. The residual mTORC1 activity may prevent Ulk1 activation, thus minimizing autophagy initiation. Therefore, the phosphorylation of Ulk1 by mTORC1 and AMPK may ensure that autophagy is not initiated unless severe starvation conditions are experienced.

The identification of Ulk1 as a direct target of mTORC1 and AMPK represents a significant step towards the understating how cellular nutrient sensor/integrator regulates autophagy machinery. Further studies directed at identifying physiological substrates of Ulk1 will be essential to understand how Ulk1 activation results in initiation of the autophagy programme. □

METHODS

Methods and any associated references are available in the online version of the paper at http://www.nature.com/naturecellbiology/

Note: Supplementary Information is available on the Nature Cell Biology website

ACKNOWLEDGEMENTS

We thank members of the Guan lab for discussions and reagents. We would especially like to thank I. Lian and C. Fang for technical assistance, and M. Farquhar, K. Kudicka and T. Meerloo for help with the electron microscopy. This work was supported by NIH grants GM51586 and GM62694 (to K.-L.G.).

AUTHOR CONTRIBUTIONS

J.K. performed the experiments; M.K. and B.V. established the AMPK and Ulk1 knockout MEFs, respectively; J.K. and K.-L.G. designed the experiments, analysed data and wrote the paper. All authors discussed the results and commented on the manuscript.

COMPETING FINANCIAL INTERESTS

The authors declare that they have no competing financial interests.

Published online at http://www.nature.com/naturecellbiology
Reprints and permissions information is available online at http://npg.nature.com/reprintsandpermissions/

1. He, C. & Klionsky, D. J. Regulation mechanisms and signaling pathways of autophagy. *Annu. Rev. Genet.* **43,** 67–93 (2009).
2. Wang, R. C. & Levine, B. Autophagy in cellular growth control. *FEBS Lett.* **584,** 1417–1426 (2010).
3. Hara, T. *et al.* FIP200, a ULK-interacting protein, is required for autophagosome formation in mammalian cells. *J. Cell Biol.* **181,** 497–510 (2008).
4. Stipanuk, M. H. Macroautophagy and its role in nutrient homeostasis. *Nutr. Rev.* **67,** 677–689 (2009).
5. Huang, J. & Klionsky, D. J. Autophagy and human disease. *Cell Cycle* **6,** 1837–1849 (2007).
6. Liang, C. & Jung, J. U. Autophagy genes as tumor suppressors. *Curr. Opin. Cell Biol.* **22,** 226–233 (2010).
7. Sarkar, S. & Rubinsztein, D. C. Huntington's disease: degradation of mutant huntingtin by autophagy. *FEBS J.* **275,** 4263–4270 (2008).
8. Cadwell, K., Stappenbeck, T. S. & Virgin, H. W. Role of autophagy and autophagy genes in inflammatory bowel disease. *Curr. Top. Microbiol. Immunol.* **335,** 141–167 (2009).
9. Lerena, M. C., Vazquez, C. L. & Colombo, M. I. Bacterial pathogens and the autophagic response. *Cell Microbiol.* **12,** 10–18 (2010).
10. Tal, M. C. & Iwasaki, A. Autophagy and innate recognition systems. *Curr. Top. Microbiol. Immunol.* **335,** 107–121 (2009).
11. Nakatogawa, H., Suzuki, K., Kamada, Y. & Ohsumi, Y. Dynamics and diversity in autophagy mechanisms: lessons from yeast. *Nat. Rev. Mol. Cell Biol.* **10,** 458–467 (2009).
12. Xie, Z. & Klionsky, D. J. Autophagosome formation: core machinery and adaptations. *Nat. Cell Biol.* **9,** 1102–1109 (2007).
13. Inoue, Y. & Klionsky, D. J. Regulation of macroautophagy in *Saccharomyces cerevisiae*. *Semin. Cell Dev. Biol.* **21,** 664–670 (2010).
14. Mizushima, N. The role of the Atg1/ULK1 complex in autophagy regulation. *Curr. Opin. Cell Biol.* **22,** 132–139 (2010).
15. Chan, E. Y. & Tooze, S. A. Evolution of Atg1 function and regulation. *Autophagy* **5,** 758–765 (2009).
16. Kamada, Y. *et al.* Tor-mediated induction of autophagy via an Apg1 protein kinase complex. *J. Cell Biol.* **150,** 1507–1513 (2000).
17. Kabeya, Y. *et al.* Atg17 functions in cooperation with Atg1 and Atg13 in yeast autophagy. *Mol. Biol. Cell* **16,** 2544–2553 (2005).
18. Chang, Y. Y. & Neufeld, T. P. An Atg1/Atg13 complex with multiple roles in TOR-mediated autophagy regulation. *Mol. Biol. Cell* **20,** 2004–2014 (2009).
19. Chan, E. Y., Kir, S. & Tooze, S. A. siRNA screening of the kinome identifies ULK1 as a multidomain modulator of autophagy. *J. Biol. Chem.* **282,** 25464–25474 (2007).
20. Young, A. R. *et al.* Starvation and ULK1-dependent cycling of mammalian Atg9 between the TGN and endosomes. *J. Cell Sci.* **119,** 3888–3900 (2006).
21. Ganley, I. G. *et al.* ULK1.ATG13.FIP200 complex mediates mTOR signaling and is essential for autophagy. *J. Biol. Chem.* **284,** 12297–12305 (2009).
22. Hosokawa, N. *et al.* Atg101, a novel mammalian autophagy protein interacting with Atg13. *Autophagy* **5,** 973–979 (2009).
23. Jung, C. H. *et al.* ULK–Atg13–FIP200 complexes mediate mTOR signaling to the autophagy machinery. *Mol. Biol. Cell* **20,** 1992–2003 (2009).
24. Sudarsanam, S. & Johnson, D. E. Functional consequences of mTOR inhibition. *Curr. Opin. Drug Discov. Devel.* **13,** 31–40 (2010).
25. Jung, C. H., Ro, S. H., Cao, J., Otto, N. M. & Kim, D. H. mTOR regulation of autophagy. *FEBS Lett.* **584,** 1287–1295 (2010).
26. Chang, Y. Y. *et al.* Nutrient-dependent regulation of autophagy through the target of rapamycin pathway. *Biochem. Soc. Trans.* **37,** 232–236 (2009).
27. Wullschleger, S., Loewith, R. & Hall, M. N. TOR signaling in growth and metabolism. *Cell* **124,** 471–484 (2006).
28. Kamada, Y., Sekito, T. & Ohsumi, Y. Autophagy in yeast: a TOR-mediated response to nutrient starvation. *Curr. Top. Microbiol. Immunol.* **279,** 73–84 (2004).
29. Funakoshi, T., Matsuura, A., Noda, T. & Ohsumi, Y. Analyses of *APG13* gene involved in autophagy in yeast, *Saccharomyces cerevisiae*. *Gene* **192,** 207–213 (1997).
30. Kamada, Y. *et al.* Tor directly controls the Atg1 kinase complex to regulate autophagy. *Mol. Cell Biol.* **30,** 1049–1058 (2010).
31. Hosokawa, N. *et al.* Nutrient-dependent mTORC1 association with the ULK1–Atg13–FIP200 complex required for autophagy. *Mol. Biol. Cell* **20,** 1981–1991 (2009).
32. Hardie, D. G. AMP-activated/SNF1 protein kinases: conserved guardians of cellular energy. *Nat. Rev. Mol. Cell Biol.* **8,** 774–785 (2007).
33. Vingtdeux, V. *et al.* AMP-activated protein kinase signaling activation by resveratrol modulates amyloid-β peptide metabolism. *J. Biol. Chem.* **285,** 9100–9113 (2010).
34. Herrero-Martin, G. *et al.* TAK1 activates AMPK-dependent cytoprotective autophagy in TRAIL-treated epithelial cells. *EMBO J.* **28,** 677–685 (2009).
35. Matsui, Y. *et al.* Distinct roles of autophagy in the heart during ischemia and reperfusion: roles of AMP-activated protein kinase and Beclin 1 in mediating autophagy. *Circ. Res.* **100,** 914–922 (2007).
36. Liang, J. *et al.* The energy sensing LKB1–AMPK pathway regulates p27(kip1) phosphorylation mediating the decision to enter autophagy or apoptosis. *Nat. Cell Biol.* **9,** 218–224 (2007).
37. Meley, D. *et al.* AMP-activated protein kinase and the regulation of autophagic proteolysis. *J. Biol. Chem.* **281,** 34870–34879 (2006).
38. Inoki, K., Zhu, T. & Guan, K. L. TSC2 mediates cellular energy response to control cell growth and survival. *Cell* **115,** 577–590 (2003).
39. Gwinn, D. M. *et al.* AMPK phosphorylation of raptor mediates a metabolic checkpoint. *Mol. Cell* **30,** 214–226 (2008).
40. Kinoshita, E., Kinoshita-Kikuta, E., Takiyama, K. & Koike, T. Phosphate-binding tag, a new tool to visualize phosphorylated proteins. *Mol. Cell Proteomics* **5,** 749–757 (2006).
41. Zhou, G. *et al.* Role of AMP-activated protein kinase in mechanism of metformin action. *J. Clin. Invest.* **108,** 1167–1174 (2001).
42. Klionsky, D. J. *et al.* Guidelines for the use and interpretation of assays for monitoring autophagy in higher eukaryotes. *Autophagy* **4,** 151–175 (2008).
43. Hawley, S. A., Gadalla, A. E., Olsen, G. S. & Hardie, D. G. The antidiabetic drug metformin activates the AMP-activated protein kinase cascade via an adenine nucleotide-independent mechanism. *Diabetes* **51,** 2420–2425 (2002).
44. Inoki, K., Li, Y., Xu, T. & Guan, K. L. Rheb GTPase is a direct target of TSC2 GAP activity and regulates mTOR signaling. *Genes Dev.* **17,** 1829–1834 (2003).
45. Zhang, Y. *et al.* Rheb is a direct target of the tuberous sclerosis tumour suppressor proteins. *Nat. Cell Biol.* **5,** 578–581 (2003).
46. Schalm, S. S., Fingar, D. C., Sabatini, D. M. & Blenis, J. TOS motif-mediated raptor binding regulates 4E-BP1 multisite phosphorylation and function. *Curr. Biol.* **13,** 797–806 (2003).
47. Inoki, K., Li, Y., Zhu, T., Wu, J. & Guan, K. L. TSC2 is phosphorylated and inhibited by Akt and suppresses mTOR signalling. *Nat. Cell Biol.* **4,** 648–657 (2002).
48. Behrends, C., Sowa, M. E., Gygi, S. P. & Harper, J. W. Network organization of the human autophagy system. *Nature* **466,** 68–76 (2010).
49. Lee, J. W., Park, S., Takahashi, Y. & Wang, H. G. The association of AMPK with ULK1 regulates autophagy. *PLoS One* **5,** e15394 (2010).
50. Scott, J. W., Norman, D. G., Hawley, S. A., Kontogiannis, L. & Hardie, D. G. Protein kinase substrate recognition studied using the recombinant catalytic domain of AMP-activated protein kinase and a model substrate. *J. Mol. Biol.* **317,** 309–323 (2002).
51. Koren, I., Reem, E. & Kimchi, A. DAP1, a novel substrate of mTOR, negatively regulates autophagy. *Curr. Biol.* **20,** 1093–1098 (2010).

DOI: 10.1038/ncb2152

METHODS

Antibodies and reagents. Anti-PARP (#9542, 1:1,000), AMPKα (#2532, 1:1,000) and LC3 (#2775, 1:2,000) antibodies were purchased from Cell Signaling technology. Anti-Ulk1 (A7481, 1:1,000), and α-tubulin (T6199, 1:10,000) antibodies were obtained from Sigma, Anti-HA (1:4,000) and Myc antibodies (1:4,000) were from Covance. Anti-phosphorylated Ser 317 and Ser 757 antibodies were generated by immunizing rabbits with phosphopeptides. The phospho-specific antibodies were affinity purified (Cell Signaling Technology). Anti-phospho Ser 777 antibody was prepared by immunizing rabbits (Biomyx). HA–Ulk1 wild-type and GFP–LC3 expression constructs were provided by J. Chung (Seoul National University, Korea) and N. Mizushima (Tokyo Medical and Dental University, Japan), respectively. Mutagenesis was performed based on Quik-Change mutagenesis (Stratagene).

Cell culture, transfection and viral infection. HEK293 cells or HEK293T were cultured in DMEM (Invitrogen) culture medium containing 10% fetal bovine serum (FBS; Invitrogen) and 50 μg ml^{-1} penicillin/streptomycin. The MEFs were grown in the DMEM culture medium (complete medium) supplemented with β-mercaptoethanol (Invitrogen), 1 mM pyruvate and non-essential amino-acid mixture (Invitrogen). Transfection with polyethylenimine (PEI) was performed as described[3]. To generate stable cells expressing wild-type or the indicated mutant mouse Ulk1 (mUlk1) proteins, retrovirus infection was performed by transfecting 293 Phoenix retrovirus packaging cells with pQCXIH (Clontech) empty vector or mUlk1 constructs expressing CBP (Calmodulin-binding peptide)/SBP (streptavidin-binding peptide) at the N-terminus of the mUlk1 protein. After transfection (48 h), retroviral supernatant was supplemented with 5 μg ml^{-1} polybrene, filtered through a 0.45-μm syringe filter, and used to infect *Ulk1*$^{-/-}$ (Ulk1-KO) MEFs. After infection (36 h), cells were selected with 0.2 mg ml^{-1} hygromycin (Invitrogen) in the complete culture medium. To establish Ulk2 knockdown stable cells in the Ulk1-KO background, lentiviral construct (pLKO.1-TRC system, Addgene) containing shRNA targeting mouse *Ulk2* (2592–2612, Forward oligonucleotide: 5′- CCGGaaccctgagctgtgcacatctCTCGAG*AGATGTGCACAGCTCAGGGTT*TTTTTC-3′; Reverse oligonucleotide: 5′- AATTGAAAAAaaccctgagctgtgcacatctCTCGAG*AGATGTGCACAGCTCAGGGTT*-3′; lower case characters and italic characters are the sense and antisense sequences for the targeting region, respectively) was generated and co-transfected with viral packaging plasmids (psPAX2 and pMD2.G) into HEK293T cells. Viral supernatant was filtered through 0.45-μm filter and applied to Ulk1-KO MEFs. Stable pools were obtained in the presence of 5 μg ml^{-1} puromycin (Sigma).

Western blot and immunoprecipitation. Cells were lysed with mild lysis buffer (MLB; 10 mM Tris at pH 7.5, 2 mM EDTA, 100 mM NaCl, 1% NP-40, 50 mM NaF, 1 mM Na_3VO_4 and protease inhibitor cocktail; Roche). These cell lysates were used for western analyses. For immunoprecipitation, the indicated antibody was coupled with protein G–Sepharose (Amersham bioscience) in 1% bovine serum albumin (BSA) in TBST (20 mM Tris at pH 8.0, 170 mM NaCl and 0.05% Tween-20). This immune complex was added to the cell lysates and incubated at 4 °C for 2 h. The resulting beads were washed with MLB five times before analysis.

Cell death assay. Cell viability was determined by cell counting with trypan blue staining (Sigma, T8154) according to the manufacturer's instructions. Also, poly-ADP ribose polymerase (PARP), an apoptotic marker protein, was examined by western blot. The index of apoptosis was determined by the ratio between the cleaved and noncleaved PARP protein level. The band intensity was quantified on ImageJ software (http://rsbweb.nih.gov/ij/index.html).

Protein purification and kinase assay. Bacterial expression constructs (pGEX-KG) containing the indicated genes were transformed into *Escherichia coli* DH5α. Cells were induced to protein overexpression under 0.5 mM IPTG (isopropyl β-D-1-thiogalactopyranoside) at 18 °C. Cells were resuspended in PBS containing 0.5% Triton X-100 and 2 mM β-mercaptoethanol, followed by ultrasonication. The proteins were purified by a single step using glutathione bead according to the manufacturer's protocol (Amersham Bioscience). Purified proteins were dialysed against 20 mM Tris at pH 8.0, and 10% glycerol. Purified bacterial GST–Ulk1 proteins (0.5 μg) were used for either mTOR or AMPK assay as substrates to determine phosphorylation sites. For mTOR assay, mTORC1 was prepared from the HEK293 cells, where Myc-mTOR and HA–Raptor were co-transfected. mTORC1 was immunoprecipitated by Raptor and eluted from the bead by adding the excess amount of HA peptide, followed by desalting with desalting spin column. For AMPK assay, 10 ng of purified AMPK α/β/γ complex (Cell signaling technology) was used. mTORC1 (ref. 4) and AMPK (ref. 5) assay were performed as previously described. Phosphorylation of GST–Ulk1 proteins was determined by ^{32}P-autoradiogram.

***In vitro* Ulk1 kinase assay.** Ulk1 proteins were immunoprecipitated with either HA (Covance) or endogenous Ulk1 (Santa Cruz, N-17) antibodies as indicated. The immune-complex was extensively washed with MLB (once) and RIPA buffer (50 mM Tris at pH 7.5, 150 mM NaCl, 50 mM NaF, 1 mM EDTA, 1 mM EGTA, 0.05% SDS, 1% Triton X-100 and 0.5% deoxycholate) twice, followed by washing with kinase assay buffer containing 20 mM HEPES at pH 7.4, 1 mM EGTA, 0.4 mM EDTA, 5 mM $MgCl_2$ and 0.05 mM DTT (dithiothreitol). For Ulk1 autophosphorylation assay, the immunoprecipitated Ulk1 bead was incubated in kinase assay buffer containing 10 μM cold ATP and 2 μCi [γ-^{32}P]ATP per reaction. For kinase assays with GST–ATG13 and/or FIP200, GST–ATG13 was bacterially purified and HA–FIP200 proteins were immunopurified from the transfected HEK293 cells and eluted by adding the excess amount of HA peptide (Sigma). HA peptide was removed by desalting spin column (Pierce). The kinase reaction was performed at 37 °C for 30 min and the reaction was terminated by adding SDS sample buffer and subjected to SDS–PAGE (polyacrylamide gel electrophoresis) and autoradiography.

Lambda phosphatase/AMPK treatment *in vitro*. To evaluate the effects of phosphorylation on Ulk1 kinase activity, Ulk1 was pre-incubated with either lambda phosphatase or AMPK *in vitro*. First, the cells were starved of glucose (4 h) and then Ulk1 (endogenous Ulk1 or HA–tagged Ulk1) was immunoprecipitated as indicated. The Ulk1 immune-complex was incubated with either 5U lambda phosphatase (Cell signaling technology) in the phosphatase buffer or 5 ng of purified AMPK (Cell Signaling Technology) in kinase assay buffer supplemented with 0.2 mM AMP and 0.1 mM cold ATP, for 15 min. The Ulk1-bound beads were extensively washed with RIPA buffer and kinase assay buffer and recovered by centrifugation. The resulting Ulk1–bead was assayed for Ulk1 autophosphorylation and/or for GST–ATG13 phosphorylation in the presence of [^{32}P]ATP. To rule out the possibility that residual AMPK or lambda phosphatase contamination might affect Ulk1 autophosphorylation (or GST–ATG13 phosphorylation), autophosphorylation of kinase-inactive Ulk1 (K46R) or dephosphorylation of ^{32}P-prelabelled GST–TSC2 (phosphorylation on Ser 1345 in the TSC2 fragment 1300–1367) were examined as controls for AMPK and lambda phosphatase, respectively.

***In vitro* pulldown assay.** CBP/SBP–Ulk1 (wild type or S757C mutant) and Myc–Rheb were co-transfected into HEK293 cells as indicated. The cells were treated with or without 50 nM rapamycin for 1 h and then Ulk1 proteins were purified by streptavidin beads. The resulting Ulk1–beads were incubated with the bacterial purified AMPKα/β/γ complex and recovered by centrifugation. The beads were extensively washed with MLB. For *in vitro* Ulk1 phosphorylation by mTOR, CBP/SBP–Ulk1 proteins were purified from the transfected HEK293 cells, which were incubated with 50 nM rapamycin for 1 h to remove any mTORC1-induced phosphorylation on Ulk1, and then incubated with mTORC1 in kinase assay buffer supplemented with 20 μM cold ATP for 30 min. The Ulk1 immune-complex was extensively washed with RIPA buffer and recovered by centrifugation. The resulting Ulk1 proteins were incubated with 100 ng of bacterially purified AMPK α/β/γ complex or the total cell lysates including endogenous AMPK complex for 15 min at 4 °C, followed by MLB washing three times. The proteins on beads were eluted by adding SDS/sample buffer and subjected to SDS–PAGE and western blot using Ulk1 and AMPKα antibodies.

GFP–LC3 fluorescence analysis. MEFs stably expressing GFP–LC3 were plated onto glass coverslips. The following day, the medium was replaced with the complete culture medium for 4 h before experiment. Autophagy was induced by glucose starvation for 4 h. Cells were fixed with 2% paraformaldehyde for 20 min and rinsed with PBS twice. Cells were mounted and visualized under a confocal microscope (Zeiss LSM, ×64 PlanAPO oil lens). To quantify GFP–LC3-positive autophagosomes, five different confocal microscopy images were randomly chosen

and GFP-positive dots were examined on the images with identical brightness and contrast setting. Cells showing more than five strong GFP-positive dots were counted as GFP–LC3 autophagosomes. Total number of cells on images was determined by nuclei staining with DAPI (4',6-diamidino-2-phenylindole).

Electron microscopy. MEFs were fixed in modified Karnovsky's fixative (1.5% glutaraldehyde, 3% paraformaldehyde and 5% sucrose in 0.1 M cacodylate buffer at pH 7.4) for 8 h, followed by treatment with 1% osmium tetroxide in 0.1 M cacodylate buffer for an additional 1 h. They were stained in 1% uranyl acetate and dehydrated in ethanol. Samples were embedded in epoxy resin, sectioned (60–70 nm), and placed on Formvar and carbon-coated copper grids. Grids were stained with uranyl acetate and lead nitrate, and the images were obtained using a JEOL 1200EX II (JEOL) transmission electron microscope and photographed on a Gatan digital camera (Gatan).

nature cell biology

SUPPLEMENTARY INFORMATION

DOI: 10.1038/ncb2152

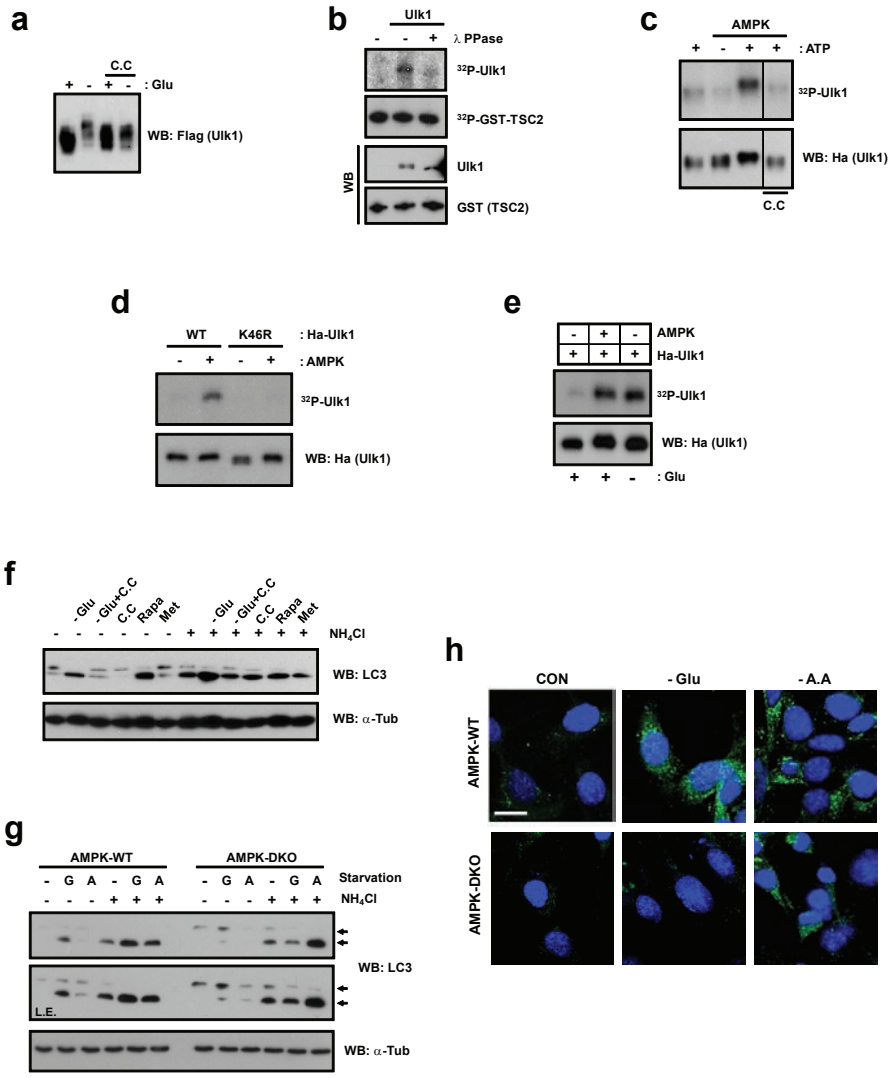

Figure S1 Ulk1 is activated by glucose starvation and by AMPK. **(a)** AMPK inhibitor blocks glucose starvation induced Ulk1 phosphorylation. Flag-Ulk1 was transfected into HEK293 cells and the cells were starved with glucose for 4hrs in the presence or absence of 20 μM Compound C (C.C) before lysis. Total cell lysates were examined for Ulk1 mobility by a Phos-tag gel, which produced a bigger mobility shift of phosphorylated protein. **(b)** Endogenous Ulk1 kinase is activated by phosphorylation. ULK1-WT MEFs were starved with glucose for 4hrs and endogenous Ulk1 protein was immunoprecipitated. Purified Ulk1 immune-complex was treated with lambda phosphatase (λ PPase) before Ulk1 autophosphorylation reaction as described in *Methods*. ^{32}P-pre-labeled GST-TSC2 was also added to Ulk1 autophosphorylation reaction mixture to monitor the possible phosphatase contaminations after RIPA buffer washing. Ulk1 autophosphorylation level was determined by ^{32}P- autoradiogram. Total protein levels for Ulk1 and GST-TSC2 were determined by western blots. **(c)** AMPK directly stimulates Ulk1 autophosphorylation activity *in vitro*. Ha-Ulk1 was immuno-purified from the transfected HEK293 cells and pre-incubated with purified AMPK complex (Cell signaling) for 15 min under the KA buffer supplemented with 0.2 mM AMP in the presence or absence of 0.1 mM cold ATP as indicated. Also, AMPK inhibitor (Compound C, 10 μM, denoted as C.C) was added to the reaction containing 0.1 mM ATP to confirm the reaction specificity toward AMPK. After *in vitro* AMPK reaction, Ulk1 immune-complex was extensively washed with RIPA buffer to remove AMPK and the Ulk1-bead was recovered by a centrifugation. The resulting Ulk1 immune-complex was used for Ulk1 autophosphorylation assay. **(d)** ^{32}P-incorporation in Ulk1 autophosphorylation is mediated by Ulk1 kinase. Ha-Ulk1 wild-type (WT) or kinase inactive (K46R) mutant was immunoprecipitated from the transfected cells under glucose-rich medium. The Ulk1 immune complex was pre-incubated with AMPK *in vitro* for 15 min and then, washed to remove AMPK. Ulk1 autophosphorylation activity was measured as described in Fig. S1b.. ^{32}P-incorporation in Ulk1 autophosphorylation was barely detected in Ulk1 K46R mutant even treated with AMPK. **(e)** AMPK co-transfection activates Ulk1 activity. Ha-Ulk1 and AMPK (α, β, and γ) were co-transfected into HEK293 cells. The cells were starved with glucose for 4hrs as indicated and then Ha-Ulk1 was immunoprecipitated to measure the Ulk1 autophosphorylation activity. **(f)** Glucose starvation and rapamycin stimulate autophagy. MEFs were starved with glucose (Glu) for 4hrs in the presence or absence of 20 μM Compound C (C.C). In parallel, cells were also treated with 50 nM rapamycin (Rapa) or 2 mM Metformin (Met) for 4hrs. To examine the autophagic flux, 10 mM NH_4Cl was added as indicated. The cell lysates were probed for LC3 antibody and α-Tubulin, respectively. **(g-h)** Glucose starvation induces autophagic markers, LC3 lipidation and LC3GFP-LC3 punctuate formation, in an AMPK-dependent manner. **(g)** AMPK-WT and DKO MEFs were incubated in either glucose-free (G) or amino acid-free (A) medium for 4hrs with or without 10 mM NH_4Cl as indicated. LC3 lipidation was monitored by LC3 western. **(h)** AMPK-WT and DKO MEFs stably expressing GFP-LC3 were incubated in either glucose-free (-Glu) or amino acid free (-A.A) media for 4hrs and GFP-positive autophagosome was analyzed by confocal microscopy. Bar, 20 μm.

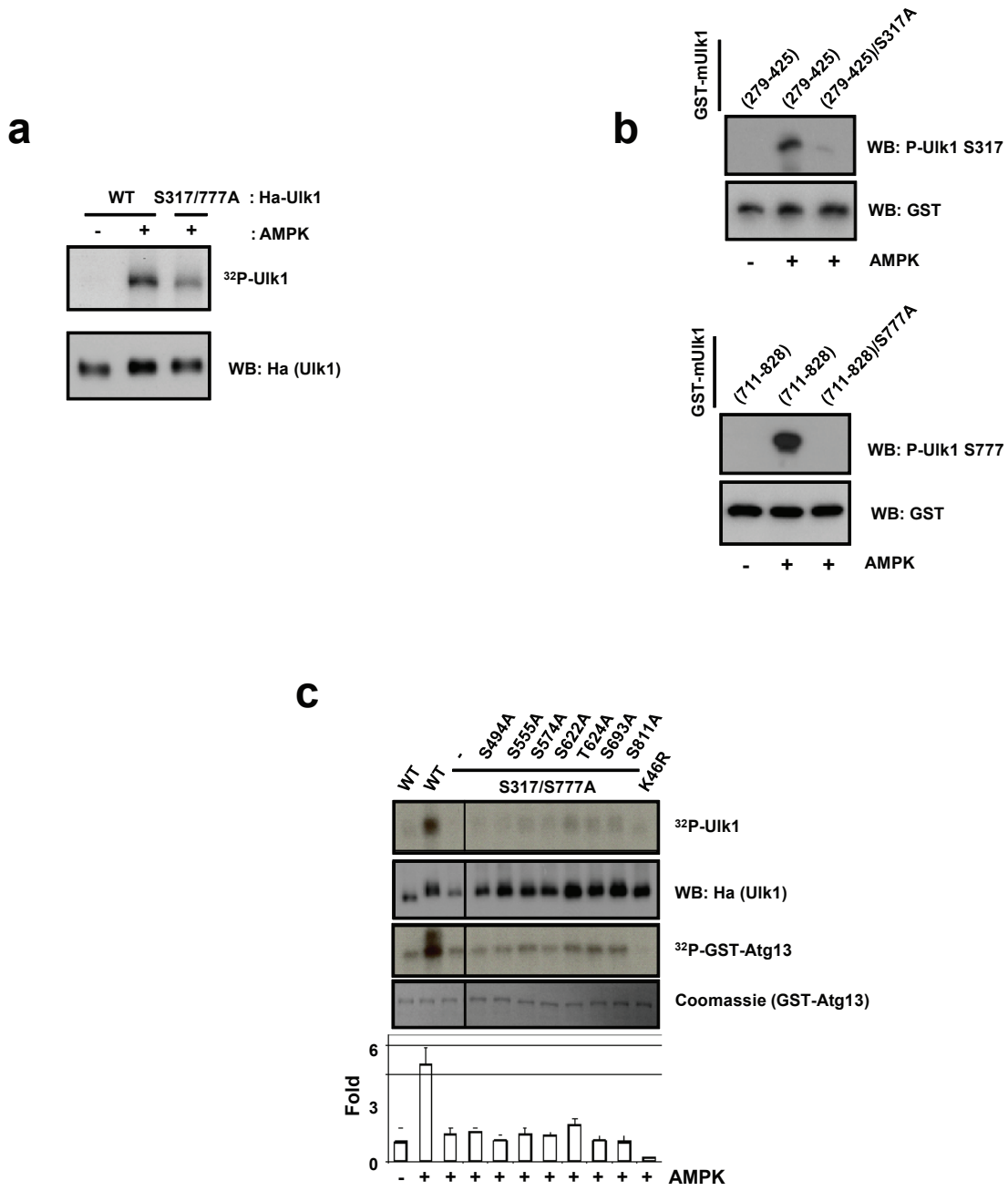

Figure S2 AMPK can activate Ulk1 by phosphorylating Ulk1 at S317 and S777 *in vitro*. **(a)** Mutation of S317 and S777 in Ulk1 decreases Ulk1 phosphorylation by AMPK *in vitro*. Ha-Ulk1 WT or S317/777A mutant were immunoprecipitated from the transfected HEK293 cells and used as substrates for *in vitro* AMPK phosphorylation. Phosphorylation level was determined by ^{32}P- autoradiogram. **(b)** Characterizations of Ulk1 S317 and S777 phospho-specific antibodies. Recombinant GST-mUlk1 fragments were purified from bacteria and 500 ng of the indicated recombinant fragments were used as a substrate for *in vitro* AMPK phosphorylation. After reaction, 5 ng of the phosphorylated GST-mUlk1 fragments were used to test specificity of S317 and S777 phospho-antibodies by western blot. Two phosphorylation defective mutant fragments, (279-425)/S317A and (711-828)/S777A, were used as negative controls. **(c)** S317 and S777 are the major sites important for Ulk1 activation by AMPK. Seven putative AMPK consensus sites in Ulk1 were individually mutated in the S317/777A background and Ulk1 proteins were prepared by immuno-purification from the transfected HEK293 cells. The immunopurified Ulk1 was subjected to *in vitro* activation by AMPK and then used in Ulk1 kinase assays. Ulk1 activity was determined by autophosphorylation (^{32}P-Ulk1) and Atg13 phosphorylation (^{32}P-GST-Atg13) and normalized to Ulk1 protein levels. Western/Coomassie staining analyses were performed on a duplicate gel to that used for autoradiogram analysis. The quantification data were obtained from three-independent experiments and one representative result was shown (mean ± S.D).

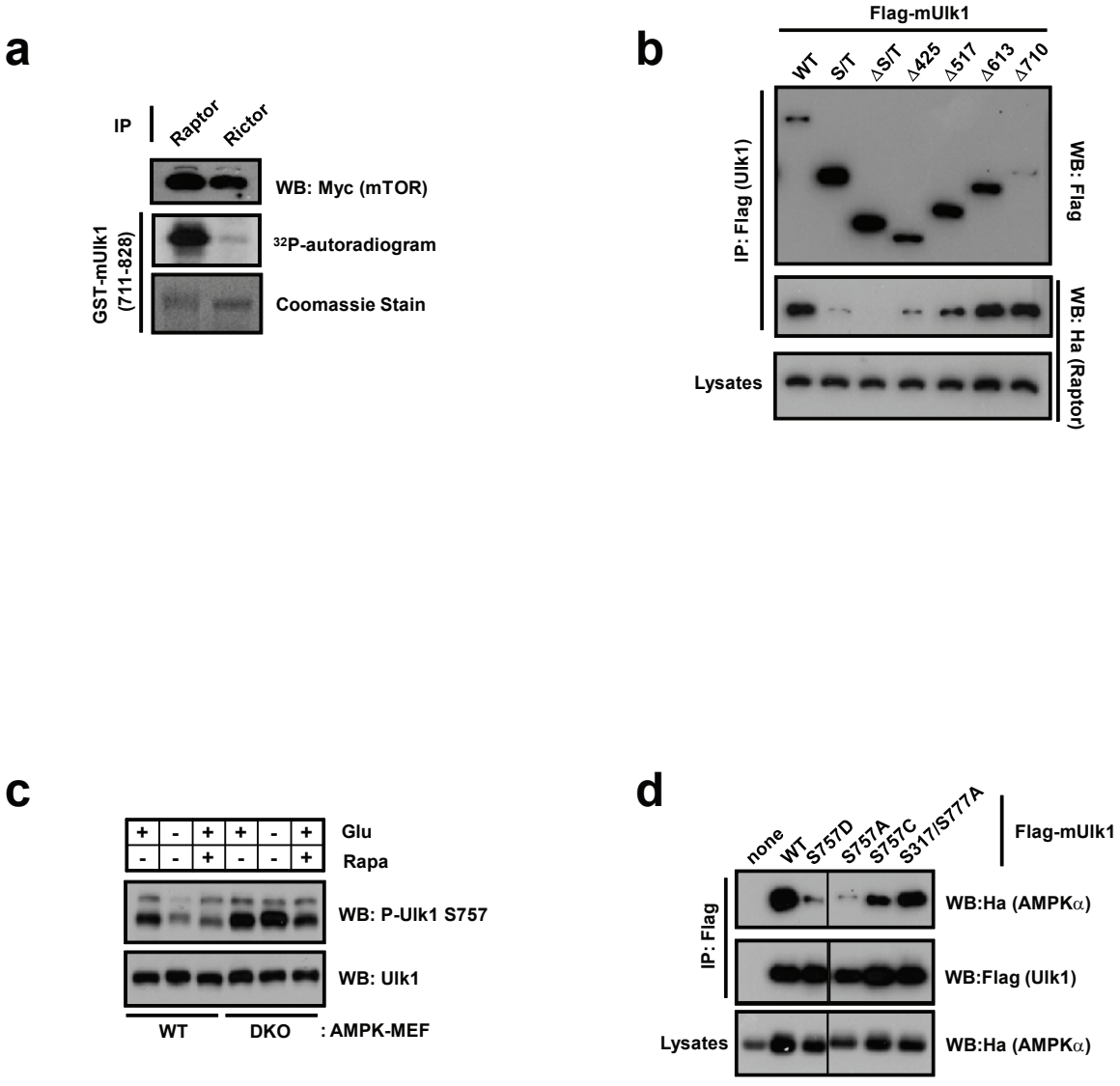

Figure S3 mTORC1 phosphorylates S757 in Ulk1. **(a)** mTORC1, but not mTORC2, phosphorylates Ulk1 *in vitro*. mTORC1 (by Raptor) and mTORC2 (by Rictor) were immuno-purified from the transfected HEK293 cells. The immune complexes were incubated with bacterially purified GST-mUlk1 (711-828) and phosphorylation of the GST-Ulk1 fragment was determined by ^{32}P-autoradiogram. Protein levels for mTOR and GST-mUlk1 (711-828) were shown by western blot and Coomassie staining, respectively. **(b)** Determination of Ulk1 domain responsible for Raptor interaction. Ha-Raptor was co-transfected with various Flag-Ulk1 deletion constructs. Ulk1 proteins were immunoprecipitated and Co-IP of Raptor was examined by western blot. **(c)** Glucose starvation fails to inhibit Ulk1 S757 phosphorylation in AMPK-DKO MEFs. AMPK WT an DKO MEF cells were starved with glucose (4hrs) or treated with 50 nM rapamycin (Rapa, 1hr), as indicated. Endogenous Ulk1 proteins were immunoprecipitated and the phosphorylation of S757 was examined. **(d)** S757 is important for Ulk1-AMPK interaction. The indicated Flag-Ulk1 mutants and Ha-AMPKα were co-transfected into HEK293 cells. Flag-Ulk1 proteins were immunoprecipitated and Co-IP of Ha-AMPKα was examined by western blot.

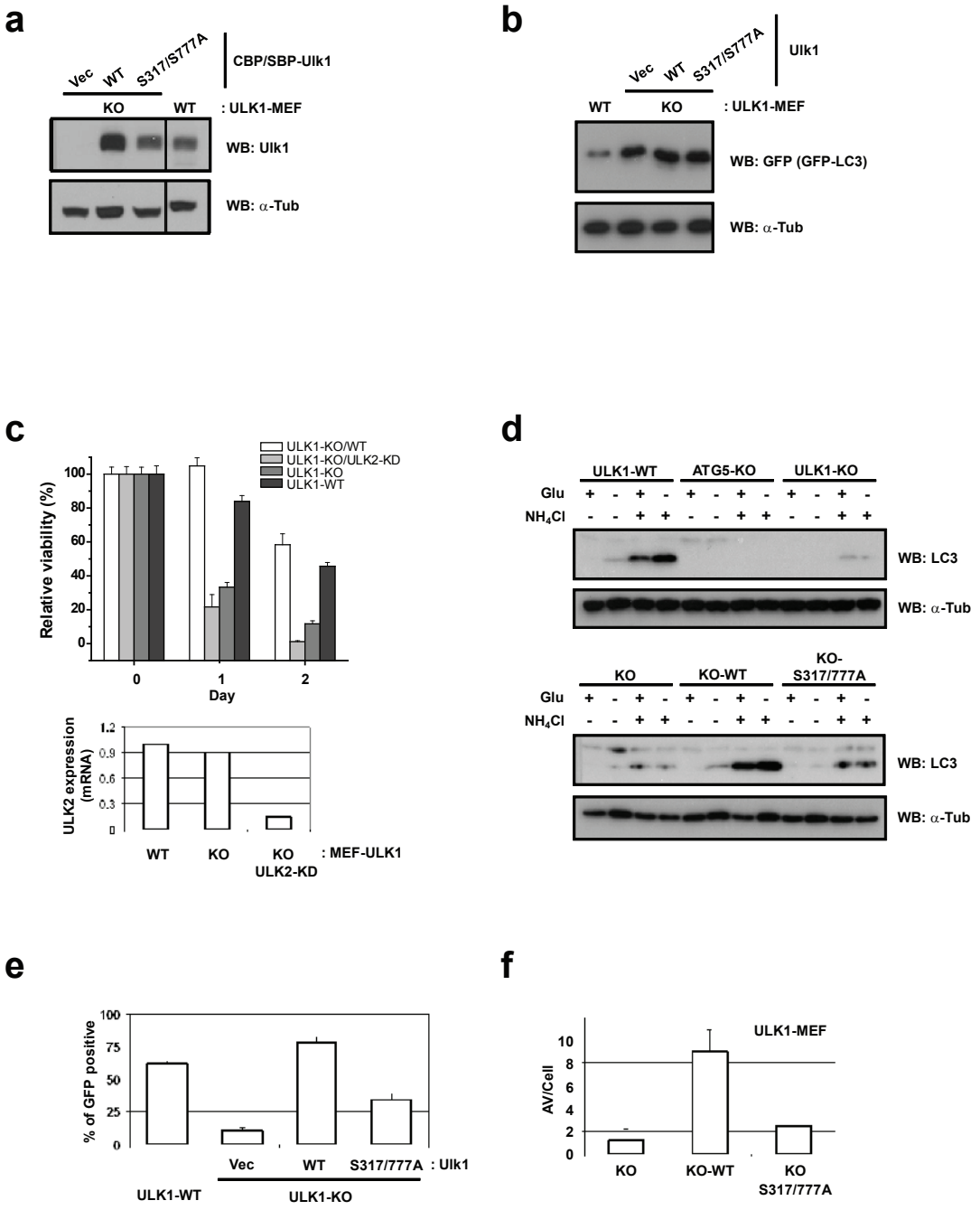

Figure S4 Analyses of Ulk1 reconstituted ULK1 -/- MEFs. **(A)** Expression levels of ectopic Ulk1 proteins in ULK1 -/- (KO) MEFs. The ULK1-KO MEFs stably expressing wild-type Ulk1 or S317/777A mutant were prepared as described in *Methods*. Expression levels of Ulk1 proteins were examined by western blot using an Ulk1 antibody. The levels of ectopic Ulk1 expression were comparable to that of the endogenous Ulk1 protein in the ULK1-WT MEFs. Protein levels were normalized against α-tubulin (α-Tub). **(b)** Expression levels of GFP-LC3 in the ectopic Ulk1 expression cell lines. GFP-LC3 was introduced to the cells by retroviral infection and the cells stably expressing GFP-LC3 were obtained by puromycin selection. The expression levels of GFP-LC3 were examined by western blot using anti-GFP antibody. **(c)** Ulk1 plays pivotal roles in cell survival under starvation. ULK1-WT, ULK1-KO, ULK1-KO/WT, and ULK1 -/- with ULK2 knockdown (ULK1-KO/ULK2-KD) MEFs were starved with glucose for the indicated time. Knock-down efficiency of ULK2 was determined by quantitative RT-PCR and shown in the lower panel (mean ± S.D, n=2). Data was normalized by GAPDH. Cell viability was determined by tryphan blue staining (mean ± S.D, n=3). Cell viability is represented as % of corresponding MEFs before starvation, which is set as 100%. **(d)** The Ulk1 S317/777A mutant is compromised in supporting glucose starvation-induced autophagy. ULK1-WT, KO, and KO expressing Ulk1-WT (KO-WT) or Ulk1 S317/777A mutant (KO-S317/777A) MEFs were starved with glucose (Glu) for 4hrs. Also, 10 mM NH4Cl was added to determine the autophagic flux in these cells. Autophagy induction was monitored by LC3-II accumulation by LC3 western. **(e)** Quantification of GFP-LC3 punta formation for Fig.7C. The cells displaying strong GFP positive dots on confocal microscopy were counted and quantified (mean ± S.D., n=30-40 cells) as described in *Supplementary Methods*. **(f)** Expression of wild type but not the S317/777A mutant restores autophagosome/autolysosome-like structures in ULK1-/- cells. The numbers of autophagosome/autolysosome-like structures (AV) from 5-7 AV positive cells were counted and mean ± S.D. are shown. This is the quantification for Fig.7d.

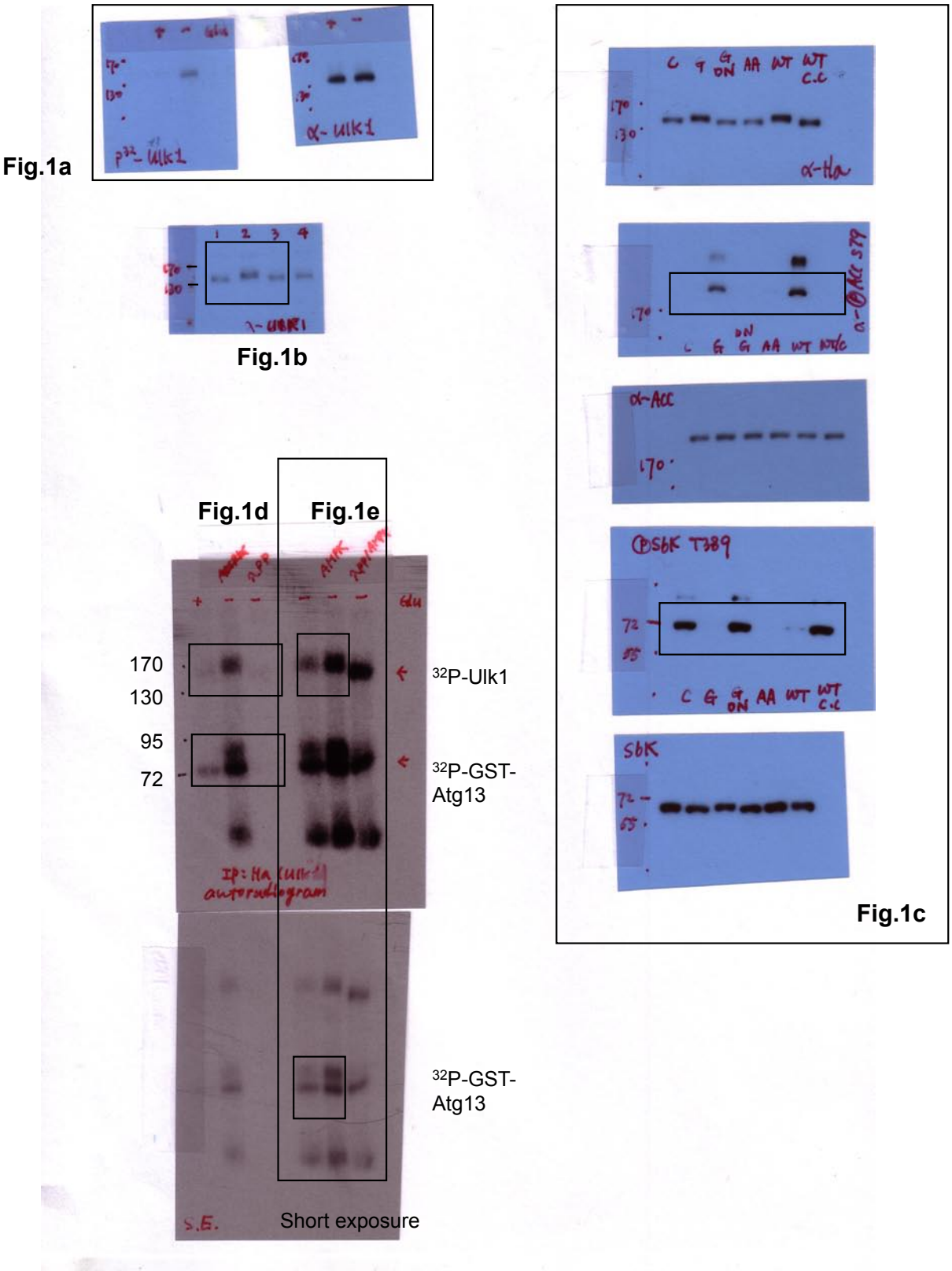

Figure S5 Full scans of original blots for data in Fig. 1, 2, 3, 4, 5, and 6. Panels corresponding to the figures in the paper are indicated.

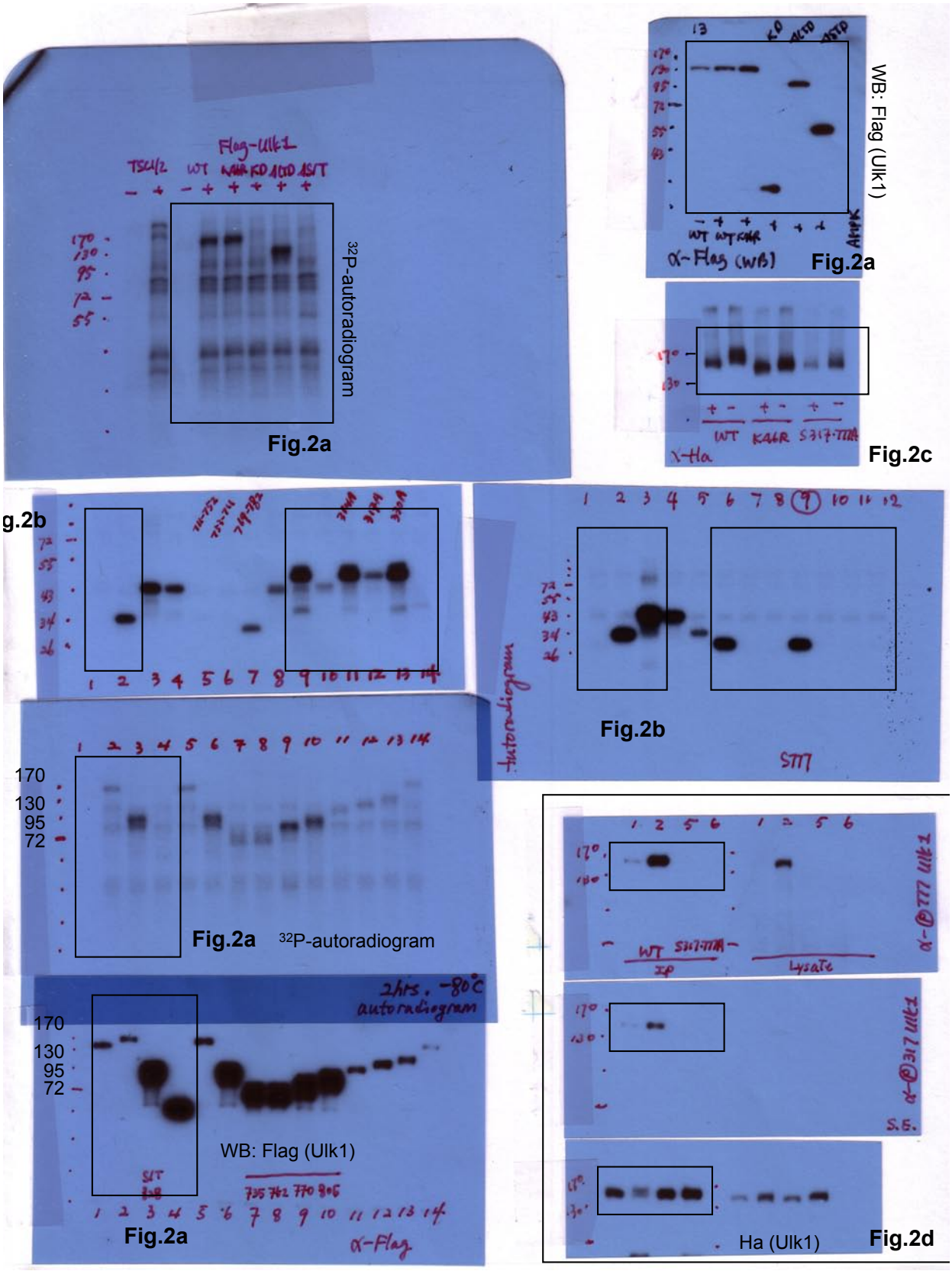

Figure S5 continued

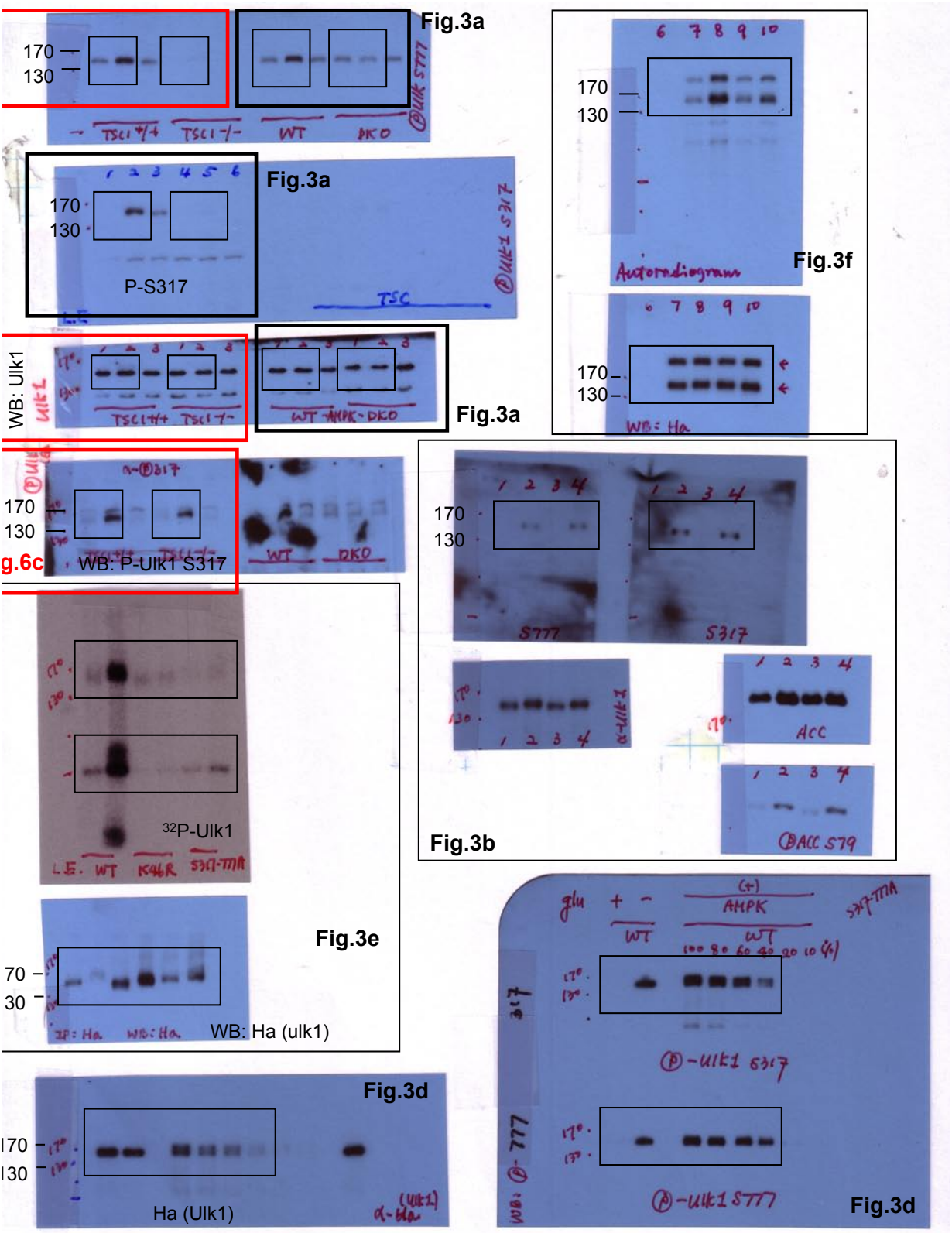

Figure S5 continued

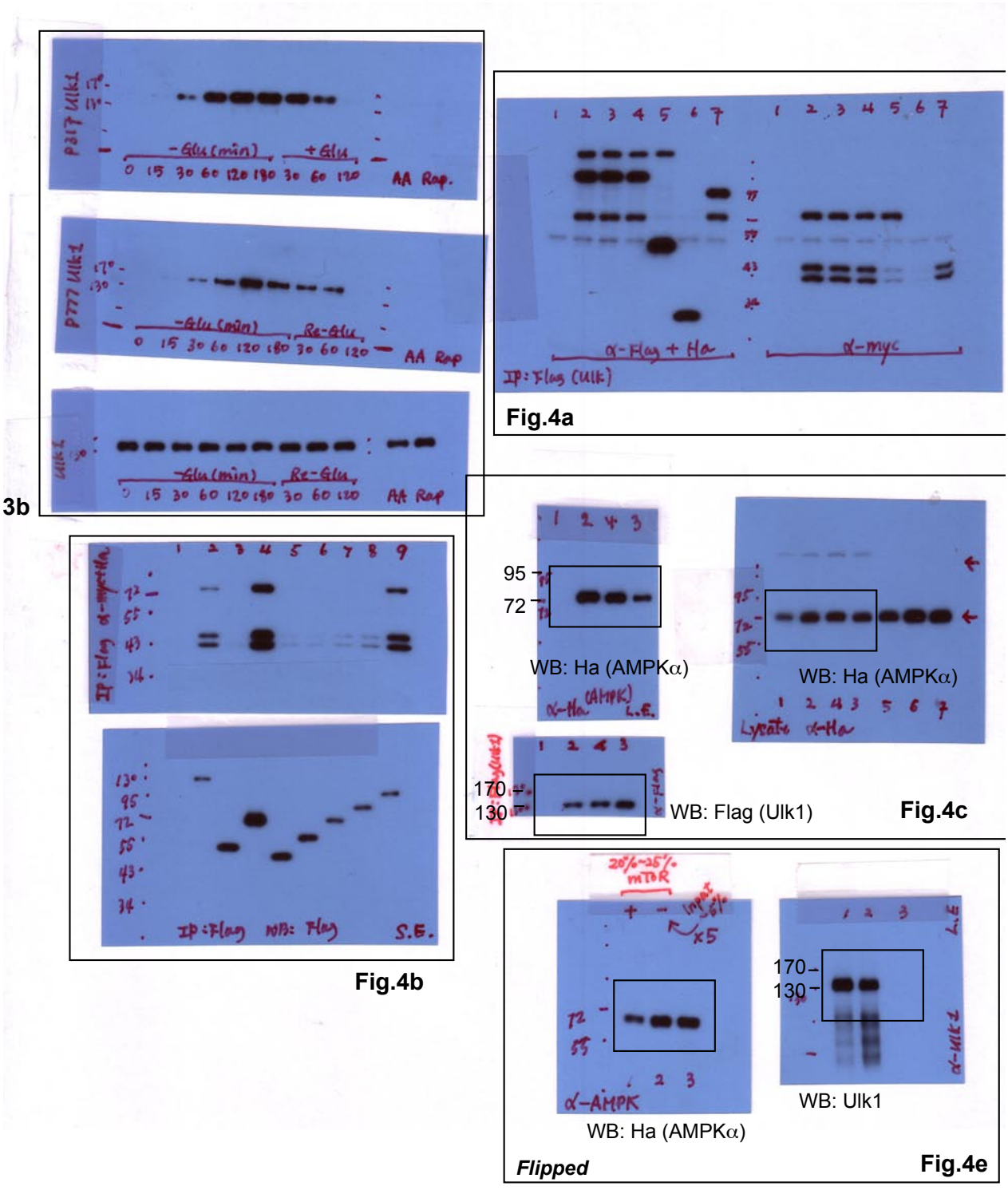

Figure S5 continued

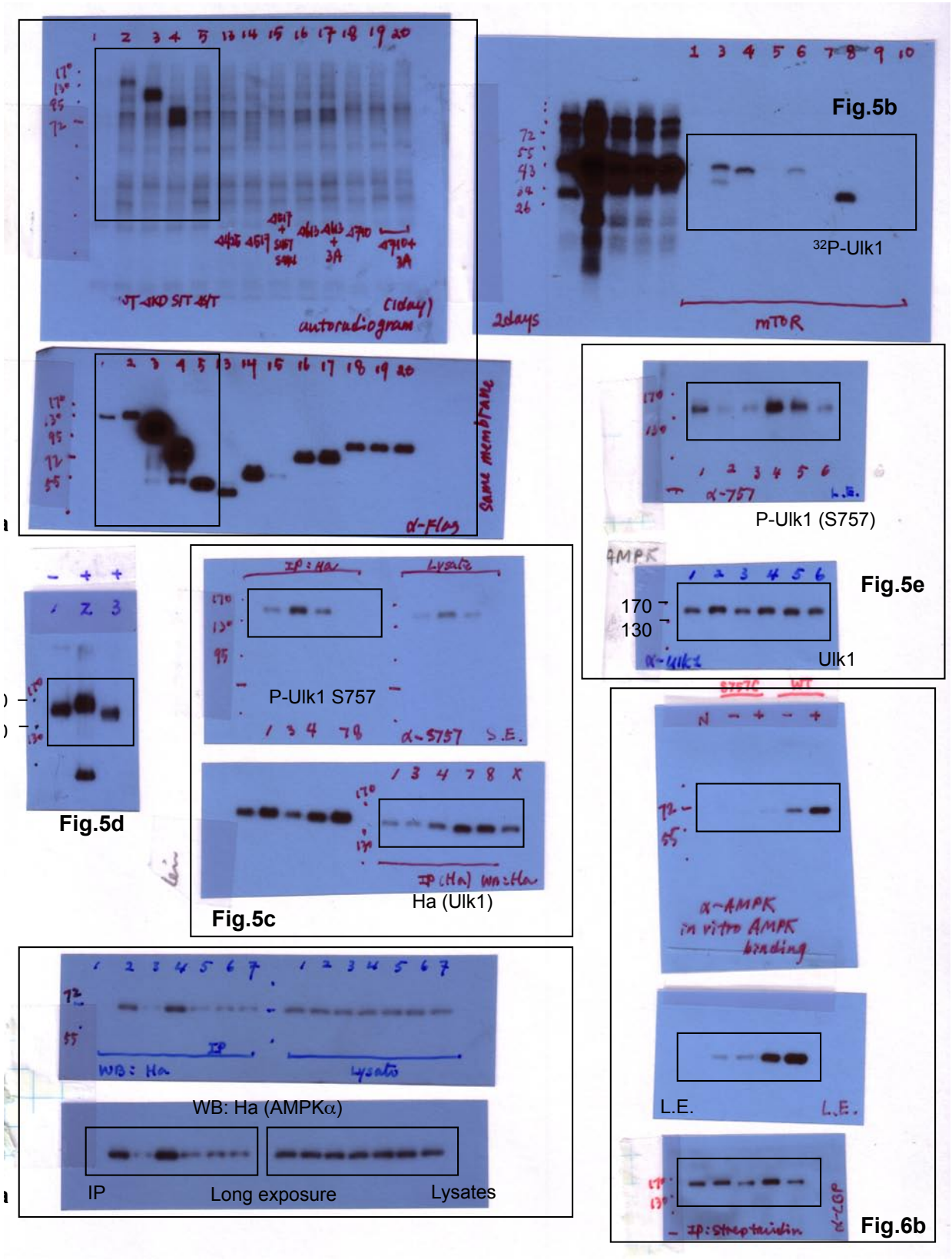

Figure S5 continued

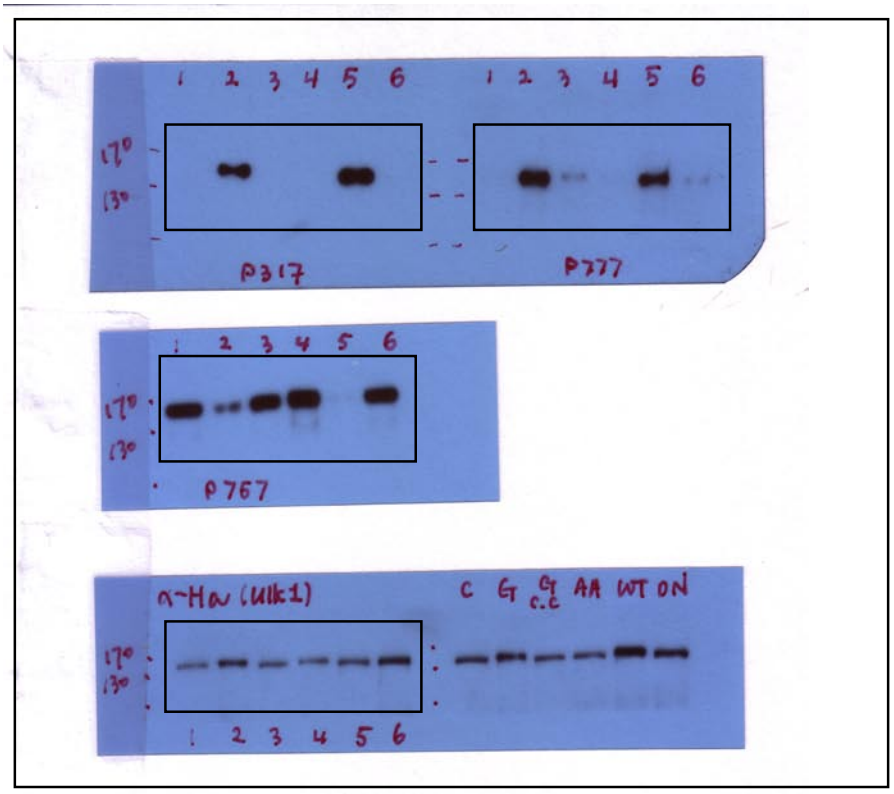

Fig.6d

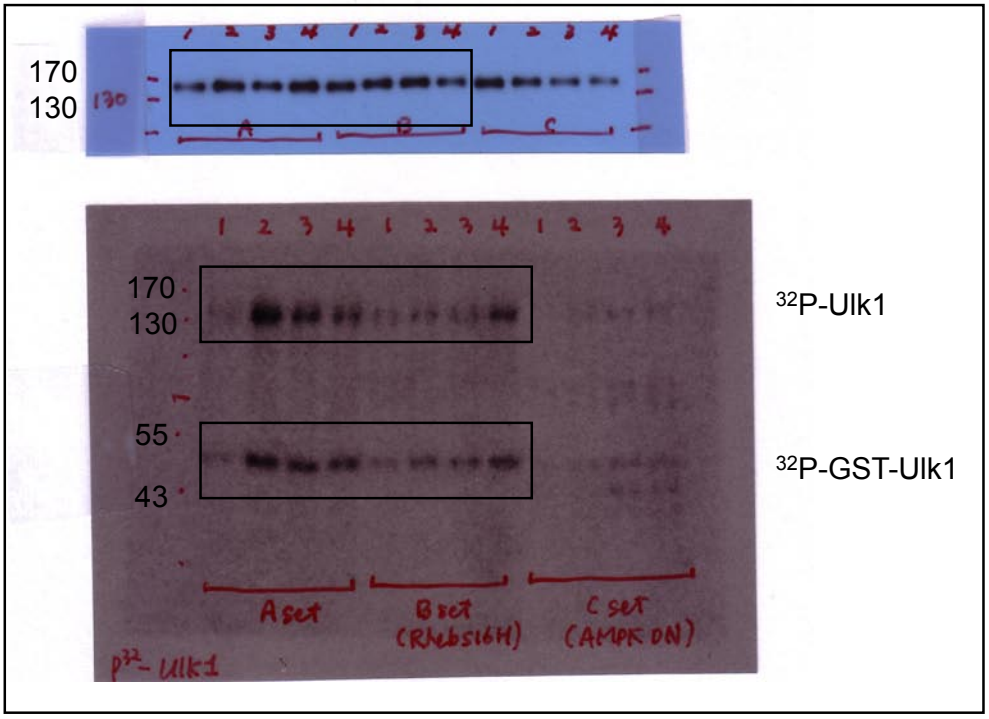

Fig.6e

Figure S5 continued

AMPK and mTOR in Cellular Energy Homeostasis and Drug Targets

Ken Inoki,[1] Joungmok Kim,[2] and Kun-Liang Guan[2]

[1]Life Sciences Institute and Department of Molecular and Integrative Physiology, University of Michigan, Ann Arbor, Michigan 48109

[2]Department of Pharmacology and Moores Cancer Center, University of California San Diego, La Jolla, California 92093-0815; email: kuguan@ucsd.edu

Annu. Rev. Pharmacol. Toxicol. 2012. 52:381–400

First published online as a Review in Advance on October 17, 2011

The *Annual Review of Pharmacology and Toxicology* is online at pharmtox.annualreviews.org

This article's doi: 10.1146/annurev-pharmtox-010611-134537

0362-1642/12/0210-0381$20.00

Keywords

rapamycin, TSC Rheb, Rag, ULK1, ribosome biogenesis

Abstract

The mammalian target of rapamycin (mTOR) is a central controller of cell growth and proliferation. mTOR forms two distinct complexes, mTOR complex 1 (mTORC1) and mTOR complex 2 (mTORC2). mTORC1 is regulated by multiple signals such as growth factors, amino acids, and cellular energy and regulates numerous essential cellular processes including translation, transcription, and autophagy. The AMP-activated protein kinase (AMPK) is a cellular energy sensor and signal transducer that is regulated by a wide array of metabolic stresses. These two pathways serve as a signaling nexus for regulating cellular metabolism, energy homeostasis, and cell growth, and dysregulation of each pathway may contribute to the development of metabolic disorders such as obesity, type 2 diabetes, and cancer. This review focuses on our current understanding of the relationship between AMPK and mTORC1 signaling and discusses their roles in cellular and organismal energy homeostasis.

AMP-ACTIVATED PROTEIN KINASE

As a key physiological energy sensor, AMP-activated protein kinase (AMPK) is a major regulator of cellular and organismal energy homeostasis that coordinates multiple metabolic pathways to balance energy supply and demand and ultimately modulate cellular and organ growth (1). AMPK is an evolutionarily conserved serine/threonine protein kinase and a member of the AMPK-related kinase family that consists of 13 kinases in the human genome. The activation of AMPK-related kinases except for MELK requires phosphorylation of their activation loops by upstream kinases such as LKB1, which was initially identified as a tumor suppressor (2, 3). LKB1 requires two adaptor proteins, STRAD and MO25, to be a functional kinase in phosphorylation of AMPK (4, 5).

The AMPK holoenzyme is a trimer consisting of one α subunit, one β subunit, and one γ subunit; α is the catalytic subunit and β and γ are regulatory subunits (6). In mammals, each subunit has multiple subtypes and expresses differentially in different tissues. For instance, there are two isoforms of the catalytic α subunit (α1 and α2), whereas β and γ subunits have two (β1 and β2) and three (γ1, γ2, and γ3) isoforms, respectively (1). AMPK phosphorylates many substrates regulating the balance of intracellular energy levels. The activation loop of AMPK in the α subunit can be phosphorylated by upstream kinases, including LKB1, calcium/calmodulin-dependent protein kinase-β (CaMKK β), and TAK1 (7–9). The β subunit functions as a hinge, bringing both α and γ subunits together. It also plays an important role in the cellular localization of the complex via its myristoylation motif and carbohydrate binding domain (10, 11). A recent study revealed that branched oligosaccharides and glycogen inhibit AMPK activity (12). Thus, the β subunit may be an important regulatory unit sensing availability of cellular energy by recognizing the levels and/or the formation of glycogen. The γ subunit contains four repeats of the CBS domain, a motif originally recognized as the Bateman domain (13, 14). Two CBS domains form a pocket and create binding sites for two adenosine molecules including AMP, ADP, and ATP. Structural analyses have revealed that two of the four binding sites appear to bind AMP, ADP, or ATP in an exchangeable manner. The third site prefers to permanently bind AMP but not other forms of adenosine. The fourth site seems unable to function as a binding site even in the presence of high concentrations of AMP (15, 16).

The activity of AMPK is allosterically enhanced by AMP binding to the γ subunit. The binding of ATP or ADP to the γ subunit does not induce allosteric activation of AMPK. However, the major effect of AMP binding is to affect the activation loop phosphorylation of AMPK, which plays the most prominent role in AMPK activation. Therefore, antibodies that recognize the activation loop phosphorylation have been widely used as an indirect measurement for AMPK activity. Binding of AMP to the γ subunit protects the activation loop from dephosphorylation by the phosphatases such as PP2C, therefore leading to AMPK activation. Recent studies have demonstrated that ADP may also play a regulatory role in AMPK activation (17). Cellular concentrations of AMP or ADP are much lower than those of ATP (18, 19). Therefore, a small decrease of ATP will result in a relatively large increase of ADP and AMP. Given the above mechanisms, AMPK is able to sense small changes in cellular energy charge by monitoring AMP and ADP. Thus, AMPK is able to maintain cellular energy homeostasis at a very constant level.

AMPK is activated by a variety of cellular stresses that decrease ATP generation including metabolic poisons as well as pathologic cues such as nutrient starvation, ischemia, and hypoxia. Under these conditions, the activated AMPK phosphorylates many substrates that turn on alternative catabolic pathways to generate more ATP. It also phosphorylates some substrates that switch off anabolic biosynthetic pathways to prevent further ATP consumption.

The role of AMPK in the metabolic regulation is not the focus of this article. Excellent reviews on this topic can be found elsewhere (20–22). Nevertheless, it is important to note that AMPK

phosphorylates acetyl CoA carboxylases (ACC1 and ACC2) (23), CERB-regulated transcriptional coactivator-2 (CRTC2) (24), TBC1D1/AS160 (25, 26), PPARγ coactivator-1α (PGC1α) (27), and histone deacetylase 5 (HDAC5) (28). ACC1 and ACC2 are key enzymes for fatty acid synthesis and oxidation (29). AMPK-dependent phosphorylation of ACC inhibits its enzyme activity to suppress malonyl-CoA synthesis, thereby relieving inhibition of fatty acid uptake into mitochondria and enhancing fatty acid oxidation. Thus, AMPK allows cells to utilize an alternative source of energy such as lipids when the cells are not able to obtain energy from carbohydrates, the preferred energy source. In addition to this metabolic switch, AMPK stimulates gene expression of glucose transporter 4 (GLUT4) by inhibiting HDAC5 activity as well as glucose uptake by inducing GLUT4 translocation through inhibition of TBC1D1 and AS160, two Rab-GAP (GTPase-activating protein) proteins (28). AMPK phosphorylates and inhibits AS160, leading to Rab activation and increased plasma membrane localization of GLUT4 and glucose uptake. Furthermore, it has been postulated that AMPK-dependent phosphorylation of PGC1α stimulates mitochondrial biogenesis in muscle, whereas the phosphorylation of CRTC2 (also known as TORC2, not to be confused with the mTOR complex 2, mTORC2) by AMPK inhibits gluconeogenic gene expression in the liver (24, 27). Activation of the AMPK system in response to acute metabolic stresses is important for the survival of cells as well as whole organisms during energy crises. In addition, chronic inactivation of the AMPK system not only may have deteriorative effects on cell or organism survival, but also can contribute to the development of metabolic disorders such as type 2 diabetes and obesity.

MAMMALIAN TARGET OF RAPAMYCIN

Mammalian target of rapamycin (mTOR) is an evolutionarily conserved serine/threonine protein kinase that regulates multiple cellular processes such as cell growth, cell cycle, cell survival, and autophagy. mTOR forms two functional complexes, mTORC1 and mTORC2 (30). mTORC1 exists as a multiprotein complex containing mTOR, Raptor, mLST8 (GβL), and PRAS40 (31–35), whereas mTORC2 consists of mTOR, Rictor, mSin1 (MAPKAP1), Protor (PRR5), and mLST8 (36–41). The configuration of each complex is conserved from yeast to mammals (30). mTORC1 is directly regulated by cellular energy and nutrient status, whereas mTORC2 is not. mTORC1 plays essential roles in the regulation of translation and autophagy and is sensitive to inhibition by rapamycin. Raptor, a component of mTORC1, functions as a scaffolding protein to recruit substrates such as S6 kinase (S6K) and eIF4E binding proteins (4EBPs) for phosphorylation by mTORC1 (42–44). Interestingly, recent studies have shown that Raptor also plays a significant role in intracellular localization of mTORC1 in response to amino acid availability, which is an essential cellular cue for mTORC1 activation (45).

DOWNSTREAM OF MTORC1

The most well-characterized substrates for mTORC1 are ribosomal protein (RP) S6 kinase (S6K) and eukaryotic initiation factor 4E binding protein 1 (4EBP1) (46–48) (**Figure 1**). mTORC1 primarily phosphorylates Thr389 of S6K1. Thr389 phosphorylation on S6K1 recruits phosphoinositide-dependent kinase-1 (PDK1) and enhances PDK1-dependent Thr229 phosphorylation in the activation loop of S6K1, a process essential for S6K1 activation. S6K1 phosphorylates many substrates such as eIF4B, PDCD4, Skar, and S6, thereby regulating translation initiation, mRNA processing, and cell growth (49–52). Ablation of *Drosophila* S6K1 results in a reduction in cell size and body size (53). Furthermore, disruption of the *S6K1* gene in mice displays a phenotype with small body size (54).

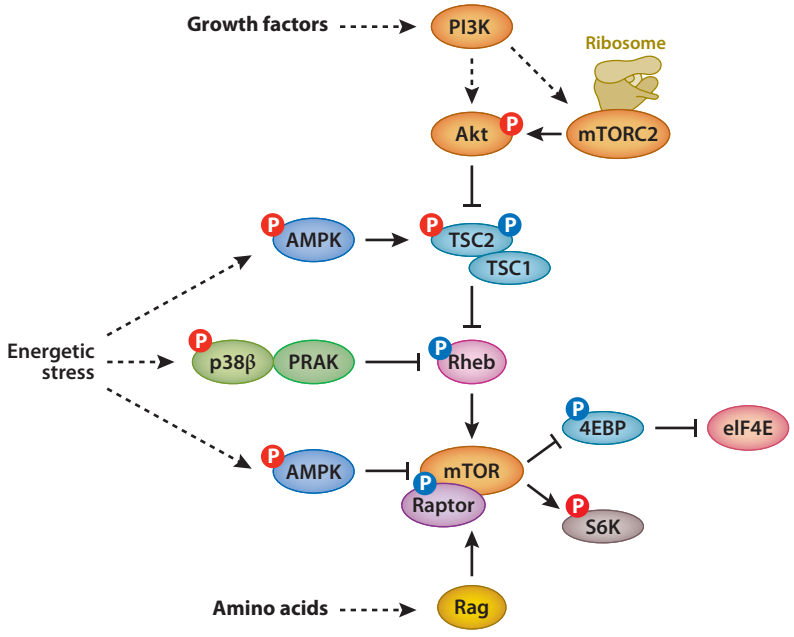

Figure 1

AMP-activated protein kinase (AMPK) inhibits the pathway of the mammalian target of rapamycin complex 1 (mTORC1) in multiple fashions. Under energetic stress conditions, AMPK phosphorylates TSC2 and Raptor to inhibit the mTORC1 pathway.

4EBP1 is a member of the 4EBP family (4EBP1, 2, and 3) that functions as a repressor of translation initiation (55). 4EBPs have a eukaryotic translation initiation factor 4E (eIF4E) binding domain, which is shared by eIF4G, an essential scaffolding protein that forms the eIF4F complex. Hypo-phosphorylated 4EBP1 strongly interacts with eIF4E, thereby interfering with the binding between eIF4E and eIF4G. Upon mTORC1-dependent 4EBP1 phosphorylation, the 4EBP1 dissociates from eIF4E, thereby relieving the inhibitory effect of 4EBP1 on eIF4E-dependent translation initiation. Recent studies have shown that 4EBPs are crucial elements of the mTORC1 pathway that regulate cell number and proliferation. mTORC1 also phosphorylates the unc-51-like kinase 1 (ULK1), a mammalian homolog of ATG1, which is the serine/threonine protein kinase that triggers autophagy initiation (56). Phosphorylation of ULK1 by mTORC1 represses the kinase activity of ULK1, thereby suppressing the initiation of autophagy (57, 58) (see discussion below).

MTORC1 AND RIBOSOME BIOGENESIS

In addition to its role in translation initiation, mTORC1 is also involved in ribosomal biogenesis. Studies in yeast and mammalian cells have demonstrated that TOR activity couples nutrient availability to regulate ribosome biogenesis. Interestingly, acute inhibition of TORC1 activity with rapamycin suppresses translation, although this occurs more slowly than does transcription of ribosomal gene expression (59, 60). Ribosome biogenesis requires the coordinated activities of all three RNA polymerases (Pol I, II, and III) and consumes a large amount of total cellular energy. Pol I accounts for the transcription of rRNA, a noncoding RNA that is an essential component of ribosomes. Upon amino acid starvation, the activity of Pol I transcription is rapidly decreased

(61). Similar results are seen with rapamycin treatment, indicating that mTORC1 plays a role in nutrient-dependent regulation of Pol I transcription (62). Pol I forms a transcription initiation complex with TIF-IA, TIF-IB/SL1, and UBF (63, 64). Among these components, TIF-IA and UBF are the targets of the mTORC1 pathway (62, 65). In recent studies, rapamycin-dependent Pol I transcriptional repression was restored by exogenous TIF-IA, mTOR, or S6K1. Upon rapamycin treatment, TIF-IA, the mammalian homolog of *Saccharomyces cerevisiae* Rrn3p, translocates from the nucleus into the cytoplasm, and the association of TIF-IA with both Pol I and TIF-IB/SL1 is diminished. Furthermore, rapamycin decreases TIF-IA activity by decreasing phosphorylation at Ser44 and increasing phosphorylation at Ser199. These results suggest that mTOR- or S6K1-dependent kinase and phosphatase regulate TIF-IA in multiple manners, thereby controlling rRNA expression. Notably, a recent study demonstrated that AMPK directly phosphorylates Ser635 of TIF-IA and inhibits rRNA synthesis, highlighting an integration of AMPK and mTOR signaling at the transcriptional level (66).

RP gene expression is mediated by Pol II. Despite a considerable body of evidence about the relationship between TORC1 and RP gene expression in yeast, there is limited information regarding the impact of mTORC1 signaling on Pol II in mammalian systems. In yeast, TORC1 upregulates RP gene expression by regulating the shuttling of a transcription factor as well as corepressors that are coupled to Pol II function in RP gene expression. SFP1, a positive regulator for RP gene transcription, binds to RP gene promoters and enhances their expression in a TOR-dependent manner. In the presence of rapamycin as well as nutritional stresses, SFP1 is restricted to the cytoplasm, thereby reducing RP gene expression (67, 68). TORC1 also controls the expression of RP genes via the forkhead transcriptional factor (FHL1) and its coactivator IFH1 and corepressor CRF1 in *S. cerevisiae* (69). Under growth conditions, FHL1 binds to RP gene promoters with IFH1 and upregulates RP transcription, whereas CRF1 is excluded from the nucleus through a TORC1-dependent protein kinase A activity (70). Upon nutrient deprivation, CRF1 translocates into the nucleus and competes with IFH1 to interact with FHL1, leading to suppression of RP gene transcription. These observations clearly indicate that TORC1-mediated RP gene expression is pivotal for ribosomal biogenesis in yeast.

In mammals, the evidence that mTORC1 is actively involved in Pol II–dependent RP gene transcription is limited, although ample studies show that mTORC1-dependent RP gene expression is largely regulated at the level of translation. All functional RP genes contain a polypyrimidine tract (5′ TOP, terminal oligopyrimidine) sequence at the 5′ end of their mRNA (71). It has been postulated that mTORC1/S6K1-dependent phosphorylation of S6 may play a critical role in the translation of 5′ TOP mRNA (72). However, two genetic studies using the phospho-defective S6 knock-in mice and S6K1/2 double-knockout mice have revealed that mTORC1-dependent 5′ TOP mRNA translation requires neither S6K nor phosphorylated S6 (73, 74). Therefore, the mechanism by which mTORC1 controls the translation of 5′ TOP mRNAs including RP mRNA remains to be elucidated (75).

Pol III synthesizes 5S rRNA and tRNA. Recent studies have demonstrated that mTORC1 interacts with TFIIIC, a Pol III–specific transcription factor, and directly phosphorylates MAF1, a repressor of Pol III in the nucleus (76, 77). mTORC1-dependent MAF1 phosphorylation relieves its inhibitory effect on transcription, thereby inducing Pol III–dependent transcriptional activity. These data indicate that mTORC1 plays an important role in the regulation of 5S rRNA and tRNA gene expression.

Given the essential roles of mTORC1 function in ribosome synthesis and its overall function, dysregulation of the mTORC1 pathway may be linked to ribosome-associated human diseases such as neurodegenerative disease and cancer (78, 79). Hyperactivation of mTORC1 and overexpression of RPs have frequently been shown to be associated with tumor development (80). Strikingly, a

recent study from Hall's group demonstrated that mTORC2 associates with and is activated by ribosomes in response to PI3K signaling (81) (**Figure 1**). Notably, the translational activity driven by the ribosomes is not required for mTORC2 activation, suggesting that ribosome functions as a platform for the kinase reactions of mTORC2 to phosphorylate its substrates such as Akt (82). Thus, both the function and the amount of cellular ribosomes are key factors in the regulation of cell growth and survival.

REGULATION OF MTORC1 BY THE GROWTH FACTOR–TSC-RHEB PATHWAY

mTORC1 activity is modulated by multiple upstream factors including growth factors and nutrients such as glucose and amino acids (**Figure 1**). The molecular mechanisms by which these upstream signals regulate mTORC1 have been extensively investigated. The results of these studies have indicated that the small GTPase Rheb is the most proximal molecule with a key role in the regulation of mTORC1 activity (83). Previous studies demonstrated that Rheb directly interacts with mTOR (84). As is the case of other small GTPases, the GTP-bound form of Rheb is active, whereas the GDP-bound form is inactive (85). Importantly, the purified active Rheb is able to activate mTORC1 kinase activity in vitro (34, 86). Although intermediates between active Rheb and mTOR could exist, compelling evidence indicates that Rheb is a direct activator of mTORC1.

The activity of Rheb is tightly regulated by the tuberous sclerosis gene products TSC1 and TSC2 (87–90). Tuberous sclerosis complex (TSC) is an autosomal dominant disease caused by mutations of either the *TSC1* or *TSC2* gene (91). TSC is characterized by the formation of multiple hamartomas in a wide array of organs (92). *TSC1* and *TSC2* gene products (hamartin and tuberin, respectively) form a physical and functional complex in vivo and function as tumor suppressors (93). TSC1 stabilizes TSC2 and may play a role in the cellular localization of the complex (93). TSC2 has a catalytic domain in its carboxyl terminus, which is a GAP for the Rheb small GTPase. The active Rheb (GTP-bound form) is converted to the GDP form of Rheb, as the late form is unable to stimulate mTORC1 activity. Thus, the TSC1/TSC2 complex is a negative regulator of the mTORC1 pathway, thereby functioning as a tumor suppressor (**Figure 1**).

Identification of the TSC as a negative regulator for the mTORC1 pathway significantly advanced our understanding as to how upstream signals such as growth factor, glucose, and many stresses regulate mTORC1. Previous studies had demonstrated that multiple growth-related kinases such as AKT, ERK, and RSK phosphorylate TSC2 and inhibit the function of the TSC, thereby activating the Rheb-mTORC1 pathway (94–99). Consistently, mTORC1 activity is constitutively active, and deprivation of growth factors fails to efficiently inhibit mTORC1 activity in TSC-deficient cells (100).

AMPK INHIBITS MTORC1 VIA MULTIPLE MECHANISMS

Extensive studies have also revealed that mTORC1 activity is modulated by intracellular energy levels via multiple mechanisms. In 2001, the first evidence demonstrating the relationship between cellular ATP levels and mTORC1 activity was reported (101). In 2002, a reciprocal relationship between the activation of AMPK and mTORC1 was shown (102). In 2003, direct evidence that AMPK inhibits mTORC1 activity was demonstrated (103). Afterward, several groups found that AMPK directly phosphorylates multiple components in the mTORC1 pathway (**Figure 1**). AMPK phosphorylates TSC2 and activates the TSC, thereby attenuating the TORC1 pathway (104). Consistent with this model, inhibition of mTORC1 activity by aminoimidazole carboxamide ribonucleotide (AICAR), an AMPK activator, or by glucose

deprivation is largely compromised in TSC1- or TSC2-deficient cells (105, 106). In AMPK α1 α2 double-knockout MEFs (mouse embryonic fibroblasts), AICAR fails to inhibit mTORC1 activity (107). Furthermore, glucose starvation inhibits cell growth in wild-type cells but not in TSC1-deficient cells (104). Concomitantly, the TSC1-deficient cells, but not wild-type cells, undergo massive cell death under glucose-deprivation conditions, and rapamycin treatment prevents the cell death in TSC-deficient cells under glucose starvation (108, 109).

Several mechanisms by which TSC-deficient cells undergo cell death upon glucose starvation have been proposed. They include accumulation of p53 tumor suppressor, enhanced endoplasmic reticulum (ER) stress, and reduction of survival kinases (108, 110–112). Therefore, multiple factors likely contribute to the hypersensitivity of TSC mutant cells to energy starvation. AMPK is able to stabilize p53, a major proapoptotic protein, via its Ser15 phosphorylation, and the constitutive activation of mTORC1 enhances p53 translation (108, 113). In combination, these two effects cause a massive accumulation of p53 in TSC-deficient cells with glucose starvation, thereby increasing susceptibility to cell death. In addition, hyperactive mTORC1 signaling has been reported to induce ER stress and activate the unfolded protein response. The continuous ER stress induced by mTORC1 activation causes a reduction in the insulin sensitive pathway as well as the survival pathway (110). Furthermore, active S6K also leads to the downregulation of insulin receptor substrate and generates the negative-feedback inhibition for the PI3K-Akt pathway (111, 114, 115). These observations indicate that survival signaling pathways are attenuated in TSC-deficient cells. More recently, Blenis and colleagues (109) demonstrated that mTORC1 inhibition in TSC-deficient cells with rapamycin allows cells to maintain ATP levels and attenuates AMPK activation under glucose-starvation conditions. These data also suggest that the TSC-mTORC1 pathway functions upstream of the AMPK. Under energetic stress conditions, inhibition of mTORC1 is critical to conserve energy for cell survival. For example, glutamate dehydrogenase–dependent glutamine metabolism via the TCA cycle becomes the main pathway to generate energy for cell survival in rapamycin-treated TSC-deficient cells under glucose-starvation conditions (109). Collectively, these observations indicate that the response of the intact AMPK-TSC signaling is essential to suppress the mTORC1 pathway to regulate cell survival and growth under energetic stress conditions.

Although the above mechanism has been highlighted as a linear signaling pathway for the regulation of mTORC1 under stress conditions, cells can also inhibit mTORC1 through AMPK-dependent direct regulation of mTORC1 involving Raptor (116) (**Figure 1**). The inverse regulation of TOR and AMPK by glucose levels is also conserved in *Caenorhabditis elegans* and *S. cerevisiae*, both of which lack a TSC2 ortholog, thereby raising the possibility that an alternative regulatory mechanism exists in the AMPK-dependent mTORC1 mediation in these organisms. Shaw and his colleagues (116) have found that AMPK also phosphorylates Ser722 and Ser792 on Raptor. Their study demonstrated that cells expressing a phospho-defective Raptor mutant with alanine substitutions at both Ser722 and Ser792 were resistant to AICAR-induced mTORC1 inhibition, indicating that AMPK-induced Raptor phosphorylation negatively regulates mTORC1 activity. However, a more recent study (106) has shown that AICAR fails to inhibit mTORC1 activity in TSC-deficient fibroblasts although Raptor is fully phosphorylated by AMPK. Interestingly, however, AICAR inhibits mTORC1 activity in TSC-deficient hepatocytes with an increase in Raptor phosphorylation. This study (106) further suggests that the involvement of the TSC in AMPK-induced mTORC1 regulation depends on the cell types and tissues studied.

A third mechanism by which glucose deprivation and AMPK activators such as AICAR and 2-deoxy-glucose (2DG) inhibit mTORC1 signaling has recently been demonstrated. Han and colleagues (105) have implicated the p38β-PRAK pathway in the downregulation of Rheb activity through a phosphorylation-dependent mechanism (**Figure 1**). Upon glucose starvation, AICAR,

or 2DG treatment, the p38β-PRAK pathway is activated in a manner independent of AMPK, and the activated PRAK directly phosphorylates Ser130 on Rheb. The phosphorylation of Rheb causes not only an impairment of its GTP binding, but also a dissociation of bound GTP from Rheb. Although it remains unclear whether Ser130 phosphorylation of Rheb induces the intrinsic Rheb GTPase activity or stimulates TSC2-dependent Rheb GTP hydrolysis, the study suggests that there is a reduction of guanine nucleotide binding, including GDP. Because p38β-PRAK-dependent Rheb phosphorylation occurs later than the initial inhibition of mTORC1 activity in AICAR-treated cells, TSC2- or Raptor-mediated mTORC1 inhibition may be responsible for the acute phase of mTORC1 suppression during energetic stress, whereas the p38β-PRAK-dependent regulation is responsible for the sustained mTORC1 inhibition.

Many studies have used different methods and chemicals to activate AMPK. For instance, glucose depletion or hypoxia is often used as a means to activate AMPK. Moreover, a variety of chemicals including AICAR, biguanides such as metformin and phenformin, glycolysis inhibitors (2DG), and metabolic poisons such as oligomycin and FCCP have been used to study the role of AMPK in the regulation of the mTORC1 pathway. As described above, the involvement of new players such as p38β-PRAK compels us to re-evaluate our view of AMPK-dependent mTORC1 regulation (105). Furthermore, Thomas and colleagues (107) have recently made the unexpected observation that metformin-induced mTORC1 inhibition depends on neither AMPK nor TSC. This work has demonstrated that phenformin inhibition of mTORC1 activity depends on Rag small GTPases, but the precise molecular mechanism by which phenformin modulates the Rag-mTORC1 pathway remains unclear.

REGULATION OF MTORC1 BY AMINO ACID–RAG PATHWAY

The mammalian Rag subfamily of GTPase is a Ras-related GTPase and consists of RagA, RagB, RagC, and RagD (117). RagA and RagB (RagA/B) are homologous to yeast Gtr1p, whereas the yeast Gtr2p is a homolog of RagC and RagD (RagC/D). A unique feature of this Rag complex is that RagA/B form a stable dimer with RagC/D. Moreover, in the Rag GTPase dimer, RagA/B must be in GTP form, whereas RagC/D must be in GDP form for the RAG complex to activate mTORC1 (45, 118). Recently Sabatini's group and our group (45, 118) found that Rag plays a crucial role in amino acid–sensitive mTORC1 regulation (**Figure 2**). Sancak et al. (45) demonstrated that the Rag heterodimer interacts with Raptor. Interestingly, the interaction between Raptor and Rag is dependent on the GTP binding state of RagA or RagB in the heterodimer. In contrast, the nucleotide binding status of RagC/D does not have a direct effect on the interaction between the Rag GTPase dimer and Raptor. Furthermore, the level of GTP-bound RagB is increased by amino acid stimulation. Knockdown of RagA/B or dominant negative RagA/B expression efficiently inhibits the mTORC1 pathway. In contrast, constitutively active RagA/B is able to activate mTORC1 activity during amino acid starvation, indicating that Rag functions downstream of amino acids to activate mTORC1 (45, 118). In *Drosophila*, loss of function of dRagA decreases cell size, wing, and fat bodies, whereas overexpression of dRagA increases cell size. Importantly, constitutively active dRagA suppresses starvation-induced autophagy in fat bodies (118). These observations indicate that Rag small GTPases relay signals from amino acids to activate the mTORC1 pathway.

The mechanism by which Rag activates mTORC1 has been further defined, revealing that Rag plays an essential role in the spatial regulation of mTORC1 in the cytoplasm. Rag small GTPases are constitutively expressed at the lysosomal membrane anchored by the MP1/p18/p14 complex (Ragulator) (119) (**Figure 2**). Unlike Rheb, active Rag has no capability to activate the kinase activity of mTORC1 in vitro, and instead it recruits mTORC1 to the lysosomal membrane

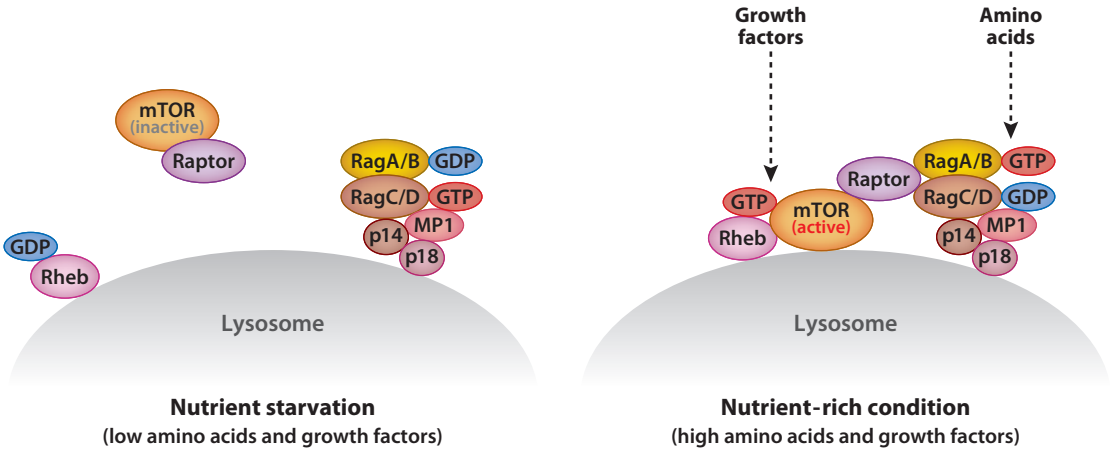

Figure 2

Spatial regulation of mammalian target of rapamycin complex 1 (mTORC1) on the lysosomal membrane. Upon amino acid stimulation, the Rag heterodimer anchored at the lysosomal membrane by the MP1/p14/p18 complex (Ragulator) recruits mTORC1 to the lysosome. Concomitantly, growth factors stimulate Rheb on the lysosomal membrane, thereby facilitating Rheb-induced mTORC1 activation.

in vivo (45). These data suggest that mTORC1 may translocate to the lysosome in a manner dependent on Rag, whose activity is regulated by amino acid availability. Because exogenous Rheb can be expressed on the lysosomes, amino acid–induced Rag activation helps to link mTORC1 and Rheb on the lysosomes, thereby enhancing mTORC1 activity (**Figure 2**). This spatial regulation of mTORC1 via Rag and Rheb explains how the signals from amino acids and growth factors are integrated and then activate the mTORC1 pathway.

More recently, Rubinsztein and colleagues (120) demonstrated that nutrients such as amino acids regulate lysosomal positioning that plays a critical role in the regulation of mTORC1 activity and autophagy. The study used mild amino acid starvation to examine mTORC1-lysosome localization and found that mTORC1 remains on lysosomes even when its activity is significantly reduced. Under these conditions, lysosomes translocate the perinuclear region with mTORC1. These observations suggest that dissociation of mTORC1 from lysosomes in response to amino acid starvation may not be the sole basis for the inhibition of mTORC1 activity. The study further demonstrated that KIF1Bβ and KIF2, two kinesin proteins, as well as ARL8B (small GTPase ADP-ribosylation factor-like 8B) play a positive role in the redistribution of lysosomes to the cell periphery and the activation of mTORC1 in response to amino acid stimulation. It is possible that mTORC1 remains in the late endosomal LAMP2-positive compartment and that subsequently these compartments redistribute to the cell periphery in response to increases in amino acid concentrations. Consistent with this idea, loss of function of p18, a component of the Ragulator, also disrupts lysosomal maturation and positioning (121). Therefore, Rag-Ragulator may function not only in the recruitment of mTORC1 but also in the trafficking of lysosomes, possibly via the kinesins and ARL8. Interestingly, expression of a loss of function of ARL8B increases autophagosome formation as well as autophagosome-lysosome fusion. The study illustrates the important role of the dynamics of lysosomes for both amino acid–induced mTORC1 activation and for limiting the process of autophagy.

The importance of organelle and protein trafficking for mTORC1 activation in response to amino acids is consistent with recent reports that the Rab small GTPases have a role in mTORC1

activation (122). The Rab family GTPases play a key role in intracellular vesicle trafficking. Expression of constitutively active Rab, including Rab5, Rab7, Rab11, and Rab31, selectively blocks mTORC1 activation in response to amino acids. Surprisingly, expression of dominant negative Rab GTPases also inhibits mTORC1. Although the precise mechanisms by which Rab family small GTPases regulate mTORC1 remain unclear, it is likely that the Rab family may be involved in the control of trafficking for the essential components in amino acid–sensitive mTORC1 signaling.

Besides the Rag family GTPases, both VPS34 and MAP4K3 have also been implicated in mTORC1 activation in response to amino acids (123, 124). The role of VPS34 is complicated; VPS34 likely regulates the mTORC1 pathway in an indirect manner, because it also plays a key role in the intracellular trafficking machinery (125). Moreover, VPS34 is essential for inducing autophagy (126), which may contribute to mTORC1 activation by increasing intracellular amino acids as a result of autophagy-based degradation of cellular proteins (see next section). Good evidence also supports a role for MAP4K3 in mTORC1 activation by amino acids. However, this role may be limited because MAP4K3 knockdown delays mTORC1 inactivation by amino acid withdrawal (124). With such a wide array of potential regulators in the amino acid–sensitive mTORC1 pathway, it is clear that the mechanisms governing mTORC1 activation by amino acids are much more complicated than anticipated, and our current understanding of these signaling pathways remains far from complete.

REGULATION OF AUTOPHAGY BY MTOR AND AMPK

Autophagy is a cellular degradative process that functions to maintain fundamental biological activities during cellular stresses, especially nutrient starvation (127). Once autophagy is activated, cellular components are embedded into a double-membrane vacuolar structure (autophagosome), which is further fused with lysosomes (autolysosome) as a means to degrade its contents, providing a nutrient source to maintain vital cellular activities (128, 129).

Many studies of *S. cerevisiae* have shown that TORC1 negatively regulates autophagy, and the observation that rapamycin treatment is sufficient to induce autophagy even in the presence of nutrients provided key evidence for this conclusion. Extensive genetic and biochemical studies indicate that ATG1 is an autophagy-initiating kinase and its activity is under the control of TORC1 (56, 130). In *S. cerevisiae*, the ATG1 mutant is defective in autophagy even under nutrient starvation or TORC1 inhibition, suggesting that ATG1 acts downstream of TORC1. ATG1 interacts with several autophagy proteins, including ATG13 and ATG17. The interaction of ATG13 and ATG17 with ATG1 is induced by rapamycin or nutrient starvation, and formation of this complex is important for ATG1 kinase activity (131). TORC1 appears to phosphorylate ATG13 on multiple residues to disrupt the ATG1 complex (132), thereby repressing autophagy induction. Consistently, starvation or rapamycin treatment enhances ATG1 kinase activity.

The function of TORC1 in the regulation of autophagy is conserved in eukaryotes (130). The human genome has ATG1 homologs, such as ULK1 and ULK2 (56). Several studies have revealed that mammalian ULK1 is involved in autophagy regulation (133, 134) and functions downstream of mTORC1. Moreover, recent reports show that mTORC1 interacts with ULK1-ATG13-FIP200 (a mammalian functional homolog of ATG17) (135) and directly phosphorylates ULK1 kinase and ATG13 proteins, even though the precise sites and functional impact of phosphorylation are yet to be established (57, 136–138). This may provide a mechanism for autophagy inhibition by mTORC1. As an energy sensor, not surprisingly, AMPK is also involved in autophagy (139–141). Typically, AMPK inhibits mTORC1 through phosphorylation of TSC2 (142) and Raptor (116); thus, AMPK is assumed to induce autophagy by suppressing mTORC1 in response to cellular energy cues.

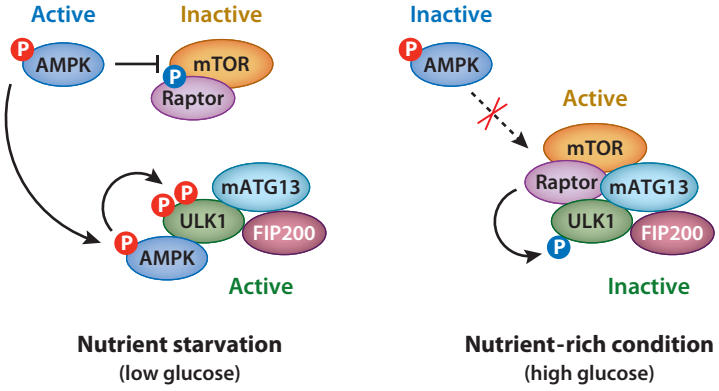

Figure 3

Regulation of ULK1 by AMP-activated protein kinase (AMPK) and mammalian target of rapamycin complex 1 (mTORC1). In the nutrient-rich condition, active mTORC1 phosphorylates ULK1, which negatively regulates the ULK1-AMPK interaction. Once the cellular energy level is decreased, AMPK phosphorylates to inhibit mTORC1 at the level of TSC2 and Raptor, relieving mTORC1-dependent ULK1 phosphorylation. It allows AMPK-ULK1 interaction, followed by ULK1 activation by AMPK-dependent phosphorylation.

In a recent paper, we provided new molecular insight into autophagy regulation by mTORC1 and AMPK (58) (**Figure 3**). We observed that ULK1 is activated by glucose starvation in a manner that depends on AMPK-mediated phosphorylation. ULK1 cannot be activated when AMPK-knockout MEFs are subjected to glucose deprivation, indicating an obligatory role of AMPK in ULK1 activation. Importantly, ULK1 can be directly activated by AMPK in vitro. Similarly, Egan et al. (143) also showed that ULK1 is a direct target of AMPK. They showed that autophagy was promoted by expression of an active AMPK in worm hypodermal cells, which was suppressed by ULK1 siRNA. These genetic data also support the ideas that AMPK lies upstream of ULK1 and that AMPK regulation of ULK1 is required for proper autophagy. Consistent with these two observations, Lee et al. (144) reported that AMPK association with ULK1 plays an important role in autophagy induction. In this study, the authors suggest that AMPK induces autophagy, at least in part, by phosphorylation of Raptor, an event that relieves the inhibitory effect of mTOR on the ULK1 autophagic complex.

In parallel, our group and others have demonstrated that AMPK directly phosphorylates multiple sites in ULK1 (S317, S467, S555, T575, S637, and S777) and promotes ULK1 function in autophagy (58, 143) (**Figure 3**). Analyses of ULK1-knockout cells reconstituted with ULK1 mutants that cannot be phosphorylated by AMPK indicate that the cells expressing the ULK1 mutants are defective in autophagy induction. These observations demonstrate the functional importance of ULK1 phosphorylation by AMPK in autophagy induction. Moreover, ULK1 can be directly activated by AMPK phosphorylation in vitro. Phosphorylation of S317 and S777 is essential for ULK1 activation by AMPK both in vitro and in vivo. These observations establish a direct role for AMPK in ULK1 activation, hence also in autophagy induction.

The mechanism of mTORC1 in ULK1 regulation and autophagy induction has also been elucidated (**Figure 3**). Our group showed that the ULK1-AMPK interaction was enhanced by rapamycin, indicating that mTORC1 may inhibit the interaction between ULK1 and AMPK. mTORC1 directly phosphorylates ULK1 on S757, which is located in the AMPK binding motif (711–828) on ULK1. Notably, phosphorylation of the AMPK sites and the mTORC1 site in ULK1 are oppositely regulated under various conditions. A recent report proposed a different

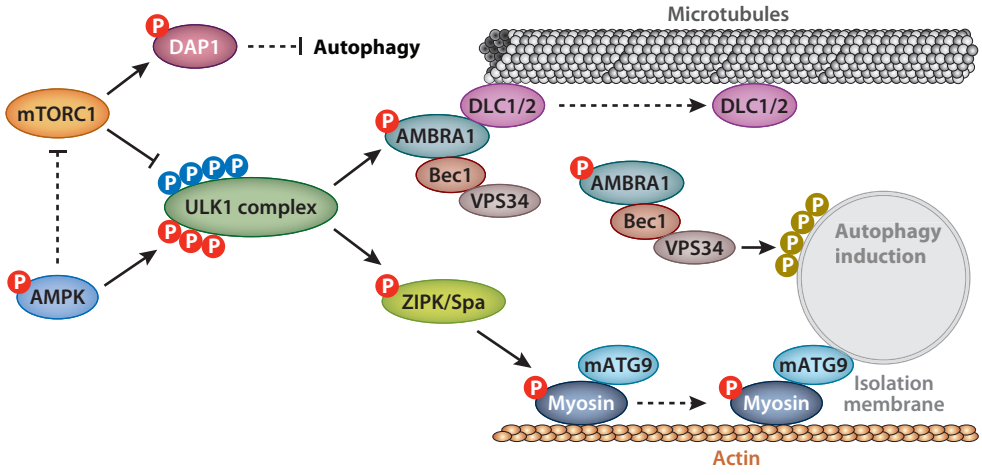

Figure 4

ULK1-dependent autophagy induction. Under autophagy-inducing conditions, such as nutrient starvation, active ULK1 phosphorylates AMBRA1, a component of the VPS34 complex. The VPS34 complex produces PI(3)P, which provides a docking platform for the autophagy protein machinery. Phosphorylation of AMBRA1 induces the release of the VPS34 complex from the dynein complex on microtubules and subsequent relocation of the autophagy core complex to the endoplasmic reticulum, which enables autophagosome nucleation. Also, actin-associated motor protein myosin II is activated by ULK1-dependent phosphorylation. The activated myosin complex delivers mammalian ATG9 (mATG9) to the isolation membrane for autophagy.

model regarding the ULK1-AMPK interaction upon nutrient starvation (145). These authors performed quantitative analysis of ULK1 phosphorylation and found that phosphorylation of S556 (for human ULK1, which is equivalent to mouse S555) was decreased more than fivefold upon starvation, whereas Egan et al. (143) showed increased S555 phosphorylation upon starvation. Further studies are needed to clarify how phosphorylation of S555 is regulated by starvation, as the phosphorylation of ULK1 S757, which is phosphorylated by mTORC1, was decreased upon starvation (58, 145). However, Shang et al. (145) argued that the ULK1-AMPK interaction was disrupted by nutrient starvation, mainly through dephosphorylation of S758 of ULK1 (equivalent to mouse S757), as evidenced by the observation that the S758A mutant impaired the ULK1-AMPK interaction. In contrast, our study (58) showed that mutation of S757 to either alanine (S757A) or aspartate (S757D) abolished AMPK binding, suggesting that the chemistry of this residue is important for ULK1-AMPK binding. More importantly, mutation of S757 to cysteine, which is structurally and chemically similar to serine but cannot be phosphorylated, retains some ULK1-AMPK binding but the binding is resistant to mTORC1, demonstrating the importance of S757 phosphorylation in regulating the association between ULK1 and AMPK in response to mTORC1 activation.

Recent studies are starting to shed light on a downstream target of ULK1. Tang et al. (146) showed that the actin-associated motor protein myosin II was activated by ATG1/ULK1-dependent phosphorylation in *Drosophila* and mammalian cells. These authors demonstrated that activation of myosin II plays important roles in the regulation of starvation-induced autophagy and mammalian ATG9 (mATG9) trafficking when cells are deprived of nutrients (**Figure 4**). Also, another recent paper reported that the VPS34 complex is a target of ULK1 (147). Di Bartolomeo et al. (147) showed that the VPS34 complex is tethered to the cytoskeleton through

an interaction between one component of the VPS34 complex, AMBRA1, and dynein light chains 1 and 2 (DLC1 and DLC2) (**Figure 4**). When autophagy is induced, ULK1 phosphorylates AMBRA1, releasing the autophagy core complex from dynein. Its subsequent relocation to the ER enables autophagosome nucleation.

In addition, DAP1 (death-associated protein 1) is a novel mTORC1 substrate with an inhibitory role in autophagy (148). Although the underlying mechanism of DAP1 in autophagy inhibition is unknown, it would be interesting to determine both if DAP1 acts upstream or downstream of ULK1 and its relative contribution in mediating the effect of mTORC1 in autophagy regulation. Surprisingly, Yu et al. (149) recently demonstrated that mTORC1 activity is also required at the late stage of autophagy to recycle lysosomes for another cycle of autophagy, even though mTORC1 has long been believed to inhibit the initiation step of this degradative process. Thus, the function of mTORC1 in autophagy is complex. It inhibits the initiation of autophagy at early stages, yet it positively contributes to the completion of autophagy at later stages.

Accumulating reports indicate that mTORC1 and AMPK serve as master switches for the process of autophagy. AMPK and mTORC1 have opposing effects on autophagy induction via coordinated phosphorylation of ULK1 (**Figure 4**). However, many questions still remain regarding how these two energy-sensing kinases, mTOR and AMPK, accomplish and coordinate their complex regulatory functions in response to the wide variety of conditions that trigger autophagy.

CONCLUSION AND PERSPECTIVE

Extensive biochemical, cell biological, genetic, and physiological studies confirm that AMPK is a key cellular energy sensor and that its activation promotes energy-producing catabolism and inhibits energy-consuming anabolism. Many of the AMPK substrates are metabolic enzymes directly involved in energy metabolism, such as glycolysis and fatty acid synthesis and oxidation. As illustrated by its effects on protein synthesis, AMPK activation also inhibits biosynthesis of macromolecules by, for example, inhibiting mTORC1 or eukaryotic elongation factor activity. Moreover, AMPK induces hydrolysis of cellular contents, such as proteins and organelles, via autophagy induction. This is accomplished in part by inhibiting mTORC1 and activating ULK1. Thus, AMPK activation modulates cellular metabolism of both small metabolites and macrobiomolecules. AMPK also plays a role in organismal energy balance by its actions in the neuroendocrine system. mTORC1 integrates cellular nutrient status, including energy levels, and plays a major role in cell growth. High mTORC1 activity promotes cell growth, whereas low mTORC1 activity inhibits growth and induces autophagy. Under nutrient starvation, decreased mTORC1 activity leads to reductions in ribosome biosynthesis and protein translation, which normally consume a large fraction of cellular energy. Therefore, mTORC1 has a key role not only in nutrient response, but also in cellular energy homeostasis. It is not surprising that mTORC1 activity is coupled to and inhibited by AMPK.

AMPK and mTORC1 are key cellular nutrient indicators and cell growth regulators. Thus, their dysregulation is associated with many human diseases. For example, uncontrolled mTORC1 activation by mutation in TSC1/TSC2 or constitutive activation of the PI3K pathway contributes to tumorigenesis. As such, mTORC1 inhibitors have been shown to have therapeutic benefits for TSC disease. Moreover, mTORC1 inhibitors, rapamycin analogs, have been approved as drugs to treat late-stage renal cancer, and many clinical trials under way use mTOR inhibitors for cancer treatment. mTORC1 can also regulate protein metabolism, targeting both synthesis and degradation (by autophagy); thus, inhibition of mTORC1 may prove useful in the development of drugs that target proteinopathies, including neurodegenerative disorders such as Alzheimer's disease. Similarly, defects in AMPK activation may be linked to tumorigenesis, given that the

upstream kinase LKB1 has long been recognized as a tumor suppressor. Moreover, metformin, the most widely used diabetic drug, has been reported to suppress cancers because patients using metformin present with a significant reduction in cancer incidence. Furthermore, the prominent role of AMPK and mTOR in energy metabolism makes them attractive drug targets for metabolic diseases, such as diabetes and obesity. Finally, inhibition of mTORC1 delays aging and extends life span in *C. elegans*, *Drosophila*, and mice. Therefore, both AMPK and mTORC1 will continue to attract wide attention from the pharmaceutical industry as prominent drug targets.

DISCLOSURE STATEMENT

The authors are not aware of any affiliations, memberships, funding, or financial holdings that might be perceived as affecting the objectivity of this review.

ACKNOWLEDGMENTS

We thank the members of Dr. Guan's and Dr. Inoki's laboratory, especially Jenna Jewell, for their critical reading of this manuscript. This study is supported by grants from the National Institutes of Health (K.I. and K.L.G.) and the Department of Defense (K.L.G.).

LITERATURE CITED

1. Hardie DG. 2007. AMP-activated/SNF1 protein kinases: conserved guardians of cellular energy. *Nat. Rev. Mol. Cell Biol.* 8:774–85
2. Lizcano JM, Goransson O, Toth R, Deak M, Morrice NA, et al. 2004. LKB1 is a master kinase that activates 13 kinases of the AMPK subfamily, including MARK/PAR-1. *EMBO J.* 23:833–43
3. Bright NJ, Thornton C, Carling D. 2009. The regulation and function of mammalian AMPK-related kinases. *Acta Physiol.* 196:15–26
4. Hawley SA, Boudeau J, Reid JL, Mustard KJ, Udd L, et al. 2003. Complexes between the LKB1 tumor suppressor, STRADα/β and MO25α/β are upstream kinases in the AMP-activated protein kinase cascade. *J. Biol.* 2:28
5. Boudeau J, Baas AF, Deak M, Morrice NA, Kieloch A, et al. 2003. MO25α/β interact with STRADα/β enhancing their ability to bind, activate and localize LKB1 in the cytoplasm. *EMBO J.* 22:5102–14
6. Hardie DG, Carling D, Carlson M. 1998. The AMP-activated/SNF1 protein kinase subfamily: metabolic sensors of the eukaryotic cell? *Annu. Rev. Biochem.* 67:821–55
7. Momcilovic M, Hong SP, Carlson M. 2006. Mammalian TAK1 activates Snf1 protein kinase in yeast and phosphorylates AMP-activated protein kinase in vitro. *J. Biol. Chem.* 281:25336–43
8. Hawley SA, Selbert MA, Goldstein EG, Edelman AM, Carling D, Hardie DG. 1995. 5′-AMP activates the AMP-activated protein kinase cascade, and Ca^{2+}/calmodulin activates the calmodulin-dependent protein kinase I cascade, via three independent mechanisms. *J. Biol. Chem.* 270:27186–91
9. Hong SP, Leiper FC, Woods A, Carling D, Carlson M. 2003. Activation of yeast Snf1 and mammalian AMP-activated protein kinase by upstream kinases. *Proc. Natl. Acad. Sci. USA* 100:8839–43
10. Warden SM, Richardson C, O'Donnell J Jr, Stapleton D, Kemp BE, Witters LA. 2001. Post-translational modifications of the β-1 subunit of AMP-activated protein kinase affect enzyme activity and cellular localization. *Biochem. J.* 354:275–83
11. Oakhill JS, Chen ZP, Scott JW, Steel R, Castelli LA, et al. 2010. β-Subunit myristoylation is the gatekeeper for initiating metabolic stress sensing by AMP-activated protein kinase (AMPK). *Proc. Natl. Acad. Sci. USA* 107:19237–41
12. McBride A, Ghilagaber S, Nikolaev A, Hardie DG. 2009. The glycogen-binding domain on the AMPK β subunit allows the kinase to act as a glycogen sensor. *Cell Metab.* 9:23–34
13. Celenza JL, Carlson M. 1986. A yeast gene that is essential for release from glucose repression encodes a protein kinase. *Science* 233:1175–80

14. Bateman A. 1997. The structure of a domain common to archaebacteria and the homocystinuria disease protein. *Trends Biochem. Sci.* 22:12–13
15. Xiao B, Heath R, Saiu P, Leiper FC, Leone P, et al. 2007. Structural basis for AMP binding to mammalian AMP-activated protein kinase. *Nature* 449:496–500
16. Oakhill JS, Scott JW, Kemp BE. 2009. Structure and function of AMP-activated protein kinase. *Acta Physiol.* 196:3–14
17. Xiao B, Sanders MJ, Underwood E, Heath R, Mayer FV, et al. 2011. Structure of mammalian AMPK and its regulation by ADP. *Nature* 472:230–33
18. Veech RL, Lawson JW, Cornell NW, Krebs HA. 1979. Cytosolic phosphorylation potential. *J. Biol. Chem.* 254:6538–47
19. Hellsten Y, Richter EA, Kiens B, Bangsbo J. 1999. AMP deamination and purine exchange in human skeletal muscle during and after intense exercise. *J. Physiol.* 520(Pt. 3):909–20
20. McBride A, Hardie DG. 2009. AMP-activated protein kinase—a sensor of glycogen as well as AMP and ATP? *Acta Physiol.* 196:99–113
21. Steinberg GR, Kemp BE. 2009. AMPK in health and disease. *Physiol. Rev.* 89:1025–78
22. Fogarty S, Hardie DG. 2010. Development of protein kinase activators: AMPK as a target in metabolic disorders and cancer. *Biochim. Biophys. Acta* 1804:581–91
23. Davies SP, Sim AT, Hardie DG. 1990. Location and function of three sites phosphorylated on rat acetyl-CoA carboxylase by the AMP-activated protein kinase. *Eur. J. Biochem.* 187:183–90
24. Koo SH, Flechner L, Qi L, Zhang X, Screaton RA, et al. 2005. The CREB coactivator TORC2 is a key regulator of fasting glucose metabolism. *Nature* 437:1109–11
25. Chen S, Murphy J, Toth R, Campbell DG, Morrice NA, Mackintosh C. 2008. Complementary regulation of TBC1D1 and AS160 by growth factors, insulin and AMPK activators. *Biochem. J.* 409:449–59
26. Geraghty KM, Chen S, Harthill JE, Ibrahim AF, Toth R, et al. 2007. Regulation of multisite phosphorylation and 14–3–3 binding of AS160 in response to IGF-1, EGF, PMA and AICAR. *Biochem. J.* 407:231–41
27. Jager S, Handschin C, St-Pierre J, Spiegelman BM. 2007. AMP-activated protein kinase (AMPK) action in skeletal muscle via direct phosphorylation of PGC-1α. *Proc. Natl. Acad. Sci. USA* 104:12017–22
28. McGee SL, van Denderen BJ, Howlett KF, Mollica J, Schertzer JD, et al. 2008. AMP-activated protein kinase regulates GLUT4 transcription by phosphorylating histone deacetylase 5. *Diabetes* 57:860–67
29. Munday MR. 2002. Regulation of mammalian acetyl-CoA carboxylase. *Biochem. Soc. Trans.* 30:1059–64
30. Loewith R, Jacinto E, Wullschleger S, Lorberg A, Crespo JL, et al. 2002. Two TOR complexes, only one of which is rapamycin sensitive, have distinct roles in cell growth control. *Mol. Cell* 10:457–68
31. Hara K, Maruki Y, Long X, Yoshino K, Oshiro N, et al. 2002. Raptor, a binding partner of target of rapamycin (TOR), mediates TOR action. *Cell* 110:177–89
32. Kim DH, Sarbassov DD, Ali SM, King JE, Latek RR, et al. 2002. mTOR interacts with raptor to form a nutrient-sensitive complex that signals to the cell growth machinery. *Cell* 110:163–75
33. Kim DH, Sarbassov DD, Ali SM, Latek RR, Guntur KV, et al. 2003. GβL, a positive regulator of the rapamycin-sensitive pathway required for the nutrient-sensitive interaction between raptor and mTOR. *Mol. Cell* 11:895–904
34. Sancak Y, Thoreen CC, Peterson TR, Lindquist RA, Kang SA, et al. 2007. PRAS40 is an insulin-regulated inhibitor of the mTORC1 protein kinase. *Mol. Cell* 25:903–15
35. Vander Haar E, Lee SI, Bandhakavi S, Griffin TJ, Kim DH. 2007. Insulin signalling to mTOR mediated by the Akt/PKB substrate PRAS40. *Nat. Cell Biol.* 9:316–23
36. Jacinto E, Loewith R, Schmidt A, Lin S, Ruegg MA, et al. 2004. Mammalian TOR complex 2 controls the actin cytoskeleton and is rapamycin insensitive. *Nat. Cell Biol.* 6(11):1122–28
37. Sarbassov DD, Ali SM, Kim DH, Guertin DA, Latek RR, et al. 2004. Rictor, a novel binding partner of mTOR, defines a rapamycin-insensitive and raptor-independent pathway that regulates the cytoskeleton. *Curr. Biol.* 14:1296–302
38. Yang Q, Inoki K, Ikenoue T, Guan KL. 2006. Identification of Sin1 as an essential TORC2 component required for complex formation and kinase activity. *Genes Dev.* 20:2820–32
39. Frias MA, Thoreen CC, Jaffe JD, Schroder W, Sculley T, et al. 2006. mSin1 is necessary for Akt/PKB phosphorylation, and its isoforms define three distinct mTORC2s. *Curr. Biol.* 16:1865–70

40. Pearce LR, Huang X, Boudeau J, Pawlowski R, Wullschleger S, et al. 2007. Identification of Protor as a novel Rictor-binding component of mTOR complex-2. *Biochem. J.* 405:513–22
41. Woo SY, Kim DH, Jun CB, Kim YM, Haar EV, et al. 2007. PRR5, a novel component of mTOR complex 2, regulates platelet-derived growth factor receptor β expression and signaling. *J. Biol. Chem.* 282:25604–12
42. Schalm SS, Fingar DC, Sabatini DM, Blenis J. 2003. TOS motif-mediated raptor binding regulates 4E-BP1 multisite phosphorylation and function. *Curr. Biol.* 13:797–806
43. Choi KM, McMahon LP, Lawrence JC Jr. 2003. Two motifs in the translational repressor PHAS-I required for efficient phosphorylation by mammalian target of rapamycin and for recognition by raptor. *J. Biol. Chem.* 278:19667–73
44. Nojima H, Tokunaga C, Eguchi S, Oshiro N, Hidayat S, et al. 2003. The mammalian target of rapamycin (mTOR) partner, raptor, binds the mTOR substrates p70 S6 kinase and 4E-BP1 through their TOR signaling (TOS) motif. *J. Biol. Chem.* 278:15461–64
45. Sancak Y, Peterson TR, Shaul YD, Lindquist RA, Thoreen CC, et al. 2008. The Rag GTPases bind raptor and mediate amino acid signaling to mTORC1. *Science* 320:1496–501
46. Jacinto E, Lorberg A. 2008. TOR regulation of AGC kinases in yeast and mammals. *Biochem. J.* 410:19–37
47. Gingras AC, Raught B, Sonenberg N. 2001. Regulation of translation initiation by FRAP/mTOR. *Genes Dev.* 15:807–26
48. Yip CK, Murata K, Walz T, Sabatini DM, Kang SA. 2010. Structure of the human mTOR complex I and its implications for rapamycin inhibition. *Mol. Cell* 38:768–74
49. Shahbazian D, Roux PP, Mieulet V, Cohen MS, Raught B, et al. 2006. The mTOR/PI3K and MAPK pathways converge on eIF4B to control its phosphorylation and activity. *EMBO J.* 25:2781–91
50. Dorrello NV, Peschiaroli A, Guardavaccaro D, Colburn NH, Sherman NE, Pagano M. 2006. S6K1- and βTRCP-mediated degradation of PDCD4 promotes protein translation and cell growth. *Science* 314:467–71
51. Richardson CJ, Broenstrup M, Fingar DC, Julich K, Ballif BA, et al. 2004. SKAR is a specific target of S6 kinase 1 in cell growth control. *Curr. Biol.* 14:1540–49
52. Blenis J, Kuo CJ, Erikson RL. 1987. Identification of a ribosomal protein S6 kinase regulated by transformation and growth-promoting stimuli. *J. Biol. Chem.* 262:14373–76
53. Montagne J, Stewart MJ, Stocker H, Hafen E, Kozma SC, Thomas G. 1999. *Drosophila* S6 kinase: a regulator of cell size. *Science* 285:2126–29
54. Shima H, Pende M, Chen Y, Fumagalli S, Thomas G, Kozma SC. 1998. Disruption of the p70(s6k)/p85(s6k) gene reveals a small mouse phenotype and a new functional S6 kinase. *EMBO J.* 17:6649–59
55. Gingras AC, Kennedy SG, O'Leary MA, Sonenberg N, Hay N. 1998. 4E-BP1, a repressor of mRNA translation, is phosphorylated and inactivated by the Akt(PKB) signaling pathway. *Genes Dev.* 12:502–13
56. Mizushima N. 2010. The role of the Atg1/ULK1 complex in autophagy regulation. *Curr. Opin. Cell Biol.* 22:132–39
57. Jung CH, Jun CB, Ro SH, Kim YM, Otto NM, et al. 2009. ULK-Atg13-FIP200 complexes mediate mTOR signaling to the autophagy machinery. *Mol. Biol. Cell* 20:1992–2003
58. Kim J, Kundu M, Viollet B, Guan KL. 2011. AMPK and mTOR regulate autophagy through direct phosphorylation of Ulk1. *Nat. Cell Biol.* 13:132–41
59. Cardenas ME, Cutler NS, Lorenz MC, Di Como CJ, Heitman J. 1999. The TOR signaling cascade regulates gene expression in response to nutrients. *Genes Dev.* 13:3271–79
60. Hardwick JS, Kuruvilla FG, Tong JK, Shamji AF, Schreiber SL. 1999. Rapamycin-modulated transcription defines the subset of nutrient-sensitive signaling pathways directly controlled by the Tor proteins. *Proc. Natl. Acad. Sci. USA* 96:14866–70
61. Grummt I, Smith VA, Grummt F. 1976. Amino acid starvation affects the initiation frequency of nucleolar RNA polymerase. *Cell* 7:439–45
62. Hannan KM, Brandenburger Y, Jenkins A, Sharkey K, Cavanaugh A, et al. 2003. mTOR-dependent regulation of ribosomal gene transcription requires S6K1 and is mediated by phosphorylation of the carboxy-terminal activation domain of the nucleolar transcription factor UBF. *Mol. Cell. Biol.* 23:8862–77

63. Schnapp A, Pfleiderer C, Rosenbauer H, Grummt I. 1990. A growth-dependent transcription initiation factor (TIF-IA) interacting with RNA polymerase I regulates mouse ribosomal RNA synthesis. *EMBO J.* 9:2857–63
64. Eberhard D, Tora L, Egly JM, Grummt I. 1993. A TBP-containing multiprotein complex (TIF-IB) mediates transcription specificity of murine RNA polymerase I. *Nucleic Acids Res.* 21:4180–86
65. Mayer C, Zhao J, Yuan X, Grummt I. 2004. mTOR-dependent activation of the transcription factor TIF-IA links rRNA synthesis to nutrient availability. *Genes Dev.* 18:423–34
66. Hoppe S, Bierhoff H, Cado I, Weber A, Tiebe M, et al. 2009. AMP-activated protein kinase adapts rRNA synthesis to cellular energy supply. *Proc. Natl. Acad. Sci. USA* 106:17781–86
67. Jorgensen P, Rupes I, Sharom JR, Schneper L, Broach JR, Tyers M. 2004. A dynamic transcriptional network communicates growth potential to ribosome synthesis and critical cell size. *Genes Dev.* 18:2491–505
68. Marion RM, Regev A, Segal E, Barash Y, Koller D, et al. 2004. Sfp1 is a stress- and nutrient-sensitive regulator of ribosomal protein gene expression. *Proc. Natl. Acad. Sci. USA* 101:14315–22
69. Martin DE, Soulard A, Hall MN. 2004. TOR regulates ribosomal protein gene expression via PKA and the Forkhead transcription factor FHL1. *Cell* 119:969–79
70. Schawalder SB, Kabani M, Howald I, Choudhury U, Werner M, Shore D. 2004. Growth-regulated recruitment of the essential yeast ribosomal protein gene activator Ifh1. *Nature* 432:1058–61
71. Levy S, Avni D, Hariharan N, Perry RP, Meyuhas O. 1991. Oligopyrimidine tract at the 5′ end of mammalian ribosomal protein mRNAs is required for their translational control. *Proc. Natl. Acad. Sci. USA* 88:3319–23
72. Jefferies HB, Fumagalli S, Dennis PB, Reinhard C, Pearson RB, Thomas G. 1997. Rapamycin suppresses 5′TOP mRNA translation through inhibition of p70s6k. *EMBO J.* 16:3693–704
73. Pende M, Um SH, Mieulet V, Sticker M, Goss VL, et al. 2004. S6K1(-/-)/S6K2(-/-) mice exhibit perinatal lethality and rapamycin-sensitive 5′-terminal oligopyrimidine mRNA translation and reveal a mitogen-activated protein kinase-dependent S6 kinase pathway. *Mol. Cell. Biol.* 24:3112–24
74. Ruvinsky I, Sharon N, Lerer T, Cohen H, Stolovich-Rain M, et al. 2005. Ribosomal protein S6 phosphorylation is a determinant of cell size and glucose homeostasis. *Genes Dev.* 19:2199–211
75. Tang H, Hornstein E, Stolovich M, Levy G, Livingstone M, et al. 2001. Amino acid-induced translation of TOP mRNAs is fully dependent on phosphatidylinositol 3-kinase-mediated signaling, is partially inhibited by rapamycin, and is independent of S6K1 and rpS6 phosphorylation. *Mol. Cell. Biol.* 21:8671–83
76. Kantidakis T, Ramsbottom BA, Birch JL, Dowding SN, White RJ. 2010. mTOR associates with TFIIIC, is found at tRNA and 5S rRNA genes, and targets their repressor Maf1. *Proc. Natl. Acad. Sci. USA* 107:11823–28
77. Michels AA, Robitaille AM, Buczynski-Ruchonnet D, Hodroj W, Reina JH, et al. 2010. mTORC1 directly phosphorylates and regulates human MAF1. *Mol. Cell. Biol.* 30:3749–57
78. Silvera D, Formenti SC, Schneider RJ. 2010. Translational control in cancer. *Nat. Rev. Cancer* 10:254–66
79. Ding Q, Markesbery WR, Chen Q, Li F, Keller JN. 2005. Ribosome dysfunction is an early event in Alzheimer's disease. *J. Neurosci.* 25:9171–75
80. Zoncu R, Efeyan A, Sabatini DM. 2011. mTOR: from growth signal integration to cancer, diabetes and ageing. *Nat. Rev. Mol. Cell Biol.* 12:21–35
81. Zinzalla V, Stracka D, Oppliger W, Hall MN. 2011. Activation of mTORC2 by association with the ribosome. *Cell* 144:757–68
82. Sarbassov DD, Guertin DA, Ali SM, Sabatini DM. 2005. Phosphorylation and regulation of Akt/PKB by the rictor-mTOR complex. *Science* 307:1098–101
83. Yamagata K, Sanders LK, Kaufmann WE, Yee W, Barnes CA, et al. 1994. *rheb*, a growth factor- and synaptic activity-regulated gene, encodes a novel Ras-related protein. *J. Biol. Chem.* 269:16333–39
84. Long X, Lin Y, Ortiz-Vega S, Yonezawa K, Avruch J. 2005. Rheb binds and regulates the mTOR kinase. *Curr. Biol.* 15:702–13
85. Tabancay AP Jr, Gau CL, Machado IM, Uhlmann EJ, Gutmann DH, et al. 2003. Identification of dominant negative mutants of Rheb GTPase and their use to implicate the involvement of human Rheb in the activation of p70S6K. *J. Biol. Chem.* 278:39921–30

86. Sato T, Nakashima A, Guo L, Tamanoi F. 2009. Specific activation of mTORC1 by Rheb G-protein in vitro involves enhanced recruitment of its substrate protein. *J. Biol. Chem.* 284:12783–91
87. Garami A, Zwartkruis FJ, Nobukuni T, Joaquin M, Roccio M, et al. 2003. Insulin activation of Rheb, a mediator of mTOR/S6K/4E-BP signaling, is inhibited by TSC1 and 2. *Mol. Cell* 11:1457–66
88. Inoki K, Li Y, Xu T, Guan KL. 2003. Rheb GTPase is a direct target of TSC2 GAP activity and regulates mTOR signaling. *Genes Dev.* 17:1829–34
89. Tee AR, Manning BD, Roux PP, Cantley LC, Blenis J. 2003. Tuberous sclerosis complex gene products, Tuberin and Hamartin, control mTOR signaling by acting as a GTPase-activating protein complex toward Rheb. *Curr. Biol.* 13:1259–68
90. Zhang Y, Gao X, Saucedo LJ, Ru B, Edgar BA, Pan D. 2003. Rheb is a direct target of the tuberous sclerosis tumour suppressor proteins. *Nat. Cell Biol.* 5:578–81
91. Kwiatkowski DJ. 2003. Tuberous sclerosis: from tubers to mTOR. *Ann. Hum. Genet.* 67:87–96
92. Crino PB, Nathanson KL, Henske EP. 2006. The tuberous sclerosis complex. *N. Engl. J. Med.* 355:1345–56
93. van Slegtenhorst M, Nellist M, Nagelkerken B, Cheadle J, Snell R, et al. 1998. Interaction between hamartin and tuberin, the TSC1 and TSC2 gene products. *Hum. Mol. Genet.* 7:1053–57
94. Dan HC, Sun M, Yang L, Feldman RI, Sui XM, et al. 2002. PI3K/AKT pathway regulates TSC tumor suppressor complex by phosphorylation of tuberin. *J. Biol. Chem.* 277:35364–70
95. Manning BD, Tee AR, Logsdon MN, Blenis J, Cantley LC. 2002. Identification of the tuberous sclerosis complex-2 tumor suppressor gene product tuberin as a target of the phosphoinositide 3-kinase/Akt pathway. *Mol. Cell* 10:151–62
96. Inoki K, Li Y, Zhu T, Wu J, Guan KL. 2002. TSC2 is phosphorylated and inhibited by Akt and suppresses mTOR signalling. *Nat. Cell Biol.* 4:648–57
97. Tee AR, Fingar DC, Manning BD, Kwiatkowski DJ, Cantley LC, Blenis J. 2002. Tuberous sclerosis complex-1 and -2 gene products function together to inhibit mammalian target of rapamycin (mTOR)-mediated downstream signaling. *Proc. Natl. Acad. Sci. USA* 99:13571–76
98. Ma L, Chen Z, Erdjument-Bromage H, Tempst P, Pandolfi PP. 2005. Phosphorylation and functional inactivation of TSC2 by Erk implications for tuberous sclerosis and cancer pathogenesis. *Cell* 121:179–93
99. Roux PP, Ballif BA, Anjum R, Gygi SP, Blenis J. 2004. Tumor-promoting phorbol esters and activated Ras inactivate the tuberous sclerosis tumor suppressor complex via p90 ribosomal S6 kinase. *Proc. Natl. Acad. Sci. USA* 101:13489–94
100. Kwiatkowski DJ, Zhang H, Bandura JL, Heiberger KM, Glogauer M, et al. 2002. A mouse model of TSC1 reveals sex-dependent lethality from liver hemangiomas, and up-regulation of p70S6 kinase activity in Tsc1 null cells. *Hum. Mol. Genet.* 11:525–34
101. Dennis PB, Jaeschke A, Saitoh M, Fowler B, Kozma SC, Thomas G. 2001. Mammalian TOR: a homeostatic ATP sensor. *Science* 294:1102–5
102. Bolster DR, Crozier SJ, Kimball SR, Jefferson LS. 2002. AMP-activated protein kinase suppresses protein synthesis in rat skeletal muscle through down-regulated mammalian target of rapamycin (mTOR) signaling. *J. Biol. Chem.* 277:23977–80
103. Kimura N, Tokunaga C, Dalal S, Richardson C, Yoshino K, et al. 2003. A possible linkage between AMP-activated protein kinase (AMPK) and mammalian target of rapamycin (mTOR) signalling pathway. *Genes Cells* 8:65–79
104. Inoki K, Zhu T, Guan KL. 2003. TSC2 mediates cellular energy response to control cell growth and survival. *Cell* 115:577–90
105. Zheng M, Wang YH, Wu XN, Wu SQ, Lu BJ, et al. 2011. Inactivation of Rheb by PRAK-mediated phosphorylation is essential for energy-depletion-induced suppression of mTORC1. *Nat. Cell Biol.* 13:263–72
106. Wolff NC, Vega-Rubin-de-Celis S, Xie XJ, Castrillon DH, Kabbani W, Brugarolas J. 2011. Cell type-dependent regulation of mTORC1 by REDD1 and the tumor suppressors TSC1/TSC2 and LKB1 in response to hypoxia. *Mol. Cell. Biol.* 31(9):1870–84
107. Kalender A, Selvaraj A, Kim SY, Gulati P, Brule S, et al. 2010. Metformin, independent of AMPK, inhibits mTORC1 in a Rag GTPase-dependent manner. *Cell Metab.* 11:390–401

108. Lee CH, Inoki K, Karbowniczek M, Petroulakis E, Sonenberg N, et al. 2007. Constitutive mTOR activation in TSC mutants sensitizes cells to energy starvation and genomic damage via p53. *EMBO J.* 26:4812–23
109. Choo AY, Kim SG, Vander Heiden MG, Mahoney SJ, Vu H, et al. 2010. Glucose addiction of TSC null cells is caused by failed mTORC1-dependent balancing of metabolic demand with supply. *Mol. Cell* 38:487–99
110. Ozcan U, Ozcan L, Yilmaz E, Düvel K, Sahin M, et al. 2008. Loss of the tuberous sclerosis complex tumor suppressors triggers the unfolded protein response to regulate insulin signaling and apoptosis. *Mol. Cell* 29:541–51
111. Shah OJ, Wang Z, Hunter T. 2004. Inappropriate activation of the TSC/Rheb/mTOR/S6K cassette induces IRS1/2 depletion, insulin resistance, and cell survival deficiencies. *Curr. Biol.* 14:1650–56
112. Ghosh S, Tergaonkar V, Rothlin CV, Correa RG, Bottero V, et al. 2006. Essential role of tuberous sclerosis genes TSC1 and TSC2 in NF-κB activation and cell survival. *Cancer Cell* 10:215–26
113. Imamura K, Ogura T, Kishimoto A, Kaminishi M, Esumi H. 2001. Cell cycle regulation via p53 phosphorylation by a 5′-AMP activated protein kinase activator, 5-aminoimidazole- 4-carboxamide-1-β-D-ribofuranoside, in a human hepatocellular carcinoma cell line. *Biochem. Biophys. Res. Commun.* 287:562–67
114. Harrington LS, Findlay GM, Gray A, Tolkacheva T, Wigfield S, et al. 2004. The TSC1-2 tumor suppressor controls insulin-PI3K signaling via regulation of IRS proteins. *J. Cell Biol.* 166:213–23
115. Um SH, Frigerio F, Watanabe M, Picard F, Joaquin M, et al. 2004. Absence of S6K1 protects against age- and diet-induced obesity while enhancing insulin sensitivity. *Nature* 431:200–5
116. Gwinn DM, Shackelford DB, Egan DF, Mihaylova MM, Mery A, et al. 2008. AMPK phosphorylation of raptor mediates a metabolic checkpoint. *Mol. Cell* 30:214–26
117. Sekiguchi T, Hirose E, Nakashima N, Ii M, Nishimoto T. 2001. Novel G proteins, Rag C and Rag D, interact with GTP-binding proteins, Rag A and Rag B. *J. Biol. Chem.* 276:7246–57
118. Kim E, Goraksha-Hicks P, Li L, Neufeld TP, Guan KL. 2008. Regulation of TORC1 by Rag GTPases in nutrient response. *Nat. Cell Biol.* 10:935–45
119. Sancak Y, Bar-Peled L, Zoncu R, Markhard AL, Nada S, Sabatini DM. 2010. Ragulator-Rag complex targets mTORC1 to the lysosomal surface and is necessary for its activation by amino acids. *Cell* 141:290–303
120. Korolchuk VI, Saiki S, Lichtenberg M, Siddiqi FH, Roberts EA, et al. 2011. Lysosomal positioning coordinates cellular nutrient responses. *Nat. Cell Biol.* 13:453–60
121. Nada S, Hondo A, Kasai A, Koike M, Saito K, et al. 2009. The novel lipid raft adaptor p18 controls endosome dynamics by anchoring the MEK-ERK pathway to late endosomes. *EMBO J.* 28:477–89
122. Li L, Kim E, Yuan H, Inoki K, Goraksha-Hicks P, et al. 2010. Regulation of mTORC1 by the Rab and Arf GTPases. *J. Biol. Chem.* 285:19705–9
123. Nobukuni T, Joaquin M, Roccio M, Dann SG, Kim SY, et al. 2005. Amino acids mediate mTOR/raptor signaling through activation of class 3 phosphatidylinositol 3OH-kinase. *Proc. Natl. Acad. Sci. USA* 102:14238–43
124. Findlay GM, Yan L, Procter J, Mieulet V, Lamb RF. 2007. A MAP4 kinase related to Ste20 is a nutrient-sensitive regulator of mTOR signalling. *Biochem. J.* 403:13–20
125. Schu PV, Takegawa K, Fry MJ, Stack JH, Waterfield MD, Emr SD. 1993. Phosphatidylinositol 3-kinase encoded by yeast VPS34 gene essential for protein sorting. *Science* 260:88–91
126. Kihara A, Noda T, Ishihara N, Ohsumi Y. 2001. Two distinct Vps34 phosphatidylinositol 3-kinase complexes function in autophagy and carboxypeptidase Y sorting in *Saccharomyces cerevisiae*. *J. Cell Biol.* 152:519–30
127. Mizushima N. 2009. Physiological functions of autophagy. *Curr. Top. Microbiol. Immunol.* 335:71–84
128. Yang Z, Klionsky DJ. 2009. An overview of the molecular mechanism of autophagy. *Curr. Top. Microbiol. Immunol.* 335:1–32
129. Mizushima N. 2007. Autophagy: process and function. *Genes Dev.* 21:2861–73
130. Chan EY, Tooze SA. 2009. Evolution of Atg1 function and regulation. *Autophagy* 5:758–65
131. Kamada Y, Funakoshi T, Shintani T, Nagano K, Ohsumi M, Ohsumi Y. 2000. Tor-mediated induction of autophagy via an Apg1 protein kinase complex. *J. Cell Biol.* 150:1507–13

132. Kamada Y, Yoshino K, Kondo C, Kawamata T, Oshiro N, et al. 2010. Tor directly controls the Atg1 kinase complex to regulate autophagy. *Mol. Cell. Biol.* 30:1049–58
133. Chan EY, Kir S, Tooze SA. 2007. siRNA screening of the kinome identifies ULK1 as a multidomain modulator of autophagy. *J. Biol. Chem.* 282:25464–74
134. Chan EY, Longatti A, McKnight NC, Tooze SA. 2009. Kinase-inactivated ULK proteins inhibit autophagy via their conserved C-terminal domains using an Atg13-independent mechanism. *Mol. Cell. Biol.* 29:157–71
135. Hara T, Takamura A, Kishi C, Iemura S, Natsume T, et al. 2008. FIP200, a ULK-interacting protein, is required for autophagosome formation in mammalian cells. *J. Cell Biol.* 181:497–510
136. Ganley IG, Lam du H, Wang J, Ding X, Chen S, Jiang X. 2009. ULK1.ATG13.FIP200 complex mediates mTOR signaling and is essential for autophagy. *J. Biol. Chem.* 284:12297–305
137. Hosokawa N, Hara T, Kaizuka T, Kishi C, Takamura A, et al. 2009. Nutrient-dependent mTORC1 association with the ULK1-Atg13-FIP200 complex required for autophagy. *Mol. Biol. Cell* 20:1981–91
138. Chan EY. 2009. mTORC1 phosphorylates the ULK1-mAtg13-FIP200 autophagy regulatory complex. *Sci. Signal.* 2:pe51
139. Meley D, Bauvy C, Houben-Weerts JH, Dubbelhuis PF, Helmond MT, et al. 2006. AMP-activated protein kinase and the regulation of autophagic proteolysis. *J. Biol. Chem.* 281:34870–79
140. Herrero-Martin G, Høyer-Hansen M, García-García C, Fumarola C, Farkas T, et al. 2009. TAK1 activates AMPK-dependent cytoprotective autophagy in TRAIL-treated epithelial cells. *EMBO J.* 28:677–85
141. Matsui Y, Takagi H, Qu X, Abdellatif M, Sakoda H, et al. 2007. Distinct roles of autophagy in the heart during ischemia and reperfusion: roles of AMP-activated protein kinase and Beclin 1 in mediating autophagy. *Circ. Res.* 100:914–22
142. Inoki K, Ouyang H, Zhu T, Lindvall C, Wang Y, et al. 2006. TSC2 integrates Wnt and energy signals via a coordinated phosphorylation by AMPK and GSK3 to regulate cell growth. *Cell* 126:955–68
143. Egan DF, Shackelford DB, Mihaylova MM, Gelino S, Kohnz RA, et al. 2011. Phosphorylation of ULK1 (hATG1) by AMP-activated protein kinase connects energy sensing to mitophagy. *Science* 331:456–61
144. Lee JW, Park S, Takahashi Y, Wang HG. 2010. The association of AMPK with ULK1 regulates autophagy. *PLoS One* 5:e15394
145. Shang L, Chen S, Du F, Li S, Zhao L, Wang X. 2011. Nutrient starvation elicits an acute autophagic response mediated by Ulk1 dephosphorylation and its subsequent dissociation from AMPK. *Proc. Natl. Acad. Sci. USA* 108:4788–93
146. Tang HW, Wang YB, Wang SL, Wu MH, Lin SY, Chen GC. 2011. Atg1-mediated myosin II activation regulates autophagosome formation during starvation-induced autophagy. *EMBO J.* 30:636–51
147. Di Bartolomeo S, Corazzari M, Nazio F, Oliverio S, Lisi G, et al. 2010. The dynamic interaction of AMBRA1 with the dynein motor complex regulates mammalian autophagy. *J. Cell Biol.* 191:155–68
148. Koren I, Reem E, Kimchi A. 2010. DAP1, a novel substrate of mTOR, negatively regulates autophagy. *Curr. Biol.* 20:1093–98
149. Yu L, McPhee CK, Zheng L, Mardones GA, Rong Y, et al. 2010. Termination of autophagy and reformation of lysosomes regulated by mTOR. *Nature* 465:942–46

Annual Review of Pharmacology and Toxicology

Volume 52, 2012

Contents

Indexes

Errata

An online log of corrections to *Annual Review of Pharmacology and Toxicology* articles may be found at http://pharmtox.annualreviews.org/errata.shtml

Crystal structure of the Gtr1p–Gtr2p complex reveals new insights into the amino acid-induced TORC1 activation

Rui Gong, Li Li, Yi Liu, et al.

Genes Dev. 2011 25: 1668-1673 originally published online August 4, 2011
Access the most recent version at doi:10.1101/gad.16968011

RESEARCH COMMUNICATION

Crystal structure of the Gtr1p–Gtr2p complex reveals new insights into the amino acid-induced TORC1 activation

Rui Gong,[1,2,5] Li Li,[3,5] Yi Liu,[1,2,5] Ping Wang,[2] Huirong Yang,[2] Ling Wang,[2] Jingdong Cheng,[2] Kun-Liang Guan,[3,6] and Yanhui Xu[1,2,4,6,7]

[1]Cancer Institute, Shanghai Cancer Center, Department of Oncology, Shanghai Medical College, Fudan University, Shanghai 200032, China; [2]Institute of Biomedical Sciences, Fudan University, Shanghai 200032, China; [3]Department of Pharmacology, Moores Cancer Center, University of California at San Diego, La Jolla, California 92093, USA; [4]State Key Laboratory of Genetic Engineering, School of Life Sciences, Fudan University, Shanghai 200433, China

The target of rapamycin (TOR) complex 1 (TORC1) is a central cell growth regulator in response to a wide array of signals. The Rag GTPases play an essential role in relaying amino acid signals to TORC1 activation through direct interaction with raptor and recruitment of the TORC1 complex to lysosomes. Here we present the crystal structure of the Gtr1p–Gtr2p complex, the Rag homologs from *Saccharomyces cerevisiae*, at 2.8 Å resolution. The heterodimeric GTPases reveal a pseudo-twofold symmetric organization. Structure-guided functional analyses of RagA–RagC, the human homologs of Gtr1p–Gtr2p, show that both G domains (N-terminal GTPase domains) and dimerization are important for raptor binding. In particular, the switch regions of the G domain in RagA are indispensible for interaction with raptor, and hence TORC1 activation. The dimerized C-terminal domains of RagA–RagC display a remarkable structural similarity to MP1/p14, which is in a complex with lysosome membrane protein p18, and directly interact with p18, therefore recruiting mTORC1 to the lysosome for activation by Rheb. Our results reveal a structural model for the mechanism of the Rag GTPases in TORC1 activation and amino acid signaling.

Supplemental material is available for this article.

Received May 5, 2011; revised version accepted July 12, 2011.

The mammalian target of rapamycin (mTOR) is an atypical protein kinase related to ATM and the DNA-PK subfamily. TOR is highly conserved from yeast to mammals and forms two distinct functional complexes: TOC complex 1 (TORC1) and TORC2. mTORC1 is a central cell growth regulator that integrates a wide range of growth stimulatory and inhibitory signals to regulate cell growth (Wullschleger et al. 2006). Key substrates of mTORC1 include S6K and 4EBP1; therefore, mTORC1 activation promotes cell growth by stimulating translation. In addition, mTORC1 plays a critical role in inhibiting catabolic processes, such as autophagy. mTORC1 inhibits autophagy at least in part by phosphorylating and inhibiting the autophagy-initiating kinase ULK1. Uncontrolled TORC1 activation has been observed in human diseases such as cancer (Inoki et al. 2005; Guertin and Sabatini 2007), indicating an important role of tight mTORC1 regulation under physiological conditions. Rapamycin is a specific TORC1 inhibitor, and its analogs are being used for cancer treatment and immunosuppression.

Growth factors act through PI3K, Akt, TSC1/TSC2, and Rheb to stimulate TORC1 (Wullschleger et al. 2006). In addition to growth factors, mTORC1 activation requires energy sufficiency (high ATP levels) and nutrients (amino acids). The AMP-dependent protein kinase AMPK plays a critical role in mTORC1 inhibition in response to cellular energy stress. Amino acids are one of the most important signals for mTORC1 activation. In the absence of amino acids, neither growth factors nor glucose (as a source of energy) can efficiently activate mTORC1. It has been shown that the Rag GTPases, which are distantly related to Ras (Kim et al. 2008; Sancak et al. 2008), play an essential role in TORC1 activation in response to amino acid signals. The requirement of amino acids for TORC1 activation and the involvement of Rag GTPases in amino acid signaling are highly conserved in all eukaryotes. For example, the *Saccharomyces cerevisiae* Gtr1 and Gtr2, which correspond to human RagA/RagB and RagC/RagD (Binda et al. 2009), respectively, also relay amino acid sufficiency to TORC1 activation in yeast.

Rag GTPases are unique in that they form heterodimers, as RagA or RagB dimerizes with RagC or RagD (Sekiguchi et al. 2001). Similarly, the yeast Gtr1 forms a heterodimer with Gtr2. Another unique property of the Rag GTPases is that the two Rag GTPases in the heterodimer bind guanine nucleotides in an apposing manner; i.e., one subunit binds GTP, and the other binds GDP. Only when RagA or RagB exist in the GTP-bound form, the heterodimer is active to stimulate TORC1 through a direct interaction with raptor (Kim et al. 2008; Sancak et al. 2008). Consistently, addition of amino acids promotes GTP binding of RagA or RagB in the heterodimer. Recently, it has been proposed that the Rag GTPases mainly function to recruit mTORC1 to lysosome, where mTORC1 can be activated by the lysosomal-localized Rheb. Once recruited to the lysosomes by the Rag GTPases, TORC1 is activated by the Rheb GTPase, another Ras family member (Kim et al. 2008; Sancak et al. 2008). The lysosomal localization of Rag is mediated by a direct interaction with the lysosomal membrane protein p18 and its associated protein, p14/MP1 (Sancak et al. 2010).

Recent studies have established an essential role of Rag GTPases in amino acid signaling; however, the molecular mechanism of Rag GTPases in mTORC1 activation is largely unknown. In this study, we report the three-dimensional structure of the Gtr1p–Gtr2p complex. Our

[*Keywords*: Rag GTPases; Gtr1p; Gtr2p; structure; raptor; TORC1]
[5]**These authors contributed equally to this work.**
[6]**These authors contributed equally to this work.**
[7]**Corresponding author.**
E-mail xuyh@fudan.edu.cn.
Article published online ahead of print. Article and publication date are online at http://www.genesdev.org/cgi/doi/10.1101/gad.16968011.

structure–function studies have revealed new molecular insights into the molecular basis of mTORC1 regulation by Rag GTPases through interaction with Raptor and the lysosomal protein p18.

Results and Discussion

Overall structure of Gtr1p–Gtr2p, the yeast homolog of RagA–RagC

Previous studies have shown that the function of Rag GTPase complexes are highly conserved across species from yeast to humans (Bun-Ya et al. 1992; Schurmann et al. 1995; Hirose et al. 1998; Nakashima et al. 1999; Sekiguchi et al. 2001; Dubouloz et al. 2005; Binda et al. 2009). The three-dimensional structures are also predicted to be conserved from yeast to humans, with the primary sequence identity of 49% for RagA/Gtr1p and 43% for RagC/Gtr2p (similarity of 75% for RagA/Gtr1p and 76% for RagC/Gtr2p) (Supplemental Fig. S1). To understand the mechanism of Rag GTPase-mediated TORC1 activation, we sought to determine the structure of Rag GTPases from yeast to mammals. After numerous trials, we succeeded in crystallizing the Gtr1p–Gtr2p complex, the yeast homolog of RagA–RagC, and the final model was refined to 2.8 Å resolution (Fig. 1A; Supplemental Fig. S2). The statistics for the structure determination are summarized in Supplemental Table S1. Gtr1p and Gtr2p form a very stable heterodimer in solution, which was copurified from *Escherichia coli* (Supplemental Fig. S3). The two proteins used for crystallization were both GTP-bound forms, through incorporation of GMPPNP, a nonhydrolyzable GTP analog commonly used in structure studies.

As shown in Figure 1A, both Gtr1p and Gtr2p comprise two domains: an N-terminal GTPase domain and a C-terminal domain (designated as the G domain and CTD, respectively). Consistent with their sequence homology, Gtr1p and Gtr2p adopt a similar fold, with a root-mean-squared deviation (RMSD) of 3.92 Å for 216 aligned Cα atoms and, if corresponding domains are superimposed individually, 1.88 Å for 171 Cα atoms of the G domains and 2.68 Å for 99 Cα atoms of the CTDs (Supplemental Fig. S4).

The Gtr1p–Gtr2p heterodimer adopts a pseudo-twofold symmetry and resembles a U-shaped horseshoe. The two G domains of Gtr1p–Gtr2p are located on the same side of the complex, with the corresponding surfaces of two G domains facing opposite directions (Fig. 1A; Supplemental Fig. S5). Interestingly, different from dimerization of G domains in the reported structures (Focia et al. 2004; Low et al. 2009; Chappie et al. 2010; Gao et al. 2010), no direct

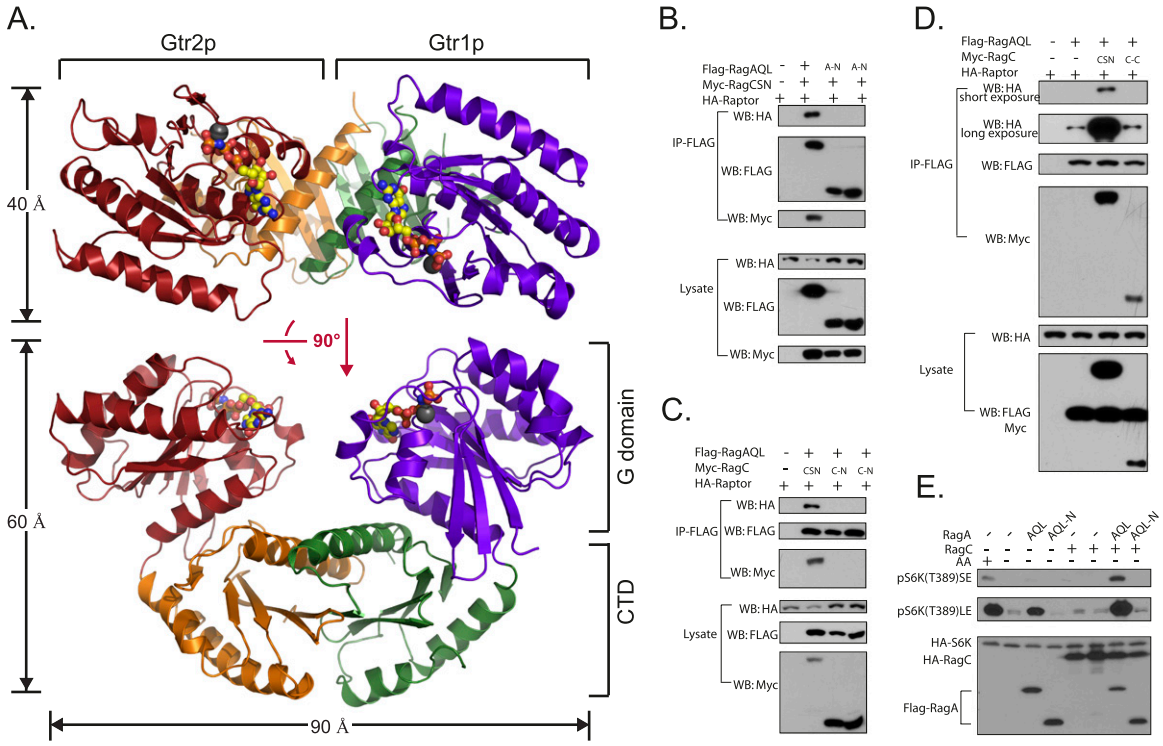

Figure 1. Overall structure of the Gtr1p–Gtr2p. (*A*) Overall structure of the Gtr1p–Gtr2p complex as a ribbon representation in two different views. G domains of Gtr1p and Gtr2p bound to GMPPNP are colored in blue and red, respectively, and CTDs are colored in green and orange, respectively. GMPPNP is shown as a ball-and-stick representation, and magnesium atoms are shown as black balls. (*B*,*C*) Dimerization is required for RagA–RagC to interact with raptor. Different RagA and RagC constructs were cotransfected with raptor into HEK293 cells. Protein interaction was determined by coimmunoprecipitation. RagAQL and RagCSN are mutants restricted to $RagA^{GTP}$ (Q66L) and $RagC^{GDP}$(S75N), respectively. (A-N) G domain of RagA; (C-N) G domain of RagC; (IP) immunoprecipitation; (WB) Western blot. (*D*) The G domain of RagC is required to promote the interaction between RagA and raptor. (CSN) RagCSN ($RagC^{GDP}$); (C-C) CTD of RagC. (*E*) The CTD of RagA is required for both basal and RagC-enhanced activity to stimulate TORC1. TORC1 activity was indirectly measured by the level of S6K phosphorylation. RagA and RagC constructs were cotransfected with HA-S6K into HEK293 cells. For amino acid starvation, cells were starved for amino acids for 1 h before harvesting. Amino acid starvation is denoted as AA^-. Sample cultured in complete medium is denoted as AA^+. Phosphorylation and protein levels were determined by immunoblotting with the indicated antibodies.

interaction was found between the two G domains in the Gtr1p–Gtr2p heterodimer structure. The dimerization is mediated by CTDs of both proteins, and the dimer interface is far away from the nucleotide pocket (Fig. 1A). The Gtr1p–Gtr2p heterodimer represents a new architecture among all GTPase structures.

In each monomer, the G domain forms extensive interactions with the CTD, with buried surfaces (G domain and CTD) of 882.2 Å^2 for Gtr1p and 878.2 Å^2 for Gtr2p, respectively. In the Gtr1p^{GTP}–Gtr2p^{GTP} heterodimer structure, with these intramolecular interactions and extensive interaction between two CTDs (buried surface of 1259 Å^2), the Gtr1p–Gtr2p complex adopts a rigid conformation and the two G domains adopt fixed orientation to each other. Nucleotide exchanges in G domains may not change the overall conformation of the complex because the switch regions are far away from both dimer and intramolecular interfaces (Supplemental Fig. S6). Thus, the Gtr1p–Gtr2p heterodimer may keep a rigid overall fold and undergo conformational changes mainly on switch regions upon nucleotide exchanges, through which they recognize raptor and activate mTORC1.

Both G domains are required for raptor interaction

Previous studies showed that the function of Rag/Gtr is highly conserved between yeast and mammals, and the interaction of Rag with raptor in mammalian cells and Gtr with Kog1 in yeast is also conserved (Bun-Ya et al. 1992; Schurmann et al. 1995; Hirose et al. 1998; Nakashima et al. 1999; Sekiguchi et al. 2001; Dubouloz et al. 2005). Compared with yeast TORC1, more extensive biochemical studies have been reported based on human mTORC1 and the Rag complexes (Kim et al. 2008; Sancak et al. 2008, 2010); thus, we used the human RagA–RagC complex to investigate their function in TORC1 binding and activation, guided by structure analyses of the Gtr1p–Gtr2p complex and highly conserved primary sequences (Supplemental Fig. S1). Previous studies have shown a direct interaction between RagA/C and raptor, which was confirmed by our in vitro pull-down assays using purified RagA/C and raptor proteins (Supplemental Fig. S7). Coimmunoprecipitation with raptor and Western blotting for S6K phosphorylation were performed to test the ability of Rag in raptor binding and TORC1 activation, respectively. RagA/C(N) and RagA/C(C) denote the G domain and CTD, respectively. RagA^{GTP} and RagC^{GDP} are mutants restricted to GTP-bound and GDP-bound, respectively.

We first examined whether both G domains are required for proper function of Rag GTPases. RagA^{GTP}–RagC^{GDP} showed strong interaction with raptor, whereas RagA(N)^{GTP}–RagC^{GDP} and RagA^{GTP}–RagC(N)^{GDP} showed little interaction with raptor (Fig. 1B,C). Moreover, expression of RagC(C) did not enhance the weak interaction between RagA^{GTP} and raptor (Fig. 1D). Consistent with these data, RagA(N)^{GTP} could not activate TORC1 in the absence of amino acids (Fig. 1E). These results indicate that both the G domains of RagA and RagC and dimerization are important for raptor binding and mTORC1 activation.

Although the Gtr1p–Gtr2p heterodimer adopts a pseudo-twofold symmetry and both G domains adopt a similar fold, structure comparison shows that the surface features of the G domains from Gtr1p and Gtr2p are rather different. For example, the surface region close to switch I and II of the Gtr1p G domain is more hydrophobic than that of Gtr2p, which is more acidic. Gtr2p and RagC share a similar electrostatic potential distribution in the switch regions of their respective G domains (Supplemental Fig. S8). Together with the finding that both G domains are required for raptor binding, these analyses suggest that Gtr1p/RagA and Gtr2p/RagC may contribute differently to raptor interaction, and together provide the specificity for raptor recognition.

RagA surface for raptor recognition

Next, we mapped the binding interface between raptor and Rag GTPases using coimmunoprecipitation. We first tested whether both G domains are equally important for raptor interaction. As shown in Figure 2A, wild-type RagA, together with either GTP-bound, GDP-bound, or the T90A/L93A/T96A mutant of RagC, strongly bound raptor, while GDP-bound RagA could not. These results indicate that the interaction with raptor was mainly determined by the nucleotide loading status of RagA, although the nucleotide-binding status of RagC modestly influenced the ability

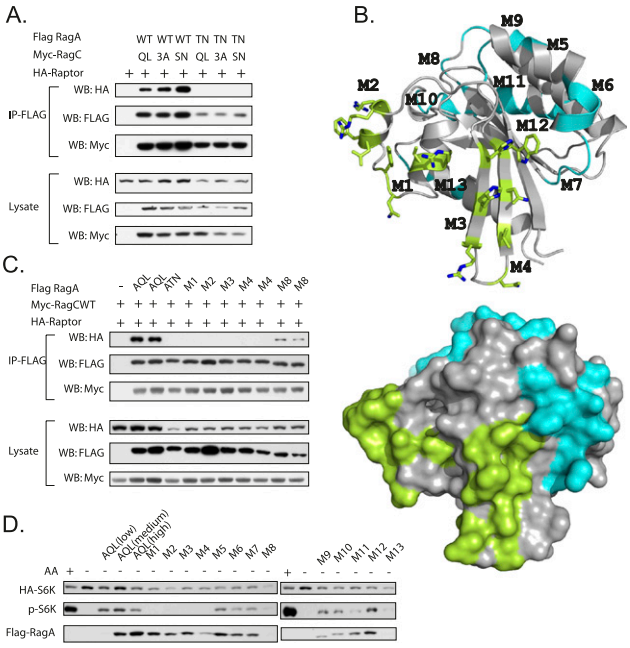

Figure 2. Mapping the raptor-interacting surface on RagA. (*A*) RagA plays a major role in raptor binding. The interaction between raptor and cotransfected RagA or RagC was examined by coimmunoprecipitation. 3A is the T90A/L93A/T96A mutation of RagC, in which mutations of the corresponding residues in Ras have been shown to abolish the effector binding. (*B*) G domain of Gtr1p is shown in a ribbon representation (*left* panel) and a surface representation (*right* panel). Corresponding residues involved in composite RagA mutations (M1–M4) are indicated with a stick representation and are colored in green, and residues mutated in M5–M13 are colored in cyan on the surface, as shown in Supplemental Figure S1 and Supplemental Table S2. All mutants were generated based on RagAQL(RagA^{GTP}). (*C*) The regions close to switch I and II in the RagA G domain are important for raptor interaction. Interaction between raptor and cotransfected RagA mutants was examined by coimmunoprecipitation. (*D*) The raptor interaction-defective RagA mutants cannot activate TORC1. RagA mutants were cotransfected with HA-S6K into HEK293 cells, and phosphorylation of HA-S6K in the absence of amino acids (indicating the activity of RagA) was determined.

of the RagA/C heterodimer to bind raptor. This observation is consistent with previous studies, which have shown that the GTP-bound RagA or RagB interacts with raptor and activates TORC1 when in complex with RagC or RagD; in contrast, the Rag dimer cannot bind mTORC1 if RagA is in the GDP form regardless of the nucleotide-binding status of the associated RagC or RagD (Kim et al. 2008; Sancak et al. 2008). These results suggest that RagA/B play a major role in raptor interaction. Thus, we focus on the RagA G domain to investigate the raptor recognition.

Based on the structural information of Gtr1p, 13 composite mutations were made in RagA-QL, which is a GTP-bound mutant, in order to map the raptor-interacting surface. The involved residues represent small patches of alanine substitutions on the surface area of the RagA G domain (Fig. 2B; Supplemental Table S2). Among the 13 mutants, four (M1–M4) abolished interaction with raptor and lost the ability to activate TORC1 (Fig. 2C,D). Notably, the four mutations are close to the P loop, switch I, and switch II regions. The above data indicate that the surface area (α1, α2 and β2, β3) of the RagA G domain is important for raptor binding and TORC1 activation. This observation is consistent with a notion that nucleotide exchanges alter the surface feature of switch I and II, and thus regulate raptor binding affinity.

Dimerized CTDs of the Rag complexes are required for function

In the structure of Gtr1p–Gtr2p, the CTDs of both proteins contain a central five-stranded anti-parallel β sheet, sandwiched by a long helix on one side of the G domains and two helices on the other side. Gtr1p and Gtr2p form a heterodimer through an edge-to-edge (β9–β9) arrangement of their β sheets (Supplemental Fig. S2). The dimerized CTDs form a compact three-layered structure, with a 10-stranded anti-parallel β sheet sandwiched by two α helices on the concave face and four α helices on the convex face (Fig. 1A; Supplemental Fig. S2). The dimerization is mediated by a network of hydrogen bonds and hydrophobic interactions, and the residues involved in dimerization are highly conserved from yeast to mammals (Fig. 3A,B). Intriguingly, in dimerized CTDs, Gtr2p α8 interacts with α8 and four β strands of Gtr1p, whereas α8 of Gtr1p only interacts with α8 and two β strands of Gtr2p. Structure analyses of Gtr1p–Gtr2p inter-

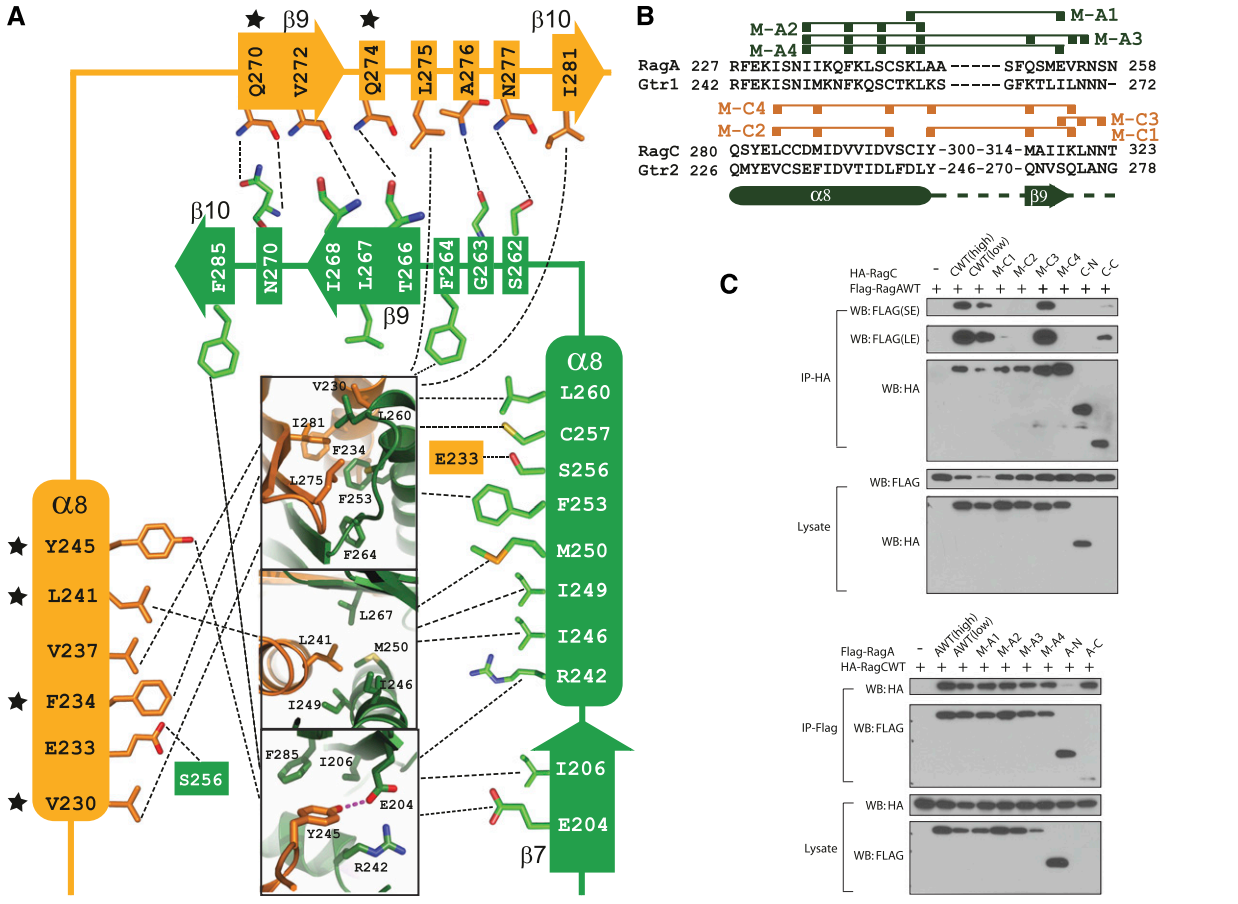

Figure 3. Mapping the dimerization critical residues. (*A*) Detailed interaction of Gtr1p–Gtr2p CTDs. Residues involved in hydrogen bond formation are connected with a dashed line directly, and hydrophobic interactions are linked by the central boxes with the detailed interactions shown. Critical residues for dimer formation are indicated as black stars. (*B*) Sequence alignment of critical regions for dimer formation in the CTDs of Rag GTPases. Composite RagA and RagC mutations are indicated *above* the sequence and are summarized in Supplemental Table S3. (*C*) The α8 and β9 of RagC are critical for dimer formation with RagA. Different RagA or RagC mutants were cotransfected as indicated. The interaction was determined by coimmunoprecipitation and Western blot. (SE) Short exposure; (LE) long exposure; (AWT) wild-type RagA; (CWT) wild-type RagC; [AWT(low)] transfection of 100 ng of DNA; [AWT(high)] transfection of 200 ng of DNA.

action show that more residues in Gtr1p than Gtr2p are involved in dimer formation, suggesting a lower contribution of individual residues in Gtr1p/RagA than Gtr2p/RagC for dimer formation (Supplemental Fig. S9).

Since the CTDs' dimerization is important for the function of Rag GTPases in TORC1 activation, we studied the interaction between the two CTDs. To determine residues critical for dimerization, we generated mutations in RagA and RagC based on the Gtr1p–Gtr2p structure and sequence alignment (Fig. 3B; Supplemental Table S3). Three mutations (M-C1, M-C2, and M-C4) of RagC abolished the interaction with RagA (Fig. 3C). In contrast, similar mutations in RagA did not abolish the interaction with RagC (Fig. 3C), consistent with previous structure analyses (Supplemental Fig. S9).

A Dali search with the Gtr1p–Gtr2p structure indicates that p14/MP1 adopt folds similar to the dimerized CTDs

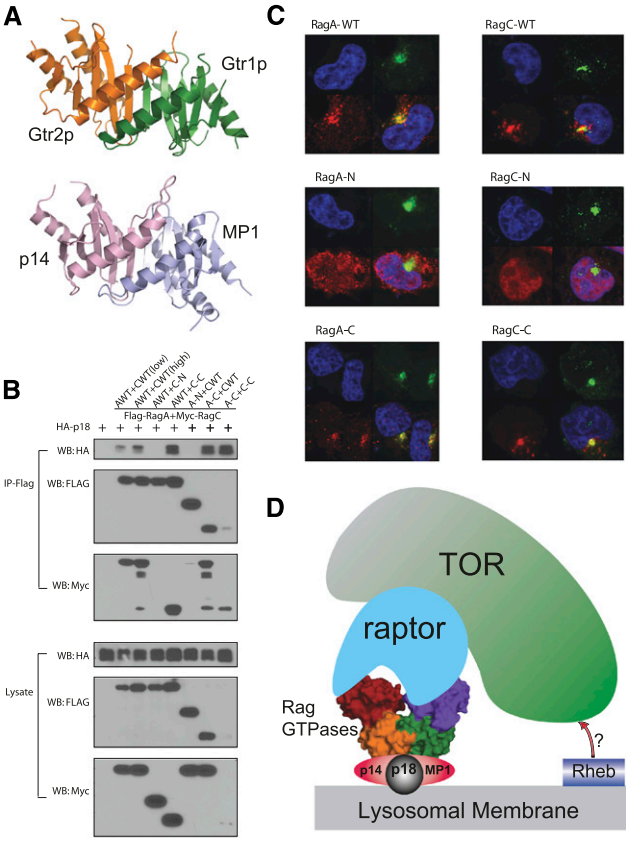

Figure 4. The CTDs of Rag GTPases share similar structures with p14/MP1 and are responsible for p18 interaction and lysosomal localization. (*A*) Structure comparison of Gtr1p–Gtr2p CTDs and the p14/MP1 complex. The structures are shown in a ribbon representation, and Gtr1p and Gtr2p CTDs are colored green and orange, respectively, while p14 and MP1 are colored pink and light blue, respectively. (*B*) The CTD dimer of RagA–RagC interacts with p18. RagA and RagC constructs were cotransfected with the p18 construct and the protein interaction was determined by coimmunoprecipitation. (*C*) The CTDs of RagA and RagC are necessary and sufficient for lysosomal localization. Different deletion mutants were transfected in 293 cells. The transfected Flag-RagA or HA-RagC was stained (red) along with DNA (blue) and lysosomal marker LAMP2 (green). (*D*) Working model of Rag GTPases in TORC1 activation. In the cartoon, the Rag CTDs interact with p18 and p14/MP1 to target the GTPases to lysosomes. The G domains of Rag associate with raptor, thus recruiting TORC1 to lysosomes for activation.

of Gtr1p–Gtr2p (Fig. 4A; Supplemental Fig. S9; Kurzbauer et al. 2004; Lunin et al. 2004). This is a rather surprising finding because these proteins do not share sequence homology. Interestingly, p14/MP1 are essential for lysosomal localization of RagB–RagD and form a complex with p18, which also binds with Rag GTPases (Sancak et al. 2010). However, surface feature differences between the two complexes suggest that they may not interact with p18 in a similar region. Notably, Ego3p, which was identified to interact with Gtr1p–Gtr2p and form an EGO complex, adopts a similar fold to p14/MP1 and was thought to be a potential p14/MP1 functional homolog in yeast, suggesting a conserved mechanism for Rag GTPase localization (Gao and Kaiser 2006; Kogan et al. 2010). Why p14/MP1 adopts a similar fold to the CTDs of Rag GTPases and how p14/MP1 is involved in Rag GTPase-mediated TORC1 activation need to be further investigated.

It has been shown that p18, together with p14/MP1, interacts with and recruits Rag GTPases to the lysosomal membrane (Sancak et al. 2010). We next studied which regions of Rag GTPase directly interact with p18. The coimmunoprecipitation results show that both CTDs are required for interaction with p18, and dimerization of Rag CTDs is necessary and sufficient for binding to p18 (Fig. 4B; Supplemental Fig. S11A,B). Consistent with the protein interaction results, immunofluorescence experiments showed that the CTDs of both RagA and RagC are necessary and sufficient for colocalization with the lysosomal marker LAMP2 (Fig. 4C). These data indicate that the localization of Rag GTPases is mediated by the interaction with p18 through their dimerized CTDs, which is consistent with the notion that the nucleotide loading status of Rag GTPases does not affect their cellular localization (Sancak et al. 2010).

This study presents the three-dimensional structure of Rag GTPase heterodimers and the structural basis of Rag GTPase-mediated raptor recognition and p18 association. Based on our data, we propose a working model for Rag GTPases in TORC1 recruitment and activation. In this model, the CTDs of Rag GTPase interact with p18, which is permanently anchored to the lysosomal surface (Fig. 4D). p14/MP1 may facilitate the interaction between p18 and Rag GTPases in an unknown mechanism. In a manner depending on GTP-binding status, the Rag heterodimer interacts with raptor mainly via the surfaces close to switch I and II on RagA, although RagC is also required. Through these interactions, the TORC1 complex is recruited to a lysosomal compartment where it is activated, presumably by the lysosome-localized Rheb. Our results provide structural insights into how the Rag GTPases recruit TORC1 to the p18 regulator complex, and thus activation of TORC1 by amino acids. Interestingly, the two p18-interacting complexes, the Gtr1p–Gtr2p CTD domains and p14/MP1, share remarkably similar three-dimensional structures. The function of the RagC/D G domain also needs to be further investigated. Although the G domain of RagC/D plays a minor role in raptor interaction, the nucleotide loading status still regulates the binding affinity. One possibility is that raptor mainly interacts with the RagA G domain, and the GDP-bound RagC G domain may facilitate the interaction and thus provide specific recognition and regulation. A key remaining issue is the activation/nucleotide exchange of Rag GTPases in response to the amino acid signal. Notably, VAM6, also known as VPS39, has been suggested as a guanine nucleotide exchange factor

for Gtr1p in yeast (Binda et al. 2009). Future study of amino acids in regulating nucleotide exchange of Rag GTPases will shed new light on this important signaling pathway in cell growth regulation.

Materials and methods

Protein purification and crystallization

Protein expression and purification were performed as described previously (Li et al. 2010). In brief, the ORFs of *gtr1p* and *gtr2p* were subcloned into a modified pETDuet-1 vector (Novagen) for bicistronic protein expression in the *Escherichia coli* strain BL21(DE3). The Gtr1p–Gtr2p complex was purified using Ni-NTA affinity columns, anion exchange, and gel filtration. The crystals were obtained using the hanging-drop, vapor diffusion method with reservoir solution containing 0.1 M HEPES (pH 7.0), 10% PEG monomethyl ether 5000, and 5% v/v Tacsimate (pH 7.0) at 277K. Crystals of the selenomethionine derivative of Gtr1p–Gtr2p were grown under similar conditions.

Data collection and structure determination

Se-SAD (single-wavelength anomalous diffraction) data were collected at a wavelength of 0.97916 Å and the diffraction was extended to 2.8 Å resolution (Hendrickson 1991). Data were indexed, integrated, and scaled using the program XDS (Kabsch 1988). Phases were initially determined by Se-SAD, and automatic model building was performed. All refinements were performed with the restraint of an experimental phase using the refinement module phenix.refine of the PHENIX package (Adams et al. 2002). The model quality was checked with the PROCHECK program (Laskowski et al. 1993).

Other procedures—including antibodies, plasmids, cell culture, transfection, immunofluorescence, and immunoprecipitation—are described in the Supplemental Material.

Accession number

The atomic coordinates of the Gtr1p–Gtr2p has been deposited in the Protein Data Bank with accession code 3R7W.

Acknowledgments

We thank Dr. Jiawei Wang at Tsinghua University for the help in data processing and structure determination. We thank staff members of beamline BL17U at SSRF (China) and other members in the Guan laboratory and the Xu laboratory for technical help. This work was supported by grants (to Y.X.) from the National Basic Research Program of China (2011CB918600 and 2009CB918600), the National Natural Science Foundation of China (31030019, 11079016, and 30870493), and the International Collaboration Program from the Science and Technology Commission of Shanghai Municipality (10430709300), and grants from the NIH (to K.L.G.).

References

Adams PD, Grosse-Kunstleve RW, Hung LW, Ioerger TR, McCoy AJ, Moriarty NW, Read RJ, Sacchettini JC, Sauter NK, Terwilliger TC. 2002. PHENIX: building new software for automated crystallographic structure determination. *Acta Crystallogr* **58:** 1948–1954.

Binda M, Peli-Gulli MP, Bonfils G, Panchaud N, Urban J, Sturgill TW, Loewith R, De Virgilio C. 2009. The Vam6 GEF controls TORC1 by activating the EGO complex. *Mol Cell* **35:** 563–573.

Bun-Ya M, Harashima S, Oshima Y. 1992. Putative GTP-binding protein, Gtr1, associated with the function of the Pho84 inorganic phosphate transporter in *Saccharomyces cerevisiae*. *Mol Cell Biol* **12:** 2958–2966.

Chappie JS, Acharya S, Leonard M, Schmid SL, Dyda F. 2010. G domain dimerization controls dynamin's assembly-stimulated GTPase activity. *Nature* **465:** 435–440.

Dubouloz F, Deloche O, Wanke V, Cameroni E, De Virgilio C. 2005. The TOR and EGO protein complexes orchestrate microautophagy in yeast. *Mol Cell* **19:** 15–26.

Focia PJ, Shepotinovskaya IV, Seidler JA, Freymann DM. 2004. Heterodimeric GTPase core of the SRP targeting complex. *Science* **303:** 373–377.

Gao M, Kaiser CA. 2006. A conserved GTPase-containing complex is required for intracellular sorting of the general amino-acid permease in yeast. *Nat Cell Biol* **8:** 657–667.

Gao S, von der Malsburg A, Paeschke S, Behlke J, Haller O, Kochs G, Daumke O. 2010. Structural basis of oligomerization in the stalk region of dynamin-like MxA. *Nature* **465:** 502–506.

Guertin DA, Sabatini DM. 2007. Defining the role of mTOR in cancer. *Cancer Cell* **12:** 9–22.

Hendrickson WA. 1991. Determination of macromolecular structures from anomalous diffraction of synchrotron radiation. *Science* **254:** 51–58.

Hirose E, Nakashima N, Sekiguchi T, Nishimoto T. 1998. RagA is a functional homologue of *S. cerevisiae* Gtr1p involved in the Ran/Gsp1–GTPase pathway. *J Cell Sci* **111:** 11–21.

Inoki K, Corradetti MN, Guan KL. 2005. Dysregulation of the TSC–mTOR pathway in human disease. *Nat Genet* **37:** 19–24.

Kabsch W. 1988. Evaluation of single-crystal X-ray diffraction data from a position-sensitive detector. *J Appl Crystallogr* **21:** 916–924.

Kim E, Goraksha-Hicks P, Li L, Neufeld TP, Guan KL. 2008. Regulation of TORC1 by Rag GTPases in nutrient response. *Nat Cell Biol* **10:** 935–945.

Kogan K, Spear ED, Kaiser CA, Fass D. 2010. Structural conservation of components in the amino acid sensing branch of the TOR pathway in yeast and mammals. *J Mol Biol* **402:** 388–398.

Kurzbauer R, Teis D, de Araujo ME, Maurer-Stroh S, Eisenhaber F, Bourenkov GP, Bartunik HD, Hekman M, Rapp UR, Huber LA, et al. 2004. Crystal structure of the p14/MP1 scaffolding complex: how a twin couple attaches mitogen-activated protein kinase signaling to late endosomes. *Proc Natl Acad Sci* **101:** 10984–10989.

Laskowski RA, MacArthur MW, Moss DS, Thornton JM. 1993. PROCHECK: a program to check the stereochemical quality of protein structures. *J Appl Crystallogr* **26:** 283–291.

Li Z, Zhao B, Wang P, Chen F, Dong Z, Yang H, Guan KL, Xu Y. 2010. Structural insights into the YAP and TEAD complex. *Genes Dev* **24:** 235–240.

Low HH, Sachse C, Amos LA, Lowe J. 2009. Structure of a bacterial dynamin-like protein lipid tube provides a mechanism for assembly and membrane curving. *Cell* **139:** 1342–1352.

Lunin VV, Munger C, Wagner J, Ye Z, Cygler M, Sacher M. 2004. The structure of the MAPK scaffold, MP1, bound to its partner, p14. A complex with a critical role in endosomal map kinase signaling. *J Biol Chem* **279:** 23422–23430.

Nakashima N, Noguchi E, Nishimoto T. 1999. *Saccharomyces cerevisiae* putative G protein, Gtr1p, which forms complexes with itself and a novel protein designated as Gtr2p, negatively regulates the Ran/Gsp1p G protein cycle through Gtr2p. *Genetics* **152:** 853–867.

Sancak Y, Peterson TR, Shaul YD, Lindquist RA, Thoreen CC, Bar-Peled L, Sabatini DM. 2008. The Rag GTPases bind raptor and mediate amino acid signaling to mTORC1. *Science* **320:** 1496–1501.

Sancak Y, Bar-Peled L, Zoncu R, Markhard AL, Nada S, Sabatini DM. 2010. Ragulator–Rag complex targets mTORC1 to the lysosomal surface and is necessary for its activation by amino acids. *Cell* **141:** 290–303.

Schurmann A, Brauers A, Massmann S, Becker W, Joost HG. 1995. Cloning of a novel family of mammalian GTP-binding proteins (RagA, RagBs, RagB1) with remote similarity to the Ras-related GTPases. *J Biol Chem* **270:** 28982–28988.

Sekiguchi T, Hirose E, Nakashima N, Ii M, Nishimoto T. 2001. Novel G proteins, Rag C and Rag D, interact with GTP-binding proteins, Rag A and Rag B. *J Biol Chem* **276:** 7246–7257.

Wullschleger S, Loewith R, Hall MN. 2006. TOR signaling in growth and metabolism. *Cell* **124:** 471–484.